University of New Mexico
UNM Digital Repository

Nuclear Engineering ETDs | Engineering ETDs

1-28-2015

PREDICTING THE SENSITIVITY OF A BERYLLIUM/SCINTILLATOR FUSION NEUTRON DETECTOR COMBINING EXPERIMENTAL METHODS AND MONTE CARLO MODELS

Jedediah Styron

Follow this and additional works at: https://digitalrepository.unm.edu/ne_etds

Recommended Citation
Styron, Jedediah. "PREDICTING THE SENSITIVITY OF A BERYLLIUM/SCINTILLATOR FUSION NEUTRON DETECTOR COMBINING EXPERIMENTAL METHODS AND MONTE CARLO MODELS." (2015). https://digitalrepository.unm.edu/ne_etds/41

This Thesis is brought to you for free and open access by the Engineering ETDs at UNM Digital Repository. It has been accepted for inclusion in Nuclear Engineering ETDs by an authorized administrator of UNM Digital Repository. For more information, please contact disc@unm.edu.

Jedediah Daniel Styron

Candidate

Nuclear Engineering

Department

This thesis is approved, and it is acceptable in quality and form for publication:

Approved by the Thesis Committee:

Dr. Gary Cooper, UNM Faculty, Chairperson

Dr. Adam Hecht, UNM Faculty

Dr. Carlos Ruiz, Sandia National Laboratories

PREDICTING THE SENSITIVITY OF A BERYLLIUM/SCINTILLATOR FUSION NEUTRON DETECTOR COMBINING EXPERIMENTAL RESULTS AND MONTE CARLO METHODS

by

JEDEDIAH D. STYRON

B.S. NUCLEAR ENGINEERING, SPRING 2013
UNIVERSITY OF NEW MEXICO

THESIS

Submitted in Partial Fulfillment of the
Requirements for the Degree of

Masters of Science
Nuclear Engineering

The University of New Mexico
Albuquerque, New Mexico

December, 2014

Acknowledgements

I would like to thank my advisor Dr. Gary Cooper for his patience, support and encouragement throughout this project. I would also like to thank the rest of the team from Org. 1677 at Sandia National Laboratories: Dr. Carlos Ruiz, Dr. Kelly Hahn, Dr. Gordon Chandler, Dr. Brett Jones, and Jose Torres for their support and advice during this work. Others who have offered support are: Dr. Alan Nelson, Bruce McWatters, Ruth Smelsner (all from Sandia National Laboratories), Dr. Adam Hecht, for sitting on my committee, and Ken Carpenter (both from the University of New Mexico) for his electronics expertise.

Most of all I would like to thank my wife Theresa and my daughter Cassandra for dealing with the several exceptionally late nights and early mornings. Thank you for not divorcing me after the fact! Thanks to all the others I have not mentioned and for your understanding when I couldn't go golfing or hunting. My grandfather, "Papa", provided me with inspiration throughout this journey. Unfortunately, he passed away prior to me receiving my B.S. degree, but he always knew I would succeed before I did. Thanks for always believing in me, big guy!

This work was performed under contract to Sandia National Laboratories, a multi-program laboratory operated by Sandia Corporation, a wholly owned subsidiary of Lockheed Martin Company, for the U.S. Department of Energy's National Nuclear Security Administration under contract DE-AC04-94AL85000.

Abstract

For this work a methodology has been developed to predict the sensitivity of a beryllium/scintillator fusion neutron detector. Neutrons may be captured by the beryllium via the ^{9}Be (n, α) ^{6}He nuclear reaction, where the product nucleus, ^{6}He, decays by beta emission. The beta particles can be detected by close coupling scintillator with the beryllium. The methodology relates beta energy deposition to absolute measured scintillation light output as a function of detector bias, reflective material, scintillator thickness, and solid angle subtended by the scintillator on the face of the PMT. Output signals were measured from thin plastic scintillator using NIST traceable beta and gamma sources and MCNP5 was used to model the energy deposition from each source. Combining the experimental and calculated results gives the desired empirical relationships. The results from this methodology were compared with previous work and the two results were in good agreement. The empirical relationships were applied to a similar detector with much larger dimensions and very different response characteristics. The correlation between the two systems produced nearly identical results. To validate, the sensitivity of the second beryllium/scintillator-layer neutron activation detector was predicted and then exposed to a known DD neutron fluence. The neutron fluence was determined by the associated particle method from which the detector sensitivity could be inferred. The predicted and the measured sensitivity agreed within a range of 8 to 38 percent difference with an average standard deviation of 25% from 8 total measurements. Predicting the detector performance within 25% is adequate enough to guide future detector design decisions. To test this methodology it was applied to the design modeled after Sandia National Laboratories current beryllium detector, which was originally designed using results from a very limited set of experimental data. The results of these calculations indicated that the design was in fact optimal within the uncertainties of this work.

Table of Contents

List of Figures ix
List of Tables xi
1. Introduction 1
2. Theory 7
Organic Scintillator and PMT Response 7
Previous Experimental Work 13
3. Experimental Set-Up 15
Detector #1 Geometry 15
Procedure 17
Detector System Electronics 18
Beta and Gamma Source Description 18
MCNP 5 model 19
4. Methodology 22
5. Statistical and Systematic Uncertainties 26
6. Detector #1 Results 29
Method Proof of Concept 29
Combining Response Functions, Detector #1 BLC Geometry 42
7. Detector #2 45
Description 45
Detector #2 Results 47
8. Validation 54
Experiment 54
Monte Carlo Calculations 55
9. Optimization 59
10. Conclusion 62
11. References 63
12. List of Appendices 66
Appendix A Experimental Data and Calculated Response Functions 69
Detector #1 69

Proof of Concept – Case 1 (Beryllium/Beryllium) 69
Proof of Concept – Case 2 (Beryllium/Polypropylene) 70
Proof of Concept – Case 3(Polypropylene/Polypropylene) 72
Proof of Concept – Case 4 (Mylar) 74
Bias Correlation – Case 1 (Beryllium/Beryllium) 75
Bias Correlation – Case 3 (Polypropylene/Polypropylene) 77
¼ and ½ mm Scintillator 80
Source Location – Case 1 (Beryllium/Beryllium) 83
Source Location – Case 2 (Beryllium/Polypropylene) 84
Source Location – Case 3 (Polypropylene/Polypropylene) 85
Source Location – Case 4 (Mylar) 86
Source Location – ¼ and ½ mm scintillator 87
View Factor – Case 3 Geometry (Polypropylene/Polypropylene) 89
View Factor – Case 1 Geometry (Beryllium/Beryllium) 92
BLC Geometry 93
Detector #2 95
BLC geometry – 10 3.175 mm layers 95
Spatial, BLC geometry –10 0.3175 mm layers 103
Single Layer Geometry – 3.175 mm scintillator 109
BLC geometry – 10 0.5 mm layers 113
Single Layer Geometry – 0.5 mm scintillator 115
BLC geometry – 10 0.25 mm layers 117
Single Layer Geometry – 0.25 mm scintillator 121
Appendix B MCNP Results 124
Detector #1 124
Proof of Concept – Case 1 (Beryllium/Beryllium) 124
Proof of Concept – Case 2 (Beryllium/Polypropylene) 126
Proof of Concept – Case 3 (Polypropylene/Polypropylene) 129
Proof of Concept – Case 4 (Mylar Wrap) 132
¼ and ½ mm Scintillator 133
Source Location – Case 1(Beryllium/Beryllium) 138
Source Location – Case 2(Beryllium/Polypropylene) 140
Source Location – Case 3(Polypropylene/Polypropylene) 141

Source Location – Case 4(Mylar Wrap) 143
Source Location – ¼ and ½ mm Scintillator 145
View Factor 149
BLC Geometry 153
Geometric Uncertainties 156
Detector #2 160
BLC Geometry – 10 3.175 mm layers 160
BLC Geometry – 10 0.5 mm layers 166
BLC Geometry – 10 0.25 mm layers 167
Single Layer Geometry – 3.175 mm 168
Single Layer Geometry – 0.50 mm 170
Single Layer Geometry – 0.25 mm 171
Appendix C Sample MCNP Inputs 173
Detector # 1 173
Na-22 Gamma Source, Case 1 Geometry 173
Na-22 Positron Source, Case 1 Geometry 175
Cs-137 gamma source, case 1 geometry 178
Cl-36 beta source, case 2 geometry 180
Pb-210 beta source, case 3 geometry 183
Pb-210 gamma source, case 3 geometry 185
Sr-90 beta source in top location, case 4 geometry 188
Co-60 gamma source, case 3 geometry, ¼ mm scintillator 191
Co-60 beta source, case 3 geometry, ¼ mm scintillator 193
Sr-90 beta source, case 3 geometry, ½ mm scintillator, bottom location 196
Co-60 gamma source, BLC Geometry 199
Detector #2 202
Co-60 gamma source, BLC geometry, 3.175 mm scintillator 202
Cs-137 gamma source, single layer geometry, ¼ mm scintillator 205
Neutron Source, Validation Experiment, BLC Geometry, 3.175 mm scintillator 207
He-6 beta source, Validation Experiment, BLC Geometry, 3.175 mm scintillator 214
Validation Experiment, Neutron Fluence at Average Detector Solid Angle 218
Appendix D Sample MCNP Output Files 226
Detector #1 226

Co-60 gamma source, BLC geometry 226
Detector #2 241
Neutron Source, Validation Experiment, BLC Geometry, 3.175 mm scintillator 241
He-6 beta source, Validation Experiment, BLC Geometry, 3.175 mm scintillator 258
Appendix E Source Data Sheets 284
Cs-137 (IPL) 284
Cs-137 (Baird-Atomic) 285
Cl-36 286
Co-60 287
Na-22 288
Pb-210/Bi-210 289
Sr-90/Y-90 290
Appendix F Beta Source Spectral Data 291
Appendix G Scintillator Data Sheets 293
Bc-404 Scintillator (St. Gobain Crystals) 293
EJ-204 (Eljen Technologies) 296
Appendix H PMT Data Sheets 297
Hamamatsu R5946 PMT 297
Hamamatsu R1250 PMT 299
Appendix J Review of Scientific Instruments Publication (Draft) 301

List of Figures

Figure 1 - Fusion Reactions of Interest 1
Figure 2 ^{9}Be (n, α) ^{6}He Cross-Section 2
Figure 3 Sandia National Laboratories Dual Paddle BLC Detector 4
Figure 4 Model for photon scattering within a scintillator 11
Figure 5 Re-purposed Beryllium Rod Detector Housing 15
Figure 6 Detector # 1 Experimental Geometries, Radial View shown on top, Axial View shown on the bottom 16
Figure 7 Preperation of experiment, Shown above is 1 mm scintillator with beryllium on either side and a Sr-90 source placed in the top location 17
Figure 8 Electronic configuration used for data acquisition 18
Figure 9 MCNP Calculated Total Differential Spectrum for a Sr-90 Source with 1 mm Scintillator and Polypropylene Reflective Material 21
Figure 10 Experimental Total Integral Spectrum for a Sr-90 Source with 1 mm Scintillator and Polypropylene Reflective Material 22
Figure 11 MCNP Total Integral Spectrum, for a Sr-90 Source with 1 mm Scintillator and Polypropylene Reflective Material 23
Figure 12 Energy Deposition vs Pulse Height for a Sr-90 Source with 1 mm Scintillator and Polypropylene Reflective Material, Comparison to Previous Work Shown 24
Figure 13 Residual Plot of Geometry and Source Knowledge Systematic Uncertainty ... 27
Figure 14 Correlation for Pp-Pp geometry, 4 sources, 1mm Scintillator 29
Figure 15 Experimental Data Taken at -1.8kV to -2.3kV 31
Figure 16 CFD Setting-Energy Deposition Correlations for Cl-36 as a Function of Detector Bias 32
Figure 17 Calculated Detector Response vs. Detector Bias, Empirical Equation Shown 32
Figure 18 Calculated Detector Response vs. Reflective Material Refraction Index, Empirical Equation Shown 33
Figure 19 CFD setting vs. Energy Deposition for the Case 1 and Case 3 geometries with the 0.25, 0.50, and 1.0 mm scintillator (-2.0 kV bias used for Case 3 and -2.3 kV bias used for Case 1) 34
Figure 20 Calculated Detector Response vs. Scintillator Thickness, Empirical Relationship Shown 36
Figure 21 CFD Setting vs. Energy Deposition as a Function of Three Different Source Locations, Calculations Shown are for a Sr-90 Source with 1 mm Scintillator and Mylar 37
Figure 22 Calculated Detector Response vs. Source Location as a Function of Reflective Material and Scintillator Size, Empirical Relationship Shown 38
Figure 23 View Factor Experimental Data, Co-60 source in Case 3 Geometry 39

Figure 24 Experimental Data Taken with Co-60 in the Case 3 Geometry with the Inclusion of the View Factor..... 40
Figure 25 CFD Setting vs. Energy Deposition, Detector #1 Energy Dependent Relationship Shown 41
Figure 26 Validation of Detector Response Function, Predicted and Experimental Sensitivity for a Co-60 Source in the BLC Geometry 44
Figure 27 Active Region of Detector #2, BLC geometry Shown with .635 mm Be and 0.318 mm Scintillator..... 46
Figure 28 Detector #2 Source Location Grid..... 46
Figure 29 Detector #2 Calculated Detector Response vs. Detector Bias, Empirical Relationship Shown 47
Figure 30 Calculated Detector Response vs. Source Location, Detector #2 BLC geometry with 10 .318 mm scintillator layers..... 49
Figure 31 Comparison of response functions produced with Cs-137 and Co-60 with 10-0.318 mm scintillator 50
Figure 32 Comparison of Detector # 2 Response Functions, Single Scintillator Layer vs. BLC Geometry..... 51
Figure 33 CFD Setting vs. Energy Deposition, Detector #2 Energy Dependent Relationship Shown 52
Figure 34 Comparison of Detectors # 1 and 2 Energy Dependent Response Functions .. 53
Figure 35 Predicted and Measured Sensitivities for Detector #2 as a function of CFD setting..... 58
Figure 36 MCNP Geometry, 2 mm BC-404 scintillator and 2 mm Beryllium Layers Shown 60
Figure 37 Detector Sensitivity as a function of scintillator and beryllium thicknesses.... 61

List of Tables

Table I Summary of UNM NIST traceable sources..... 19
Table II Source Photon Energies and Branching Ratios used in MCNP Models..... 20
Table III Source Particle Energies and Branching Ratios used in MCNP Models..... 20
Table IV Comparison of Detector # 2 Sensitivities, Measured and Predicted 57

1. Introduction

Inertial-confinement-fusion (ICF) experiments are conducted at several national laboratories to study nuclear fusion as a viable energy source. The detection of the neutrons produced from these experiments give critical information about the performance of the fusion plasma. There are several fusion reactions, but the three reactions typically studied are shown in Figure 1, where the last two reactions produce the neutrons of interest.

$$^{2}_{1}H + ^{2}_{1}H \xrightarrow{yields\ 50\%} ^{3}_{1}H + ^{1}_{1}H + 4.03\ MeV$$

$$^{2}_{1}H + ^{2}_{1}H \xrightarrow{yields\ 50\%} ^{3}_{2}He + ^{1}_{0}n + 3.27\ MeV$$

$$^{3}_{1}H + ^{2}_{1}H \xrightarrow{yields} ^{4}_{2}He + ^{1}_{0}n + 17.6\ MeV$$

Figure 1 - Fusion Reactions of Interest

The neutron yield from a fusion experiment, assuming a certain source isotropy, can be inferred by measuring the induced activity of a radioisotope that is produced by activation via a neutron reaction. The primary activation diagnostic that has historically been used to measure DD neutrons at Sandia National Laboratories' Z machine is the activation of indium [1]. In indium activation the primary reaction of interest is ^{115}In (n, n') ^{115m}In which has a threshold of 336 keV. The neutron yield is determined by measuring the gamma line radiation of 336 keV that occurs from the isomeric transition from the metastable state to the ground state. To measure DD neutrons, indium samples are placed near the source of neutrons, then after exposure are manually recovered and measured with a High Purity Germanium detector (HPGe). For Z experiments it takes at least one hour and often twelve hours or more before the indium samples can be recovered. Fortunately, the 4.49-hour half-life makes such delays acceptable but the quality of the data can be significantly decreased. Depending on induced activity, the sample may have to be counted for one or two half-lives, thus yields cannot be determined for several hours after an experiment.

At the Z facility, DD neutron measurements are made in a very harsh radiation environment. The Z-machine, when fired, creates a very intense bremsstrahlung background that can have an endpoint energy exceeding 10 MeV. This bremsstrahlung interferes with most neutron detectors including the activation of indium since ^{115m}In can also be produced via the nuclear reaction ^{115}In (γ, γ') ^{115m}In. This is a direct interference with the neutron measurement since one cannot infer which reaction produced the measured ^{115m}In.

In 1983 Rowland [2] proposed the use of a beryllium activation detector as an alternative to indium activation for measuring DD and DT neutrons produced in ICF experiments. Beryllium neutron detectors are based on the nuclear reaction, ^{9}Be (n, α) ^{6}He. Unlike the product of the indium reaction, ^{6}He can only be produced via a neutron reaction. This reaction has a threshold of 0.67 MeV, which makes it somewhat selective to DD (2.45 MeV) and DT (14.1 MeV) neutron energies and insensitive to low-energy thermal neutrons. The cross-section for this reaction, shown on a semi-log scale in Figure 2, is more sensitive for DD neutrons at 82.5 mb compared with10.4 mb for DT neutrons [3].

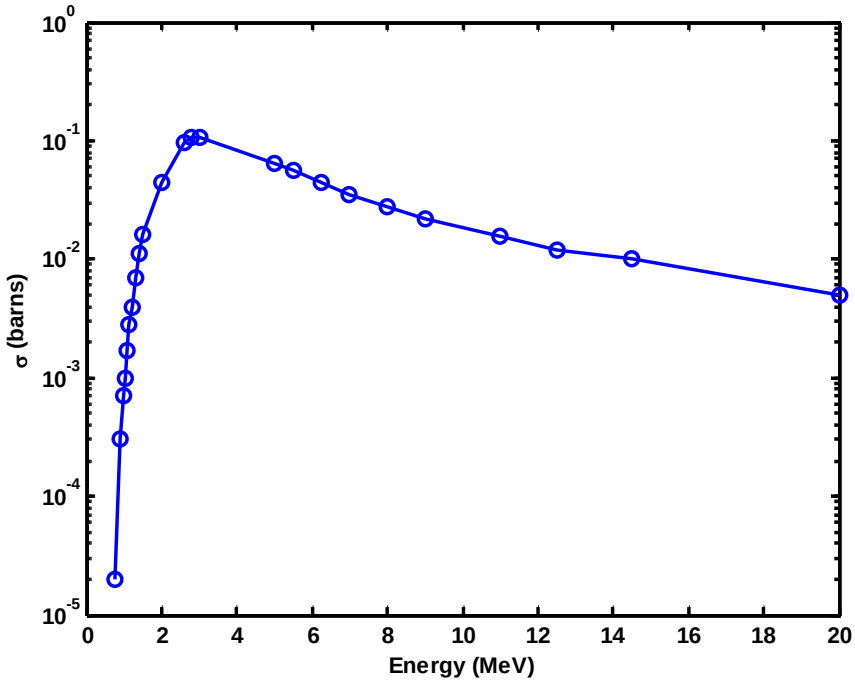

Figure 2 ^{9}Be (n, α) ^{6}He Cross-Section

Since the product nucleus, ^{6}He, decays with a half-life of only 807 ms [4], obviously there is no time to manually recover and count the ^{6}He decay beta particles, so it must be measured *in situ.* This was accomplished in the original Rowland design by alternating layers of moderately thick beryllium and plastic scintillator sheets that were coupled to a photomultiplier tube (PMT). This design is very practical since the ^{6}He nucleus decays by emitting a beta particle with an end-point energy of 3.51 MeV, allowing for a large fraction of the betas to escape the activation region and deposit energy in the scintillator. Murphy proposed an alternative design that consisted of several beryllium rods imbedded in a cylinder of plastic scintillator [5]. Another, more recent design, is a gas proportional counter concept where the beryllium layer is sandwiched between two gas filled tubes [7]. In either case, these designs have practical advantages over indium activation in that samples do not have to be "recovered" and the yields can be determined within a few minutes after an experiment.

The designs by both Rowland and Murphy have both been used at the Z-facility. For experiments on the Z-machine these designs are desirable since the bremsstrahlung background does not directly interfere with the neutron measurement. However, the negative consequence of both these designs is that the plastic scintillator will also measure the instantaneous bremsstrahlung pulse. While it does not directly interfere with the measurement of the ^{6}He decay a large enough pulse can overdrive the constant fraction discriminator (CFD) that is used in the detection scheme on the Z-machine resulting in total loss of data. In the event data are recoverable, gamma rays from materials that have been activated in and around the detector will also be measured, thus, superimposing additional background on the ^{6}He decay which may hinder inference of the neutron yield by decreasing the signal to noise ratio. The detector sensitivity must be significantly reduced by increasing the discriminator settings to mitigate this consequence.

To improve these deficiencies, the volume ratio of scintillator to beryllium was reduced in a newer version of the beryllium activation detector designed at Sandia National Laboratories (Org. 1677, Target Physics and Diagnostics), which is referred to as the

beryllium “layer cake” (BLC) geometry. Similar to the Rowland design, the active detector region has alternating layers of 3.18 mm thick beryllium and 1.00 mm thick BC-404 scintillator [8] encased in 0.10 mm thick reflective Mylar® [9]. The detection region is enclosed on two sides with Lexan light guides coupled to two PMTs as shown in Figure 3. The two PMTs allow the option for taking data at two different gains and/or discriminator settings to cover a larger range of sensitivity than with a single detector. Since the geometry and design of this detector has performed well in the Z-environment and provided satisfactory data it was decided that a performance predictive capability shall be developed that concentrates on the “layer cake” geometry.

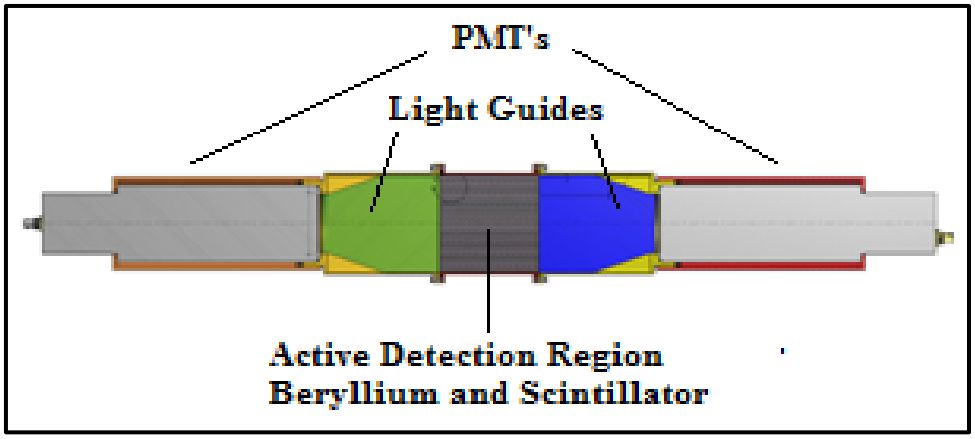

Figure 3 Sandia National Laboratories Dual Paddle BLC Detector

For the purpose of developing a methodology the design criteria for this detector will be discussed. The improvements to the design are driven by two desired outputs, a maximum sensitivity (counts per incident neutron) and a maximum signal to noise ratio (real counts to background counts). To achieve these objectives three coupled problems have to be solved. First, the ideal detector should produce the largest number of ^{6}He nuclei. Second, the detector should measure a large fraction of the decay betas and finally the amount of light produced per beta interaction within the scintillator needs to be larger than some threshold value. This threshold value is largely a function of the amount of light produced by background radiation. Thus an optimal detector should be designed to be as insensitive to background as possible. This can be done by minimizing the volume of scintillator used. However, the volume of scintillator should not be minimized to the

point where a sufficiently large prompt signal is compromised. This suggests that an ideal configuration exists only if the thicknesses of the beryllium and scintillator layers are ideal for detecting the radiation of interest and the arrangement of these layers is ideal for collecting the largest quantity of light produced from the beta particles.

For this type of detector the first two problems can be solved directly using models in MCNP5 [10]. MCNP5 is a very powerful tool used throughout the nuclear industry, but it is particularly useful for doing detector design since virtually any geometry can be modeled and the model parameters can be varied rather easily. Unfortunately, the results of an MCNP5 calculation do not directly translate to experimentally verifiable results. The variables considered in MCNP5 are limited to energy and frequency of events that occur within a geometric region of interest. Experimentally the variables of interest are the frequency of events not as a function of energy but as a function of electronic pulses that are discrete. The problem becomes then: how can we translate a simple MNCP5 calculation to a predictable, useful, and experimentally measurable quantity? For this work, the goal is to predict and quantize the number of events that occur at a given magnitude of measurable electronic pulse as a function of the calculated energy deposition.

There are typically three ways of determining a detector response function: experimentally [11, 12], theoretically, or a semi-empirical formulation that couples either analytical formulation or Monte Carlo calculations to experimental data [13]. Semi-empirical formulations are widely used to smooth spectral data measured with NaI(Tl) detectors [14] or semi-conductor detectors [15,16,17]. In neutron applications, specifically for organic scintillators, most of the focus has been on developing response functions for recoil protons [18]. The response function for recoil protons needs to be well known and is absolutely necessary when unfolding neutron time of flight data for recovering neutron energy spectra and plasma temperatures [19]. Monte Carlo techniques, in general, are used for a wide variety of calculations across the nuclear industry and while this is not a complete literature review of Monte Carlo applications,

several good references can be found within the given references for the application of Monte Carlo techniques to detector design.

For this thesis work, Monte Carlo calculations will be combined with experimental data for a simple detector system to develop a semi-empirical formulation that will characterize specific detector parameters that are known to affect the magnitude of the signal from a scintillation detector. The parameters discussed in the literature that will be investigated are the system electronics, reflectivity of materials around the scintillator, location of scintillating events, scintillator size, and the solid angle subtended by the scintillator on the photocathode [20-22]. This technique will then be applied to data from a similar, but larger detector that has very different response characteristics, verified through a set of separate neutron experiments, and then applied to an optimization study. The rest of this thesis will discuss the theory of organic scintillators, the detector geometries/systems used, development of the methodology, simulated and experimental results, validation of the methodology, an optimization study, and concluding remarks.

2. Theory

Organic Scintillator and PMT Response

Organic scintillators typically come in the form of liquid or plastic media and will be briefly described here. A more complete and thorough discussion of organic scintillators can be found in Birks [23]. Plastic scintillators have a number of advantages: they are affordable, can be fabricated into any shape, are sensitive to neutrons, and have very fast time response characteristics. Organic scintillator detectors, in general, work on the principle of absorbing kinetic energy from charged particles passing through the medium and then reemitting a fraction of that energy in the form of visible light that is subsequently collected with a PMT. The detection of neutral particles can be accomplished by measuring the recoil particles from scattering interactions. For neutrons and gammas the recoil particles of interest are protons and electrons, respectively. The number of scintillation photons created and the energy that each photon is emitted with after an energy loss event is a highly statistical process and is dependent on the energy level structure of the organic molecules present in the scintillating medium. These values also vary as a function of the type of charged particle that is interacting and with how much kinetic energy is lost. Typical values for fast electrons in the low MeV range interacting in most plastic scintillators result in 8-10 photons emitted, in the energy range of 3-4 eV, per keV absorbed within the scintillator [24]. This value is rather low when compared with sodium iodide crystals which produce ~40 photons per keV absorbed, which is why organic scintillators are known for poor energy resolution. However, the time it takes to create and collect the visible light is in the nano-second range for organics where the response for sodium iodide crystals is in the micro-second range. This makes organics ideal for pulsed neutron experiments where time response and count rates are of a concern.

The physical relationship between energy deposition and light yield from organic scintillation processes is well known and the functional representation that relates the two quantities, The Birks formula [23], is given in Equation 1.

$$\frac{dL}{dx} = \frac{S\frac{dE}{dx}}{1 + kB\frac{dE}{dx}} \tag{1}$$

In this equation dL/dx is the amount of light produced per unit path length, dE/dx is the energy loss per unit path length, S is the scintillation efficiency, B is the ionization density, and k is the fraction of the ionization density that leads to quenching. In the absence of quenching (k is small) or if dE/dx is comparatively small, Birks formula predicts the amount of light produced per unit energy loss is a constant. This is the case for gammas and fast electrons [24].

$$\frac{dL}{dx} = S\frac{dE}{dx} \quad or \quad \frac{dL}{dE} = S \tag{2}$$

In this equation the scintillation efficiency, S, becomes the absolute normalization constant for the amount of light produced per unit energy loss. The number of scintillation photons that contribute to the measured output pulse, and thus the scintillation efficiency, S, will vary depending on the optical and physical properties of the system. Here the system can be defined as the scintillator material, reflective materials around the scintillator, and the PMT.

The number of photons that contribute to the output pulse depend on how well the photons are transported through the system from the initial scintillation location to the photocathode. The transport can be improved by reflecting the light at the boundaries of the scintillator not exposed to the photocathode where the escape of light is desirable. The reflection that will occur at the interface between two materials can be described as either specular or diffuse, where the dominant mode for most materials, such as plastics or metals is diffuse. If the material is glass or a highly polished metal then the reflection of light, in addition to being diffuse, will have a specular component. The difference between the two types of reflections is the angular dependence between the incident and reflected photon. Diffuse reflection is caused by surface roughness which causes the light to be reflected in random directions. This can be described by a statistical distribution, shown in Equation 3, known as Lamberts Law. In this equation the intensity of the reflected light will vary proportional to the scattering angle.

$$\frac{dI(\psi)}{dI_o} = \cos\psi \tag{3}$$

Both diffuse and specular reflection are highly dependent on the types of materials interfaced and can be described by a ratio of the two refraction indices. The refraction index is material specific and consists of a real and imaginary component, where the real part of the refractive index (n) is a measure of the reflectivity and the imaginary component, also called the extinction coefficient (κ), is a measure of the absorption. The one component that defines specular reflection is the critical angle, which can be derived from Snell's Law, as shown in Equation 4, where n_o is the refraction index of the scintillator and n_1 is the refraction index of the reflective material.

$$\theta_c = \sin^{-1}\frac{n_1}{n_o} \tag{4}$$

The critical angle defines the angle with the surface normal where 100% internal reflection will occur if the incident photon angle is greater than the critical angle, where the angle of reflection will be the same as the incident angle. Consequently, if the incident light interacts with the surface at an angle less than the critical angle only partial reflection will occur and the remaining light will be transmitted through the secondary surface. Knowing this relationship, an ideal reflector for a scintillator detector should have an index of refraction lower than the index of the scintillator at the interfaces where internal reflection is desirable.

Whether the reflection is specular or diffuse, reflectance is a measure of the incident photon flux that will be reflected. Reflectance depends on the polarization of the incident light, which is considered s-polarized if the electric field is normal to the transverse plane and p-polarized if the electric field is parallel to the transverse plane. The reflectance can be calculated for s-polarized light using equation 5a and equation 5b for p-polarized light. In these equations, the reflectance (R) relates the photon angle of incidence (θ_i) with the surface normal vector and the refraction indices of two adjacent materials where n_0 corresponds to the refraction index of the scintillator and n_1 corresponds to the refraction index of the reflecting material. 100% reflection will occur if the incident angle is

equivalent to the critical angle. Here the critical angle is equivalent to the inverse ratio of the refraction indices under the square root term which reduces the square root term to zero. Consequently, the reflectivity approaches zero as the refraction indices approach unity. For either case (s or p polarization) this is easy to see when the photon angle of incidence is normal to the surface ($\theta_i = 0$) as shown by equation 5c.

$$R_s = \left[\frac{\left(n_0 \cos\theta_i - n_1\sqrt{1-\left(\frac{n_0}{n_1} sin\theta_i\right)^2}\right)}{\left(n_0 \cos\theta_i + n_1\sqrt{1-\left(\frac{n_0}{n_1} sin\theta_i\right)^2}\right)}\right]^2 \qquad (5a)$$

$$R_p = \left[\frac{\left(n_0\sqrt{1-\left(\frac{n_0}{n_1} sin\theta_i\right)^2} - n_1 \cos\theta_i\right)}{\left(n_0\sqrt{1-\left(\frac{n_0}{n_1} sin\theta_i\right)^2} + n_1 \cos\theta_i\right)}\right]^2 \qquad (5b)$$

$$R = \left[\frac{(n_1 - n_0)}{(n_1 + n_0)}\right]^2 \qquad (5c)$$

The opposite of reflectance is transmittance, which by conservation of energy is the amount of light remaining after one reflection. If multiple reflections occur before the scintillation photon leaves the scintillator the remaining energy of a single photon can be approximated by Equation 6, where I_F represents the final intensity and can be written in terms of the transmittance and a power function based on the number of reflections, N, a photon will encounter before leaving the desired edge of the scintillator. A simple model and pictorial derivation of the number of reflections a single photon might encounter is shown in Figure 4. This assumes specular reflection where only internal reflection is considered at all reflecting boundaries and the angle of reflectance is equivalent to the angle of incidence. This is a simplified derivation to determine the parameters that will affect the photon transport. If a more detailed analysis is needed, this equation can be implemented for diffuse reflection, where the number of reflections would depend on the average value of the distribution from Lamberts Law.

$$I_f = I_o(1-R)^N, N = \frac{H}{z}, z = t\tan\theta \tag{6}$$

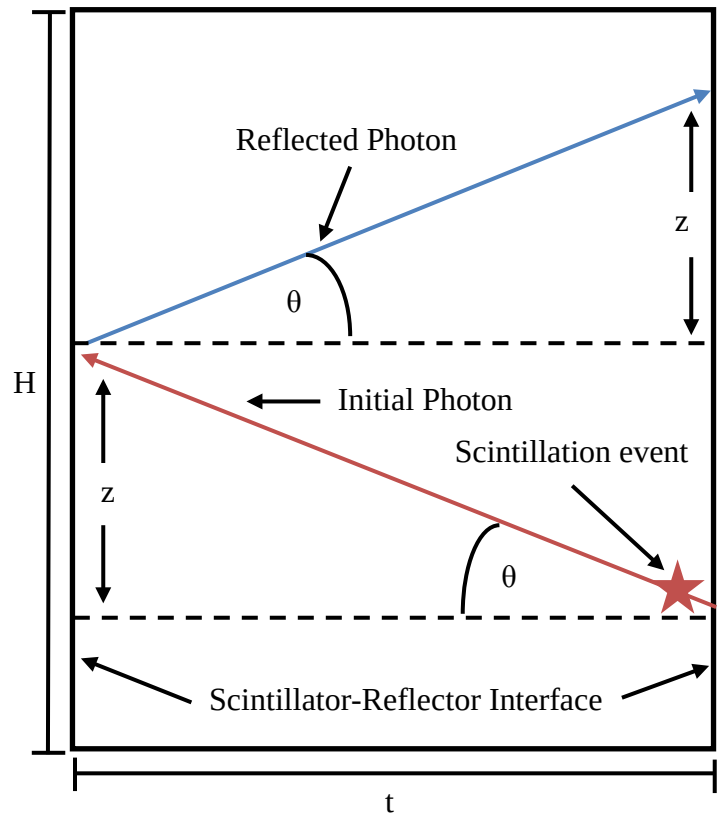

Figure 4 Model for photon scattering within a scintillator

In the event the photon remains within the scintillator there is still a chance the photon will be absorbed within the scintillation medium prior to escaping. The probability of a photon being absorbed in any material can be described by Equation 7, where λ is an energy dependent, material specific constant that describes the probability of absorption per unit path length of travel.

$$I = I_o e^{-\frac{x}{\lambda}} \tag{7}$$

The light that is not transmitted through the reflective boundary or lost to an absorption event will eventually be emitted through the edge of the scintillator viewed by the PMT. Here the light is collected at the photocathode and converted into photoelectrons. The quality of this process can be characterized by two parameters: a view factor and the

quantum efficiency. The view factor, in this case, is defined as the ratio of the photons incident on the photocathode to the number of photons emitted from the scintillator. Mathematically the view factor is a similar concept to what is used in radiative transport [25] to describe black body radiation and is defined in Equation 8.

$$f \equiv \frac{1}{A_1} \int \int \frac{cos\theta_1 cos\theta_2 dA_1 dA_2}{\pi r^2} \tag{8}$$

In this equation, θ is the angle between the surface normal vector and the vector, r, between the two surfaces. If isotropic light emission is assumed to be into a half sphere then the view factor becomes twice the solid angle subtended by the scintillator on the photocathode. If the photocathode is coupled directly to the edge of the scintillator then the view factor becomes one and the transport of light between interfaces is dictated by the reflectance parameters as described previously. To enhance the light transmission, the coupling material should be index matched with the scintillator.

The quantum efficiency is defined as the ratio of the number of photoelectrons ejected from the photocathode per incident photon. This efficiency can change across the face of the photocathode if the photon flux is non-uniform or the thickness of the photocathode varies across the surface. For this analysis the photon flux is considered isotropic and the photocathode is considered uniform. This assumption seems valid since there is a slight air gap between the PMT and the edge of the scintillator which promotes further dispersion of the visible light by scattering events with electrons in the air molecules. If the number of photons leaving the scintillator is large then this will naturally promote a more uniform coverage across the face of the photocathode.

Once the photoelectrons are created they are accelerated through a series of dynode stages where electron multiplication takes place. The electron multiplication starts with a single photoelectron from the photocathode being accelerated to the first dynode stage. At this stage additional electrons are ejected from the surface of the dynode given the energy of the initial electron is sufficient enough to overcome the electron binding energy of the dynode material. The electrons that are ejected are then accelerated to the next

dynode, where the process is repeated throughout each dynode stage. This process is a function of the detector bias, which is split between the dynode stages and provides the acceleration potential for the electrons. It is also a function of the electron affinity of the dynode material which is dominated by the binding energy of the orbital electrons within the dynode material. The total number of electrons collected at the anode is dominated statistically by the number of electrons created at the first dynode surface. Mathematically the entire electron multiplication process can be described by Equation 9 [23].

$$G = \alpha\delta^N \tag{9}$$

In this equation G is the overall gain of the PMT, α is the fraction of photoelectrons collected in the multiplication structure, δ is the ratio of emitted to incident photoelectrons at the first dynode, and N is the number of dynode stages in the multiplication chain. This equation is only valid if the overall gain of the PMT is a linear function of detector bias.

Previous Experimental Work

There are two types of experimental techniques commonly discussed in the literature to characterize scintillation detectors: the Compton Coincidence Technique (CCT) [12] and the Compton Edge Method (CEM) [22, 26, 27]. In CCT, the electron energy is inferred by exposing the scintillator to a collimated gamma source and measuring the kinematic relationship of scattered photon and electron pairs given by the Compton Scattering Formula shown in Equation 10. The recoil electron energy is calculated by measuring the photon scattering angle, θ, from an initial gamma ray of known energy, hν. This method requires a coincidence measurement between a calibrated photon detector, typically an HPGe detector at a known angle and location, and the scintillator detector of interest, where full energy deposition from the recoil electron is presumed.

$$T = h\upsilon \frac{1 - cos\theta}{\frac{mc^2}{h\nu} + 1 - cos\theta} \tag{10}$$

The CEM method is used to determine the response of the detector at the maximum obtainable energy (T_{max}) of a recoil electron from a collision with a gamma of known energy ($h\nu$) as shown in Equation 11. This equation can be found by solving Equation 10 for a scattering angle of 180° [28]. Experimentally in the CEM method this maximum energy corresponds to the channel location of the half-height of the Compton edge that can be determined from a differential spectrum. This method requires several known gamma sources of varying energies and some knowledge of the detector resolution.

$$T_{max} = \frac{2h\nu}{2 + \frac{mc^2}{h\nu}} \tag{11}$$

The most recent investigation was done by Pozzi et al.[18], where they developed a correlation for the relative pulse height in terms of MeV_{ee} (mega electron volt electron equivalent) which by definition is the amount of light produced from a 1 MeV electron. The Pozzi et al. correlation is shown in Equation 12, where R is the amount of light produced in MeV_{ee} and E_e is the kinetic energy of the electron in MeV.

$$R = 0.99E_e + .008 \tag{12}$$

The correlation from Pozzi is implemented in the MCNP-Pollimi code [27] to calculate the amount of light produced in MeV_{ee}. This correlation can be used to find the absolute magnitude of the light produced from a given energy deposition by multiplying R by the amount of light produced by a 1 MeV electron if that value is known.

3. Experimental Set-Up

Detector #1 Geometry

For this work, an existing cylindrical beryllium detector was adopted and is shown in Figure 5. The housing is a 3.18 mm thick steel tube with an inside diameter of 4.22 cm and a height of 11.90 cm. The inside of the housing was retrofitted with a polystyrene insert that was designed to accept a variation of rectangular geometries, where the geometry is defined as a slab of plastic scintillator sandwiched between two reflecting materials. The reflective materials that were chosen for this study are beryllium, polypropylene, and Mylar. The arrangements of these geometries within the detector are shown in Figure 6.

Figure 5 Re-purposed Beryllium Rod Detector Housing

The primary geometry of interest, which is representative of the BLC geometry, consists of alternating 30 x 65 mm layers of 3.18 mm thick beryllium metal (3 total) and 1.00 mm thick Bicron BC-404 plastic scintillator (4 total). Within the primary geometry (shown in the left image of Figure 6) are two distinct geometries that are symmetric with the axial center of the detector. The two inner scintillator layers have beryllium on both sides of the scintillator and the outermost scintillator layers are reflected with beryllium and a 1.00 mm white polypropylene layer. These two geometries, shown with a source in place, are labeled Cases 1 and 2 and are shown 2nd and 3rd from the left in Figure 6,

respectively. Case 1 and Case 2 are studied independently and then coupled to develop the response function for the primary BLC geometry. The other geometries studied are shown in the two right images of Figure 6. Case 3 has a slab of scintillator sandwiched between two 1.00 mm thick polypropylene layers and Case 4 has a slab of scintillator enclosed in an aluminized Mylar wrap.

The scintillator used for these experiments was 1.00 mm thick BC-404 from St. Gobain [8] and the equivalent from Eljen Technologies, EJ-204 [29] in thicknesses of 0.50 and 0.25 mm. Both these scintillators have negligible self-absorption with an attenuation length of 160 cm. The peak emission wavelength of 408 nm and a decay constant of only 1.9 ns (Appendix G) allows for high frequency counting that is required for pulsed neutron experiments, such as those conducted on the Z machine. The Hamamatsu R5946 PMT [30] is enclosed in the detector housing and is located above the scintillator in all cases by a 5.50 mm air gap. This PMT has a quantum efficiency of 23% at 390 nm and a maximum response at 420 ± 50 nm, which closely matches the peak wavelength emission of the scintillator. This PMT is also ideal for high frequency applications with short transit and rise times of 7.2 and 1.9 ns, respectively (Appendix H).

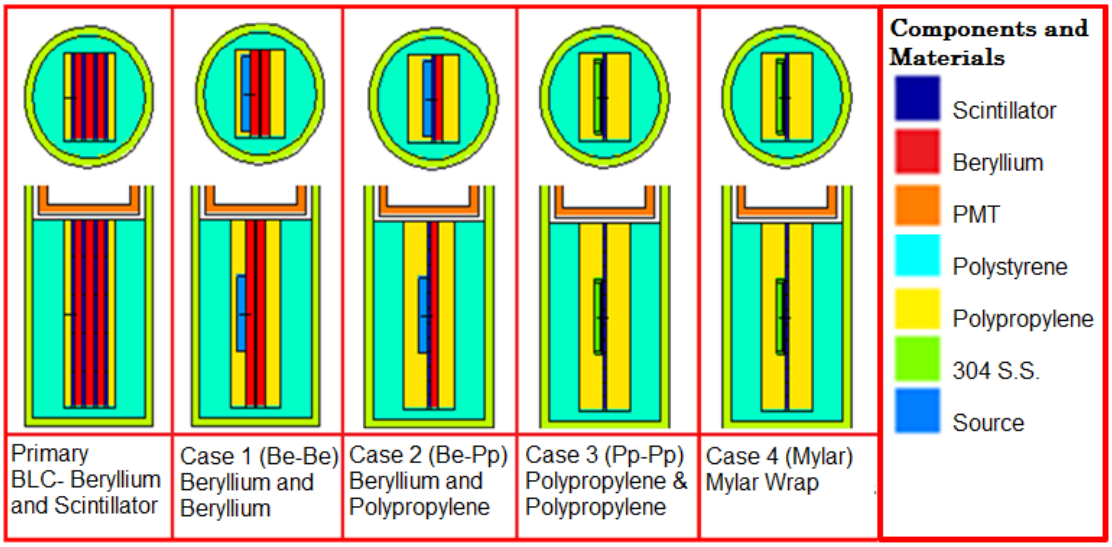

Figure 6 Detector # 1 Experimental Geometries, Radial View shown on top, Axial View shown on the bottom

Procedure

A slab of scintillator was placed between two reflective materials to form a “sandwich” arrangement. The “sandwich” was then wrapped with a poly vinyl chloride (PVC) tape to couple the scintillator to the reflective material as tightly as possible to minimize the air gaps and the loss of light through the vertical edges and the bottom of the scintillator. A source was placed in the source holder in one of three locations: centered on the face of the scintillator or as shown in Figure 7, 1.00 mm from either end. In the event that polypropylene was being used, the source could be placed directly on the scintillator. If the beryllium or Mylar was in use then the incident radiation would have to be attenuated by the reflecting material prior to reaching the scintillator. The sandwich configuration, with the source in place, was placed in the polystyrene insert in one of five locations: the axial center of the detector housing or 2, 4, 6, 8 mm off axis. The remaining space of the insert was filled in with polypropylene spacers to maintain the scintillator alignment with the PMT and then placed in the bottom of the detector housing as shown in the right image of Figure 7. The lower housing was then attached to the detector base and checked for light leaks. The detector was powered on and monitored for a minimum of 15 minutes prior to taking measurements to avoid measuring false-positive events that occur from dark current build-up on the photocathode.

Case 1 Geometry with PVC wrap and Sr-90 source in top location	Polystyrene Insert Placed in Housing	Insert Seated in Bottom Of Detector Housing

Figure 7 Preperation of experiment, Shown above is 1 mm scintillator with beryllium on either side and a Sr-90 source placed in the top location

Detector System Electronics

The electronic configuration used in the detection scheme is shown in Figure 8. The output signal of the detector was routed through a 5 Volt clipper circuit and then split to an Ortec 584 Constant Fraction Discriminator (CFD) and a Tektronix DPO 3032 digitizer. The positive TTL output signal of the 584 was processed with an Ortec Easy-MCS for fluctuation monitoring and the negative logic output pulse signal was processed through a Tennelec TC 536 counter/timer. For each source-geometry combination counts were first measured at a minimum CFD setting of 20 mV and then at 20 mV increments until the number of counts in a 300 second interval diminished to background.

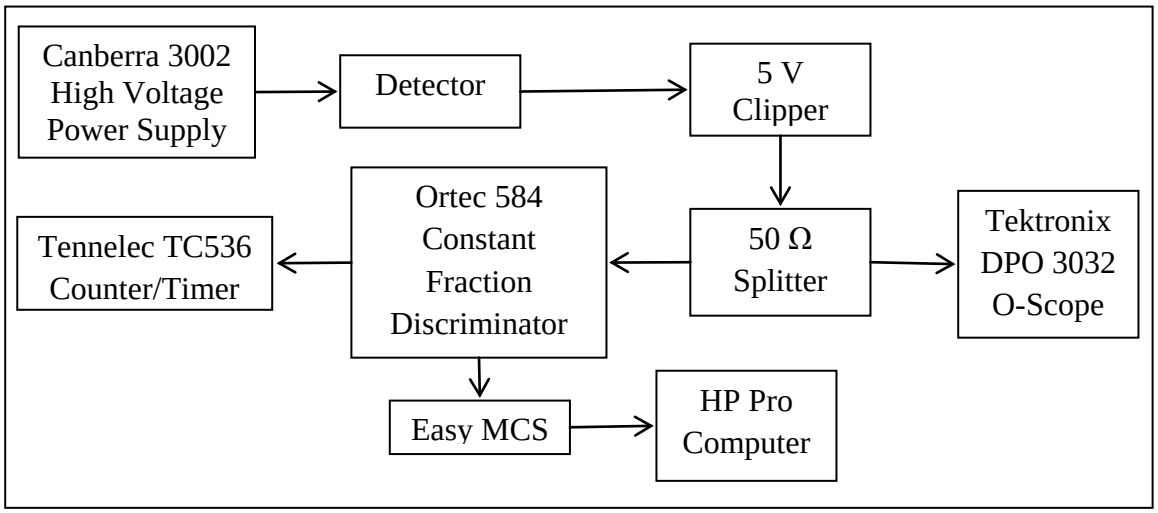

Figure 8 Electronic configuration used for data acquisition

Beta and Gamma Source Description

Data were collected with several NIST traceable beta and gamma sources for the geometries of interest. The isotopes used throughout were ^{60}Co, ^{36}Cl, ^{137}Cs, ^{210}Pb/^{210}Bi, ^{90}Sr/^{90}Y, and ^{22}Na. Each source has an accompanying data sheet (Appendix E) that specifies the calibration date, activity at time of calibration, calibration procedure, and specifics of the source geometry. In the event data were missing from the data sheet it was supplemented with data from Ref. 31. A summary of the source descriptions are

shown in Table I. These sources were chosen for their varying decay modes, energies of the decay particles, and source geometries.

Table I Summary of UNM NIST traceable sources

Source	Decay Mode(s)	Cal. Date	Activity (µCi)	Window	Backer
Cs-137	Beta Gamma	08/01/1969	1.35	1 mm plastic	1 mm plastic
Cl-36	Beta (98.1%)	11/21/1977	0.0209	0.90 mg/cm2 Mylar	0.25 mm S.S.
Co-60	Beta Gamma	08/01/2006	10.71	1 mm plastic	1 mm plastic
Na-22	Positron Gamma	08/01/2006	10.12	1 mm plastic	1 mm plastic
Pb-210/Bi-210	Beta Gamma	03/15/1994	0.01017	0.0254 mm Aluminum	0.254 mm S.S.
Sr-90/Y-90	Beta	03/15/1994	0.00993	0.90 mg/cm2 Mylar	0.25 mm S.S.

MCNP 5 model

For every experiment conducted, the specific geometry-source configuration used was modeled using the transport code MCNP5 [10]. Materials used in the model were of theoretical density and the compositions were obtained from the NIST database [32]. Since the material thicknesses used in the problem are very thin a special treatment for the electron transport was implemented [33]. This ensures that the electron ionization path is sampled at a minimum of 10 times for every region of interest. The beta and gamma source distributions are planar geometries and are equally distributed over 22.0 mm and 5.0 mm diameter circular regions, respectively. Discreet photon energies and branching ratios for each source were found in ref. 34 and the spectral data for the beta emitters were found in ref. 35. The beta spectra were modeled as a probability function that was continuous and linear between points. A summary of the energy and branching ratio for each source are shown in Table II for the gamma-ray emissions and Table III for the beta-particle emissions. The tabular data for each beta spectrum is shown in Appendix F. The implementation of the probability functions in MCNP5 for the spatial and energy dependence of the particle emissions can be seen in the sample input files shown in Appendix C.

Table II Source Photon Energies and Branching Ratios used in MCNP Models

Source	X-ray/Gamma Energy in keV (Branching Ratio, %)
Co-60	7.461 (.00322), 7.478 (.0063), 8.265 (.001151), 347.14 (.0075), 826.10 (.0076), 1173.228 (99.85) 1332.492 (99.9826), 2158.57 (.00120)
Cs-137	31.817 (1.99), 32.194 (3.64), 36.304 (0.348), 36.378 (0.672), 37.255 (0.213), 661.657 (85.1)
Na-22	511.0 (180.76), 1274.537 (99.941)
Pb-210/Bi210	10.8 (23.6), 46.539 (4.25)

Table III Source Particle Energies and Branching Ratios used in MCNP Models

Source	β^-,β^+, C.E. End-Point Energy in keV (Branching Ratio, %)
Co-60	β^-, 317.05 (99.88) β^-, 1490.29 (0.12)
Cl-36	β^-, 705.55 (98.1)
Cs-137	β^-, 513.97 (94.70) β^-, 1175.63 (5.30) C.E. 624.216 (7.79) 655.668 (1.402) 660.364 (0.300) 661.404 (0.0646) 661,637 (0.00965)
Na-22	β^+, 545.7 (90.326) β^+, 1820.3 (0.056)
Pb-210/Bi210	β^-, 17.0 (84) β^-, 63.5 (16) C.E. 30.1515 (60.3) 42.54 (14.28) **β^-, 1162.1 (100)**
Sr-90/Y-90	β^-, 546.0 (100) **β^-, 519.4 (0.011) β^-, 2280.1 (99.989)**

The output quantity calculated using an MCNP5 F8 pulse-height tally was the number of events that occur within user-defined energy bins. In this case, the energy bins were divided into 50 keV increments ranging from the MCNP5 threshold limit of 1 keV to a maximum energy that was source dependent. For these calculations there was no correction implemented for energy broadening due to the detector response. This implementation requires an experimental measurement of the FWHM of a specific energy deposition. Given the poor energy resolution of plastic scintillators and the inability to measure a single energy this correction was deemed unnecessary. A separate MCNP5 model was developed for each type of emission, e.g. beta or gamma. For each type of emission (beta or gamma) all decay modes with a branching ratio >0.001% were used to define discrete probabilities for each decay particle and energy. The total differential spectrum for each isotope was then found by taking the product of the result from the MNCP5 calculation and the total branching ratio for each type of emission and then summing the products over all possible emission types as shown in Equation 13.

$$N = T_\gamma Br_\gamma + T_\beta Br_\beta \tag{13}$$

In this equation T_γ and Br_γ are the results obtained from the MCNP calculation and the sum of all the gamma branching ratios, respectively. Similarly, T_β and Br_β is representative of the beta source calculations. The units that result from the MCNP calculation are in counts per source particle, and the branching ratio has units of particle per decay, thus the product of these two quantities gives the solution in units of counts per decay. For example, a ^{60}Co source was modeled separately as both a beta and gamma emitter for a given detector geometry. The gamma calculation for the ^{60}Co source used a discreet probability for the gamma ray energy where the probability for that energy emission was the corresponding branching ratio as shown in Table II. The result from that calculation was multiplied by the total gamma branching ratio, 1.996. Similarly, the beta model results were multiplied by a branching ratio of one. The sum of these two separate calculations gives the expected number of detectable events per a single decay. A plot of a typical result from an MCNP calculation is shown in Figure 9. The overall statistical uncertainty, typical for all MCNP calculations is on the order of 1 – 2 %.

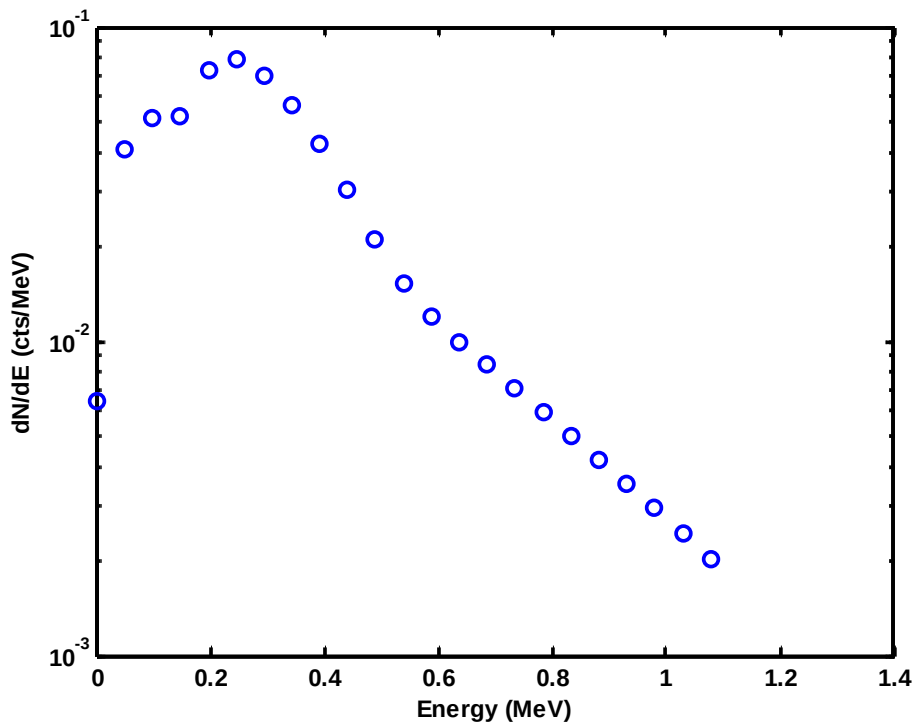

Figure 9 MCNP Calculated Total Differential Spectrum for a Sr-90 Source with 1 mm Scintillator and Polypropylene Reflective Material

4. Methodology

An integral spectrum was obtained by measuring the counts as a function of CFD setting for each experimental set-up. Here the counts measured at a given discriminator setting include all events that resulted in a pulse larger than the discriminator value. Background counts were subtracted from the total counts to obtain the number of net events, which were normalized to the decay corrected source activity using Equation 14. In this equation (C - B) is the net count rate, A_o is the initial source activity in becquerels, λ is the decay constant in inverse years, and t is the elapsed time in years since the calibration date. An example of an experimentally obtained integral spectrum is shown in Figure 10.

$$\frac{(C - B)}{A_o e^{-\lambda t}} \tag{14}$$

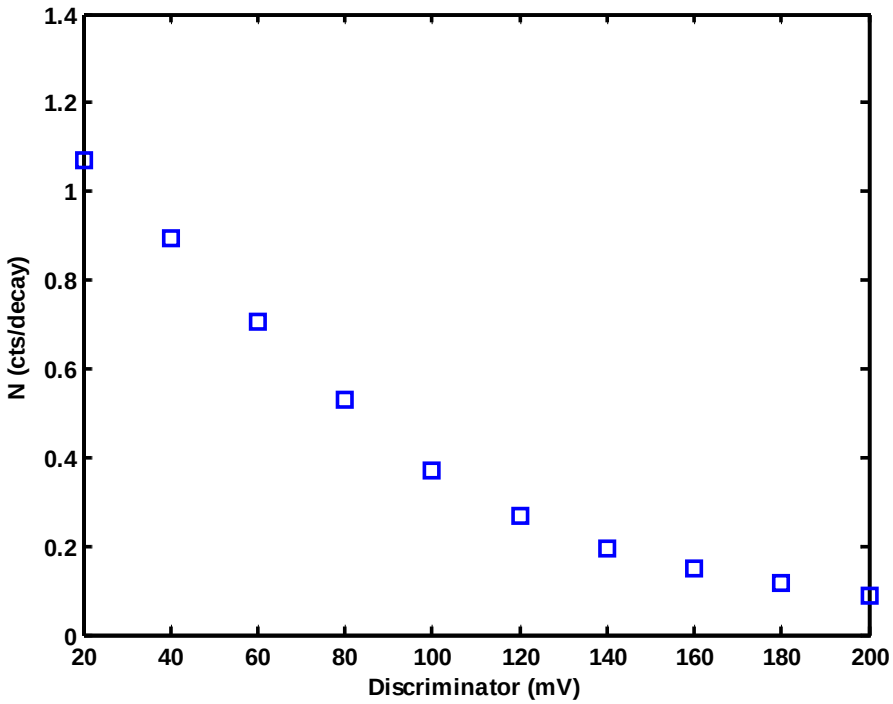

Figure 10 Experimental Total Integral Spectrum for a Sr-90 Source with 1 mm Scintillator and Polypropylene Reflective Material

This type of curve was deemed more appropriate for this analysis instead of the more commonly used differential curve for several reasons. First, the integral curve is a smooth, continually decreasing function that can be easily normalized or interpolated.

Differential curves are dependent on the energy resolution of the scintillation material and the features of the spectrum can change with the choice of energy bin width in MCNP5, which makes normalization difficult. For these reasons the MCNP results were also converted into integral form to allow for direct comparison to the experimental results. Since the values of the differential spectrum are discrete the integral spectrum was obtained by summation. The count rate was summed over all the events that occurred above the lower limit of each energy bin. An example of an integrated MCNP result is shown in Figure 11.

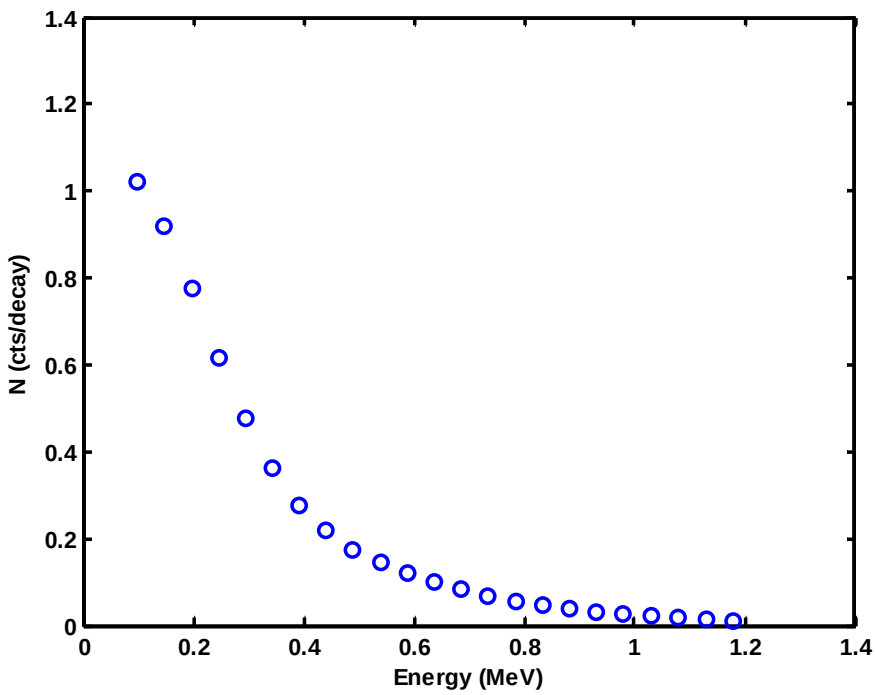

Figure 11 MCNP Total Integral Spectrum, for a Sr-90 Source with 1 mm Scintillator and Polypropylene Reflective Material

The independent variable for both the experimental function and the MCNP calculated function are the same (counts/decay), therefore, the dependent variable for one function can be solved in terms of the other. Since the shapes of the curves are unique, a point-wise interpolation method was used to obtain a discrete energy deposition value for each CFD threshold level at every experimental data point that was bounded by two MCNP calculated values. Mathematically this can be described by a simple interpolation function as shown in Equation 15.

$$E(\varepsilon) = \frac{(\varepsilon - \varepsilon_a)}{(\varepsilon_b - \varepsilon_a)} * \left(E(\varepsilon_b) - E(\varepsilon_a)\right) + E(\varepsilon_a) \tag{15}$$

In this formula, ε is the calculated experimental efficiency for a given CFD setting that is bounded by efficiencies obtained from MCNP calculations, ε, with a and b subscripts. E is the energy at which the corresponding MCNP efficiency was calculated, and E(ε) is the calculated energy that corresponds to the experimental efficiency obtained at that CFD setting. Thus, the interpolated value and the discriminator setting can be viewed as a set of discrete points that can be used to determine an analytical expression for the expected discriminator value as a function of energy deposition for a specific detector configuration. Doing this analysis for several configurations allows the user to see how the light yield changes as a function of a detector specific parameter. This method is similar to the CEM method except the whole range of data is used instead of just the Compton Edges. An example of the correlation developed using the results from Figures 10 and 11 are shown in Figure 12. For comparison, the relationship developed by Pozzi et al [18] using the CEM method is also shown.

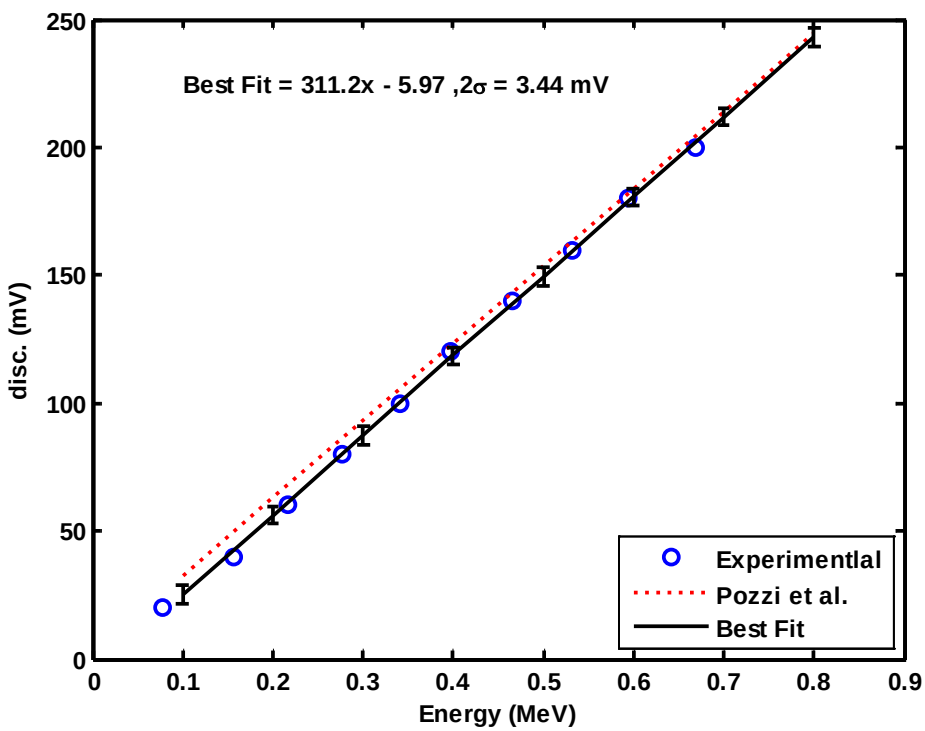

Figure 12 Energy Deposition vs Pulse Height for a Sr-90 Source with 1 mm Scintillator and Polypropylene Reflective Material, Comparison to Previous Work Shown

In the Pozzi et al. correlation it is important to note that the threshold value, the intercept, is always 0.80% of the light produced from a 1 MeV electron, which in this case corresponds to an intercept value of 3 mV. The largest error associated with this linear fit is the value of the intercept at ± 20 % at the 68% confidence interval. Statistically this places the correlation from this work in good agreement with the Pozzi et al. correlation. The error bars shown in Figure 12 are at the 2 sigma confidence interval (95%) and correspond to twice the standard deviation from a weighted linear regression fit, where the weights are determined by propagating the statistical uncertainty in both the experimental and calculated data. A weighted fit was deemed more appropriate than a standard linear regression since the propagation of statistical uncertainty does vary slightly point by point and can be accounted for using this type of analysis. Systematic uncertainty is not included in this figure, but is discussed in the next section.

5. Statistical and Systematic Uncertainties

Statistical uncertainties for this analysis are present in the independent variable (counts per decay) in both the experimental and calculated data. The experimental statistical uncertainty is typically less than 3%, while the MCNP statistical uncertainty in most cases is 1 – 2 %. Since the relationship of the experimental and calculated quantities depend on the uncertainty associated with the dependent variable (CFD setting and the energy deposition) the statistical uncertainties in the count rate have to be converted. The uncertainties in the count rates can be converted to uncertainties in both the CFD setting and the energy deposited values rather easily if the data is assumed linear between points. If the relationship is assumed linear between points the error in the x value corresponds to the inverse slope multiplied by the uncertainty in the y-direction as given by Equation 16. This of course requires the uncertainty in the y-direction be bounded by two values.

$$\frac{\Delta y}{\Delta x} = slope, \Delta x = \frac{\Delta y}{slope}, \sigma_x = \sigma_y \frac{(x_2 - x_1)}{(y_2 - y_1)} \tag{16}$$

Propagating these uncertainties through the interpolation scheme results in a relative uncertainty on the order of 3-4%, where the propagation is dominated by the uncertainties in the experimental data. In addition to the statistical uncertainties, there are also systematic uncertainties associated with each experiment-calculation pair.

There are several geometric factors within the detector set-up that can vary. An approximation to the magnitude of the systematic uncertainty can be found by adjusting the MCNP model to reflect the unknowns in the detector set-up. Source knowledge and two geometric factors were considered. They include a distributed versus point source, attenuating material thickness and scintillator thickness. To determine how much each factor contributed to the answer, models were run with the expected geometric or source change that is the departure from the ideal case and compared to the same set of experimental data. The resulting changes in the correlation for each case were then compared. For consistency, the uncertainty analysis was done for the same data set as shown in Figures 10-12. The set-up includes a ^{90}Sr source centered, in the Case 3 (poly-poly) geometry with the scintillator centered axially. The first model parameter varied

changed the source from an equally distributed source to a point source. The second analysis increased the window thickness on the source by a factor of two. The third and fourth cases increased and decreased the scintillator thickness by 10%, which is the uncertainty quoted by the manufacturer (Appendix G). The departure from the ideal case is shown in the residual plot shown in Figure 13 for each parameter varied. Clearly, the uncertainty is dominated by the uncertainty in the scintillator thickness. To encapsulate all of these uncertainties at once a total standard deviation of 15 mV was calculated. It is important to note that the calculated standard deviation of 15 mV is only relevant for this set-up. To determine the relative value that will be globally applicable, this value was divided by the calculated slope for this data set shown in Figure 12, which gives a relative uncertainty of 5%. This value will be used to represent the uncertainty associated with the detector geometry.

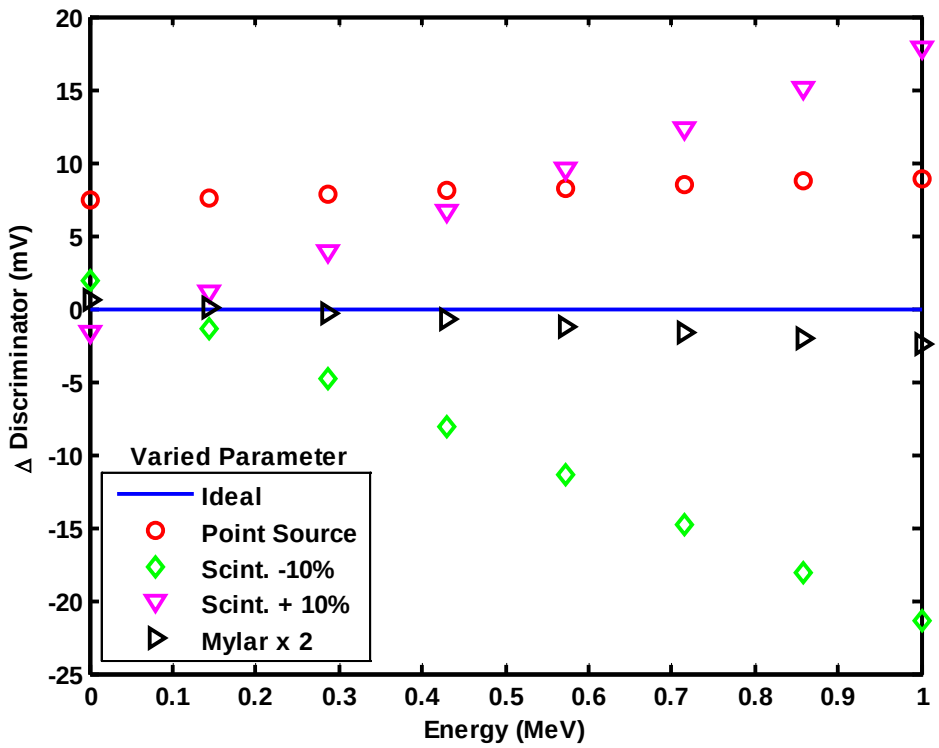

Figure 13 Residual Plot of Geometry and Source Knowledge Systematic Uncertainty

Other forms of systematic error that were included in this analysis are associated with the electronics used in the detection scheme. To see the effect on the outcome of the data

from changes in the bias supply a counting plateau experiment was conducted to investigate the change in count rate as a function of bias setting. In the linear region that is expected with such a plateau, the count rate changed by 1 count per second per 10 Volts. This contribution can be neglected at the frequencies encountered in these experiments. The largest source of uncertainty associated with the electronics is from the Ortec 584 module, which quotes an uncertainty of less than ± 5% in reflections with a 50 Ω termination. The reflections contribute to the measuring of false-positives. Thus, the count rate will have, in addition to the statistical uncertainty, a ± 5% contribution from the Ortec 584 module. Another component is the CFD dial setting, which is ± 2 mV. Since the mean CFD setting for most of these experiments is ~100 mV the average contribution from the discriminator setting would be ± 2%. Adding in quadrature the uncertainty contributions from the detector configuration, cable reflections and the dial setting results in a total systematic uncertainty of 8%. For the subsequent results sections the systematic uncertainty is not included in the parameterization study. This is a constant uncertainty throughout all the data and the main goal of the parameterization is to show the relationship in the data, therefore the following data only includes error bars that show twice the standard deviation (95% Confidence Interval) of the curve fit. The total uncertainty (systematic and statistical) will be included only in the final correlation and in all applications of the final correlation.

6. Detector #1 Results

Method Proof of Concept

For a method-proof of concept a series of four experiments, each with a different source, were conducted to see if the results using the established methodology could be duplicated. The sources chosen for these experiments (^{60}Co, ^{90}Sr, ^{210}Pb, and ^{36}Cl) each have unique decay modes, geometries, and a wide range of energy distributions associated with each emission. For each experiment the source was placed in the source holder at the central location adjacent to the face of the 1 mm scintillator and then placed in the axial center of the detector housing. Data was taken for each source at a detector bias of -2.0 kV and the discriminator setting was varied in 20 mV increments. The results after resolving the data using the established methodology are shown in Figure 14.

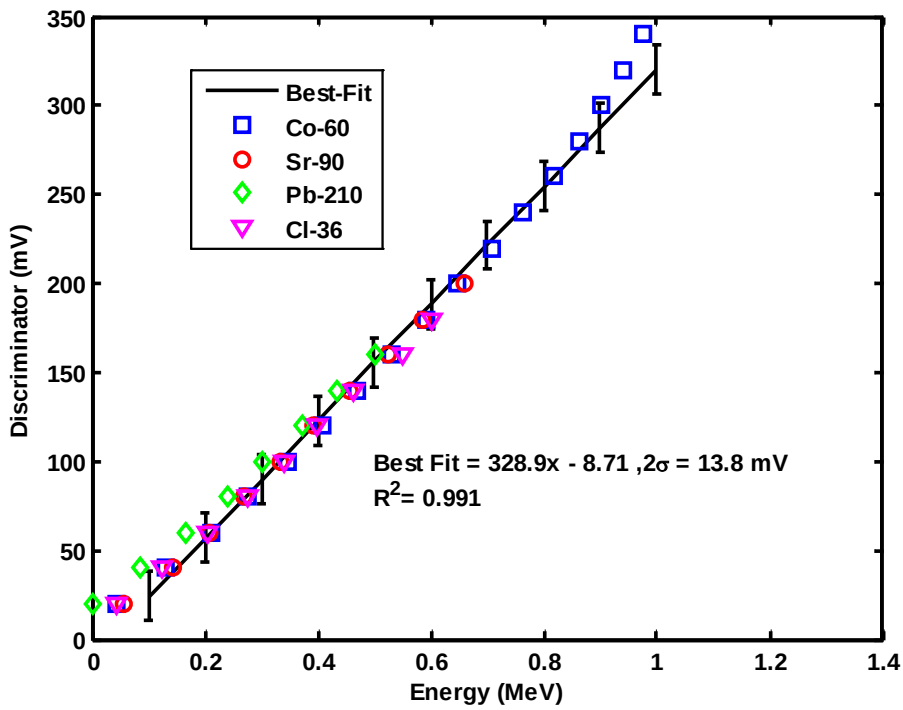

Figure 14 Correlation for Pp-Pp geometry, 4 sources, 1mm Scintillator

By visual inspection the four different data sets are in very good agreement with one another as shown by the linear determination coefficient (R^2) and the ratio of the standard deviation to the slope at the 95% confidence interval of only 4%. There are two

interesting features that can be seen in this graph. First, the correlation for the ^{60}Co experiment, shown using blue squares tends to deviate from linear around 920 keV. This is in good agreement with the expected departure at the first ^{60}Co Compton Edge energy of 962 keV. Second, the response curves for each experiment deviate from linear at ~100 keV. This tends to agree with previous work, where the deviation of the response for electrons in organic scintillators was measured at 125 keV [22]. The Pozzi et al. correlation extends to a much lower threshold of 8.1 keV. These experiments were repeated for Case 1 (beryllium-beryllium) with a ^{60}Co, ^{22}Na, and ^{137}Cs source and also for Case 2 (beryllium-polypropylene) with a ^{60}Co, ^{36}Cl, and ^{90}Sr source. The results are shown in Appendix A.

De-convolution of the Response Function

It has been shown in the previous section that for a specific geometry-scintillator arrangement the detector response function can be consistently obtained regardless of the source geometry or decay energies used. Since good agreement was obtained a parametric study of what parameters impact the light yield, and thus the detector response was undertaken. Several experiments were conducted with a specific parameter varied to develop an overall response function that is a product of parameter specific constants. The parameters investigated were the detector bias, reflective material, scintillator size, the location of scintillation events, and the solid angle subtended on the PMT by the scintillator.

The first parameter varied was the detector bias. The bias determines the acceleration potential across each dynode stage in the PMT. Thus, changing the electron multiplication dynamic directly varies the amount of current collected at the anode. For this set of measurements the detector bias was varied from -1.8 kV to -2.3 kV in 0.1 kV increments. A ^{36}Cl source was placed in the central location of the Case 3 (poly-poly) geometry and placed in the axial center of the detector housing. The experimental results for each bias setting are shown in a semi-log plot in Figure 15. From this figure it is obvious that much higher CFD settings are obtainable as the magnitude of the detector bias is increased. Since the source configuration and the detector geometry did not change, the energy deposition should be constant. Thus, the increase in CFD setting

should only be a function of the detector bias. The data was processed using the established methodology and is shown in Figure 16. An analytical expression was found by plotting the calculated slope of the response from each data set shown in Figure 16 to the corresponding detector bias setting. The unit for the slope is mV/MeV and is representative of the gain of the PMT. The empirical expression shown in Figure 17 is in good agreement with the expected analytical form shown in Equation 8.

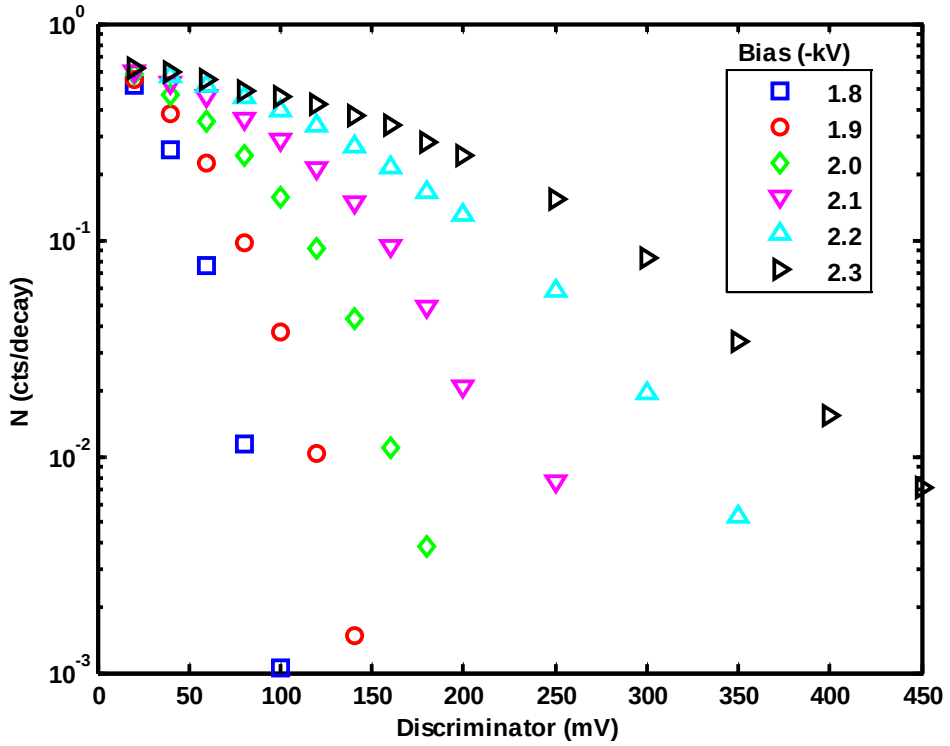

Figure 15 Experimental Data Taken at -1.8kV to -2.3kV

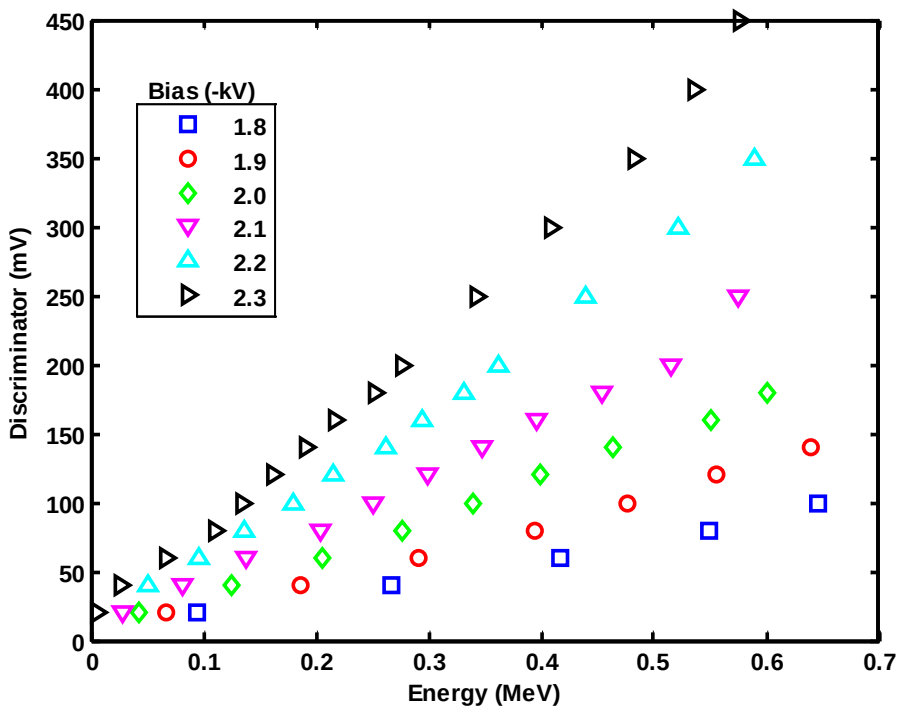

Figure 16 CFD Setting-Energy Deposition Correlations for Cl-36 as a Function of Detector Bias

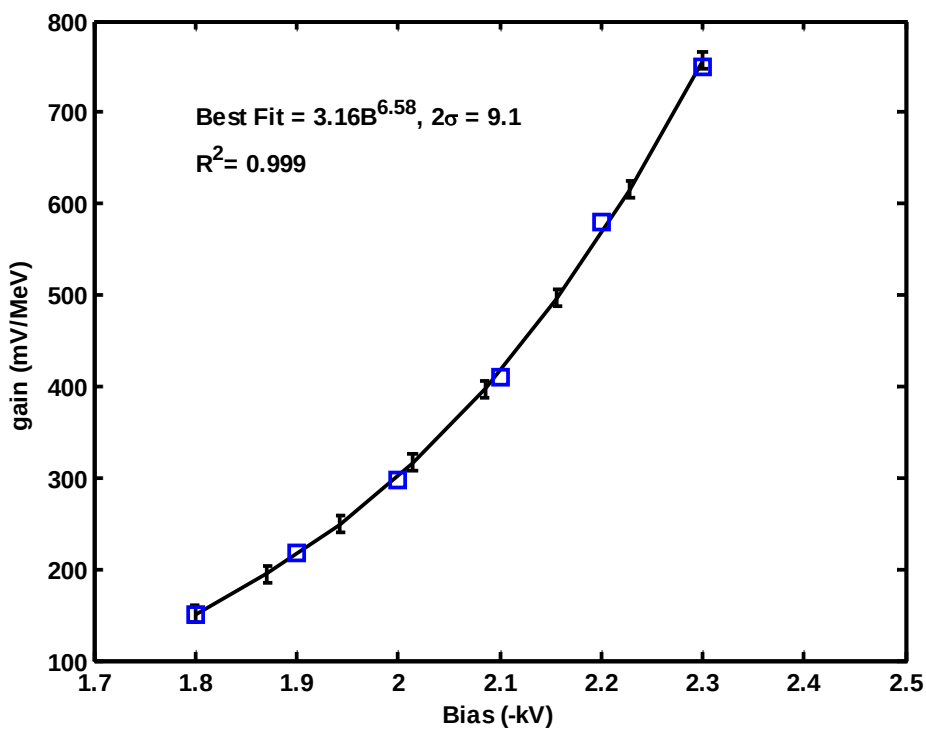

Figure 17 Calculated Detector Response vs. Detector Bias, Empirical Equation Shown

The second parameter varied was the reflective material surrounding the scintillator. As a reminder, the geometries considered are Case 1 - the beryllium reflected geometry, Case 2 - the combination of beryllium and polypropylene, Case 3 - the polypropylene and Case 4 - the Mylar. For this parameterization the data from the proof of concept was used in addition to one more data set using the Case 4 geometry. The values of the response function slopes found for each geometry (units of mV/MeV) were 95, 207, 329, and 322, respectively. The refraction index for each case, for an average wavelength of 420 nm, are 2.96 [36], 2.33, 1.70 [37], and 1.67 [38], respectively. For the Case 2 geometry the index of refraction was calculated as an average to reflect the combination of reflective materials. This assumes that scintillation light is isotropic upon creation and thus an equal contribution from each material. The response function slopes obtained from each reflective geometry were plotted as a function of refraction index. The empirical relationship shown in Figure 18 is linear with a decreasing slope.

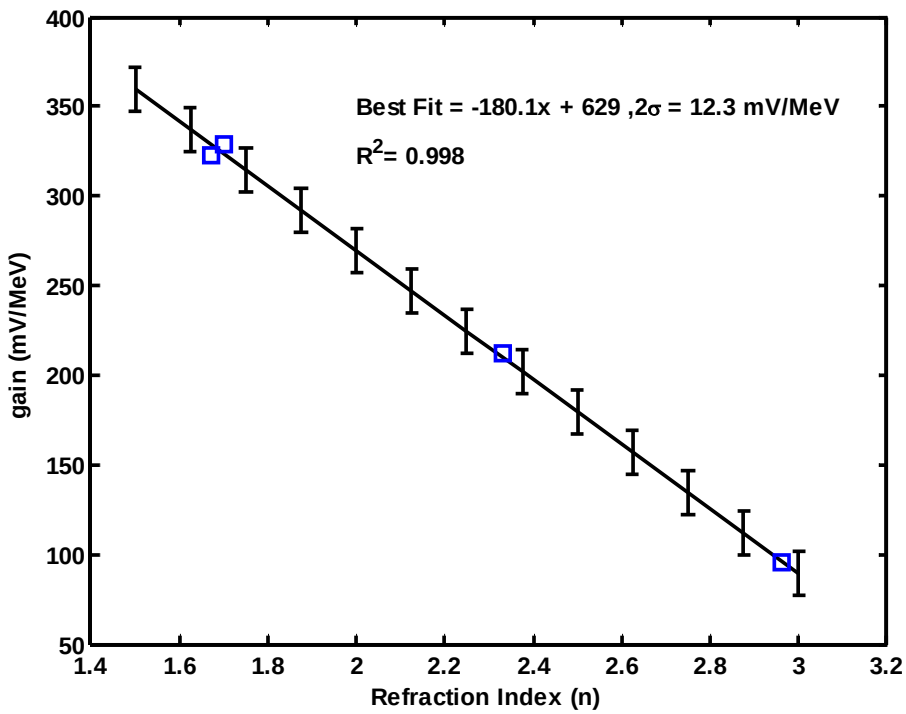

Figure 18 Calculated Detector Response vs. Reflective Material Refraction Index, Empirical Equation Shown

This is an expected result since reflectance losses are expected to increase with an increase in the refraction index as given by the relationship shown previously in Equation

6. For this analysis the reflectivity of the edge wrapping material was neglected since the ratio of the edge thickness to the face width is 0.03.

The next parameterization was the effect of scintillator size on the reflectivity relationship. The thicknesses of scintillator used in addition to the 1.00 mm were 0.50 and 0.25 mm thick. Data were taken for each scintillator size using the Case 1 (poly-poly) and Case 3 (beryllium-beryllium) geometries. For consistency, a ^{60}Co source was used for the Case 1 geometry and a ^{90}Sr source was used for Case 3. The data were taken at different bias settings: -2.0 kV for the Case 1 geometry and -2.3 kV for the Case 3 geometry. The magnitude of the detector bias had to be increased for Case 3 to get meaningful data to compensate for the thinner scintillator. In both set-ups the source was placed in the central location and the scintillator was placed in the axial center of the detector housing. The response functions for each of the three sizes are shown for both geometries in Figure 19.

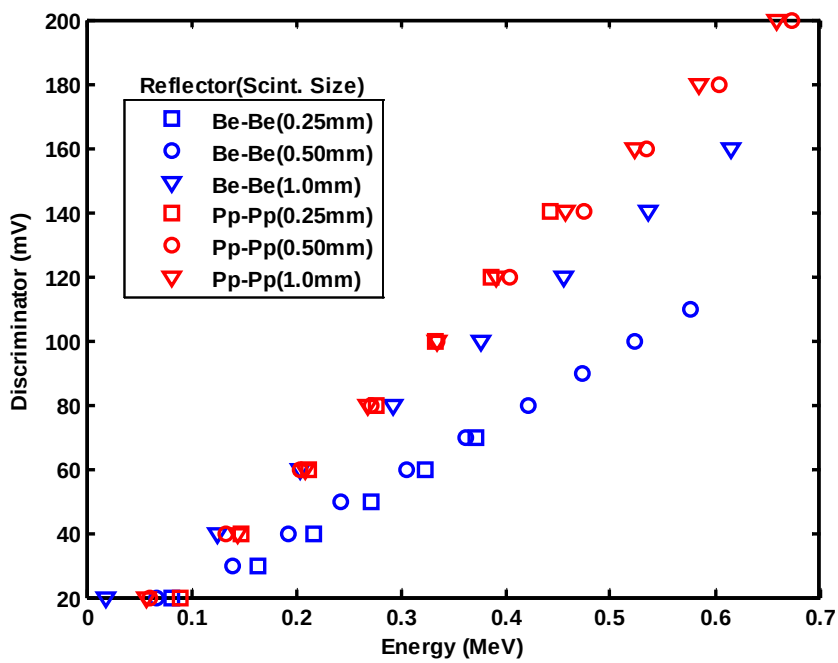

Figure 19 CFD setting vs. Energy Deposition for the Case 1 and Case 3 geometries with the 0.25, 0.50, and 1.0 mm scintillator (-2.0 kV bias used for Case 3 and -2.3 kV bias used for Case 1)

As a consequence of the light yield being proportional to the energy deposition and independent of the path-length (Equation 2), which is indicative of the scintillator

thickness, the light yield curve was expected to be constant regardless of the scintillator size. However, from Figure 19, it is apparent for the Case 1 (beryllium-beryllium) geometry there was a significant change in the detector response when the scintillator size was reduced, but there is no apparent effect seen for the Case 3 (poly-poly) geometry. This is directly related to the losses due to multiple reflections, where the expected loss from one reflection for the Case 1 geometry is ~10% greater than that for the Case 3 geometry. In Equation 6 the number of reflections is inversely related to the scintillator thickness, therefore more reflections occur within a thinner scintillator. Since the reflectance losses are negligible for the Case 1 geometry the relationship is not seen until a material with a higher refractive index is used where the losses are no longer negligible.

Equation 17 was used to derive the analytical expression for the value of the exponent shown in Figure 19. In this equation F represents the exponent, R is the beryllium reflectance coefficient, x is the scintillator thickness, and the slope corresponds to each individual response function for the Case 3 geometry that is dependent upon the scintillator thickness. The values of the slopes for each of the three scintillator sizes were normalized to a bias setting of -2.0 kV and the correlation relating the detector response to refractive index was factored out using n = 2.96 (Equation from Figure 18).

$$F = \frac{\ln\left[\frac{slope(x)}{(629 - 180n)}\left(\frac{2^{6.58}}{2.3^{6.58}}\right)\right]}{\ln(R)} \tag{17}$$

The expression that provides the relationship for the reflectance exponent can be found by plotting the value, F, as a function of the scintillator thickness, x. From Figure 20 it can be seen that the exponent varies as a logarithmic function of the scintillator thickness, x. If Equation 6 is integrated as a function of scintillator thickness to determine the total number of reflections a logarithmic dependence is found, which agrees with the empirical result presented here.

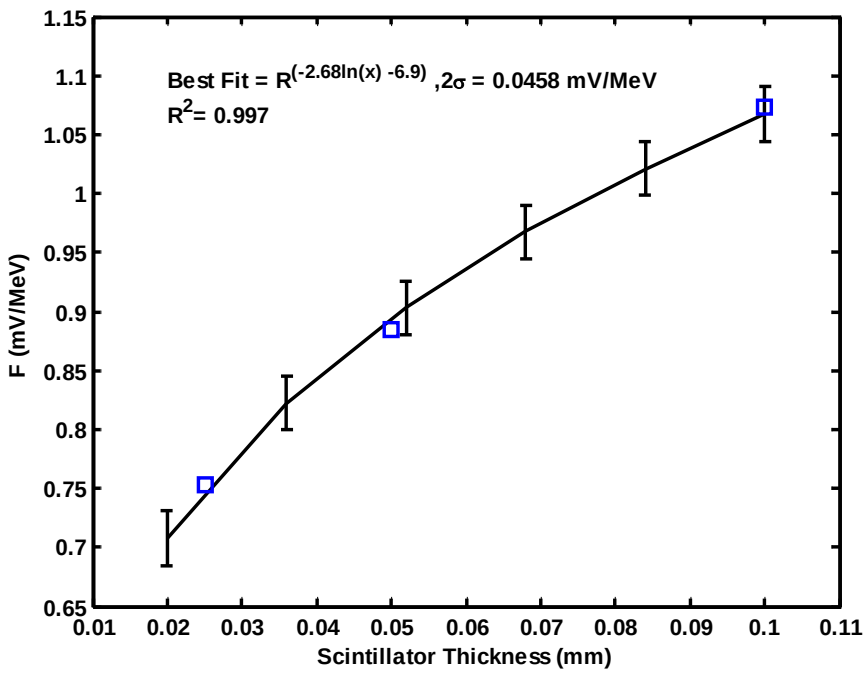

Figure 20 Calculated Detector Response vs. Scintillator Thickness, Empirical Relationship Shown

To further characterize the detector response function several more data sets were taken that utilized multiple source locations, reflective materials, and scintillator thicknesses. Three sets of data were taken for each of the geometries with the source located in the top, central and bottom locations using the 1.0 mm scintillator. Measured from the top of the scintillator to the center of the source these dimensions are 1.37, 3.25, and 5.13 cm. Since meaningful results were hard to obtain with the thinner scintillator in the Case 1 geometry, data were taken with the thinner scintillator using only the Case 3, polypropylene geometry. A ^{90}Sr source was used for Cases 2, 3 and 4, and a ^{60}Co source was used for the Case 1 beryllium geometry. In each experiment the bias was kept constant at -2.0 kV and the scintillator was placed in the axial center of the detector housing.

Using the same methodology the data were resolved into response functions for each geometry and source location. The resolved data for the Case 3 (poly-poly) geometry are shown in Figure 21. Four curves are shown, one for each source location and another that shows a correlation that corresponds to a point-wise average. For this parameterization an average would be a better mathematical choice since the uncertainty

in the location of the scintillation event is not well known. The uncertainty is dominated by the source spatial distribution to scintillator size ratio, which is approximately 1/3.

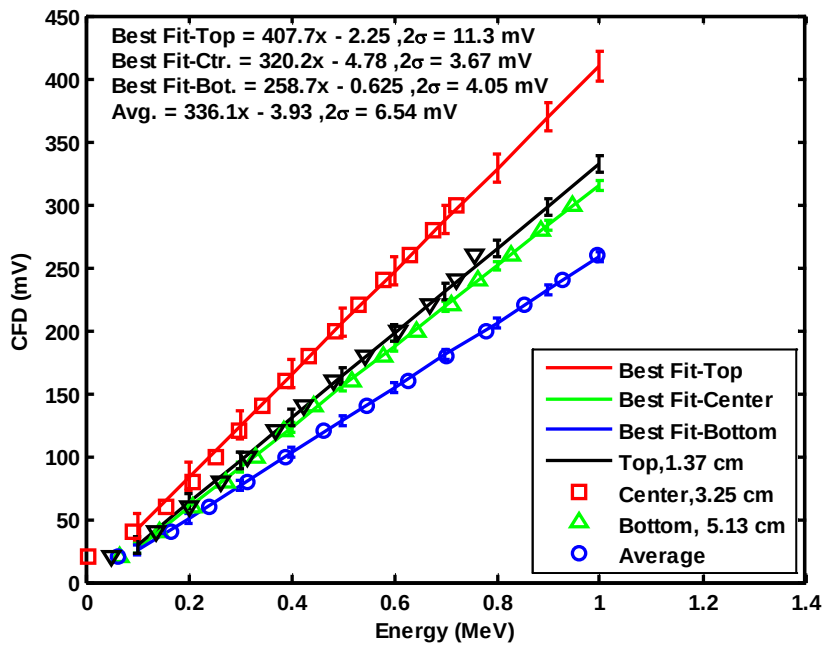

Figure 21 CFD Setting vs. Energy Deposition as a Function of Three Different Source Locations, Calculations Shown are for a Sr-90 Source with 1 mm Scintillator and Mylar

However, for completeness an analytical solution was sought by plotting the slope of the correlation from each geometry-source configuration as a function of the corresponding source location, which in this case is taken to be the center of the source. Of course, a more appropriate analytical solution can be found if a collimated source or a larger scintillator is used.

To compare all the data sets as a whole the value of the slope at each source location was normalized for the material and reflectance dependencies using the relationships shown in Figures 18 and 19, respectively. The expected analytical expression would be exponential if the dominant loss mode is the absorption of the scintillation photons within the scintillator and it is independent of the reflecting material. This was the relationship assumed and is shown in Figure 22, where the normalized data and exponential fit are shown. As expected, the error bars are rather large for this relationship given the uncertainty of the location of the scintillation event. Also of interest, there is no apparent pattern based on scintillator size or reflective material. This justifies the assumption that

the reflectance and absorption losses can be calculated independently. If the detector is presumably uniformly irradiated and the location of the scintillation events is neglected then the average value could be used. If the equation shown in Figure 22 (y = $1.52e^{-0.136Z}$) is normalized, the average value (y) from this fit would be 0.67 and correspond to a source location just above the center of the scintillator at 3.0 cm.

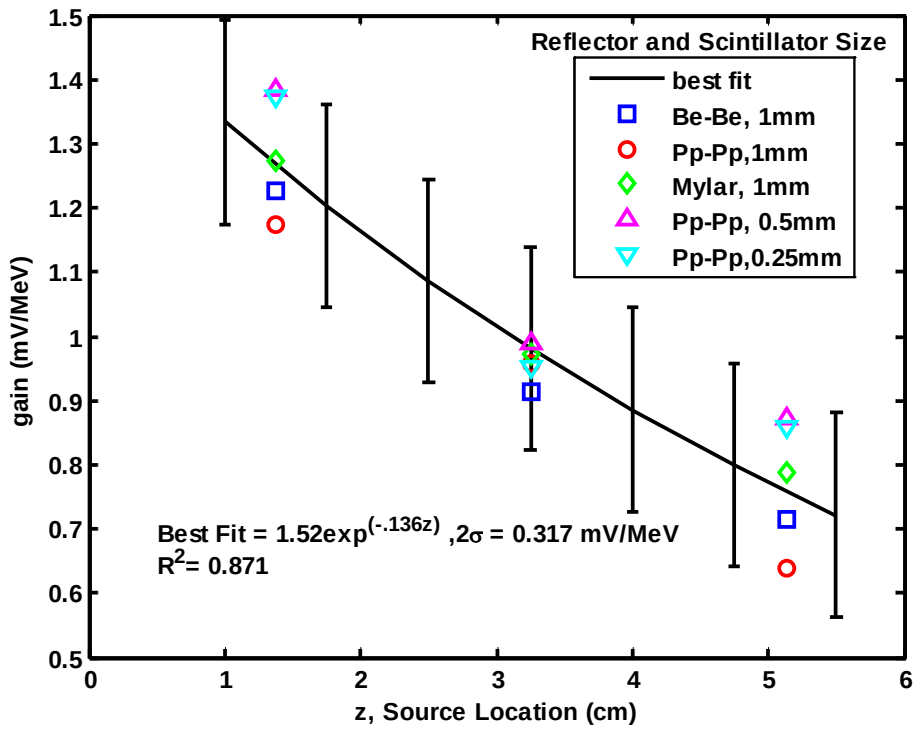

Figure 22 Calculated Detector Response vs. Source Location as a Function of Reflective Material and Scintillator Size, Empirical Relationship Shown

The last parameter varied was the view factor, which directly affects the amount light incident on the photocathode as seen in the correlations by Schonfelder [21] and Kuijper [20]. The view factor is a geometric relationship that describes how the scintillator is viewed by the PMT. In this case it can be defined as the ratio of light incident on the PMT versus the light emitted from the scintillator. To confirm their findings, data were taken using the Case 3 (poly-poly) geometry with a ^{60}Co source centered on the scintillator, at five scintillator positions: on axis and 2, 4, 6, and 8 mm off-axis. The results from the five data sets are shown in Figure 23.

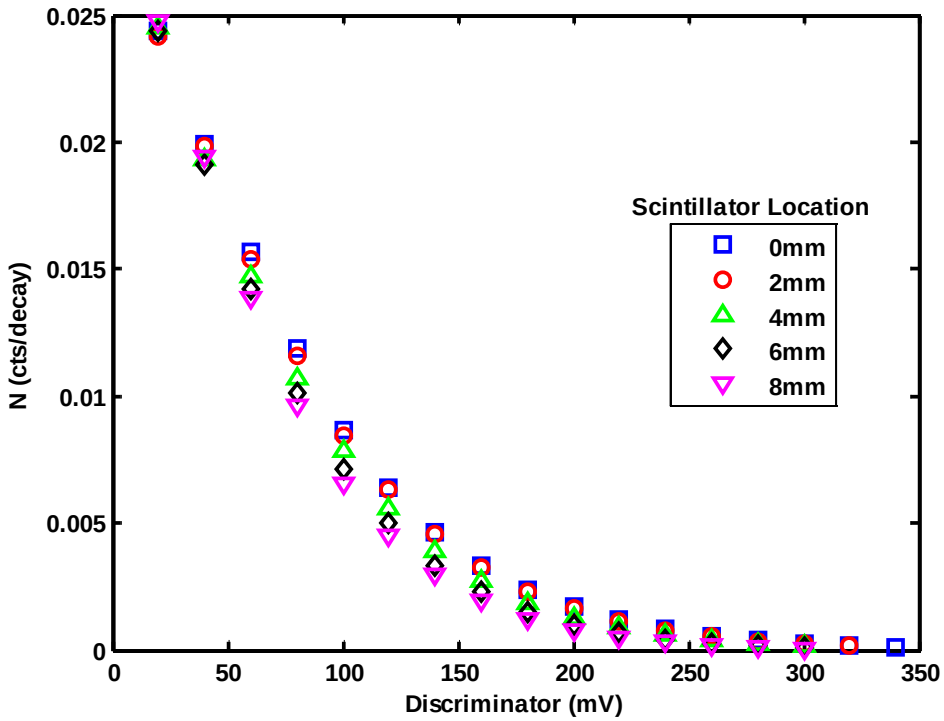

Figure 23 View Factor Experimental Data, Co-60 source in Case 3 Geometry

Assuming isotropic emission of light into a half sphere from the top edge of the scintillator, the corresponding view factors were calculated to be 0.503, 0.500, 0.478, 0.447, and 0.398 with an uncertainty at the one sigma level of 3%. This error includes a systematic component corresponding to the error associated with the scintillator placement with respect to the PMT. These view factors were calculated by solving Equation 7 with Monte Carlo calculations since the integral equation that dictates the view factor cannot be solved analytically very easily for the geometries used. For the Monte Carlo calculation photons are uniformly distributed across a cross-sectional area that is representative of the top of the scintillator. These photons are then transported in vacuum to a circular area that is representative of the photocathode surface. The number of photons that cross this surface is the expected value for the view factor. The use of the Monte Carlo method was verified by comparing Monte Carlo solutions to analytical solutions for simple planar geometries [25]. The two methods used to calculate the solutions agreed to the fourth decimal place. For comparison the data from Figure 23 is plotted in Figure 24 with the discriminator setting divided by the view factor, Ω. As can

be seen, the five data sets converge to one uniform set when the view factor is accounted for, thus confirming the findings of Schonfelder and Kuijper.

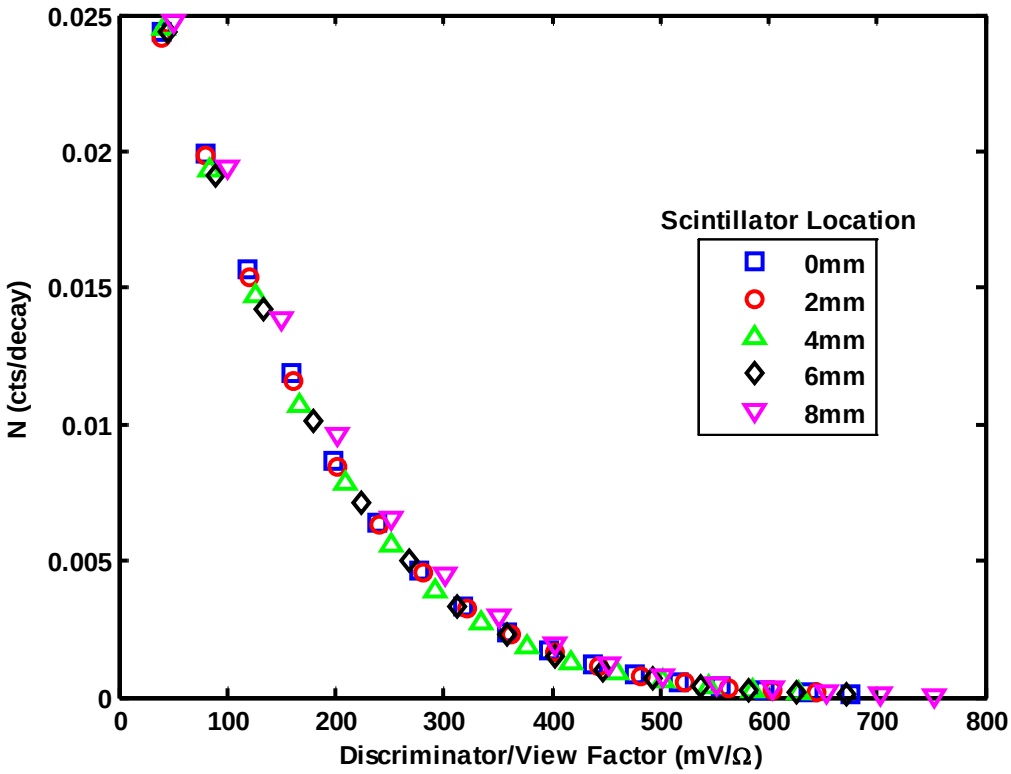

Figure 24 Experimental Data Taken with Co-60 in the Case 3 Geometry with the Inclusion of the View Factor

The final correlation can now be described empirically by factoring out the dependence of each parameter over the entire suite of experimental data. This provides a correlation between constant fraction discriminator setting and the energy deposited as a function of the detector bias, the reflective material, the scintillator thickness, location of the scintillating event, the amount of light incident on the photocathode, and the quantum efficiency. The correlation is shown in Figure 25 where all the dependencies developed have been factored out. The units are still in mV and MeV since all the dependencies are constants that describe the change in light yield for each parameter and thus are unitless quantities.

Equation 18 shows the correlation developed for each parameter and includes the energy dependent term. In this equation B is the absolute value of the detector bias in kV, Ω is

the view factor, x is the location of the scintillation event in cm, t is the scintillator thickness in cm, δ is the quantum efficiency, R is the material reflectance, CFD is the discriminator level, and E is the amount of energy deposited in MeV. The average value, neglecting the location of the scintillation event, can be found by solving this equation for x = 3.00.

$$CFD = \Omega\delta B^{6.58} e^{-0.136x} (1-R)^{(-2.68\ln(t)-6.2)} (1-0.29n)(86.4E-0.33) \qquad (18)$$

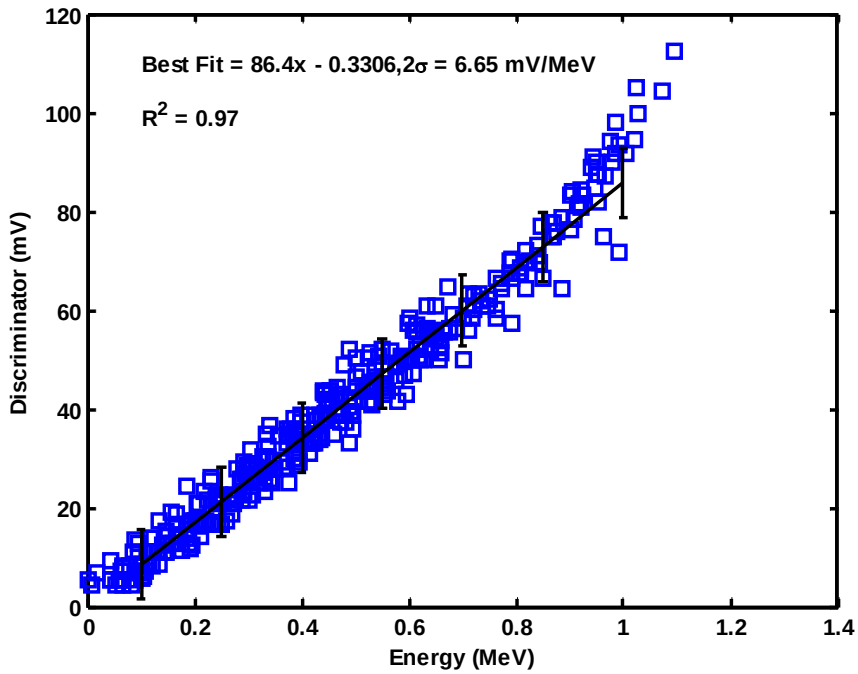

Figure 25 CFD Setting vs. Energy Deposition, Detector #1 Energy Dependent Relationship Shown

This equation is only valid for this particular set-up within the bounds used to develop this correlation and is good for energy deposition events in the range of 125 to 970 keV. These values correspond to the non-linearity boundary as discussed in the Methodology section. The error bars shown in Figure 25 correspond to the 2 sigma level, which is twice the calculated standard deviation from the linear fit. In addition to the standard deviation, 8% uncertainty should be included for the systematic contribution. The uncertainty in the standard deviation neglects the individual error contributions from each parameter correlation used to de-convolve the response function and are viewed as constants that are specific to a detector geometry and set-up. This assumption seems

valid since the same data used in the final analytical expression was used to develop the fit for each constant. The uncertainty calculated above was done using six degrees of freedom, where the degrees of freedom are: one for the experimental data, one for the original fit of the data, and one for each application of this data to the four parameters discussed in the de-convolution of the response function. This analytical expression will now be tested for its compatibility by applying the correlation to the multi-layered beryllium "layer cake" (BLC) geometry within the same detector.

Combining Response Functions, Detector #1 BLC Geometry

The initial validation for this method involves predicting and then measuring the detector response function experimentally for detector #1 with the primary BLC geometry in place. For this experiment a ^{60}Co source was placed inside the detector housing as shown in the left image of Figure 5. Data was collected at a fixed bias setting of -2.0 kV and counts were taken as a function of CFD setting as described previously. The predictive function for this geometry was determined by calculating a weighted average of the two different response functions that correspond to the two different geometries within the primary BLC geometry. The appropriate weighting factors can be determined by calculating the expected light contribution from each layer. Since a ^{60}Co source is being used the contribution from each layer can be approximated by the expected gamma ray attenuation in each layer. With having multiple materials, beryllium and scintillator, the attenuation needs to be calculated for each layer. The attenuation coefficients for a 1.25 MeV gamma ray for scintillator and beryllium are 0.0636 and 0.0933 cm, respectively [39]. The calculated attenuation then for fixed thicknesses of scintillator and beryllium is 0.994 and 0.971, respectively. The contribution from each scintillator layer can then be calculated by propagating the attenuation by taking a product of the calculated value and the attenuation value from the next layer. The expected contribution from each layer, with the starting layer being the closest to the source, was 1.000, 0.964, 0.931, and 0.898. Since the problem is symmetric the expected contribution from layers 1 and 4 (case 2 geometry) is 50%. Consequently, the other 50% contribution will come from layers 2 and 3 (case 1 geometry).

Using MCNP5 the sensitivity of this detector was calculated as a function of energy deposition, as described previously. The absolute response function in terms of discriminator level as a function of energy deposition can be found using Equation 18 with the appropriate constants for each geometry. The refraction indices are 2.96 and 2.33 for the inner and outer layers and the corresponding view factors are 0.496 and 0.440, respectively. The reflectance coefficients were calculated to be 0.092 and 0.037. The detector bias is -2.0 kV, the scintillator thickness was 1.0 mm, the quantum efficiency was 0.23, and the value used for the scintillation location was 3.25 cm. The absolute response function, after accounting for the contribution from each layer is shown in Equation 19. For comparison, Equation 20 shows the directly measured response function. Both equations statistically agree within the uncertainties of the correlation, where the uncertainty includes 8% of the value of the slope and the standard deviation associated with Equation 18.

$$CFD = 126.8E - 0.18, \sigma = 15\ mV \tag{19}$$

$$CFD = 158E - 6.70, \sigma = 20\ mV \tag{20}$$

Shown in Figure 26 are the experimental data and the predicted values using Equation 19. The predicted sensitivity deviates largely from the measured values between 100 and 150 mV. From the MCNP calculations these discriminator levels occur between 800 and 900 keV. This deviation is caused by the summing of events in multiple layers within the detector. Since the correlation was developed for only a single layer the correlation is not equipped to deal with the summing of events. The single layer correlation predicts a drastic change in the count rate, which means it predicts the Compton Edge. The summing of events in multiple layers blurs this expected feature as can be seen by the constant exponential trend in the count rate. This limitation can be approximated by considering how the correlation changes if multiple events were to occur. For example, if a particle deposited energy in two or more layers within the resolving time of the detector the correlation would under estimate the pulse amplitude by a factor of 0.2 (the intercept value) times the number of contributing layers. For this detector that could lead to a maximum underestimation of 0.8 mV. This can be seen in the comparison of Equations 19 and 20 where the intercept value for the directly measured value is much greater in

magnitude. This limitation between the correlation and current capabilities of MCNP5 is tolerable since the deviation occurs, for this case, well past a desired operating range. Since the main goal of the correlation is to have a predictive capability, these results are promising.

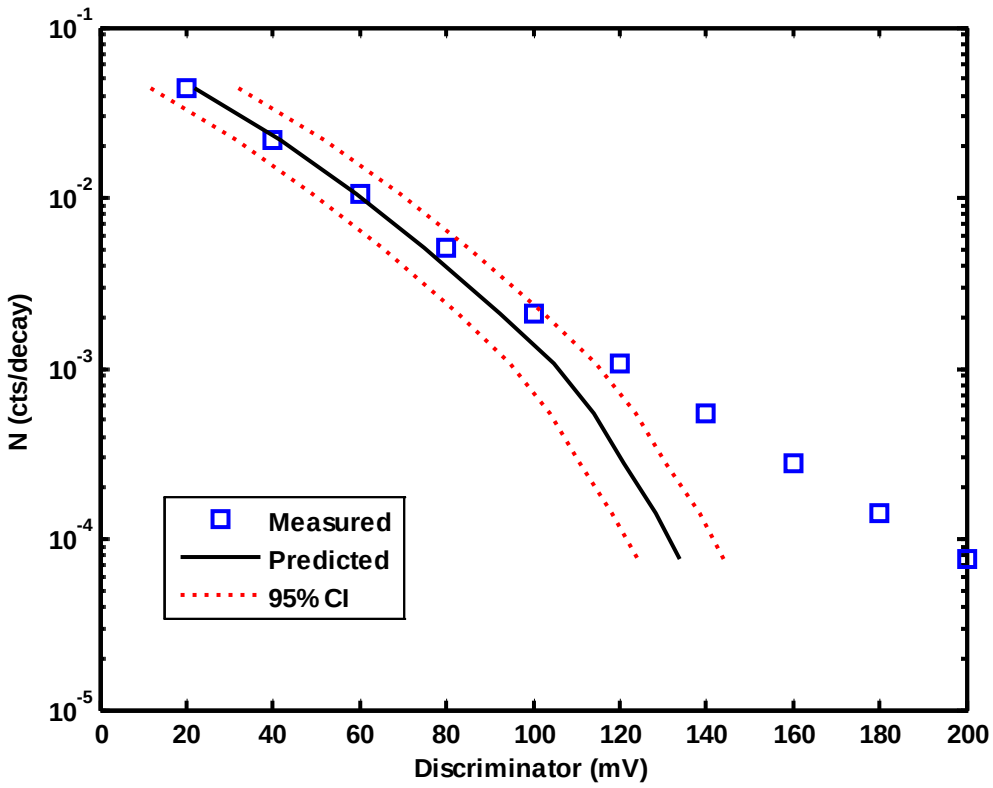

Figure 26 Validation of Detector Response Function, Predicted and Experimental Sensitivity for a Co-60 Source in the BLC Geometry

7. Detector #2

Description

To test the validity of the correlation another type of beryllium activation detector was investigated, detector #2, affectionately called the “Big BLC”. Detector #2 in principle is the same as detector #1 in that it has alternating layers of beryllium and scintillator. However, the detectors have two components that are drastically different. First, the beryllium used in this detector is 0.635 cm thick and the active region of this detector is substantially larger with a square cross-sectional area, 15.875 cm per side. The second difference is the PMT used in detector #2, a Hamamatsu R1250, which is much larger than the R5496, has an active cathode diameter of 12.7 cm versus 2.7 cm. The quantum efficiencies for both are similar at 22% for the R1250 versus 23% for the R5496 (Appendix H). Aside from geometrical differences these two PMT’s have different electron multiplication structures. The R1250 has a linear focused dynode structure and the Hamamatsu R5496 used in the small detector has a micro channel plate structure. As a consequence the R1250 has a longer transit and rise time. However, the difference in the timing characteristics for this work is non-consequential. The bigger concern was the factor of 14 increase in the gain of the R1250 versus the R5496.

To compare detectors several sets of data were taken with detector #2 using the same electronic configuration and the data was resolved using the same methodology as for detector #1. Three scintillator sizes were used independently: 0.318, 0.050, and 0.025 cm in two configurations: a single layer and the traditional BLC geometry with alternating layers of 0.635 mm beryllium. For this detector the 0.318 cm BC-404 scintillator was adopted from a previous application and the 0.05 and 0.025 cm scintillator was purchased new for these experiments from Eljen Technologies [29]. To provide some clarity on the detector configuration, the BLC geometry with the 0.318 cm scintillator is shown in Figure 27.

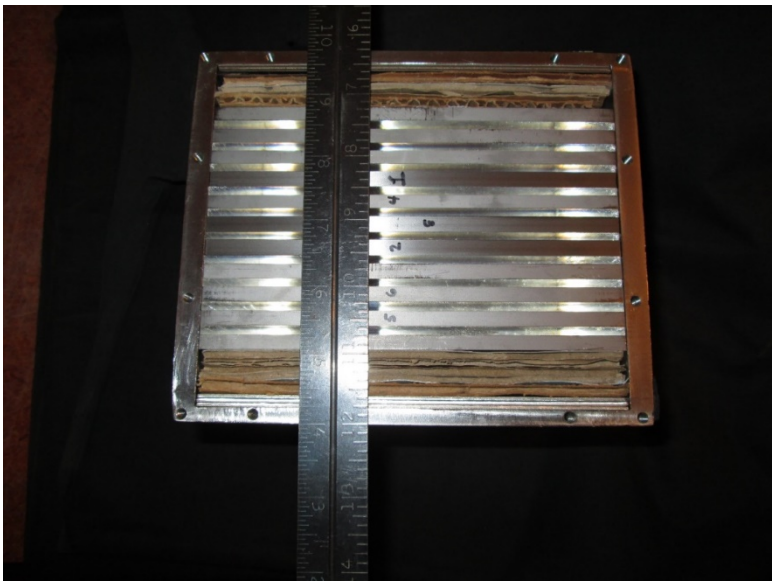

Figure 27 Active Region of Detector #2, BLC geometry Shown with .635 mm Be and 0.318 mm Scintillator

In all cases the geometric configuration was centered axially under the PMT using cardboard for spacing. This detector housing was not as easily disassembled as the small rod detector; therefore data was taken with the source placed on the exterior of the housing in position #13 as shown in Figure 28. This location corresponds to the center of the scintillator face within the detector housing.

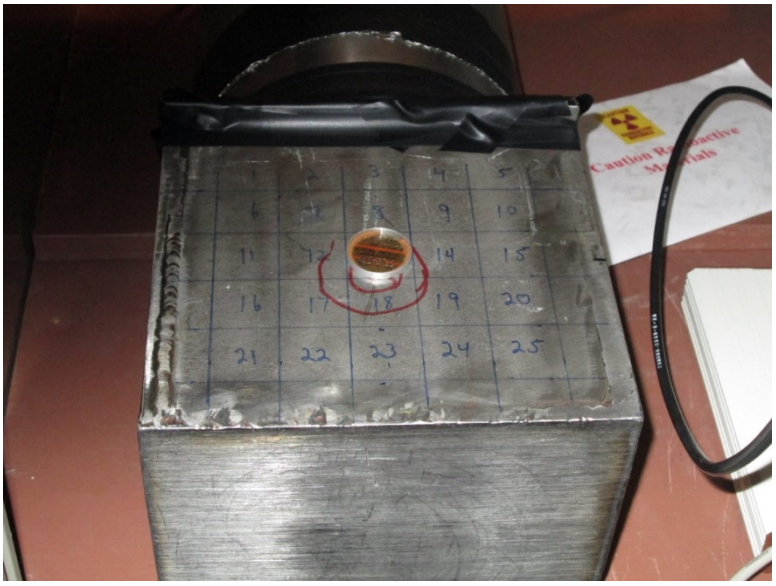

Figure 28 Detector #2 Source Location Grid

Much like the small detector, counts versus discriminator setting were taken as a function of detector bias. Data was taken at -1.6 kV to 2.1 kV for the larger scintillator and from -1.8 kV to -2.1 kV for the 0.025 and 0.05 cm scintillator. The 2.1 kV ceiling was chosen to prevent damage to the Ortec 584 module since at this bias 4 V pulses were observable which approaches the maximum allowable input pulse of 5V.

Detector #2 Results

As discussed in the previous section the PMT used in this detector has a factor of 14 increase in gain. Analytically it is unclear on how to correct the bias term from Equation 18 to reflect this increase. Thus, the first sets of experiments were conducted to correct this term. Six sets of data were taken with the BLC geometry shown in Figure 26 at bias settings of -1.6 kV to 2.1 kV in .1 kV increments with a ^{60}Co source placed in location #13. The data was resolved using the same method to find the bias term for detector #1. The results are shown in Figure 29, where the slope from each resolved data set is plotted versus the corresponding bias.

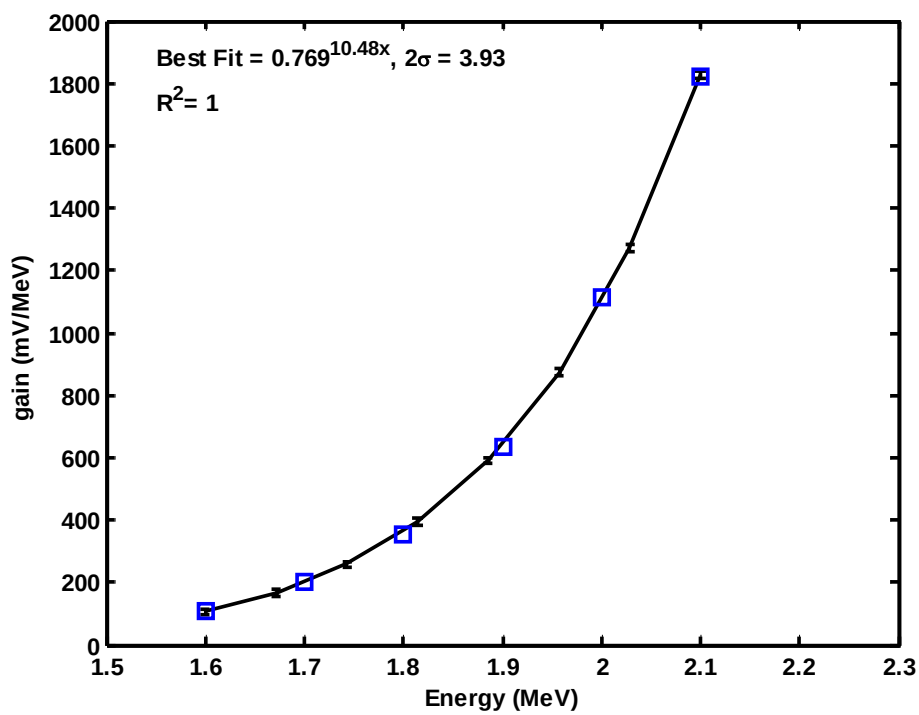

Figure 29 Detector #2 Calculated Detector Response vs. Detector Bias, Empirical Relationship Shown

If the gain was related as shown in Equation 21, a reference bias for detector #2 could be found.

$$GB_1^{6.56} = B_2^{10.48} \tag{21}$$

In this equation G represents the factor of 14 increase in the gain, B_1 the reference bias (2.0 kV) for detector #1, and similarly B_2 is a reference bias for detector #2. This equation can be re-arranged to solve for B_2, which gives a reference bias of 2 kV which is equivalent to the reference bias for detector #1. This suggests the coefficient in the exponent (10.48) for the new bias term in Equation 21 can be found if the reference bias for detector #2 is set equivalent to the bias used to develop the initial relationship. Since there are only two data points to correlate for Equation 21, this isn't substantial, but this could provide a quick reference if another PMT is used.

The second parameter that could be different for detector #2 is the coefficient for the spatial dependence. Using the equation shown in Figure 22 ($y = 1.52e^{-0.136z}$), normalized to unity, an average value, for this size of scintillator, would be 0.41 and corresponds to a vertical distance of 6.56 cm from the top edge of the scintillator. To see how this average correlates a set of 9 experiments were conducted using the BLC geometry shown in Figure 26 at a bias of -1.8 kV with a ^{60}Co source placed independently in locations: 1,3,5,11,13,15,21,23, and 25 as shown in Figure 28. The data was resolved using the same methodology and the slope of each response function was plotted as a function of the corresponding source location as shown in Figure 30. For reference the dimensions are measured from left to right and from top to bottom on the detector face.

From Figure 30 it is unclear as to why the response was greater on the left edge (-5.08) versus the right edge, but the response can be considered uniform, within 3% deviation, across the horizontal direction. The change in response is far more substantial in the vertical direction. This confirms the lack of a horizontal correction in the correlation and the one dimensional derivation shown in Figure 4 is justifiable. The mean slope for the response from these 9 measurements is 398 mV/MeV and would coincide to a source

location just above the center, which agrees with the predicted value of 402 mV/MeV at a source location of 6.56 cm.

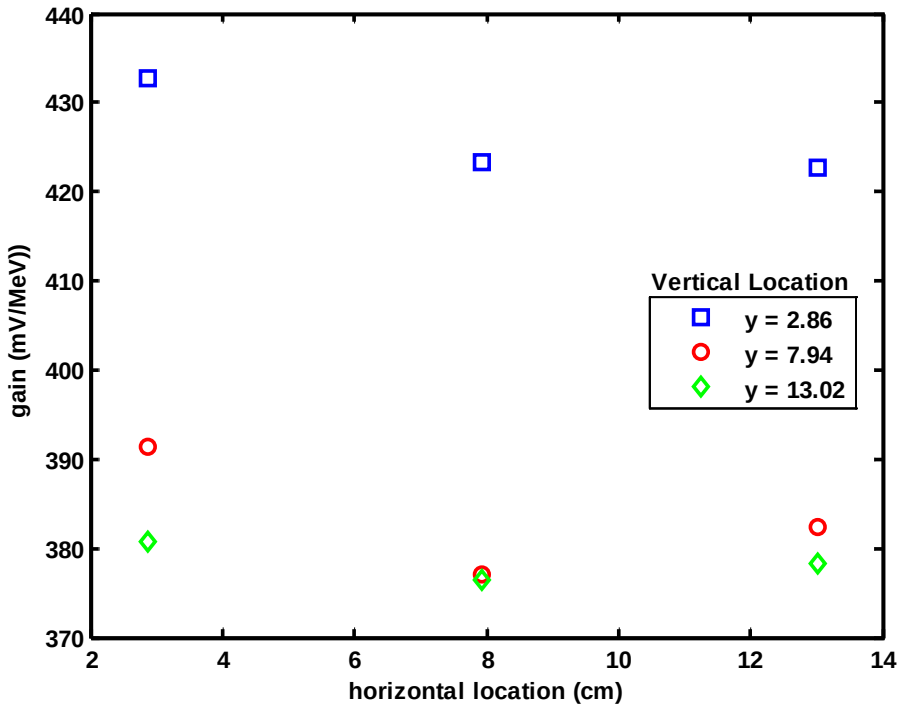

Figure 30 Calculated Detector Response vs. Source Location, Detector #2 BLC geometry with 10 .318 mm scintillator layers

Another concern with the larger detector and the increase in scintillator volume was the possibility of summing events from the cascade gamma rays associated with the decay of ^{60}Co. Data was taken with both a ^{137}Cs and ^{60}Co source independently in location #13 using the geometry shown in figure 27 at a bias of -2.0 kV. The response functions for each source are shown in Figure 31. In this figure there is excellent agreement between the two sources. Also, there are two distinct slopes that can be seen in the ^{137}Cs response function, where the steepest slope begins at the Compton Edge for ^{137}Cs (477 keV) and is a result of summing in multiple layers. This confirms the treatment of the ^{60}Co gamma rays as independent events was a valid assumption.

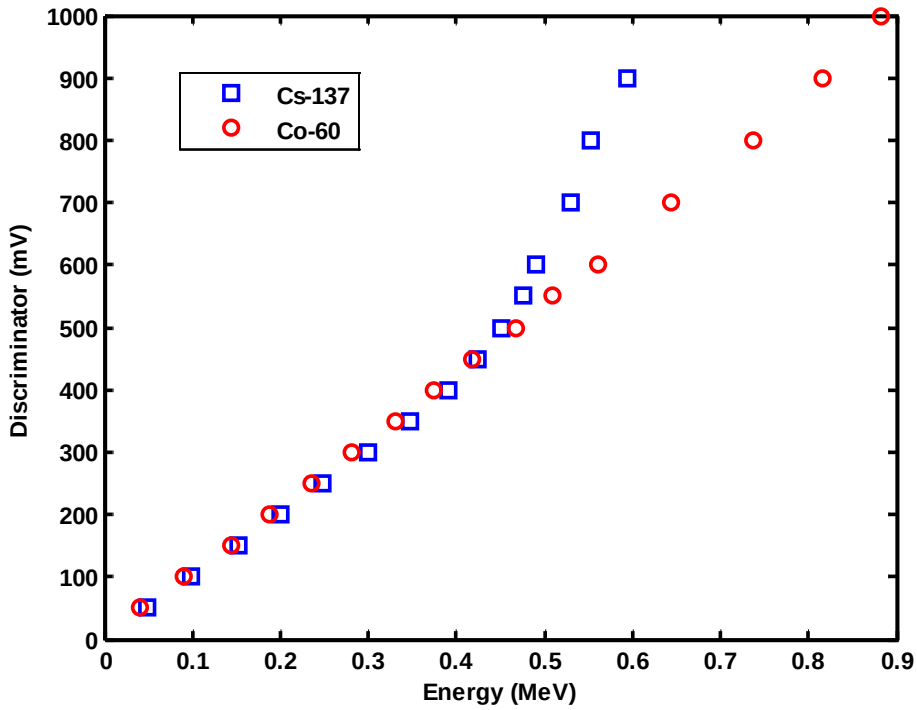

Figure 31 Comparison of response functions produced with Cs-137 and Co-60 with 10-0.318 mm scintillator

From the small rod detector correlation using multiple layers produced a slightly different correlation than with a single layer (see Equations 19 and 20). The concern with the bigger detector is that these differences would no longer be negligible. Data was compared for a single layer of 0.318 mm scintillator and the full BLC geometry shown in Figure 27 using a ^{60}Co source in position # 13 at a bias of -1.8 kV. The resolved data is shown in Figure 32. There are two distinct slopes for the BLC geometry response curve, where the steepest slope corresponds to multiple layer events. The other slope is a combination of both single and multiple events, which can be inferred from direct comparison with the single layer data. As a review, the predicted value of the CFD setting for a multi-layer geometry will change by some multiple of the intercept value, where the multiplier is dependent on the number of individual layers where energy loss events have occurred that contribute to the signal within the resolving time of the detector. The results shown here are expected since the single layer correlation has a negative slope, the value of the CFD setting within the same energy range is less for a multi-layer geometry. Although the two response functions do not agree within the

standard deviation of each fit, they do agree if the 8% systematic uncertainty is included. A more detailed analysis on the effects of layering could be undertaken at a later date. All of the previous experiments for this detector were repeated for both the 0.25 and 0.50 mm scintillator. The results were similar and the data can be found in Appendix A.

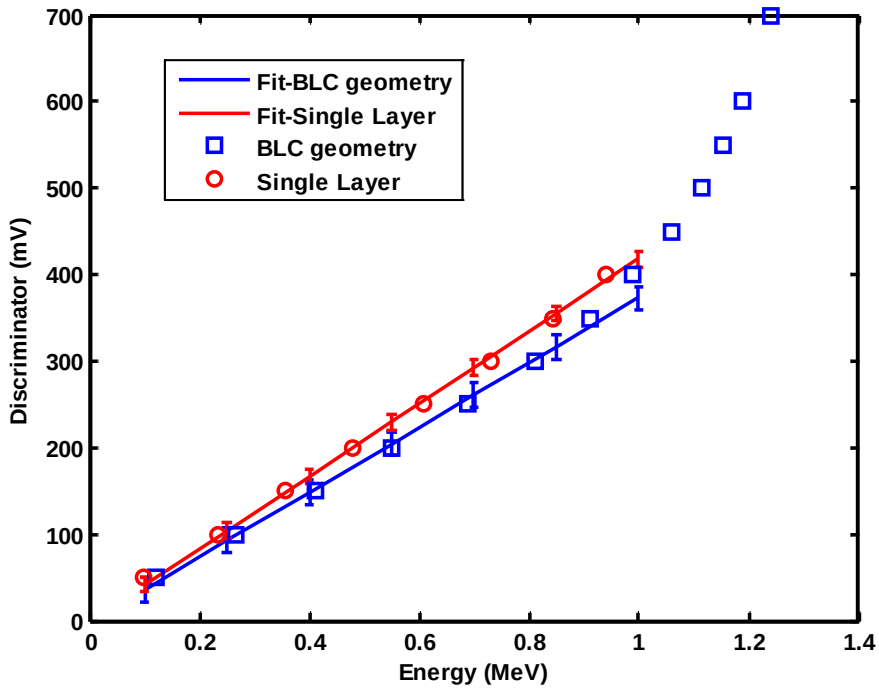

Figure 32 Comparison of Detector # 2 Response Functions, Single Scintillator Layer vs. BLC Geometry

To directly compare the data between detectors the data from detector #2 was resolved using a modified version of the parameter coefficient equation and is shown in Equation 22.

$$CFD = \Omega\delta B^{10.48} e^{-0.136x} (1-R)^{(-2.68\ln(t)-6.2)} (1-0.29n) \qquad (22)$$

The only difference in the parameters is the modified bias term, the quantum efficiency (δ) is 0.22 instead of 0.23 and the spatial term is solved for x = 7.94, which corresponds to the center of the detector where all the data was taken. The other factors remain the same: 2.96 for the refraction index (n), 0.092 for the reflectance coefficient (R) and the view factor, Ω was geometry specific. The calculation for the view factor was solved in similar fashion as discussed previously except the contribution of light from each layer in

the multi-layered geometries was inferred from the results of the MCNP5 calculation. This can be done by calculating the energy deposition as a function of a single layer in addition to calculating the energy deposition in all the layers. All the data taken with this detector was modified where the CFD setting was factored by the constants shown in Equation 22. The data was plotted as a function of energy as shown in Figure 33. For comparison the two energy dependent portions of the overall correlation for both detector #1 and #2 are shown in Equations 23 and 24, respectively. A pictorial comparison of the same two correlations is shown in Figure 34. There is excellent agreement between the two correlations, which confirms that the application of the methodology can be transferred between two detector systems.

$$D_1 = 86.40E - 0.33, 2\sigma = 6.7\ mV \tag{23}$$

$$D_2 = 93.33E - 4.74, 2\sigma = 6.7\ mV \tag{24}$$

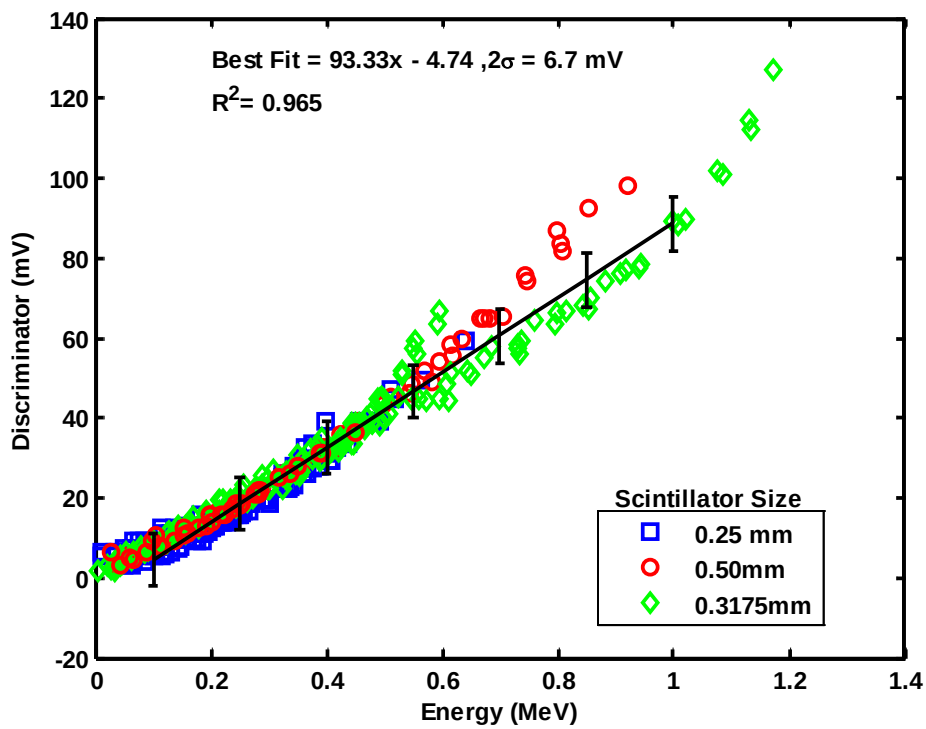

Figure 33 CFD Setting vs. Energy Deposition, Detector #2 Energy Dependent Relationship Shown

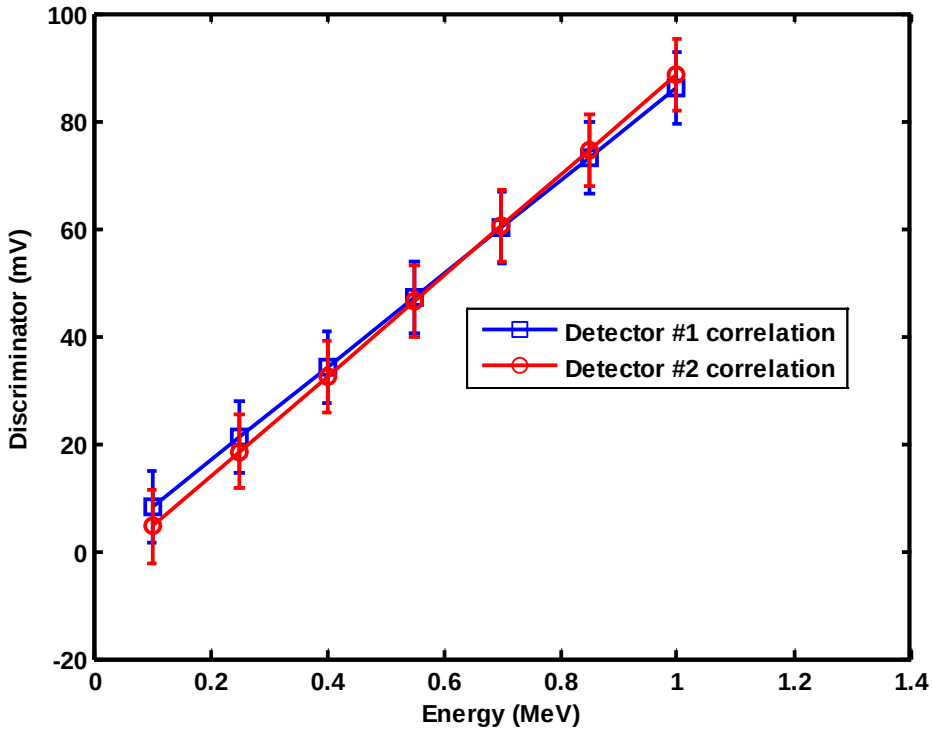

Figure 34 Comparison of Detectors # 1 and 2 Energy Dependent Response Functions

8. Validation

Experiment

Detector # 1 and # 2, both with the BLC geometry configuration in place, were exposed to a known neutron fluence at the Ion Beam Laboratory located at Sandia National Laboratories. D-D neutrons were generated by accelerating 175 keV D^+ ions into a thin ErD_2 (erbium-deuteride) target using a 350 keV Cockroft-Walton accelerator. The ErD_2 target is located inside a six inch diameter cylindrical vacuum chamber made of thin walled aluminum. There are three penetrations within the chamber wall, one for the beam line and two for SBD (surface barrier detectors) at angles of 110 and 165 degrees with respect to the beam line. The SBD detectors are nearly 100% efficient at measuring the protons produced from the D-D reactions that also produce tritium.

Nine total measurements were taken, one for the small rod detector and eight for the big BLC detector. Data was taken using the same electronic configuration as shown in Figure 7. The validation for the small rod detector has been discussed elsewhere [40] (Appendix J) so only the results for detector #2 will be presented here. Detector #2 was used for eight separate runs, where two of the runs were at a distance of 40.33 cm from the face of the detector to the source and the other six runs were conducted at a distance of 12.06 cm. In all cases the layer configuration was placed normal to the incident neutron fluence.

Given the short half-life of the ^{6}He nucleus, this detector is only useful for pulsed neutron sources since the number of nuclei produced would saturate in ~4 seconds. The overall experimental set-up and the collection of data is discussed elsewhere [41] but a brief description will be provided here. To emulate this short pulse, the D^+ beam was cycled in 20 second intervals, where the beam was on target for four seconds and then off target for sixteen seconds. This ensured a maximum build-up rate of ^{6}He in the beryllium layers. Counts were then taken for the first 12 seconds of the 16 second beam off interval in 100 ms increments. This cycling was repeated until ~ 10,000 counts were obtained in the first time bin. An average background rate per 100 ms was obtained by integrating the last four seconds of the counting time and then dividing by the number of bins. This method for obtaining the background assumes that 99.99% of the ^{6}He has decayed since the

background counts were taken after approximately ten ^{6}He half-lives (~8 sec.) had transpired. The net counts per 100 ms interval were obtained by subtracting the background, bin by bin, from the total counts. The initial amount of ^{6}He produced, A_o, was found by the integral method as shown in Equation 23.

$$A_o = \frac{(C - B)\lambda}{(e^{-\lambda t_1} - e^{-\lambda t_2})(1 - e^{-\lambda t_0})} \tag{23}$$

In this equation (C-B) is the integrated count rate from t_1 to t_2, λ is the decay constant and t_o is the total irradiation time (4 sec.). The initial activity was then divided by the number of neutrons incident at the average detector solid angle ($\varphi_{\bar{\Omega}}$), which corresponds to the mid-point of the detector, using Equation 24 to obtain the detector sensitivity, η.

$$\eta = \frac{A_o}{\varphi_{\bar{\Omega}}} \tag{24}$$

The calculation of the neutron fluence was done using the Associated Particle Method (APM) as described in detail by Ruiz *et al.* [42] and Cooper *et al.* [43]. APM is a well-established method for accurately measuring the neutron fluence for both D-D and D-T neutrons. These calculations are widely accepted and used for determining cross calibration factors for neutron detector systems. A brief summary of the method will be described here. Based on the kinematic relationship of accelerating 175 keV D+ ions into a target one can infer from the number of protons detected by the two SBD detectors the number of neutrons incident at a given solid angle. The sensitivity calculations were performed independently by C.L. Ruiz [41] and then compared to the sensitivities predicted using the methodology presented here.

Monte Carlo Calculations

The prediction of the detector sensitivity required three Monte Carlo calculations. Two are used to determine the production and decay of ^{6}He and the third is used to determine the number of source neutrons at the average solid angle of the detector. The neutron source used to determine the production of the ^{6}He was a distributed energy neutron source consistent with the kinematics of accelerating 175 keV D^+ ions into an ErD_2 target

[1]. The number of ^{6}He nuclei produced per beryllium layer can be found in MCNP5 using Equation 25.

$$R = \phi N \sigma V \tag{25}$$

Where R is the number of ^{6}He nuclei produced per layer normalized per source neutron, ϕ is the neutron scalar flux in cm^{-2}, N is the atom density of beryllium in atoms-cm^{-3}, σ is the energy dependent ^{9}Be (n, α) ^{6}He cross-section in barns (10^{-24}cm^{2}), and V is the volume of each beryllium layer in cm^{3}. This value can be calculated directly in MCNP5 by using a flux multiplier, FM4 (Appendix D). The flux multiplier tells the model to multiply the energy dependent neutron fluence by the energy dependent ^{9}Be (n, α) ^{6}He cross-section by the atom density and volume of the material. These values are then used to define the spatial location (in terms of which layer the nuclei was produced) of the ^{6}He beta particles for the second calculation, which simulates the beta decay of ^{6}He.

Since the amount of ^{6}He nuclei is calculated per layer, the starting location for the ^{6}He beta particles are assumed to be uniformly distributed throughout the beryllium layer. The initial beta particle energy was sampled from an experimentally obtained energy spectra found in previous work by others[44]. The calculated beta spectrum is a discreet probability distribution and was linearly interpolated between points. An F8 tally, as described previously, was then used to determine the number of measurable events as a function of differential energy loss. The results from these calculations were used to determine the contribution from each layer for the view factor calculation and the total number of measurable events as a function of energy as described previously. Thus the total number of results needed from this calculation numbered one more than the number of scintillator layers in the detector. The number of neutrons incident at the average solid angle was found with another Monte Carlo calculation. The neutron source term used in the first calculation was used again here to determine the number of particles crossing a square plane, the size of the beryllium layer, at 90 degrees to the source at the distance that corresponds to the mid-point of the detector. Taking the product of the three calculations gives the detector sensitivity as a function of energy deposition given by Equation 26. In this equation η_P is the predicted sensitivity as a function of energy, R/n_s

is the result from the first calculation in ^{6}He produced per source neutron, Cts/R is the result from the second calculation in number of counts per ^{6}He produced, and finally n_s/n_Ω is the inverse ratio of the final calculation in number of neutrons incident at the average solid angle per source neutron.

$$\eta_P(E) = \left[\frac{\mathrm{R}}{n_s}\right]\left[\frac{Cts}{\mathrm{R}}\right]\left[\frac{n_s}{n_\Omega}\right] \tag{26}$$

This can then be converted to a sensitivity as a function of discriminator setting by applying Equation 22. Alternatively, if the discriminator setting is known, as is the case here, Equation 22 can be inverted to find the corresponding energy. A summary of the experimental conditions and a comparison of the measured and predicted sensitivity are shown in Table IV. A visual comparison of the values calculated using APM and the correlation developed here for detector #2 are shown graphically in Figure 35. The blue line depicts the predicted sensitivity as a function of discriminator setting and the two red lines show the 68% confidence interval that corresponds to ± 9 mV for the systematic error and 4 mV for the correlation standard deviation.

Table IIV Comparison of Detector # 2 Sensitivities, Measured and Predicted

CFD (mV)	Distance (inches)	Measured (M) Sensitivity	Predicted (P) Sensitivity	% Difference |M – P|/M
25	12.06	1.86E-2	1.14E-2	38.5%
50	12.06	1.36E-2	1.01E-2	26.0%
50	12.06	1.43E-2	1.01E-2	29.6%
75	12.06	8.53E-3	7.77E-3	8.92%
75	40.33	8.99E-3	7.77E-3	13.6%
75	40.33	7.10E-3	7.77E-3	9.43%
100	12.06	5.55E-3	4.73E-3	14.8%
150	12.06	2.26E-3	1.41E-3	37.5%

5 of the 8 measurements agree statistically with the prediction with an overall average fractional standard deviation for the 8 values of 25%. It is uncertain why the predicted sensitivity does not match the measured data at lower CFD settings, where the predicted

sensitivity predicts a much steadier range of operation between 20 and 75 mV. The deviation between the measured and predicted values can possibly be attributed to two factors: the spectral data used for the ^{6}He is not accurately modeled, which the spectral shape will affect the predicted values or there is activated material that the model does not account for. The goal of this work is to be able to have a predictive capability and these results conclusively show a predictive capability that produce the expected result within 25% for this data set, but with some investigation and improvement to the model this predictive capability could extend to within as little as 12-15% as suggested by the trend at higher CFD settings as shown in Figure 35. While this isn't the most desirable result it will provide sufficient direction for future work.

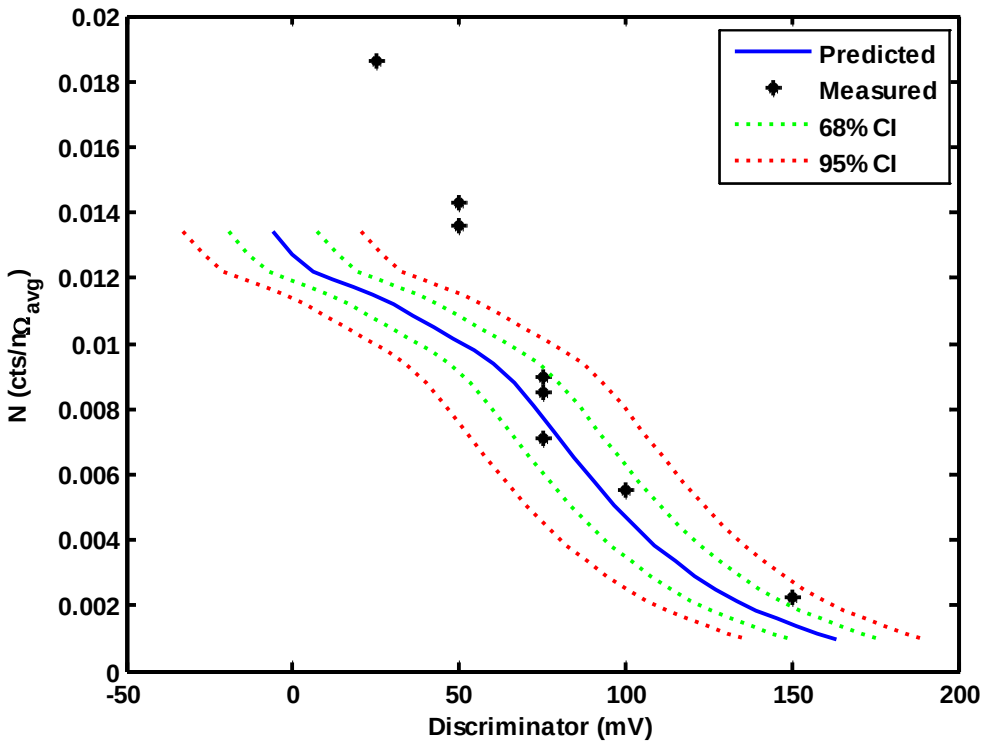

Figure 35 Predicted and Measured Sensitivities for Detector #2 as a function of CFD setting

9. Optimization

The current design of the existing BLC detector used by Sandia National Laboratories, shown in Figure 3, was used as reference geometry for an optimization study. The current design came to fruition after several prototype designs. Originally two designs were considered a “layer cake” design and a “rod design” which had several beryllium rods encased in a cylinder of scintillator. These designs suffered from having too much scintillator for the Z-environment. The initial bremsstrahlung pulse damaged the Ortec 584 CFD module that resulted in the total loss of data. In addition, if data was recoverable, gamma rays from activated material within and surrounding the detector reduced the signal-to-noise of the detectors. An investigation into an appropriate volume ratio of beryllium to scintillator was investigated. It was determined from a very limited set of experimental data that 3.18 mm thick beryllium and 1.00 mm thick scintillator would be sufficient enough to reduce the expected background on Z while maintaining the integrity of the signal of interest. The purpose of this study is to see if any improvements can be made to the existing design given the newly established methodology.

For this study four thicknesses of beryllium and scintillator were investigated: 3.0, 2.0, 1.0, and 0.25 mm each having a square cross-sectional area, 10.16 cm per side. In each case, constant thicknesses of beryllium and scintillator were alternated in a similar fashion as to what is shown in Figure 36, except for this study an extra layer of scintillator was added such that the two outer most layers were always scintillator. In addition, 0.01 cm thick pieces of reflective Mylar were sandwiched between each layer of scintillator and beryllium. The entire BLC assembly was encased in a 0.8-mm thick aluminum housing. For each of the four thicknesses of beryllium assumed, four thicknesses of scintillator were modeled, so that the total number of geometrical permutations was sixteen. For reference, the dimensions in the x and y directions are both 10.4 cm, while the dimension in the z direction is 10.4 with a variation of ± 0.2 cm to accommodate differences in the variations of the scintillator and beryllium stacked dimensions. It was important to keep the z-dimension as close as possible to 10.4 cm so

each configuration was comparable without having to correct for the source-to-detector solid angle and attenuation.

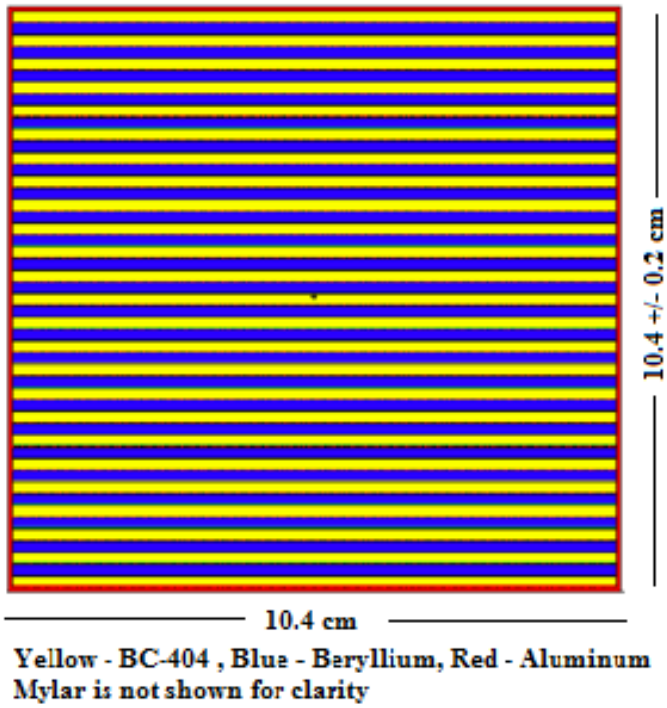

Figure 36 MCNP Geometry, 2 mm BC-404 scintillator and 2 mm Beryllium Layers Shown

For this study an isotropic-point D-D neutron source was considered at a neutron temperature of 10 keV, 50 cm from the detector face. The lower limit for this study was chosen at an energy of 200 keV, which corresponds to a discriminator level of 95 mV if the following parameters are assumed: a R5496 PMT at a bias of -2.0 kV, a view factor of 1 assuming no loss in the Lexan light guides, the average value of 0.541 was used for the spatial dependence and Mylar is used for the reflective material. The method used to determine the sensitivity was the same for this study as discussed in the Validation section. The final results of this study are shown in Figure 37.

From this figure it appears the optimized configuration will consist of alternating layers of 2 mm beryllium (33 total) and 1mm scintillator (34 total). This is only a modest improvement over the current design of 10%, but with a predictive capability within 25%, these results suggest the current detector is satisfactorily designed.

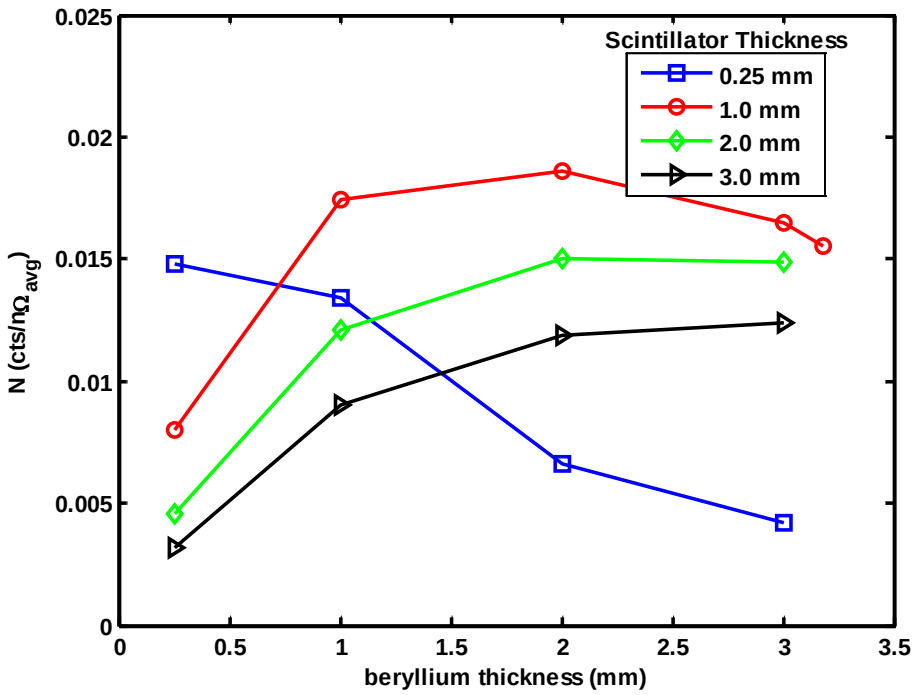

Figure 37 Detector Sensitivity as a function of scintillator and beryllium thicknesses

10. Conclusion

For this work a methodology has been developed to predict the sensitivity of a beryllium/scintillator fusion neutron detector. Neutrons may be captured by the beryllium via the ^{9}Be (n, α) ^{6}He nuclear reaction, where the product nucleus, ^{6}He, decays by beta emission. The beta particles can be detected by close coupling scintillator with the beryllium. The methodology relates beta energy deposition to absolute measured scintillation light output as a function of detector bias, reflective material, scintillator thickness, and solid angle subtended by the scintillator on the face of the PMT. Output signals were measured from thin plastic scintillator using NIST traceable beta and gamma sources and MCNP5 was used to model the energy deposition from each source. Combining the experimental and calculated results gives the desired empirical relationships. The results from this methodology were compared with previous work and the two results were in good agreement. The empirical relationships were applied to a similar detector with much larger dimensions and very different response characteristics. The correlation between the two systems produced nearly identical results. To validate, the sensitivity of the second beryllium/scintillator-layer neutron activation detector was predicted and then exposed to a known DD neutron fluence. The neutron fluence was determined by the associated particle method from which the detector sensitivity could be inferred. The predicted and the measured sensitivity agreed within a range of 8 to 38 percent difference with an average standard deviation of 25% from 8 total measurements. Predicting the detector performance within 25% is adequate enough to guide future detector design decisions. To test this methodology it was applied to the design modeled after Sandia National Laboratories current beryllium detector, which was originally designed using results from a very limited set of experimental data. The results of these calculations indicated that the design was in fact optimal within the uncertainties of this work.

11. References

[1] C.L. Ruiz et. al., Rev. Sci. Instr., **63**, (1992), 4889, http://dx.doi.org/10.1063/1.1143541.

[2] M.S. Rowland and J.C. Roberson, Nucl. Instr. Meth., **224**, (1984), 322.

[3] National Nuclear Data Center, Brookhaven National Laboratories, ENDF/B-VII.0 Library, (2006).

[4] Chart of the Nuclides,16 ed.,Knolls Atomic Power Laboratory, Bechtel, (2002).

[5] T.J.MURPHY, "A Practical Beryllium Activation Detector For Measuring DD Neutron Yield From ICF Targets," LA-UR-96-1649, Los Alamos National Laboratory (1996).

[6] National Nuclear Data Center, Brookhaven National Laboratories, NuDat 2.6 Library, http://www.nndc.bnl.gov/nudat2/, (2012).

[7] A. Talebitaher,S.V. Springham, R.S. Rawat, P. Lee, Nucl. Instr. and Meth. **659**, (2011), 361.

[8] St-Gobain Detectors, "Plastic Scintillation," http://www.crystals.saint-gobain.com/, (2008)

[9] Mylar registered trademark of Dupont Teijin Films

[10] X-5 Monte Carlo Team, "MCNP - A General Monte Carlo N-Particle Transport Code, Version 5," LA-UR-03-1987, Los Alamos National Laboratory (2008).

[11] J.B. Czirr, D. R. Nygren, Nucl. Instr. And Meth.. **31**, (1964), 226.

[12] D.L. Smith, R.G. Polk,T.G. Miller, Nucl. Instr. Meth., **64**, (1968), 157.

[13] A. Snood, R.P. Gardner, Nucl. Instr. and Meth. **213**, (2004), 100.

[14] M.J. Berger, S.M. Seltzer, Nucl. Instr. and Meth. **104**, (1972), 317.

[15] R.P. Gardner, A.M. Yacout, J. Zhang, and K. Verghese, Nucl. Instr. and Meth. **A242**, (1986), 399.

[16] Y. Jin, R.P. Gardner, and K. Verghese, Nucl. Instr. and Meth. **A242**, (1986), 116.

[17] H. Vincke, E. Gschwendtner, C.W. Fabjan, T. Otto, Nucl. Instr. and Meth. **A484**, (2002), 102.

[18] Sarah A. Pozzi, Marek Flaska, Andreas Enqvist, Imre Pazsit, Nucl. Instr. Meth. **582**, (2007), 629.

[19] A.J. Nelson et al., Rev. Sci. Instrum. 83, 10D915 (2012), http://dx.doi.org/10.1063/1.4742140.

[20] P. Kuijper, C.J. Tiesinga, C.C. Jonker, Nucl. Instr. Meth., 42, (1966), 56.G. Keil, Nucl. Instr. And Meth.. **87,** (1970).

[21] V.Schonfelder, Nucl. Instr. And Meth., **86**, (1970), 327.

[22] G. Dietze and H. Klein, Nucl. Instr. Meth., **193**, (1982), 549.

[23] J.B. Birks, "The Theory and Practice of Scintillation Counting," Pergamon Press, Oxford, (1964).

[24] G.F. Knoll, "Radiation Detection and Measurement", Fourth Ed., Wiley,New York, (2010), pg. 231.

[25] Howell, J.R., "A catalog of radiation configuration factors", McGraw-Hill, (1982).

[26] Lisa G. Chiang, Richard B. Oberer, Sara A. Pozzi , "Method to Correlate CFD Discriminator Level and Energy Deposition by Neutrons and Photons in A Fast Plastic Scintillating Detector", ORNL/TM-2000/193, (2000).

[27] M. Marseguerra, E. Padovani, S.A, Pozzi, Prog. In Nucl. Engr. **43**, (2003), 35.

[28] JAMES TURNER, "Atoms, Radiation, and Radiation Protection," 3rd ed., Wiley, Germany, (2007).

[29] Eljen Technologies, "Technical Information" http://www.eljentechnology.com/index.php/technical-information , (2011).

[30] Hamamatsu Photonics, "Photomultiplier Tubes," http://www.hamamatsu.com/us/en/index.html, (2014).

[31] Eckert & Ziegler, "Reference and Calibration Sources Catalog vers. 1.0", (2007), http://www.ezag.com

[32] NIST, ESTAR, Database, http://physics.nist.gov, (2013).

[33] H.G. HUGHES, "Treating Electron Transport in MCNP,", Los Alamos National Laboratories, LA-UR-96-4583, (1996)

[34] Brookhaven National Laboratories, "Decay Radiaton Results," http://www.nndc.bnl.gov/nudat2/

[35] M.G. Stabin and C.Q. da Luz, Health Phys., **83**, (2002), 471 http://www.doseinfo-radar.com/RADARDecay.html.

[36] RefractiveIndex.info, "Refractive Index Database," http://refractiveindex.info/, (2014).

[37] S.H. Mortazavi, M. Ghoranneviss, S. Faryadras, Journ. Fusion Energy **31,** (2012), 211.

[38] Filmetrics, "Refractive Index Database," http://filmetrics.com/refractive-index-database, (2014).

[39] NIST, "Mass Attenuation Coefficient Database," http://physics.nist.gov, (2014).

[40] Styron et al., Rev. Sci. Instrum. 85, 11E617 (2014), http://dx.doi.org/10.1063/1.4896176.

[41] Ruiz et al. (Manuscript in Progress, to be submitted to Phys. Rev.)

[42] C.L. Ruiz et al, Rev. Sci. Instr. **83**, (2012), 10D913, http://dx.doi.org/10.1063/1.4729495.

[43] G.W. Cooper et al, Rev. Sci. Instr. **83**, (2012), 10D918, http://dx.doi.org/10.1063/1.4746999.

[44] J.B. Vise and B.M. Rustad, Phys. Rev., 132, (1963), 2573.

12. List of Appendices

Appendix A Experimental Data and Calculated Response Functions 69

Detector #1 69

Proof of Concept – Case 1 (Beryllium/Beryllium) 69

Proof of Concept – Case 2 (Beryllium/Polypropylene) 70

Proof of Concept – Case 3(Polypropylene/Polypropylene) 72

Proof of Concept – Case 4 (Mylar) 74

Bias Correlation – Case 1 (Beryllium/Beryllium) 75

Bias Correlation – Case 3 (Polypropylene/Polypropylene) 77

¼ and ½ mm Scintillator 80

Source Location – Case 1 (Beryllium/Beryllium) 83

Source Location – Case 2 (Beryllium/Polypropylene) 84

Source Location – Case 3 (Polypropylene/Polypropylene) 85

Source Location – Case 4 (Mylar) 86

Source Location – ¼ and ½ mm scintillator 87

View Factor – Case 3 Geometry (Polypropylene/Polypropylene) 89

View Factor – Case 1 Geometry (Beryllium/Beryllium) 92

BLC Geometry 93

Detector #2 95

BLC geometry – 10 3.175 mm layers 95

Spatial, BLC geometry –10 0.3175 mm layers 103

Single Layer Geometry – 3.175 mm scintillator 109

BLC geometry – 10 0.5 mm layers 113

Single Layer Geometry – 0.5 mm scintillator 115

BLC geometry – 10 0.25 mm layers 117

Single Layer Geometry – 0.25 mm scintillator 121

Appendix B MCNP Results 124

Detector #1 124

Proof of Concept – Case 1 (Beryllium/Beryllium) 124

Proof of Concept – Case 2 (Beryllium/Polypropylene) 126

Proof of Concept – Case 3 (Polypropylene/Polypropylene) 129

Proof of Concept – Case 4 (Mylar Wrap) 132
¼ and ½ mm Scintillator 133
Source Location – Case 1(Beryllium/Beryllium) 138
Source Location – Case 2(Beryllium/Polypropylene) 140
Source Location – Case 3(Polypropylene/Polypropylene) 141
Source Location – Case 4(Mylar Wrap) 143
Source Location – ¼ and ½ mm Scintillator 145
View Factor 149
BLC Geometry 153
Geometric Uncertainties 156
Detector #2 160
BLC Geometry – 10 3.175 mm layers 160
BLC Geometry – 10 0.5 mm layers 166
BLC Geometry – 10 0.25 mm layers 167
Single Layer Geometry – 3.175 mm 168
Single Layer Geometry – 0.50 mm 170
Single Layer Geometry – 0.25 mm 171
Appendix C Sample MCNP Inputs 173
Detector # 1 173
Na-22 Gamma Source, Case 1 Geometry 173
Na-22 Positron Source, Case 1 Geometry 175
Cs-137 gamma source, case 1 geometry 178
Cl-36 beta source, case 2 geometry 180
Pb-210 beta source, case 3 geometry 183
Pb-210 gamma source, case 3 geometry 185
Sr-90 beta source in top location, case 4 geometry 188
Co-60 gamma source, case 3 geometry, ¼ mm scintillator 191
Co-60 beta source, case 3 geometry, ¼ mm scintillator 193
Sr-90 beta source, case 3 geometry, ½ mm scintillator, bottom location 196
Co-60 gamma source, BLC Geometry 199
Detector #2 202
Co-60 gamma source, BLC geometry, 3.175 mm scintillator 202
Cs-137 gamma source, single layer geometry, ¼ mm scintillator 205

Neutron Source, Validation Experiment, BLC Geometry, 3.175 mm scintillator 207
He-6 beta source, Validation Experiment, BLC Geometry, 3.175 mm scintillator 214
Validation Experiment, Neutron Fluence at Average Detector Solid Angle 218
Appendix D Sample MCNP Output Files 226
Detector #1 226
Co-60 gamma source, BLC geometry 226
Detector #2 241
Neutron Source, Validation Experiment, BLC Geometry, 3.175 mm scintillator 241
He-6 beta source, Validation Experiment, BLC Geometry, 3.175 mm scintillator 258
Appendix E Source Data Sheets 284
Cs-137 (IPL) 284
Cs-137 (Baird-Atomic) 285
Cl-36 286
Co-60 287
Na-22 288
Pb-210/Bi-210 289
Sr-90/Y-90 290
Appendix F Beta Source Spectral Data 291
Appendix G Scintillator Data Sheets 293
Bc-404 Scintillator (St. Gobain Crystals) 293
EJ-204 (Eljen Technologies) 296
Appendix H PMT Data Sheets 297
Hamamatsu R5946 PMT 297
Hamamatsu R1250 PMT 299
Appendix J Review of Scientific Instruments Publication (Draft) 301

Appendix A Experimental Data and Calculated Response Functions

Detector #1

Proof of Concept – Case 1 (Beryllium/Beryllium)

Co60 Source		Scintillator Thickness (mm)	1
Collected Data	2/7/14	Detector Bias (-kV)	2
Calibration Date	8/1/06	Source Location	center
Initial Activity	396100	Scintillator Location	on axis
Current Activity	147227	Material	beryllium/beryllium
Slope [mV/MeV]	92.33	σ-slope [mV/MeV]	1.17
Intercept [mV]	1.16	σ-Intercept [mV]	2.16
R^2	1.000	σ-Linear Fit (Std. Dev.) [mV]	0.52

Disc (mV)	Time (Sec.)	Total Counts	$\frac{Counts}{Sec.}$	$\frac{BG}{Sec.}$	$\frac{Net\ Cts.}{Sec.}$	$\frac{(C-B)}{A_o}$	MeV Calc.	Disc. Error %
20	10	17082	1708.2	16.08	1692.1	1.15E-02	0.201	3.97
30	20	20126	1006.3	2.03	1004.2	6.82E-03	0.311	2.34
40	20	10972	548.6	0.96	547.6	3.72E-03	0.424	1.99
50	40	12257	306.4	0.50	305.9	2.08E-03	0.527	1.46
60	90	13411	149.0	0.25	148.7	1.01E-03	0.641	1.31
70	100	7102	71.0	0.00	71.0	4.82E-04	0.747	1.43
80	300	9956	33.1	0.00	33.1	2.25E-04	0.843	2.11
100	300	2655	8.8	0.00	8.8	6.01E-05	0.966	3.21
120	300	567	1.8	0.00	1.8	1.28E-05	1.073	3.02

Co60 Source		Scintillator Thickness (mm)	1
Collected Data	5/27/14	Detector Bias (-kV)	2
Calibration Date	8/1/06	Source Location	center
Initial Activity	396100	Scintillator Location	on axis
Current Activity	141762	Material	beryllium/beryllium
Slope [mV/MeV]	95.16	σ-slope [mV/MeV]	1.84
Intercept [mV]	-0.91	σ-Intercept [mV]	2.92
R^2	0.999	σ-Linear Fit (Std. Dev.) [mV]	1.02

Disc (mV)	Time (Sec.)	Total Counts	$\frac{Counts}{Sec.}$	$\frac{BG}{Sec.}$	$\frac{Net\ Cts.}{Sec.}$	$\frac{(C-B)}{A_o}$	MeV Calc.	Disc. Error %
20	10	16027	1602.7	16.08	1586.6	1.12E-02	0.208	3.98
40	20	10389	519.4	2.03	517.4	3.65E-03	0.427	1.90
60	60	8355	139.2	0.96	138.3	9.76E-04	0.646	1.16
80	100	3179	31.7	0.50	31.3	2.21E-04	0.844	1.24
100	300	2087	6.9	0.25	6.7	4.73E-05	0.984	1.33

120	300	425	1.4	0.00	1.4	9.99E-06	1.082	0.57

Cs-137 Source			Scintillator Thickness (mm)					1
Collected Data		2/7/14	Detector Bias (-kV)					2
Calibration Date		8/1/69	Source Location					center
Initial Activity		49580	Scintillator Location					on axis
Current Activity		17712.1	Material					beryllium/beryllium
Slope [mV/MeV]			119.71	σ-slope [mV/MeV]				4.09
Intercept [mV]			-6.96	σ-Intercept [mV]				11.68
R^2			0.983	σ-Linear Fit (Std. Dev.) [mV]				2.08
Disc (mV)	Time (Sec.)	Total Counts	$\frac{Counts}{Sec.}$	$\frac{BG}{Sec.}$	$\frac{Net\ Cts.}{Sec.}$	$\frac{(C-B)}{A_o}$	MeV Calc.	Disc. Error %
20	200	12126	60.63	16.08	44.55	2.52E-03	0.222	4.63
30	300	8143	27.14	2.79	24.35	1.37E-03	0.308	2.40
40	300	3562	11.87	2.03	9.84	5.56E-04	0.396	2.16
50	300	1375	4.58	1.46	3.12	1.76E-04	0.452	5.97
60	300	545	1.82	0.96	0.86	4.84E-05	0.489	4.63

Na-22 Source			Scintillator Thickness (mm)					1
Collected Data		2/7/14	Detector Bias (-kV)					2
Calibration Date		8/1/06	Source Location					center
Initial Activity		374500	Scintillator Location					on axis
Current Activity		50437	Material					beryllium/beryllium
Slope [mV/MeV]			94.70	σ-slope [mV/MeV]				0.95
Intercept [mV]			1.66	σ-Intercept [mV]				1.79
R^2			0.997	σ-Linear Fit (Std. Dev.) [mV]				1.51
Disc (mV)	Time (Sec.)	Total Counts	$\frac{Counts}{Sec.}$	$\frac{BG}{Sec.}$	$\frac{Net\ Cts.}{Sec.}$	$\frac{(C-B)}{A_o}$	MeV Calc.	Disc. Error %
20	20	9889	494.45	16.08	478.37	9.48E-03	0.209	3.43
30	40	9565	239.13	2.79	236.34	4.69E-03	0.304	2.16
40	90	10428	115.87	2.03	113.84	2.26E-03	0.392	1.60
50	200	11765	58.83	1.46	57.37	1.14E-03	0.514	1.55
60	300	8884	29.61	0.96	28.65	5.68E-04	0.630	1.42
70	300	4435	14.78	0.68	14.10	2.80E-04	0.738	1.85
80	300	2492	8.31	0.50	7.81	1.55E-04	0.820	1.75
90	300	1155	3.85	0.35	3.50	6.94E-05	0.909	1.58

Proof of Concept – Case 2 (Beryllium/Polypropylene)

Co-60 Source	Scintillator Thickness (mm)	1

Collected Data	2/7/14	Detector Bias (-kV)	2
Calibration Date	8/1/06	Source Location	center
Initial Activity	396100	Scintillator Location	on axis
Current Activity	147227	Material	beryllium/polypropylene
Slope [mV/MeV]	214.52	σ-slope [mV/MeV]	1.65
Intercept [mV]	-9.43	σ-Intercept [mV]	2.94
R^2	0.992	σ-Linear Fit (Std. Dev.) [mV]	5.18

Disc (mV)	Time (Sec.)	Total Counts	$\frac{Counts}{Sec.}$	$\frac{BG}{Sec.}$	$\frac{Net\ Cts.}{Sec.}$	$\frac{(C-B)}{A_o}$	MeV Calc.	Disc. Error %
20	5	19036	3807.2	2.83	3804.3	2.58E-02	0.078	10.04
40	5	13074	2614.8	1.39	2613.4	1.78E-02	0.213	4.14
60	10	16099	1609.9	0.65	1609.2	1.09E-02	0.322	2.59
80	10	9665	966.5	0.35	966.15	6.56E-03	0.423	2.05
100	20	11346	567.30	0.22	567.08	3.85E-03	0.524	1.56
120	30	9404	313.47	0.26	313.21	2.13E-03	0.629	1.93
140	60	12178	202.97	0.15	202.82	1.38E-03	0.700	1.22
160	100	10979	109.79	0.10	109.69	7.45E-04	0.793	1.34
180	200	12142	60.71	0.08	60.63	4.12E-04	0.869	1.62
200	300	10299	34.33	0.08	34.25	2.33E-04	0.925	1.51
220	300	5035	16.78	0.00	16.78	1.14E-04	0.986	2.35
240	300	3045	10.15	0.00	10.15	6.89E-05	1.028	2.08

Cl-36 Source		Scintillator Thickness (mm)	1
Collected Data	5/23/14	Detector Bias (-kV)	2
Calibration Date	10/31/77	Source Location	center
Initial Activity	773.3	Scintillator Location	on axis
Current Activity	773	Material	beryllium/polypropylene
Slope [mV/MeV]	185.90	σ-slope [mV/MeV]	1.32
Intercept [mV]	-8.73	σ-Intercept [mV]	2.73
R^2	0.995	σ-Linear Fit (Std. Dev.) [mV]	2.30

Disc (mV)	Time (Sec.)	Total Counts	$\frac{Counts}{Sec.}$	$\frac{BG}{Sec.}$	$\frac{Net\ Cts.}{Sec.}$	$\frac{(C-B)}{A_o}$	MeV Calc.	Disc. Error %
20	30	11906	396.87	2.83	394.04	5.10E-01	0.105	6.44
40	50	11152	223.04	1.39	221.65	2.87E-01	0.254	2.17
60	100	9001	90.01	0.65	89.36	1.16E-01	0.377	1.12
80	300	7411	24.70	0.35	24.35	3.15E-02	0.489	0.78
100	300	1661	5.54	0.22	5.32	6.88E-03	0.580	0.49

Sr-90 Source		Scintillator Thickness (mm)	1
Collected Data	2/7/14	Detector Bias (-kV)	2
Calibration Date	3/15/94	Source Location	center

Initial Activity		367	Scintillator Location			on axis		
Current Activity		226	Material			beryllium/polypropylene		
Slope [mV/MeV]			193.96	σ-slope [mV/MeV]				1.50
Intercept [mV]			-3.35	σ-Intercept [mV]				2.85
R^2			0.999	σ-Linear Fit (Std. Dev.) [mV]				1.95
Disc (mV)	Time (Sec.)	Total Counts	$\frac{Counts}{Sec.}$	$\frac{BG}{Sec.}$	$\frac{Net\ Cts.}{Sec.}$	$\frac{(C-B)}{A_o}$	MeV Calc.	Disc. Error %
20	40	8984	224.60	2.83	221.77	9.81E-01	0.119	12.60
40	70	10684	152.63	1.39	151.24	6.69E-01	0.228	3.47
60	100	8838	88.38	0.65	87.73	3.88E-01	0.330	2.42
80	200	10825	54.13	0.35	53.78	2.38E-01	0.418	1.64
100	300	9803	32.68	0.22	32.46	1.44E-01	0.530	1.49
120	300	6211	20.70	0.26	20.44	9.04E-02	0.651	1.76
140	300	4197	13.99	0.15	13.84	6.12E-02	0.752	1.90
160	300	2979	9.93	0.10	9.83	4.35E-02	0.838	1.56
180	300	1953	6.51	0.08	6.43	2.84E-02	0.942	1.31

Proof of Concept – Case 3(Polypropylene/Polypropylene)

Cl-36 Source			Scintillator Thickness (mm)			1		
Collected Data		2/6/14	Detector Bias (-kV)			2		
Calibration Date		10/31/77	Source Location			center		
Initial Activity		773.3	Scintillator Location			on axis		
Current Activity		773	Material			polypropylene/polypropylene		
Slope [mV/MeV]			300.48	σ-slope [mV/MeV]				1.46
Intercept [mV]			-0.80	σ-Intercept [mV]				3.15
R^2			0.997	σ-Linear Fit (Std. Dev.) [mV]				2.79
Disc (mV)	Time (Sec.)	Total Counts	$\frac{Counts}{Sec.}$	$\frac{BG}{Sec.}$	$\frac{Net\ Cts.}{Sec.}$	$\frac{(C-B)}{A_o}$	MeV Calc.	Disc. Error %
20	20	9057	452.85	2.83	450.02	5.82E-01	0.053	18.07
40	30	11008	366.93	1.39	365.54	4.73E-01	0.131	5.75
60	40	11008	275.20	0.65	274.55	3.55E-01	0.211	3.09
80	60	11478	191.30	0.35	190.95	2.47E-01	0.280	1.82
100	80	9701	121.26	0.22	121.04	1.57E-01	0.342	1.27
120	100	7082	70.82	0.26	70.56	9.13E-02	0.400	0.84
140	200	6784	33.92	0.15	33.77	4.37E-02	0.466	0.54
160	300	2580	8.60	0.10	8.50	1.10E-02	0.553	0.88
180	300	911	3.04	0.08	2.96	3.82E-03	0.601	0.45

Co-60 Source	Scintillator Thickness (mm)	1

Collected Data		10/21/13	Detector Bias (-kV)					2
Calibration Date		8/1/2006	Source Location					center
Initial Activity		396100	Scintillator Location					on axis
Current Activity		153124	Material					polypropylene/polypropylene
Slope [mV/MeV]			334.73	σ-slope [mV/MeV]				2.03
Intercept [mV]			-14.08	σ-Intercept [mV]				3.65
R^2			0.993	σ-Linear Fit (Std. Dev.) [mV]				7.69
Disc (mV)	Time (Sec.)	Total Counts	$\frac{Counts}{Sec.}$	$\frac{BG}{Sec.}$	$\frac{Net\ Cts.}{Sec.}$	$\frac{(C-B)}{A_o}$	MeV Calc.	Disc. Error %
20	3	12119	4039.67	2.83	4036.84	2.64E-02	0.009	18.49
40	4	13341	3335.25	1.39	3333.86	2.18E-02	0.092	8.64
60	4	10454	2613.50	0.65	2612.85	1.71E-02	0.187	4.96
80	5	10080	2016.00	0.35	2015.65	1.32E-02	0.254	3.09
100	8	12163	1520.38	0.22	1520.16	9.93E-03	0.317	2.64
120	10	11081	1108.10	0.26	1107.84	7.23E-03	0.383	2.36
140	10	8024	802.40	0.15	802.25	5.24E-03	0.446	1.90
160	20	11922	596.10	0.10	596.00	3.89E-03	0.502	1.67
180	30	12898	429.93	0.08	429.85	2.81E-03	0.564	1.53
200	40	12444	311.10	0.08	311.02	2.03E-03	0.621	1.27
220	40	8604	215.10		215.10	1.40E-03	0.681	1.53
240	50	7462	149.24		149.24	9.75E-04	0.738	1.31
260	80	8220	102.75		102.75	6.71E-04	0.792	1.57
280	100	6787	67.87		67.87	4.43E-04	0.845	1.64
300	200	9005	45.03		45.03	2.94E-04	0.893	1.76
350	300	4486	14.95		14.95	9.77E-05	0.993	1.55
400	600	3139	5.23		5.23	3.42E-05	1.068	1.70

Pb-210 Source			Scintillator Thickness (mm)					1
Collected Data		1/14/14	Detector Bias (-kV)					2
Calibration Date		3/15/94	Source Location					center
Initial Activity		372	Scintillator Location					on axis
Current Activity		200.72	Material					polypropylene/polypropylene
Slope [mV/MeV]			301.58	σ-slope [mV/MeV]				3.47
Intercept [mV]			8.68	σ-Intercept [mV]				9.14
R^2			0.999	σ-Linear Fit (Std. Dev.) [mV]				0.95
Disc (mV)	Time (Sec.)	Total Counts	$\frac{Counts}{Sec.}$	$\frac{BG}{Sec.}$	$\frac{Net\ Cts.}{Sec.}$	$\frac{(C-B)}{A_o}$	MeV Calc.	Disc. Error %
20	100	10700	107.00	2.83	104.17	5.19E-01	0.001	28.20
40	100	8906	89.06	1.39	87.67	4.37E-01	0.085	13.30
60	200	14028	70.14	0.65	69.49	3.46E-01	0.167	5.06
80	200	9866	49.33	0.35	48.98	2.44E-01	0.240	3.57

100	300	10295	34.32	0.22	34.10	1.70E-01	0.302	2.46
120	300	6586	21.95	0.26	21.69	1.08E-01	0.372	2.12
140	300	4256	14.19	0.15	14.04	6.99E-02	0.433	1.60
160	300	2502	8.34	0.10	8.24	4.11E-02	0.502	1.32

Sr-90 Source			Scintillator Thickness (mm)			1		
Collected Data		1/14/14	Detector Bias (-kV)			2		
Calibration Date		3/15/94	Source Location			center		
Initial Activity		367	Scintillator Location			on axis		
Current Activity		226.47	Material			polypropylene/polypropylene		
Slope [mV/MeV]			313.82	σ-slope [mV/MeV]				2.14
Intercept [mV]			-4.35	σ-Intercept [mV]				5.06
R^2			1.000	σ-Linear Fit (Std. Dev.) [mV]				1.30
Disc (mV)	Time (Sec.)	Total Counts	$\frac{Counts}{Sec.}$	$\frac{BG}{Sec.}$	$\frac{Net\ Cts.}{Sec.}$	$\frac{(C-B)}{A_o}$	MeV Calc.	Disc. Error %
20	40	9804	245.10	2.83	242.27	1.07E+00	0.058	18.23
40	50	10192	203.84	1.39	202.45	8.94E-01	0.144	8.63
60	60	9654	160.90	0.65	160.25	7.08E-01	0.209	3.86
80	70	8428	120.40	0.35	120.05	5.30E-01	0.269	2.36
100	90	7532	83.69	0.22	83.47	3.69E-01	0.335	2.11
120	200	12287	61.44	0.26	61.18	2.70E-01	0.391	1.39
140	200	8875	44.38	0.15	44.23	1.95E-01	0.458	1.69
160	300	10137	33.79	0.10	33.69	1.49E-01	0.523	1.60
180	300	7995	26.65	0.08	26.57	1.17E-01	0.585	1.32
200	300	6112	20.37	0.08	20.29	8.96E-02	0.658	1.18

Proof of Concept – Case 4 (Mylar)

Sr-90 Source			Scintillator Thickness (mm)			1		
Collected Data		4/24/14	Detector Bias (-kV)			2		
Calibration Date		3/15/94	Source Location			center		
Initial Activity		367	Scintillator Location			on axis		
Current Activity		224.96	Material			Mylar Wrap		
Slope [mV/MeV]			322.84	σ-slope [mV/MeV]				1.74
Intercept [mV]			-6.26	σ-Intercept [mV]				3.52
R^2			1.000	σ-Linear Fit (Std. Dev.) [mV]				1.42
Disc (mV)	Time (Sec.)	Total Counts	$\frac{Counts}{Sec.}$	$\frac{BG}{Sec.}$	$\frac{Net\ Cts.}{Sec.}$	$\frac{(C-B)}{A_o}$	MeV Calc.	Disc. Error %
20	50	11619	232.38	2.83	229.55	1.02E+00	0.065	24.71
40	100	20006	200.06	1.39	198.67	8.83E-01	0.142	8.95

60	100	15860	158.60	0.65	157.95	7.02E-01	0.208	3.59
80	100	11538	115.38	0.35	115.03	5.11E-01	0.272	2.76
100	200	16858	84.29	0.22	84.07	3.74E-01	0.330	2.02
120	200	12327	61.64	0.26	61.38	2.73E-01	0.387	1.79
140	200	9153	45.77	0.15	45.62	2.03E-01	0.445	1.52
160	300	10182	33.94	0.10	33.84	1.50E-01	0.517	1.96
180	300	8084	26.95	0.08	26.87	1.19E-01	0.578	1.71
200	300	6332	21.11	0.08	21.03	9.35E-02	0.643	1.53
220	300	4893	16.31	0.00	16.31	7.25E-02	0.710	1.98
240	300	3983	13.28	0.00	13.28	5.90E-02	0.763	1.61
260	300	3105	10.35	0.00	10.35	4.60E-02	0.826	1.63
280	300	2442	8.14	0.00	8.14	3.62E-02	0.885	1.53
300	300	1884	6.28	0.00	6.28	2.79E-02	0.947	1.35

Bias Correlation – Case 1 (Beryllium/Beryllium)

Co60 Source			Scintillator Thickness (mm)					1
Collected Data		8/20/14	Detector Bias (-kV)					1.9
Calibration Date		8/1/2006	Source Location					center
Initial Activity		396100	Scintillator Location					on axis
Current Activity		137289	Material					beryllium/beryllium
Slope [mV/MeV]			67.68	σ-slope [mV/MeV]				0.66
Intercept [mV]			7.23	σ-Intercept [mV]				1.73
R^2			1.000	σ-Linear Fit (Std. Dev.) [mV]				0.34
Disc (mV)	Time (Sec.)	Total Counts	$\frac{Counts}{Sec.}$	$\frac{BG}{Sec.}$	$\frac{Net\ Cts.}{Sec.}$	$\frac{(C-B)}{A_o}$	MeV Calc.	Disc. Error %
20	10	7706	770.60	1.49	769.11	5.60E-03	0.187	2.21
30	50	12036	240.72	0.73	239.99	1.75E-03	0.342	1.66
40	100	7793	77.93	0.34	77.59	5.65E-04	0.480	1.56
50	300	6206	20.69	0.17	20.52	1.49E-04	0.632	1.43

Co60 Source		Scintillator Thickness (mm)		1
Collected Data	8/20/14	Detector Bias (-kV)		2.0
Calibration Date	8/1/2006	Source Location		center
Initial Activity	396100	Scintillator Location		on axis
Current Activity	137289	Material		beryllium/beryllium
Slope [mV/MeV]		96.29	σ-slope [mV/MeV]	0.64
Intercept [mV]		7.58	σ-Intercept [mV]	1.80
R^2		1.000	σ-Linear Fit (Std. Dev.) [mV]	0.45

Disc (mV)	Time (Sec.)	Total Counts	$\frac{Counts}{Sec.}$	$\frac{BG}{Sec.}$	$\frac{Net\ Cts.}{Sec.}$	$\frac{(C-B)}{A_o}$	MeV Calc.	Disc. Error %
20	10	11702	1170.20	2.82	1167.38	8.50E-03	0.133	2.84
30	20	11257	562.85	1.62	561.23	4.09E-03	0.230	2.05
40	50	13017	260.34	1.09	259.25	1.89E-03	0.333	1.55
50	100	10929	109.29	0.52	108.77	7.92E-04	0.439	1.38
60	200	8406	42.03	0.23	41.80	3.04E-04	0.550	1.59
70	300	5090	16.97		16.97	1.24E-04	0.651	1.56

Co60 Source		Scintillator Thickness (mm)	1
Collected Data	8/20/14	Detector Bias (-kV)	2.1
Calibration Date	8/1/2006	Source Location	center
Initial Activity	396100	Scintillator Location	on axis
Current Activity	137289	Material	beryllium/beryllium
Slope [mV/MeV]	129.79	σ-slope [mV/MeV]	1.00
Intercept [mV]	9.92	σ-Intercept [mV]	2.82
R^2	1.000	σ-Linear Fit (Std. Dev.) [mV]	0.48

Disc (mV)	Time (Sec.)	Total Counts	$\frac{Counts}{Sec.}$	$\frac{BG}{Sec.}$	$\frac{Net\ Cts.}{Sec.}$	$\frac{(C-B)}{A_o}$	MeV Calc.	Disc. Error %
20	10	15220	1522.00	6.37	1515.63	1.10E-02	0.096	5.11
30	10	9525	952.50	2.60	949.90	6.92E-03	0.158	2.88
40	20	11196	559.80	1.84	557.96	4.06E-03	0.231	2.04
50	30	9620	320.67	1.01	319.66	2.33E-03	0.304	1.76
60	50	8450	169.00	0.47	168.53	1.23E-03	0.386	1.48
70	100	8773	87.73	0.37	87.36	6.36E-04	0.465	1.62
80	200	8961	44.81	0.25	44.56	3.25E-04	0.544	1.67
90	300	7270	24.23		24.23	1.77E-04	0.613	1.94

Co60 Source		Scintillator Thickness (mm)	1
Collected Data	8/20/14	Detector Bias (-kV)	2.2
Calibration Date	8/1/2006	Source Location	center
Initial Activity	396100	Scintillator Location	on axis
Current Activity	137289	Material	beryllium/beryllium
Slope [mV/MeV]	180.92	σ-slope [mV/MeV]	1.05
Intercept [mV]	9.87	σ-Intercept [mV]	2.63
R^2	0.999	σ-Linear Fit (Std. Dev.) [mV]	2.32

Disc (mV)	Time (Sec.)	Total Counts	$\frac{Counts}{Sec.}$	$\frac{BG}{Sec.}$	$\frac{Net\ Cts.}{Sec.}$	$\frac{(C-B)}{A_o}$	MeV Calc.	Disc. Error %
20	10	19326	1932.60	45.31	1887.29	1.37E-02	0.043	6.09
30	10	13170	1317.00	4.81	1312.19	9.56E-03	0.118	3.55
40	10	9022	902.20	3.64	898.56	6.55E-03	0.166	2.84

50	20	12208	610.40	1.94	608.46	4.43E-03	0.219	1.99
60	30	11698	389.93	1.48	388.45	2.83E-03	0.280	1.75
70	40	10023	250.58	0.89	249.69	1.82E-03	0.337	1.47
80	90	13772	153.02	0.73	152.29	1.11E-03	0.397	1.59
90	100	10142	101.42	0.40	101.02	7.36E-04	0.447	1.43
100	100	6321	63.21	0.33	62.88	4.58E-04	0.502	4.05
110	200	10357	51.79	0.27	51.52	3.75E-04	0.528	0.90
120	300	6563	21.88	0.29	21.59	1.57E-04	0.627	0.96

Co60 Source			Scintillator Thickness (mm)					1
Collected Data		8/20/14	Detector Bias (-kV)					2.3
Calibration Date		8/1/2006	Source Location					center
Initial Activity		396100	Scintillator Location					on axis
Current Activity		137289	Material					beryllium/beryllium
Slope [mV/MeV]			242.06	σ-slope [mV/MeV]				1.49
Intercept [mV]			9.84	σ-Intercept [mV]				4.54
R^2			1.000	σ-Linear Fit (Std. Dev.) [mV]				0.87
Disc (mV)	Time (Sec.)	Total Counts	$\frac{Counts}{Sec.}$	$\frac{BG}{Sec.}$	$\frac{Net\ Cts.}{Sec.}$	$\frac{(C-B)}{A_o}$	MeV Calc.	Disc. Error %
20	10	22241	2224.10	189.94	2034.16	1.48E-02	0.018	9.46
40	10	12549	1254.90	5.08	1249.82	9.10E-03	0.125	3.38
60	20	13483	674.15	2.67	671.48	4.89E-03	0.203	2.47
80	30	10584	352.80	1.78	351.02	2.56E-03	0.292	1.83
100	50	9154	183.08		183.08	1.33E-03	0.376	1.78
120	100	9366	93.66		93.66	6.82E-04	0.456	1.93
140	200	9646	48.23		48.23	3.51E-04	0.536	1.69
160	300	7147	23.82		23.82	1.74E-04	0.616	1.86

Bias Correlation – Case 3 (Polypropylene/Polypropylene)

Cl-36 Source			Scintillator Thickness (mm)					1
Collected Data		2/6/14	Detector Bias (-kV)					1.8
Calibration Date		10/31/77	Source Location					Center
Initial Activity		773.3	Scintillator Location					on axis
Current Activity		773	Material					Polypropylene/polypropylene
Slope [mV/MeV]			160.98	σ-slope [mV/MeV]				1.13
Intercept [mV]			-5.35	σ-Intercept [mV]				2.10
R^2			0.990	σ-Linear Fit (Std. Dev.) [mV]				3.19
Disc (mV)	Time (Sec.)	Total Counts	$\frac{Counts}{Sec.}$	$\frac{BG}{Sec.}$	$\frac{Net\ Cts.}{Sec.}$	$\frac{(C-B)}{A_o}$	MeV Calc.	Disc. Error %

20	30	11994	399.80	1.21	398.59	5.15E-01	0.101	5.73
40	40	8152	203.80	0.39	203.41	2.63E-01	0.270	1.88
60	100	5942	59.42	0.16	59.26	7.66E-02	0.418	1.04
80	300	2699	9.00	0.12	8.88	1.15E-02	0.550	0.84
100	300	244	0.81	0.00	0.81	1.05E-03	0.647	0.44

Cl-36 Source			Scintillator Thickness (mm)					1
Collected Data		2/6/14	Detector Bias (-kV)					1.9
Calibration Date		10/31/77	Source Location					Center
Initial Activity		773.3	Scintillator Location					on axis
Current Activity		773	Material					Polypropylene/polypropylene
Slope [mV/MeV]			227.99	σ-slope [mV/MeV]				1.17
Intercept [mV]			-6.91	σ-Intercept [mV]				2.33
R^2			0.995	σ-Linear Fit (Std. Dev.) [mV]				2.91
Disc (mV)	Time (Sec.)	Total Counts	$\frac{Counts}{Sec.}$	$\frac{BG}{Sec.}$	$\frac{Net\ Cts.}{Sec.}$	$\frac{(C-B)}{A_o}$	MeV Calc.	Disc. Error %
20	30	12882	429.40	2.01	427.39	5.53E-01	0.074	8.96
40	40	11953	298.83	0.95	297.88	3.85E-01	0.191	3.34
60	60	10509	175.15	0.45	174.70	2.26E-01	0.293	1.46
80	100	7482	74.82	0.23	74.59	9.65E-02	0.395	1.03
100	200	5816	29.08	0.13	28.95	3.74E-02	0.478	0.77
120	300	2426	8.09	0.13	7.96	1.03E-02	0.557	0.79
140	300	362	1.21	0.06	1.15	1.48E-03	0.639	0.43

Cl-36 Source			Scintillator Thickness (mm)					1
Collected Data		2/6/14	Detector Bias (-kV)					2.1
Calibration Date		10/31/77	Source Location					Center
Initial Activity		773.3	Scintillator Location					on axis
Current Activity		773	Material					Polypropylene/polypropylene
Slope [mV/MeV]			415.61	σ-slope [mV/MeV]				2.10
Intercept [mV]			-4.52	σ-Intercept [mV]				5.24
R^2			0.986	σ-Linear Fit (Std. Dev.) [mV]				7.72
Disc (mV)	Time (Sec.)	Total Counts	$\frac{Counts}{Sec.}$	$\frac{BG}{Sec.}$	$\frac{Net\ Cts.}{Sec.}$	$\frac{(C-B)}{A_o}$	MeV Calc.	Disc. Error %
20	20	9306	465.30	3.99	461.31	5.97E-01	0.040	29.84
40	30	12414	413.80	2.07	411.73	5.32E-01	0.089	9.54
60	40	14106	352.65	0.90	351.75	4.55E-01	0.144	4.31
80	40	11127	278.18	0.62	277.56	3.59E-01	0.208	3.53
100	50	11142	222.84	0.53	222.31	2.88E-01	0.254	2.19
120	60	9914	165.23	0.45	164.78	2.13E-01	0.301	1.45
140	80	9119	113.99	0.28	113.71	1.47E-01	0.349	1.04

160	100	7278	72.78	0.30	72.48	9.37E-02	0.398	0.70
180	200	7576	37.88	0.25	37.63	4.87E-02	0.456	0.58
200	300	4934	16.45	0.13	16.32	2.11E-02	0.517	1.26
250	300	1760	5.87	0.00	5.87	7.59E-03	0.576	0.79

Cl-36 Source			Scintillator Thickness (mm)			1		
Collected Data		2/6/14	Detector Bias (-kV)			2.2		
Calibration Date		10/31/77	Source Location			Center		
Initial Activity		773.3	Scintillator Location			on axis		
Current Activity		773	Material			Polypropylene/polypropylene		
Slope [mV/MeV]			617.05	σ-slope [mV/MeV]				2.22
Intercept [mV]			-18.63	σ-Intercept [mV]				5.10
R^2			0.994	σ-Linear Fit (Std. Dev.) [mV]				7.20
Disc (mV)	Time (Sec.)	Total Counts	$\frac{Counts}{Sec.}$	$\frac{BG}{Sec.}$	$\frac{Net\ Cts.}{Sec.}$	$\frac{(C-B)}{A_o}$	MeV Calc.	Disc. Error %
20	20	10363	518.15	17.25	500.90	6.48E-01	#N/A	#N/A
40	30	13382	446.07	3.04	443.03	5.73E-01	0.051	12.76
60	30	11961	398.70	1.62	397.08	5.14E-01	0.095	8.23
80	40	14154	353.85	1.10	352.75	4.56E-01	0.137	4.94
100	40	12248	306.20	0.81	305.39	3.95E-01	0.179	3.91
120	40	10542	263.55	0.67	262.88	3.40E-01	0.216	2.24
140	50	10438	208.76	0.63	208.13	2.69E-01	0.262	2.18
160	60	10214	170.23	0.39	169.84	2.20E-01	0.294	1.40
180	70	9099	129.99	0.37	129.62	1.68E-01	0.332	1.41
200	90	9126	101.40	0.33	101.07	1.31E-01	0.362	1.22
250	200	9029	45.15	0.00	45.15	5.84E-02	0.440	0.70
300	300	4553	15.18	0.00	15.18	1.96E-02	0.521	0.71
350	300	1228	4.09	0.00	4.09	5.29E-03	0.590	0.41

Cl-36 Source			Scintillator Thickness (mm)			1		
Collected Data		2/6/14	Detector Bias (-kV)			2.3		
Calibration Date		10/31/77	Source Location			Center		
Initial Activity		773.3	Scintillator Location			on axis		
Current Activity		773	Material			Polypropylene/polypropylene		
Slope [mV/MeV]			770.15	σ-slope [mV/MeV]				3.04
Intercept [mV]			-11.62	σ-Intercept [mV]				7.43
R^2			0.996	σ-Linear Fit (Std. Dev.) [mV]				8.06
Disc (mV)	Time (Sec.)	Total Counts	$\frac{Counts}{Sec.}$	$\frac{BG}{Sec.}$	$\frac{Net\ Cts.}{Sec.}$	$\frac{(C-B)}{A_o}$	MeV Calc.	Disc. Error %
20	20	12213	610.65	130.30	480.35	6.21E-01	0.017	87.47
40	30	14044	468.13	4.57	463.56	6.00E-01	0.037	17.41

60	30	12865	428.83	2.53	426.30	5.51E-01	0.075	8.42
80	30	11476	382.53	1.69	380.84	4.93E-01	0.117	10.38
100	40	14279	356.98	1.35	355.63	4.60E-01	0.140	6.12
120	40	13034	325.85	0.94	324.91	4.20E-01	0.167	4.31
140	40	11691	292.28	0.91	291.37	3.77E-01	0.196	4.04
160	50	13168	263.36	0.58	262.78	3.40E-01	0.220	2.06
180	50	11031	220.62	0.43	220.19	2.85E-01	0.256	2.37
200	60	11520	192.00	0.51	191.49	2.48E-01	0.279	1.73
250	80	9510	118.88	0.00	118.88	1.54E-01	0.344	1.11
300	200	12825	64.13	0.00	64.13	8.29E-02	0.410	0.70
350	300	7936	26.45	0.00	26.45	3.42E-02	0.485	0.68
400	300	3561	11.87	0.00	11.87	1.54E-02	0.537	0.79
450	300	1667	5.56	0.00	5.56	7.19E-03	0.578	0.64

¼ and ½ mm Scintillator

Co-60 Source			Scintillator Thickness (mm)			1/4		
Collected Data		3/13/14	Detector Bias (-kV)			2		
Calibration Date		8/1/2006	Source Location			Center		
Initial Activity		396100	Scintillator Location			on axis		
Current Activity		148506	Material			Polypropylene/polypropylene		
Slope [mV/MeV]			283.72	σ-slope [mV/MeV]				8.51
Intercept [mV]			2.18	σ-Intercept [mV]				27.29
R^2			0.998	σ-Linear Fit (Std. Dev.) [mV]				2.35
Disc (mV)	Time (Sec.)	Total Counts	$\frac{Counts}{Sec.}$	$\frac{BG}{Sec.}$	$\frac{Net\ Cts.}{Sec.}$	$\frac{(C-B)}{A_o}$	MeV Calc.	Disc. Error %
20	5	10150	2030.00	2.26	2027.74	1.39E-02	0.052	12.73
40	10	9186	918.60	0.80	917.80	6.31E-03	0.123	7.34
60	20	8644	432.20	0.29	431.91	2.97E-03	0.203	7.59
80	50	10215	204.30	0.14	204.16	1.40E-03	0.277	7.12
100	100	10068	100.68	0.10	100.59	6.92E-04	0.345	7.13
120	200	10315	51.58	0.00	51.58	3.55E-04	0.411	9.17
140	300	7227	24.09	0.00	24.09	1.66E-04	0.486	10.62
160	300	3476	11.59	0.00	11.59	7.97E-05	0.550	9.09
180	300	1593	5.31	0.00	5.31	3.65E-05	0.644	20.77
200	300	749	2.50	0.00	2.50	1.72E-05	0.704	14.38

Sr-90 Source		Scintillator Thickness (mm)	1/4
Collected Data	3/24/14	Detector Bias (-kV)	2

Calibration Date	3/15/94	Source Location	Center
Initial Activity	367	Scintillator Location	on axis
Current Activity	225.43	Material	Polypropylene/polypropylene
Slope [mV/MeV]	336.35	σ-slope [mV/MeV]	1.35
Intercept [mV]	-10.60	σ-Intercept [mV]	4.86
R^2	0.998	σ-Linear Fit (Std. Dev.) [mV]	1.69

Disc (mV)	Time (Sec.)	Total Counts	$\frac{Counts}{Sec.}$	$\frac{BG}{Sec.}$	$\frac{Net\ Cts.}{Sec.}$	$\frac{(C-B)}{A_o}$	MeV Calc.	Disc. Error %
20	100	15588	155.88	2.26	153.62	6.81E-01	0.090	4.82
40	200	17021	85.11	0.80	84.31	3.74E-01	0.148	2.15
60	200	8954	44.77	0.29	44.48	1.97E-01	0.212	2.02
80	300	7256	24.19	0.14	24.05	1.07E-01	0.276	1.69
100	500	7026	14.05	0.10	13.96	6.19E-02	0.333	1.49
120	600	5183	8.64	0.00	8.64	3.83E-02	0.386	1.32
140	600	3205	5.34	0.00	5.34	2.37E-02	0.443	1.06

Co-60 Source		Scintillator Thickness (mm)	1/4
Collected Data	9/20/14	Detector Bias (-kV)	2.3
Calibration Date	8/1/2006	Source Location	Center
Initial Activity	396100	Scintillator Location	on axis
Current Activity	135764	Material	beryllium/beryllium
Slope [mV/MeV]	138.70	σ-slope [mV/MeV]	0.84
Intercept [mV]	3.43	σ-Intercept [mV]	3.80
R^2	0.989	σ-Linear Fit (Std. Dev.) [mV]	2.02

Disc (mV)	Time (Sec.)	Total Counts	$\frac{Counts}{Sec.}$	$\frac{BG}{Sec.}$	$\frac{Net\ Cts.}{Sec.}$	$\frac{(C-B)}{A_o}$	MeV Calc.	Disc. Error %
20	20	12413	620.65	33.82	586.83	4.32E-03	0.063	2.57
30	50	10467	209.34	4.08	205.26	1.51E-03	0.148	3.37
40	90	10369	115.21	2.42	112.79	8.31E-04	0.204	2.60
50	200	11846	59.23	1.84	57.39	4.23E-04	0.269	2.31
60	200	5853	29.27	1.27	28.00	2.06E-04	0.334	2.07
70	300	3917	13.06	0.90	12.16	8.95E-05	0.403	2.41

Co-60 Source		Scintillator Thickness (mm)	1/2
Collected Data	6/27/14	Detector Bias (-kV)	2
Calibration Date	8/1/2006	Source Location	Center
Initial Activity	396100	Scintillator Location	on axis
Current Activity	139985	Material	Polypropylene/polypropylene
Slope [mV/MeV]	354.49	σ-slope [mV/MeV]	1.55
Intercept [mV]	-9.08	σ-Intercept [mV]	3.74
R^2	0.998	σ-Linear Fit (Std. Dev.) [mV]	4.06

Disc (mV)	Time (Sec.)	Total Counts	$\frac{Counts}{Sec.}$	$\frac{BG}{Sec.}$	$\frac{Net\ Cts.}{Sec.}$	$\frac{(C-B)}{A_o}$	MeV Calc.	Disc. Error %
20	5	13979	2795.80	3.04	2792.76	2.00E-02	0.062	12.89
40	5	10029	2005.80	1.09	2004.71	1.43E-02	0.129	4.54
60	10	13047	1304.70	0.37	1304.33	9.32E-03	0.192	2.96
80	10	8560	856.00	0.16	855.84	6.11E-03	0.256	2.87
100	20	11465	573.25	0.00	573.25	4.10E-03	0.316	2.39
120	30	11807	393.57	0.00	393.57	2.81E-03	0.371	1.96
140	40	10537	263.43	0.00	263.43	1.88E-03	0.427	1.80
160	50	8823	176.46	0.00	176.46	1.26E-03	0.481	1.60
180	80	9109	113.86	0.00	113.86	8.13E-04	0.538	1.54
200	100	7318	73.18	0.00	73.18	5.23E-04	0.593	1.65
220	200	9645	48.23	0.00	48.23	3.44E-04	0.643	1.62
240	300	9333	31.11	0.00	31.11	2.22E-04	0.693	1.54
260	300	5671	18.90	0.00	18.90	1.35E-04	0.748	1.77
280	300	3477	11.59	0.00	11.59	8.28E-05	0.801	2.16
300	300	2155	7.18	0.00	7.18	5.13E-05	0.843	2.29

Sr-90 Source		Scintillator Thickness (mm)	1/2
Collected Data	6/27/14	Detector Bias (-kV)	2
Calibration Date	3/15/94	Source Location	Center
Initial Activity	367	Scintillator Location	on axis
Current Activity	224	Material	Polypropylene/polypropylene

Slope [mV/MeV]	336.35	σ-slope [mV/MeV]	1.35
Intercept [mV]	-10.60	σ-Intercept [mV]	4.86
R^2	0.998	σ-Linear Fit (Std. Dev.) [mV]	1.69

Disc (mV)	Time (Sec.)	Total Counts	$\frac{Counts}{Sec.}$	$\frac{BG}{Sec.}$	$\frac{Net\ Cts.}{Sec.}$	$\frac{(C-B)}{A_o}$	MeV Calc.	Disc. Error %
20	50	12027	240.54	3.04	237.50	1.06E+00	0.062	12.42
40	60	10243	170.72	1.09	169.63	7.57E-01	0.134	3.65
60	80	8201	102.51	0.37	102.14	4.56E-01	0.205	2.75
80	200	12491	62.46	0.16	62.30	2.78E-01	0.272	1.86
100	200	7759	38.80	0.00	38.80	1.73E-01	0.336	1.58
120	300	7318	24.39	0.00	24.39	1.09E-01	0.404	1.68
140	300	4855	16.18	0.00	16.18	7.22E-02	0.476	1.91
160	300	3513	11.71	0.00	11.71	5.23E-02	0.536	1.63
180	300	2432	8.11	0.00	8.11	3.62E-02	0.605	1.77
200	300	1683	5.61	0.00	5.61	2.50E-02	0.675	1.44

Co-60 Source		Scintillator Thickness (mm)	1/2
Collected Data	8/28/14	Detector Bias (-kV)	2.3

Calibration Date		8/1/2006	Source Location					Center
Initial Activity		396100	Scintillator Location					on axis
Current Activity		136893	Material					beryllium/beryllium
Slope [mV/MeV]			179.38	σ-slope [mV/MeV]				1.34
Intercept [mV]			5.50	σ-Intercept [mV]				5.24
R^2			0.999	σ-Linear Fit (Std. Dev.) [mV]				0.64
Disc (mV)	Time (Sec.)	Total Counts	$\frac{Counts}{Sec.}$	$\frac{BG}{Sec.}$	$\frac{Net\ Cts.}{Sec.}$	$\frac{(C-B)}{A_o}$	MeV Calc.	Disc. Error %
20	10	17378	1737.80	15.31	1722.49	1.26E-02	0.067	4.78
30	10	11036	1103.60	3.29	1100.31	8.04E-03	0.140	2.91
40	20	14689	734.45	2.03	732.42	5.35E-03	0.193	2.33
50	20	10188	509.40	1.24	508.16	3.71E-03	0.242	1.62
60	40	12658	316.45	0.65	315.80	2.31E-03	0.305	1.63
70	50	10188	203.76	0.39	203.37	1.49E-03	0.362	1.37
80	90	11422	126.91	0.36	126.55	9.24E-04	0.421	1.31
90	100	8153	81.53		81.53	5.96E-04	0.473	1.34
100	200	10659	53.30		53.30	3.89E-04	0.523	1.20
110	300	10156	33.85		33.85	2.47E-04	0.577	1.03

Source Location – Case 1 (Beryllium/Beryllium)

Co-60 Source			Scintillator Thickness (mm)					1
Collected Data		5/27/14	Detector Bias (-kV)					2
Calibration Date		8/1/2006	Source Location					Top
Initial Activity		396100	Scintillator Location					on axis
Current Activity		141762	Material					beryllium/beryllium
Slope [mV/MeV]			118.01	σ-slope [mV/MeV]				1.59
Intercept [mV]			4.04	σ-Intercept [mV]				3.10
R^2			0.985	σ-Linear Fit (Std. Dev.) [mV]				4.47
Disc (mV)	Time (Sec.)	Total Counts	$\frac{Counts}{Sec.}$	$\frac{BG}{Sec.}$	$\frac{Net\ Cts.}{Sec.}$	$\frac{(C-B)}{A_o}$	MeV Calc.	Disc. Error %
20	5	10892	2178.40	16.08	2162.32	1.53E-02	0.087	6.19
40	10	9732	973.20	2.03	971.17	6.85E-03	0.295	2.26
60	30	10132	337.73	0.96	336.77	2.38E-03	0.488	1.69
80	100	11337	113.37	0.50	112.87	7.96E-04	0.660	1.81
100	200	7927	39.64	0.25	39.39	2.78E-04	0.804	2.06
120	300	3758	12.53	0.00	12.53	8.84E-05	0.922	2.48
140	300	1126	3.75	0.00	3.75	2.65E-05	1.023	2.31

Co-60 Source	Scintillator Thickness (mm)	1

Collected Data	5/27/14	Detector Bias (-kV)	2
Calibration Date	8/1/2006	Source Location	Bottom
Initial Activity	396100	Scintillator Location	on axis
Current Activity	141762	Material	beryllium/beryllium
Slope [mV/MeV]	80.21	σ-slope [mV/MeV]	4.08
Intercept [mV]	-4.75	σ-Intercept [mV]	6.53
R^2	0.990	σ-Linear Fit (Std. Dev.) [mV]	2.86

Disc (mV)	Time (Sec.)	Total Counts	$\frac{Counts}{Sec.}$	$\frac{BG}{Sec.}$	$\frac{Net\ Cts.}{Sec.}$	$\frac{(C-B)}{A_o}$	MeV Calc.	Disc. Error %
20	10	10913	1091.30	16.08	1075.22	7.58E-03	0.273	3.40
40	40	8784	219.60	2.03	217.57	1.53E-03	0.558	1.97
60	200	8008	40.04	0.96	39.08	2.76E-04	0.807	2.38
80	300	2013	6.71	0.50	6.21	4.38E-05	0.980	3.60
100	300	361	1.20	0.25	0.95	6.72E-06	1.094	8.64

Source Location – Case 2 (Beryllium/Polypropylene)

Cl-36 Source		Scintillator Thickness (mm)	1
Collected Data	5/23/14	Detector Bias (-kV)	2
Calibration Date	10/31/77	Source Location	Top
Initial Activity	773.3	Scintillator Location	on axis
Current Activity	773	Material	beryllium/polypropylene
Slope [mV/MeV]	238.48	σ-slope [mV/MeV]	1.43
Intercept [mV]	-15.43	σ-Intercept [mV]	3.22
R^2	0.983	σ-Linear Fit (Std. Dev.) [mV]	5.41

Disc (mV)	Time (Sec.)	Total Counts	$\frac{Counts}{Sec.}$	$\frac{BG}{Sec.}$	$\frac{Net\ Cts.}{Sec.}$	$\frac{(C-B)}{A_o}$	MeV Calc.	Disc. Error %
20	30	12708	423.60	2.83	420.77	5.44E-01	0.080	7.79
40	40	10951	273.78	1.39	272.39	3.52E-01	0.212	2.92
60	80	11594	144.93	0.65	144.28	1.87E-01	0.320	1.42
80	200	12052	60.26	0.35	59.91	7.75E-02	0.416	0.98
100	300	6792	22.64	0.22	22.42	2.90E-02	0.494	0.72
120	300	2133	7.11	0.26	6.85	8.86E-03	0.566	1.10
140	300	676	2.25	0.15	2.10	2.72E-03	0.619	0.87

Cl-36 Source		Scintillator Thickness (mm)	1
Collected Data	5/23/14	Detector Bias (-kV)	2
Calibration Date	10/31/77	Source Location	Bottom
Initial Activity	773.3	Scintillator Location	on axis
Current Activity	773	Material	beryllium/polypropylene

Slope [mV/MeV]			140.18	σ-slope [mV/MeV]				0.64
Intercept [mV]			-6.72	σ-Intercept [mV]				1.66
R^2			0.973	σ-Linear Fit (Std. Dev.) [mV]				5.23
Disc (mV)	Time (Sec.)	Total Counts	$\frac{Counts}{Sec.}$	$\frac{BG}{Sec.}$	$\frac{Net\ Cts.}{Sec.}$	$\frac{(C-B)}{A_o}$	MeV Calc.	Disc. Error %
20	40	13905	347.63	2.83	344.80	4.46E-01	0.150	4.21
40	80	10360	129.50	1.39	128.11	1.66E-01	0.336	1.47
60	300	8933	29.78	0.65	29.13	3.77E-02	0.478	0.90
80	300	1324	4.41	0.35	4.06	5.25E-03	0.594	2.63

Source Location – Case 3 (Polypropylene/Polypropylene)

Sr-90 Source			Scintillator Thickness (mm)					1
Collected Data		6/27/14	Detector Bias (-kV)					2
Calibration Date		3/15/94	Source Location					Top
Initial Activity		367	Scintillator Location					on axis
Current Activity		224	Material					polypropylene/polypropylene
Slope [mV/MeV]			385.57	σ-slope [mV/MeV]				2.12
Intercept [mV]			-10.31	σ-Intercept [mV]				4.62
R^2			1.000	σ-Linear Fit (Std. Dev.) [mV]				1.57
Disc (mV)	Time (Sec.)	Total Counts	$\frac{Counts}{Sec.}$	$\frac{BG}{Sec.}$	$\frac{Net\ Cts.}{Sec.}$	$\frac{(C-B)}{A_o}$	MeV Calc.	Disc. Error %
20	50	12428	248.56	2.83	245.73	1.10E+00	0.064	23.95
40	80	17177	214.71	1.39	213.32	9.52E-01	0.132	11.08
60	80	14417	180.21	0.65	179.56	8.02E-01	0.187	5.37
80	80	11555	144.44	0.35	144.09	6.43E-01	0.237	3.30
100	100	11162	111.62	0.22	111.40	4.97E-01	0.287	2.33
120	100	8424	84.24	0.26	83.98	3.75E-01	0.338	2.23
140	100	6560	65.60	0.15	65.45	2.92E-01	0.384	1.93
160	200	10099	50.50	0.10	50.40	2.25E-01	0.434	1.49
180	200	7789	38.95	0.08	38.87	1.73E-01	0.492	1.96
200	300	9436	31.45	0.08	31.37	1.40E-01	0.547	1.73
220	300	7649	25.50	0.00	25.50	1.14E-01	0.603	1.82
240	300	6361	21.20	0.00	21.20	9.47E-02	0.653	1.64
260	300	5221	17.40	0.00	17.40	7.77E-02	0.704	1.66
280	300	4325	14.42	0.00	14.42	6.44E-02	0.753	1.45
300	300	3495	11.65	0.00	11.65	5.20E-02	0.807	1.30

Sr-90 Source	Scintillator Thickness (mm)	1

Collected Data		6/27/14	Detector Bias (-kV)					2
Calibration Date		3/15/94	Source Location					Bottom
Initial Activity		367	Scintillator Location					on axis
Current Activity		224	Material					polypropylene/polypropylene
Slope [mV/MeV]			209.27	σ-slope [mV/MeV]				1.52
Intercept [mV]			-2.97	σ-Intercept [mV]				2.73
R^2			1.000	σ-Linear Fit (Std. Dev.) [mV]				1.03
Disc (mV)	Time (Sec.)	Total Counts	$\frac{Counts}{Sec.}$	$\frac{BG}{Sec.}$	$\frac{Net\ Cts.}{Sec.}$	$\frac{(C-B)}{A_o}$	MeV Calc.	Disc. Error %
20	50	11409	228.18	2.83	225.35	1.01E+00	0.107	13.27
40	60	9911	165.18	1.39	163.79	7.31E-01	0.210	4.12
60	70	7255	103.64	0.65	102.99	4.60E-01	0.301	2.75
80	100	6335	63.35	0.35	63.00	2.81E-01	0.390	1.84
100	200	7863	39.32	0.22	39.10	1.75E-01	0.490	1.73
120	300	8114	27.05	0.26	26.79	1.20E-01	0.590	1.70
140	300	5511	18.37	0.15	18.22	8.13E-02	0.692	1.80
160	300	3907	13.02	0.10	12.92	5.77E-02	0.780	1.56
180	300	2742	9.14	0.08	9.06	4.04E-02	0.870	1.40
200	300	1817	6.06	0.08	5.98	2.67E-02	0.971	1.15

Source Location – Case 4 (Mylar)

Sr-90 Source			Scintillator Thickness (mm)					1
Collected Data		4/24/14	Detector Bias (-kV)					2
Calibration Date		3/15/94	Source Location					Top
Initial Activity		367	Scintillator Location					on axis
Current Activity		224.96	Material					Mylar wrap
Slope [mV/MeV]			426.37	σ-slope [mV/MeV]				2.56
Intercept [mV]			-6.98	σ-Intercept [mV]				6.11
R^2			1.000	σ-Linear Fit (Std. Dev.) [mV]				1.17
Disc (mV)	Time (Sec.)	Total Counts	$\frac{Counts}{Sec.}$	$\frac{BG}{Sec.}$	$\frac{Net\ Cts.}{Sec.}$	$\frac{(C-B)}{A_o}$	MeV Calc.	Disc. Error %
20	50	12378	247.56	2.83	244.73	1.09E+00	0.005	37.73
40	60	13282	221.37	1.39	219.98	9.78E-01	0.091	13.23
60	70	13435	191.93	0.65	191.28	8.50E-01	0.156	5.91
80	70	11046	157.80	0.35	157.45	7.00E-01	0.208	4.02
100	80	10099	126.24	0.22	126.02	5.60E-01	0.254	3.16
120	100	10001	100.01	0.26	99.75	4.43E-01	0.297	2.15
140	200	15484	77.42	0.15	77.27	3.43E-01	0.344	1.79
160	200	12157	60.79	0.10	60.69	2.70E-01	0.389	1.70
180	200	9656	48.28	0.08	48.20	2.14E-01	0.434	1.61

200	300	11514	38.38	0.08	38.30	1.70E-01	0.486	1.77
220	300	9564	31.88	0.00	31.88	1.42E-01	0.532	1.76
240	300	7984	26.61	0.00	26.61	1.18E-01	0.580	1.66
260	300	6623	22.08	0.00	22.08	9.81E-02	0.630	1.72
280	300	5566	18.55	0.00	18.55	8.25E-02	0.676	1.73
300	300	4689	15.63	0.00	15.63	6.95E-02	0.721	1.59

Sr-90 Source			Scintillator Thickness (mm)					1
Collected Data		4/24/14	Detector Bias (-kV)					2
Calibration Date		3/15/94	Source Location					Bottom
Initial Activity		367	Scintillator Location					on axis
Current Activity		224.96	Material					Mylar wrap
Slope [mV/MeV]			261.18	σ-slope [mV/MeV]				1.60
Intercept [mV]			-2.36	σ-Intercept [mV]				3.13
R^2			1.000	σ-Linear Fit (Std. Dev.) [mV]				1.19
Disc (mV)	Time (Sec.)	Total Counts	$\frac{Counts}{Sec.}$	$\frac{BG}{Sec.}$	$\frac{Net\ Cts.}{Sec.}$	$\frac{(C-B)}{A_o}$	MeV Calc.	Disc. Error %
20	50	11687	233.74	2.83	230.91	1.03E+00	0.061	17.62
40	50	9311	186.22	1.39	184.83	8.22E-01	0.166	6.29
60	100	13596	135.96	0.65	135.31	6.01E-01	0.240	2.86
80	100	9147	91.47	0.35	91.12	4.05E-01	0.315	2.32
100	200	12181	60.91	0.22	60.69	2.70E-01	0.389	1.75
120	200	8506	42.53	0.26	42.27	1.88E-01	0.462	1.85
140	300	9054	30.18	0.15	30.03	1.33E-01	0.547	1.71
160	300	6752	22.51	0.10	22.41	9.96E-02	0.626	1.77
180	300	5070	16.90	0.08	16.82	7.48E-02	0.701	1.53
200	300	3737	12.46	0.08	12.38	5.50E-02	0.780	1.60
220	300	2742	9.14	0.00	9.14	4.06E-02	0.854	1.74
240	300	2034	6.78	0.00	6.78	3.01E-02	0.928	1.73
260	300	1518	5.06	0.00	5.06	2.25E-02	0.997	1.51

Source Location – ¼ and ½ mm scintillator

Sr-90 Source		Scintillator Thickness (mm)		1/4
Collected Data	3/24/14	Detector Bias (-kV)		2
Calibration Date	3/15/94	Source Location		Top
Initial Activity	367	Scintillator Location		on axis
Current Activity	225.43	Material		polypropylene/polypropylene
Slope [mV/MeV]		504.36	σ-slope [mV/MeV]	2.36
Intercept [mV]		-22.57	σ-Intercept [mV]	8.36

R^2			0.999	σ-Linear Fit (Std. Dev.) [mV]				1.77
Disc (mV)	Time (Sec.)	Total Counts	$\frac{Counts}{Sec.}$	$\frac{BG}{Sec.}$	$\frac{Net\ Cts.}{Sec.}$	$\frac{(C-B)}{A_o}$	MeV Calc.	Disc. Error %
20	50	8470	169.40	2.26	167.14	7.41E-01	0.083	9.94
40	100	11971	119.71	0.80	118.91	5.27E-01	0.115	3.74
60	200	14953	74.77	0.29	74.48	3.30E-01	0.161	2.59
80	200	9595	47.98	0.14	47.84	2.12E-01	0.203	2.30
100	300	9583	31.94	0.10	31.85	1.41E-01	0.245	1.56
120	400	8660	21.65	0.00	21.65	9.60E-02	0.286	1.44
140	600	8926	14.88	0.00	14.88	6.60E-02	0.326	1.61
160	600	6549	10.92	0.00	10.92	4.84E-02	0.358	1.39
180	600	4536	7.56	0.00	7.56	3.35E-02	0.399	0.96

Sr-90 Source		Scintillator Thickness (mm)	1/4
Collected Data	3/24/14	Detector Bias (-kV)	2
Calibration Date	3/15/94	Source Location	Bottom
Initial Activity	367	Scintillator Location	on axis
Current Activity	225.43	Material	polypropylene/polypropylene

Slope [mV/MeV]	298.48	σ-slope [mV/MeV]	1.51
Intercept [mV]	-11.60	σ-Intercept [mV]	5.03
R^2	0.999	σ-Linear Fit (Std. Dev.) [mV]	1.30

Disc (mV)	Time (Sec.)	Total Counts	$\frac{Counts}{Sec.}$	$\frac{BG}{Sec.}$	$\frac{Net\ Cts.}{Sec.}$	$\frac{(C-B)}{A_o}$	MeV Calc.	Disc. Error %
20	100	14205	142.05	2.26	139.79	6.20E-01	0.097	3.91
40	200	13617	68.09	0.80	67.29	2.98E-01	0.172	2.42
60	300	10357	34.52	0.29	34.24	1.52E-01	0.239	1.58
80	400	6904	17.26	0.14	17.12	7.60E-02	0.310	1.63
100	600	5551	9.25	0.10	9.16	4.06E-02	0.380	1.60
120	600	3306	5.51	0.00	5.51	2.44E-02	0.439	1.43
140	600	1961	3.27	0.00	3.27	1.45E-02	0.502	1.44

Sr-90 Source		Scintillator Thickness (mm)	1/2
Collected Data	6/27/14	Detector Bias (-kV)	2
Calibration Date	3/15/94	Source Location	Top
Initial Activity	367	Scintillator Location	on axis
Current Activity	224	Material	polypropylene/polypropylene

Slope [mV/MeV]	435.71	σ-slope [mV/MeV]	1.90
Intercept [mV]	-4.70	σ-Intercept [mV]	5.83
R^2	1.000	σ-Linear Fit (Std. Dev.) [mV]	1.13

Disc (mV)	Time (Sec.)	Total Counts	$\frac{Counts}{Sec.}$	$\frac{BG}{Sec.}$	$\frac{Net\ Cts.}{Sec.}$	$\frac{(C-B)}{A_o}$	MeV Calc.	Disc. Error %

20	50	12439	248.78	3.04	245.74	1.10E+00	0.052	19.49
40	60	12406	206.77	1.09	205.68	9.18E-01	0.103	6.43
60	80	12477	155.96	0.37	155.59	6.95E-01	0.146	3.09
80	100	10939	109.39	0.16	109.23	4.88E-01	0.196	2.40
100	200	15633	78.17	0.00	78.17	3.49E-01	0.242	1.79
120	200	11122	55.61	0.00	55.61	2.48E-01	0.287	1.54
140	200	7832	39.16	0.00	39.16	1.75E-01	0.335	1.84
160	300	8988	29.96	0.00	29.96	1.34E-01	0.374	1.41
180	300	6551	21.84	0.00	21.84	9.75E-02	0.424	1.54
200	300	4971	16.57	0.00	16.57	7.40E-02	0.472	1.87
220	300	3977	13.26	0.00	13.26	5.92E-02	0.512	1.51
240	300	3012	10.04	0.00	10.04	4.48E-02	0.564	1.79
260	300	2385	7.95	0.00	7.95	3.55E-02	0.608	1.64

Sr-90 Source			Scintillator Thickness (mm)			1/2		
Collected Data		6/27/14	Detector Bias (-kV)			2		
Calibration Date		3/15/94	Source Location			Bottom		
Initial Activity		367	Scintillator Location			on axis		
Current Activity		224	Material			polypropylene/polypropylene		
Slope [mV/MeV]			268.99	σ-slope [mV/MeV]				1.47
Intercept [mV]			-0.34	σ-Intercept [mV]				3.97
R^2			1.000	σ-Linear Fit (Std. Dev.) [mV]				0.58
Disc (mV)	Time (Sec.)	Total Counts	$\frac{Counts}{Sec.}$	$\frac{BG}{Sec.}$	$\frac{Net\ Cts.}{Sec.}$	$\frac{(C-B)}{A_o}$	MeV Calc.	Disc. Error %
20	50	11766	235.32	3.04	232.28	1.04E+00	0.069	10.44
40	60	9082	151.37	1.09	150.28	6.71E-01	0.151	3.35
60	80	7131	89.14	0.37	88.77	3.96E-01	0.225	2.40
80	100	5077	50.77	0.16	50.61	2.26E-01	0.298	1.84
100	300	9105	30.35	0.00	30.35	1.35E-01	0.372	1.62
120	300	5797	19.32	0.00	19.32	8.63E-02	0.444	1.41
140	300	3744	12.48	0.00	12.48	5.57E-02	0.524	1.67
160	300	2506	8.35	0.00	8.35	3.73E-02	0.598	1.60
180	300	1695	5.65	0.00	5.65	2.52E-02	0.672	1.48

View Factor – Case 3 Geometry (Polypropylene/Polypropylene)

Co-60 Source		Scintillator Thickness (mm)	1
Collected Data	1/14/14	Detector Bias (-kV)	2
Calibration Date	8/1/2006	Source Location	Center
Initial Activity	396100	Scintillator Location	2 mm off axis

Current Activity		148506	Material			polypropylene/polypropylene		
Slope [mV/MeV]			339.76	σ-slope [mV/MeV]				2.03
Intercept [mV]			-25.79	σ-Intercept [mV]				3.57
R^2			0.992	σ-Linear Fit (Std. Dev.) [mV]				8.11
Disc (mV)	Time (Sec.)	Total Counts	$\frac{Counts}{Sec.}$	$\frac{BG}{Sec.}$	$\frac{Net\ Cts.}{Sec.}$	$\frac{(C-B)}{A_o}$	MeV Calc.	Disc. Error %
20	3	10757	3585.67	2.83	3582.84	2.41E-02	0.101	19.85
40	5	14762	2952.40	1.39	2951.01	1.99E-02	0.176	7.63
60	5	11448	2289.60	0.65	2288.95	1.54E-02	0.244	4.35
80	8	13774	1721.75	0.35	1721.40	1.16E-02	0.308	3.11
100	8	10062	1257.75	0.22	1257.53	8.47E-03	0.374	2.70
120	10	9342	934.20	0.26	933.94	6.29E-03	0.433	2.16
140	20	13599	679.95	0.15	679.80	4.58E-03	0.493	1.64
160	30	14425	480.83	0.10	480.73	3.24E-03	0.556	1.68
180	30	10233	341.10	0.08	341.02	2.30E-03	0.618	1.55
200	40	9583	239.58	0.08	239.50	1.61E-03	0.676	1.46
220	60	10073	167.88		167.88	1.13E-03	0.733	1.33
240	80	9172	114.65		114.65	7.72E-04	0.790	1.32
260	100	7779	77.79		77.79	5.24E-04	0.841	1.40
280	200	10554	52.77		52.77	3.55E-04	0.884	1.47
300	300	10732	35.77		35.77	2.41E-04	0.920	1.98
320	300	7327	24.42		24.42	1.64E-04	0.949	1.68

Co-60 Source			Scintillator Thickness (mm)			1		
Collected Data		1/14/14	Detector Bias (-kV)			2		
Calibration Date		8/1/2006	Source Location			Center		
Initial Activity		396100	Scintillator Location			4 mm off axis		
Current Activity		148506	Material			polypropylene/polypropylene		
Slope [mV/MeV]			320.50	σ-slope [mV/MeV]				2.06
Intercept [mV]			-26.26	σ-Intercept [mV]				3.66
R^2			0.992	σ-Linear Fit (Std. Dev.) [mV]				7.64
Disc (mV)	Time (Sec.)	Total Counts	$\frac{Counts}{Sec.}$	$\frac{BG}{Sec.}$	$\frac{Net\ Cts.}{Sec.}$	$\frac{(C-B)}{A_o}$	MeV Calc.	Disc. Error %
20	3	10940	3646.67	2.83	3643.84	2.45E-02	0.100	15.86
40	5	14384	2876.80	1.39	2875.41	1.94E-02	0.191	7.29
60	5	10958	2191.60	0.65	2190.95	1.48E-02	0.260	4.11
80	8	12739	1592.38	0.35	1592.03	1.07E-02	0.331	3.10
100	10	11701	1170.10	0.22	1169.88	7.88E-03	0.394	2.25
120	20	16652	832.60	0.26	832.34	5.60E-03	0.460	1.90
140	20	11580	579.00	0.15	578.85	3.90E-03	0.530	1.79
160	30	12304	410.13	0.10	410.03	2.76E-03	0.592	1.45

180	40	11209	280.23	0.08	280.15	1.89E-03	0.655	1.56
200	50	9570	191.40	0.08	191.32	1.29E-03	0.717	1.49
220	80	10424	130.30		130.30	8.77E-04	0.774	1.45
240	100	8865	88.65		88.65	5.97E-04	0.826	1.39
260	200	11635	58.18		58.18	3.92E-04	0.877	1.48
280	300	11583	38.61		38.61	2.60E-04	0.919	1.87
300	300	7499	25.00		25.00	1.68E-04	0.952	2.21

Co-60 Source			Scintillator Thickness (mm)					1
Collected Data		1/14/14	Detector Bias (-kV)					2
Calibration Date		8/1/2006	Source Location					Center
Initial Activity		396100	Scintillator Location					6 mm off axis
Current Activity		148506	Material					polypropylene/polypropylene
Slope [mV/MeV]			301.83	σ-slope [mV/MeV]				2.06
Intercept [mV]			-24.06	σ-Intercept [mV]				3.66
R^2			0.994	σ-Linear Fit (Std. Dev.) [mV]				7.64
Disc (mV)	Time (Sec.)	Total Counts	$\frac{Counts}{Sec.}$	$\frac{BG}{Sec.}$	$\frac{Net\ Cts.}{Sec.}$	$\frac{(C-B)}{A_o}$	MeV Calc.	Disc. Error %
20	3	10856	3618.67	2.83	3615.84	2.43E-02	0.104	16.35
40	5	14181	2836.20	1.39	2834.81	1.91E-02	0.196	6.81
60	5	10553	2110.60	0.65	2109.95	1.42E-02	0.269	3.89
80	8	12043	1505.38	0.35	1505.03	1.01E-02	0.342	2.70
100	10	10573	1057.30	0.22	1057.08	7.12E-03	0.414	2.35
120	20	14809	740.45	0.26	740.19	4.98E-03	0.483	1.69
140	20	9928	496.40	0.15	496.25	3.34E-03	0.558	1.87
160	30	10338	344.60	0.10	344.50	2.32E-03	0.622	1.48
180	40	9112	227.80	0.08	227.72	1.53E-03	0.689	1.40
200	60	8984	149.73	0.08	149.65	1.01E-03	0.751	1.35
220	90	8974	99.71		99.71	6.71E-04	0.808	1.42
240	200	12471	62.36		62.36	4.20E-04	0.867	1.53
260	300	12176	40.59		40.59	2.73E-04	0.914	1.85
280	300	7537	25.12		25.12	1.69E-04	0.950	1.49
300	300	4794	15.98		15.98	1.08E-04	0.992	1.58

Co-60 Source		Scintillator Thickness (mm)			1
Collected Data	1/14/14	Detector Bias (-kV)			2
Calibration Date	8/1/2006	Source Location			Center
Initial Activity	396100	Scintillator Location			8 mm off axis
Current Activity	148506	Material			polypropylene/polypropylene
Slope [mV/MeV]		278.84	σ-slope [mV/MeV]		1.90
Intercept [mV]		-18.00	σ-Intercept [mV]		3.33

R^2			0.995	σ-Linear Fit (Std. Dev.) [mV]				5.59
Disc (mV)	Time (Sec.)	Total Counts	$\frac{Counts}{Sec.}$	$\frac{BG}{Sec.}$	$\frac{Net\ Cts.}{Sec.}$	$\frac{(C-B)}{A_o}$	MeV Calc.	Disc. Error %
20	3	11039	3679.67	2.83	3676.84	2.48E-02	0.097	15.30
40	3	8637	2879.00	1.39	2877.61	1.94E-02	0.190	6.54
60	5	10312	2062.40	0.65	2061.75	1.39E-02	0.273	3.65
80	10	14323	1432.30	0.35	1431.95	9.64E-03	0.351	2.38
100	10	9728	972.80	0.22	972.58	6.55E-03	0.429	2.21
120	20	13313	665.65	0.26	665.39	4.48E-03	0.500	1.59
140	20	8796	439.80	0.15	439.65	2.96E-03	0.577	1.61
160	30	8612	287.07	0.10	286.97	1.93E-03	0.648	1.36
180	50	9209	184.18	0.08	184.10	1.24E-03	0.720	1.39
200	100	11546	115.46	0.08	115.38	7.77E-04	0.788	1.36
220	200	14709	73.55		73.55	4.95E-04	0.847	1.27
240	200	8936	44.68		44.68	3.01E-04	0.904	1.91
260	300	8332	27.77		27.77	1.87E-04	0.945	1.55
280	300	5128	17.09		17.09	1.15E-04	0.987	2.02
300	300	3250	10.83		10.83	7.29E-05	1.024	1.95

View Factor – Case 1 Geometry (Beryllium/Beryllium)

Co-60 Source		Scintillator Thickness (mm)		1
Collected Data	5/23/14	Detector Bias (-kV)		2
Calibration Date	8/1/2006	Source Location		Center
Initial Activity	396100	Scintillator Location		2 mm off axis
Current Activity	141762	Material		Beryllium/beryllium
Slope [mV/MeV]		91.85	σ-slope [mV/MeV]	2.35
Intercept [mV]		-0.53	σ-Intercept [mV]	4.03
R^2		0.998	σ-Linear Fit (Std. Dev.) [mV]	1.24

Disc (mV)	Time (Sec.)	Total Counts	$\frac{Counts}{Sec.}$	$\frac{BG}{Sec.}$	$\frac{Net\ Cts.}{Sec.}$	$\frac{(C-B)}{A_o}$	MeV Calc.	Disc. Error %
20	10	15538	1553.80	16.08	1537.72	1.08E-02	0.215	4.18
40	20	9687	484.35	2.03	482.32	3.40E-03	0.439	2.03
60	100	11993	119.93	0.96	118.97	8.39E-04	0.668	1.78
80	200	5452	27.26	0.50	26.76	1.89E-04	0.863	2.22
100	300	1647	5.49	0.25	5.24	3.70E-05	1.003	4.81
120	300	342	1.14	0.00	1.14	8.04E-06	1.085	1.91

Co-60 Source	Scintillator Thickness (mm)	1

Collected Data		5/23/14	Detector Bias (-kV)					2
Calibration Date		8/1/2006	Source Location					Center
Initial Activity		396100	Scintillator Location					4 mm off axis
Current Activity		141762	Material					Beryllium/beryllium
Slope [mV/MeV]			85.62	σ-slope [mV/MeV]				2.46
Intercept [mV]			-0.91	σ-Intercept [mV]				3.95
R^2			0.996	σ-Linear Fit (Std. Dev.) [mV]				1.92
Disc (mV)	Time (Sec.)	Total Counts	$\frac{Counts}{Sec.}$	$\frac{BG}{Sec.}$	$\frac{Net\ Cts.}{Sec.}$	$\frac{(C-B)}{A_o}$	MeV Calc.	Disc. Error %
20	10	15101	1510.10	16.08	1494.02	1.05E-02	0.222	3.78
40	20	7944	397.20	2.03	395.17	2.79E-03	0.475	2.06
60	100	8299	82.99	0.96	82.03	5.79E-04	0.723	1.83
80	300	4461	14.87	0.50	14.37	1.01E-04	0.926	2.41
100	300	712	2.37	0.25	2.12	1.50E-05	1.063	1.97

BLC Geometry

Co-60 Source			Scintillator Thickness (mm)					4 pieces/1 mm
Collected Data		3/24/14	Detector Bias (-kV)					2
Calibration Date		8/1/2006	Source Location					Top
Initial Activity		396100	Scintillator Location					BLC Geometry
Current Activity		144859	Material					Beryllium/polypropylene
Slope [mV/MeV]			277.12	σ-slope [mV/MeV]				1.77
Intercept [mV]			-27.84	σ-Intercept [mV]				3.12
R^2			0.994	σ-Linear Fit (Std. Dev.) [mV]				5.42
Disc (mV)	Time (Sec.)	Total Counts	$\frac{Counts}{Sec.}$	$\frac{BG}{Sec.}$	$\frac{Net\ Cts.}{Sec.}$	$\frac{(C-B)}{A_o}$	MeV Calc.	Disc. Error %
20	2	15460	7730.00	16.23	7713.77	5.32E-02	0.086	8.88
40	2	9925	4962.50	5.56	4956.94	3.42E-02	0.225	4.69
60	5	16316	3263.20	2.22	3260.98	2.25E-02	0.311	2.95
80	5	10586	2117.20	1.07	2116.13	1.46E-02	0.394	2.20
100	10	13781	1378.10	0.54	1377.56	9.51E-03	0.473	1.86
120	20	17964	898.20	0.39	897.81	6.20E-03	0.546	1.45
140	20	11665	583.25	0.00	583.25	4.03E-03	0.619	1.50
160	30	11401	380.03	0.00	380.03	2.62E-03	0.685	1.26
180	40	9494	237.35	0.00	237.35	1.64E-03	0.751	1.33
200	60	8714	145.23	0.00	145.23	1.00E-03	0.817	1.33
220	100	8988	89.88	0.00	89.88	6.20E-04	0.872	1.29
240	200	10771	53.86	0.00	53.86	3.72E-04	0.923	1.54
260	300	9719	32.40	0.00	32.40	2.24E-04	0.963	1.66
280	300	5800	19.33	0.00	19.33	1.33E-04	1.007	2.02

300	300	3575	11.92	0.00	11.92	8.23E-05	1.044	1.58

Co-60 Source			Scintillator Thickness (mm)			4 pieces/1 mm		
Collected Data		3/24/14	Detector Bias (-kV)			2		
Calibration Date		8/1/2006	Source Location			Bottom		
Initial Activity		396100	Scintillator Location			BLC Geometry		
Current Activity		144859	Material			Beryllium/polypropylene		
Slope [mV/MeV]			166.09	σ-slope [mV/MeV]				1.77
Intercept [mV]			-17.03	σ-Intercept [mV]				3.08
R^2			0.973	σ-Linear Fit (Std. Dev.) [mV]				8.74
Disc (mV)	Time (Sec.)	Total Counts	$\frac{Counts}{Sec.}$	$\frac{BG}{Sec.}$	$\frac{Net\ Cts.}{Sec.}$	$\frac{(C-B)}{A_o}$	MeV Calc.	Disc. Error %
20	2	12177	6088.50	16.23	6072.27	4.19E-02	0.172	6.41
40	5	14940	2988.00	5.56	2982.44	2.06E-02	0.329	2.69
60	10	14045	1404.50	2.22	1402.28	9.68E-03	0.469	1.81
80	20	12525	626.25	1.07	625.18	4.32E-03	0.606	1.69
100	40	12009	300.23	0.54	299.68	2.07E-03	0.720	1.48
120	60	8575	142.92	0.39	142.53	9.84E-04	0.820	1.53
140	100	6711	67.11	0.00	67.11	4.63E-04	0.901	2.03
160	200	6665	33.33	0.00	33.33	2.30E-04	0.960	3.14
180	300	6260	20.87	0.00	20.87	1.44E-04	0.998	1.65
200	300	2774	9.25	0.00	9.25	6.38E-05	1.057	1.91

Co-60 Source			Scintillator Thickness (mm)			4 pieces/1 mm		
Collected Data		2/25/14	Detector Bias (-kV)			2		
Calibration Date		8/1/2006	Source Location			Center		
Initial Activity		396100	Scintillator Location			BLC Geometry		
Current Activity		146275	Material			Beryllium/polypropylene		
Slope [mV/MeV]			170.09	σ-slope [mV/MeV]				1.73
Intercept [mV]			-19.13	σ-Intercept [mV]				2.90
R^2			0.973	σ-Linear Fit (Std. Dev.) [mV]				8.67
Disc (mV)	Time (Sec.)	Total Counts	$\frac{Counts}{Sec.}$	$\frac{BG}{Sec.}$	$\frac{Net\ Cts.}{Sec.}$	$\frac{(C-B)}{A_o}$	MeV Calc.	Disc. Error %
20	2	13050	6525.00	16.23	6508.77	4.45E-02	0.176	6.37
40	5	16139	3227.80	5.56	3222.24	2.20E-02	0.332	2.70
60	8	12361	1545.13	2.22	1542.91	1.05E-02	0.470	2.00
80	20	15026	751.30	1.07	750.23	5.13E-03	0.594	1.26
100	30	9343	311.43	0.54	310.89	2.13E-03	0.732	1.53
120	50	7743	154.86	0.39	154.47	1.06E-03	0.826	1.64
140	100	7927	79.27	0.00	79.27	5.42E-04	0.898	1.62
160	200	8173	40.87	0.00	40.87	2.79E-04	0.954	2.07

180	300	6260	20.87	0.00	20.87	1.43E-04	1.012	2.34
200	300	3318	11.06	0.00	11.06	7.56E-05	1.057	2.36

Co-60 Source			Scintillator Thickness (mm)			4 pieces/1 mm		
Collected Data		2/25/14	Detector Bias (-kV)			2		
Calibration Date		8/1/2006	Source Location			Center		
Initial Activity		396100	Scintillator Location			BLC Geometry		
Current Activity		146275	Material			Beryllium/polypropylene		
Slope [mV/MeV]			188.03	σ-slope [mV/MeV]				1.73
Intercept [mV]			-22.19	σ-Intercept [mV]				2.89
R^2			0.983	σ-Linear Fit (Std. Dev.) [mV]				6.80
Disc (mV)	Time (Sec.)	Total Counts	$\frac{Counts}{Sec.}$	$\frac{BG}{Sec.}$	$\frac{Net\ Cts.}{Sec.}$	$\frac{(C-B)}{A_o}$	MeV Calc.	Disc. Error %
20	2	13791	6895.50	2.83	6892.67	4.71E-02	0.159	6.63
40	5	17625	3525.00	1.39	3523.61	2.41E-02	0.314	2.94
60	5	8906	1781.20	0.65	1780.55	1.22E-02	0.443	2.06
80	10	9006	900.60	0.35	900.25	6.15E-03	0.564	1.87
100	30	14329	477.63	0.22	477.41	3.26E-03	0.667	1.45
120	40	9719	242.98	0.26	242.72	1.66E-03	0.767	1.49
140	100	12623	126.23	0.15	126.08	8.62E-04	0.849	1.26
160	200	12526	62.63	0.10	62.53	4.27E-04	0.922	1.53
180	300	9237	30.79	0.08	30.71	2.10E-04	0.981	1.74
200	300	4671	15.57	0.08	15.49	1.06E-04	1.036	2.15
220	300	2359	7.86	0.00	7.86	5.38E-05	1.076	2.30

Detector #2

BLC geometry – 10 3.175 mm layers

Co-60 Source			Scintillator Thickness (mm)			10 pieces/0.3175 mm		
Collected Data		5/29/14	Detector Bias (-kV)			1.6		
Calibration Date		8/1/2006	Source Location			#13		
Initial Activity		396100	Scintillator Location			BLC Geometry		
Current Activity		141456	Material			Beryllium		
Slope [mV/MeV]			117.39	σ-slope [mV/MeV]				3.13
Intercept [mV]			-8.39	σ-Intercept [mV]				3.99
R^2			0.661	σ-Linear Fit (Std. Dev.) [mV]				46.05
Disc (mV)	Time (Sec.)	Total Counts	$\frac{Counts}{Sec.}$	$\frac{BG}{Sec.}$	$\frac{Net\ Cts.}{Sec.}$	$\frac{(C-B)}{A_o}$	MeV Calc.	Disc. Error %
50	5	20172	4034.40	116.46	3917.94	2.77E-02	0.489	2.83
100	20	9513	475.65	29.55	446.10	3.15E-03	0.946	1.35

150	40	1082	27.05	8.43	18.62	1.32E-04	1.166	3.34
200	300	1569	5.23	4.63	0.60	4.24E-06	1.252	10.59

Co-60 Source			Scintillator Thickness (mm)			10 pieces/0.3175 mm		
Collected Data		5/29/14	Detector Bias (-kV)			1.7		
Calibration Date		8/1/2006	Source Location			#13		
Initial Activity		396100	Scintillator Location			BLC Geometry		
Current Activity		141456	Material			Beryllium		
Slope [mV/MeV]			207.62	σ-slope [mV/MeV]				3.02
Intercept [mV]			-4.33	σ-Intercept [mV]				4.34
R^2			0.992	σ-Linear Fit (Std. Dev.) [mV]				6.98
Disc (mV)	Time (Sec.)	Total Counts	$\frac{Counts}{Sec.}$	$\frac{BG}{Sec.}$	$\frac{Net\ Cts.}{Sec.}$	$\frac{(C-B)}{A_o}$	MeV Calc.	Disc. Error %
50	2	15990	7995.00	198.07	7796.93	5.51E-02	0.242	4.92
100	5	18511	3702.20	106.35	3595.85	2.54E-02	0.517	2.28
150	10	14375	1437.50	55.48	1382.02	9.77E-03	0.772	1.42
200	20	8740	437.00	26.75	410.25	2.90E-03	0.956	1.11
250	50	5371	107.42	13.82	93.60	6.62E-04	1.088	0.93
300	200	5048	25.24	8.16	17.08	1.21E-04	1.170	3.23
350	200	2639	13.20	5.59	7.61	5.38E-05	1.196	2.08

Co-60 Source			Scintillator Thickness (mm)			10 pieces/0.3175 mm		
Collected Data		5/29/14	Detector Bias (-kV)			1.8		
Calibration Date		8/1/2006	Source Location			#13		
Initial Activity		396100	Scintillator Location			BLC Geometry		
Current Activity		141456	Material			Beryllium		
Slope [mV/MeV]			386.40	σ-slope [mV/MeV]				4.97
Intercept [mV]			-9.21	σ-Intercept [mV]				7.21
R^2			0.996	σ-Linear Fit (Std. Dev.) [mV]				6.78
Disc (mV)	Time (Sec.)	Total Counts	$\frac{Counts}{Sec.}$	$\frac{BG}{Sec.}$	$\frac{Net\ Cts.}{Sec.}$	$\frac{(C-B)}{A_o}$	MeV Calc.	Disc. Error %
50	1	11635	11635.00	464.56	11170.44	7.90E-02	0.122	8.26
100	2	14971	7485.50	188.70	7296.80	5.16E-02	0.266	4.58
150	4	20256	5064.00	137.81	4926.19	3.48E-02	0.410	2.83
200	4	13296	3324.00	99.88	3224.12	2.28E-02	0.551	2.04
250	4	8175	2043.75	70.50	1973.25	1.39E-02	0.689	1.55
300	10	11810	1181.00	47.81	1133.19	8.01E-03	0.812	1.20
350	20	12877	643.85	32.27	611.58	4.32E-03	0.910	0.94
400	40	13019	325.48	22.36	303.12	2.14E-03	0.989	0.71
450	80	12219	152.74	15.32	137.42	9.71E-04	1.061	0.80
500	100	6878	68.78	10.72	58.06	4.10E-04	1.115	1.02

550	200	6378	31.89	8.63	23.26	1.64E-04	1.154	1.57
600	300	4950	16.50	6.21	10.29	7.27E-05	1.189	1.53
700	300	1919	6.40	4.73	1.67	1.18E-05	1.241	3.70

Co-60 Source			Scintillator Thickness (mm)			10 pieces/0.3175 mm		
Collected Data		7/21/14	Detector Bias (-kV)			1.8		
Calibration Date		8/1/2006	Source Location			#13		
Initial Activity		396100	Scintillator Location			BLC Geometry		
Current Activity		138780	Material			Beryllium		
Slope [mV/MeV]			369.79	σ-slope [mV/MeV]				3.02
Intercept [mV]			-10.78	σ-Intercept [mV]				4.59
R^2			0.994	σ-Linear Fit (Std. Dev.) [mV]				9.46
Disc (mV)	Time (Sec.)	Total Counts	$\frac{Counts}{Sec.}$	$\frac{BG}{Sec.}$	$\frac{Net\ Cts.}{Sec.}$	$\frac{(C-B)}{A_o}$	MeV Calc.	Disc. Error %
50	5	52334	10466.80	270.93	10195.88	7.35E-02	0.143	6.48
100	5	33496	6699.20	180.97	6518.23	4.70E-02	0.300	3.94
150	5	22387	4477.40	129.53	4347.87	3.13E-02	0.447	2.49
200	5	14129	2825.80	94.37	2731.43	1.97E-02	0.596	1.83
250	5	8419	1683.80	64.60	1619.20	1.17E-02	0.733	1.45
300	10	9168	916.80	43.83	872.97	6.29E-03	0.855	1.24
350	20	9605	480.25	28.19	452.06	3.26E-03	0.943	0.83
400	40	9331	233.28	19.44	213.84	1.54E-03	1.022	0.86
450	100	11014	110.14	13.16	96.98	6.99E-04	1.084	0.72
500	200	10052	50.26	9.81	40.45	2.91E-04	1.133	0.56

Cs-137 Source			Scintillator Thickness (mm)			10 pieces/0.3175 mm		
Collected Data		7/21/14	Detector Bias (-kV)			1.8		
Calibration Date		3/1/1994	Source Location			#13		
Initial Activity		392570	Scintillator Location			BLC Geometry		
Current Activity		245013	Material			Beryllium		
Slope [mV/MeV]			348.84	σ-slope [mV/MeV]				3.49
Intercept [mV]			-6.90	σ-Intercept [mV]				10.10
R^2			0.991	σ-Linear Fit (Std. Dev.) [mV]				6.84
Disc (mV)	Time (Sec.)	Total Counts	$\frac{Counts}{Sec.}$	$\frac{BG}{Sec.}$	$\frac{Net\ Cts.}{Sec.}$	$\frac{(C-B)}{A_o}$	MeV Calc.	Disc. Error %
50	2	10588	5294.00	270.93	5023.08	2.05E-02	0.156	4.45
100	5	10615	2123.00	180.97	1942.03	7.93E-03	0.323	2.19
150	20	14774	738.70	129.53	609.17	2.49E-03	0.443	1.24
200	50	11464	229.28	94.37	134.91	5.51E-04	0.500	0.93
250	100	8138	81.38	64.60	16.78	6.85E-05	0.557	4.60

Co-60 Source			Scintillator Thickness (mm)			10 pieces/0.3175 mm		
Collected Data		5/29/14	Detector Bias (-kV)			1.9		
Calibration Date		8/1/2006	Source Location			#13		
Initial Activity		396100	Scintillator Location			BLC Geometry		
Current Activity		141456	Material			Beryllium		
Slope [mV/MeV]			674.48	σ-slope [mV/MeV]				5.28
Intercept [mV]			-0.57	σ-Intercept [mV]				8.68
R^2			0.999	σ-Linear Fit (Std. Dev.) [mV]				6.07
Disc (mV)	Time (Sec.)	Total Counts	$\frac{Counts}{Sec.}$	$\frac{BG}{Sec.}$	$\frac{Net\ Cts.}{Sec.}$	$\frac{(C-B)}{A_o}$	MeV Calc.	Disc. Error %
50	1	16402	16402.00	2805.90	13596.10	9.61E-02	0.074	19.87
100	2	21430	10715.00	309.30	10405.70	7.36E-02	0.142	6.84
150	2	17109	8554.50	204.86	8349.64	5.90E-02	0.217	5.28
200	2	13869	6934.50	171.51	6762.99	4.78E-02	0.294	4.01
250	3	16940	5646.67	147.35	5499.32	3.89E-02	0.371	2.89
300	3	13385	4461.67	121.25	4340.42	3.07E-02	0.454	2.74
350	5	17954	3590.80	103.05	3487.75	2.47E-02	0.527	1.92
400	5	13935	2787.00	85.34	2701.66	1.91E-02	0.604	1.71
450	5	10658	2131.60	68.21	2063.39	1.46E-02	0.678	1.53
500	10	16274	1627.40	57.76	1569.64	1.11E-02	0.744	1.06
550	10	11675	1167.50	44.82	1122.68	7.94E-03	0.814	1.05
600	10	8322	832.20	38.07	794.13	5.61E-03	0.873	1.11
700	30	12097	403.23	24.41	378.82	2.68E-03	0.965	0.85
800	60	10741	179.02	16.09	162.93	1.15E-03	1.047	0.68
900	100	7365	73.65	11.25	62.40	4.41E-04	1.110	1.03
1000	100	3090	30.90	8.33	22.57	1.60E-04	1.156	1.20

Co-60 Source			Scintillator Thickness (mm)			10 pieces/0.3175 mm		
Collected Data		7/21/14	Detector Bias (-kV)			1.9		
Calibration Date		8/1/2006	Source Location			#13		
Initial Activity		396100	Scintillator Location			BLC Geometry		
Current Activity		138780	Material			Beryllium		
Slope [mV/MeV]			657.01	σ-slope [mV/MeV]				5.04
Intercept [mV]			-17.72	σ-Intercept [mV]				7.94
R^2			0.996	σ-Linear Fit (Std. Dev.) [mV]				10.46
Disc (mV)	Time (Sec.)	Total Counts	$\frac{Counts}{Sec.}$	$\frac{BG}{Sec.}$	$\frac{Net\ Cts.}{Sec.}$	$\frac{(C-B)}{A_o}$	MeV Calc.	Disc. Error %
50	5	71135	14227.00	455.15	13771.85	9.92E-02	0.067	7.92
100	5	48820	9764.00	246.10	9517.90	6.86E-02	0.165	6.72
150	5	38937	7787.40	200.50	7586.90	5.47E-02	0.244	4.33
200	5	31023	6204.60	167.69	6036.91	4.35E-02	0.329	3.57

250	5	24919	4983.80	143.29	4840.51	3.49E-02	0.409	2.76
300	5	19614	3922.80	119.17	3803.63	2.74E-02	0.492	2.17
350	5	15223	3044.60	97.38	2947.22	2.12E-02	0.573	1.88
400	5	11652	2330.40	80.91	2249.49	1.62E-02	0.650	1.46
450	10	17100	1710.00	66.36	1643.64	1.18E-02	0.729	1.29
500	10	12608	1260.80	53.64	1207.16	8.70E-03	0.796	1.11
550	10	9036	903.60	42.32	861.28	6.21E-03	0.857	1.15
600	20	12932	646.60	33.72	612.88	4.42E-03	0.907	0.98
700	30	8722	290.73	21.74	268.99	1.94E-03	0.998	0.77
800	100	12465	124.65	14.64	110.01	7.93E-04	1.076	0.78
900	100	5236	52.36	9.61	42.75	3.08E-04	1.130	0.96
1000	100	2266	22.66	6.80	15.86	1.14E-04	1.173	1.09

Cs-137 Source			Scintillator Thickness (mm)				10 pieces/0.3175 mm	
Collected Data		7/21/14	Detector Bias (-kV)				1.9	
Calibration Date		3/1/1994	Source Location				#13	
Initial Activity		392570	Scintillator Location				BLC Geometry	
Current Activity		245013	Material				Beryllium	
Slope [mV/MeV]			673.43	σ-slope [mV/MeV]				5.27
Intercept [mV]			-27.36	σ-Intercept [mV]				15.01
R^2			0.985	σ-Linear Fit (Std. Dev.) [mV]				11.16
Disc (mV)	Time (Sec.)	Total Counts	$\frac{Counts}{Sec.}$	$\frac{BG}{Sec.}$	$\frac{Net\ Cts.}{Sec.}$	$\frac{(C-B)}{A_o}$	MeV Calc.	Disc. Error %
50	1	8331	8331.00	455.15	7875.85	3.21E-02	0.084	6.10
100	3	14033	4677.67	246.10	4431.57	1.81E-02	0.180	3.55
150	5	14941	2988.20	200.50	2787.70	1.14E-02	0.264	2.13
200	8	13872	1734.00	167.69	1566.31	6.39E-03	0.353	1.67
250	10	9862	986.20	143.29	842.91	3.44E-03	0.420	1.28
300	20	10505	525.25	119.17	406.08	1.66E-03	0.466	1.20
350	50	13363	267.26	97.38	169.88	6.93E-04	0.495	0.72
400	80	11231	140.39	80.91	59.48	2.43E-04	0.532	1.74
450	100	8547	85.47	66.36	19.11	7.80E-05	0.551	1.29
500	200	11529	57.65	53.64	4.01	1.63E-05	0.592	2.78

Co-60 Source		Scintillator Thickness (mm)	10 pieces/0.3175 mm	
Collected Data	5/29/14	Detector Bias (-kV)	2.0	
Calibration Date	8/1/2006	Source Location	#13	
Initial Activity	396100	Scintillator Location	BLC Geometry	
Current Activity	141456	Material	Beryllium	
Slope [mV/MeV]	1,132.02	σ-slope [mV/MeV]		14.47
Intercept [mV]	19.52	σ-Intercept [mV]		43.83

R^2			1.000	σ-Linear Fit (Std. Dev.) [mV]				2.20
Disc (mV)	Time (Sec.)	Total Counts	$\frac{Counts}{Sec.}$	$\frac{BG}{Sec.}$	$\frac{Net\ Cts.}{Sec.}$	$\frac{(C-B)}{A_o}$	MeV Calc.	Disc. Error %
50	1	20993	20993.00	5270.40	15722.60	1.11E-01	0.047	54.66
100	1	14674	14674.00	1801.60	12872.40	9.10E-02	0.086	23.18
150	1	11679	11679.00	417.27	11261.73	7.96E-02	0.120	8.35
200	2	20111	10055.50	244.22	9811.28	6.94E-02	0.161	6.15
250	2	17614	8807.00	212.27	8594.73	6.08E-02	0.206	5.80
300	2	15715	7857.50	191.42	7666.08	5.42E-02	0.247	4.78
350	2	14097	7048.50	172.57	6875.93	4.86E-02	0.288	3.79
400	2	12475	6237.50	157.03	6080.47	4.30E-02	0.334	3.43
500	3	14504	4834.67	128.49	4706.18	3.33E-02	0.426	2.69
600	3	11207	3735.67	105.67	3630.00	2.57E-02	0.514	2.28
700	5	14222	2844.40	85.97	2758.43	1.95E-02	0.598	1.62
800	5	10455	2091.00	67.63	2023.37	1.43E-02	0.683	1.44
900	10	15038	1503.80	53.60	1450.20	1.03E-02	0.762	1.19
1000	10	10536	1053.60	41.59	1012.01	7.15E-03	0.833	0.83

Co-60 Source		Scintillator Thickness (mm)	10 pieces/0.3175 mm
Collected Data	7/21/14	Detector Bias (-kV)	2.0
Calibration Date	8/1/2006	Source Location	#13
Initial Activity	396100	Scintillator Location	BLC Geometry
Current Activity	138780	Material	Beryllium

Slope [mV/MeV]			1135.34	σ-slope [mV/MeV]				6.59
Intercept [mV]			-21.98	σ-Intercept [mV]				11.69
R^2			0.999	σ-Linear Fit (Std. Dev.) [mV]				10.26
Disc (mV)	Time (Sec.)	Total Counts	$\frac{Counts}{Sec.}$	$\frac{BG}{Sec.}$	$\frac{Net\ Cts.}{Sec.}$	$\frac{(C-B)}{A_o}$	MeV Calc.	Disc. Error %
50	5	85471	17094.20	664.75	16429.45	1.18E-01	0.041	8.69
100	5	63931	12786.20	375.60	12410.60	8.94E-02	0.090	6.63
150	5	52163	10432.60	268.33	10164.28	7.32E-02	0.144	6.71
200	5	45557	9111.40	231.88	8879.53	6.40E-02	0.189	5.37
250	5	39891	7978.20	205.64	7772.56	5.60E-02	0.236	4.76
300	5	35281	7056.20	185.47	6870.73	4.95E-02	0.281	3.84
350	5	31001	6200.20	169.69	6030.51	4.35E-02	0.330	3.57
400	5	27435	5487.00	150.27	5336.73	3.85E-02	0.375	3.23
450	5	24345	4869.00	138.76	4730.24	3.41E-02	0.418	2.50
500	5	21134	4226.80	123.16	4103.64	2.96E-02	0.467	2.59
550	5	18666	3733.20	114.62	3618.58	2.61E-02	0.509	1.85
600	5	15828	3165.60	100.66	3064.94	2.21E-02	0.561	2.10
700	5	11923	2384.60	80.35	2304.25	1.66E-02	0.644	1.43

800	10	16493	1649.30	63.66	1585.64	1.14E-02	0.737	1.22
900	10	11427	1142.70	49.22	1093.48	7.88E-03	0.815	1.15
1000	10	7748	774.80	38.46	736.34	5.31E-03	0.882	0.80

Cs-137 Source			Scintillator Thickness (mm)			10 pieces/0.3175 mm		
Collected Data		7/21/14	Detector Bias (-kV)			2.0		
Calibration Date		3/1/1994	Source Location			#13		
Initial Activity		392570	Scintillator Location			BLC Geometry		
Current Activity		245013	Material			Beryllium		
Slope [mV/MeV]			1177.96	σ-slope [mV/MeV]				5.55
Intercept [mV]			-42.86	σ-Intercept [mV]				16.18
R^2			0.986	σ-Linear Fit (Std. Dev.) [mV]				17.56
Disc (mV)	Time (Sec.)	Total Counts	$\frac{Counts}{Sec.}$	$\frac{BG}{Sec.}$	$\frac{Net\ Cts.}{Sec.}$	$\frac{(C-B)}{A_o}$	MeV Calc.	Disc. Error %
50	10	108945	10894.50	664.75	10229.75	4.18E-02	0.048	5.93
100	10	73801	7380.10	375.60	7004.50	2.86E-02	0.099	3.67
150	10	53980	5398.00	268.33	5129.68	2.09E-02	0.152	3.57
200	10	41529	4152.90	231.88	3921.03	1.60E-02	0.201	2.52
250	10	32507	3250.70	205.64	3045.06	1.24E-02	0.248	1.83
300	10	24391	2439.10	185.47	2253.63	9.20E-03	0.299	1.51
350	10	17987	1798.70	169.69	1629.01	6.65E-03	0.348	1.34
400	10	13100	1310.00	150.27	1159.73	4.73E-03	0.391	1.26
450	10	9459	945.90	138.76	807.14	3.29E-03	0.424	1.09
500	20	12859	642.95	123.16	519.79	2.12E-03	0.451	1.05
550	30	13232	441.07	114.62	326.45	1.33E-03	0.476	1.05
600	40	12290	307.25	100.66	206.59	8.43E-04	0.491	0.79
700	60	8564	142.73	80.35	62.38	2.55E-04	0.530	1.82
800	100	8189	81.89	63.66	18.23	7.44E-05	0.553	4.93
900	200	10521	52.61	49.22	3.39	1.38E-05	0.594	3.06

Co-60 Source			Scintillator Thickness (mm)			10 pieces/0.3175 mm		
Collected Data		7/21/14	Detector Bias (-kV)			2.1		
Calibration Date		8/1/2006	Source Location			#13		
Initial Activity		396100	Scintillator Location			BLC Geometry		
Current Activity		138780	Material			Beryllium		
Slope [mV/MeV]			1832.54	σ-slope [mV/MeV]				14.06
Intercept [mV]			-4.70	σ-Intercept [mV]				42.67
R^2			1.000	σ-Linear Fit (Std. Dev.) [mV]				4.30
Disc (mV)	Time (Sec.)	Total Counts	$\frac{Counts}{Sec.}$	$\frac{BG}{Sec.}$	$\frac{Net\ Cts.}{Sec.}$	$\frac{(C-B)}{A_o}$	MeV Calc.	Disc. Error %
50	5	95853	19170.60	845.60	18325.00	1.32E-01	0.029	17.10

100	5	78460	15692.00	525.75	15166.25	1.09E-01	0.048	6.66
150	5	66252	13250.40	367.83	12882.57	9.28E-02	0.082	7.53
200	5	58353	11670.60	298.13	11372.47	8.19E-02	0.111	7.53
250	5	52801	10560.20	264.10	10296.10	7.42E-02	0.140	6.36
300	5	48455	9691.00	246.50	9444.50	6.81E-02	0.168	7.10
350	5	45163	9032.60	225.20	8807.40	6.35E-02	0.191	4.40
400	5	41248	8249.60	211.42	8038.18	5.79E-02	0.224	5.36
450	5	38464	7692.80	197.82	7494.98	5.40E-02	0.249	4.34
500	5	35812	7162.40	187.72	6974.68	5.03E-02	0.276	4.58
550	5	33534	6706.80	177.45	6529.35	4.70E-02	0.299	3.25
600	5	30963	6192.60	166.32	6026.28	4.34E-02	0.330	3.30
700	5	26517	5303.40	148.44	5154.96	3.71E-02	0.387	3.14
800	5	23044	4608.80	131.94	4476.86	3.23E-02	0.437	2.22
900	5	19293	3858.60	117.81	3740.79	2.70E-02	0.497	2.30
1000	5	16541	3308.20	104.39	3203.81	2.31E-02	0.547	1.90

Co-60 Source			Scintillator Thickness (mm)			10 pieces/0.3175 mm		
Collected Data		5/29/14	Detector Bias (-kV)			2.1		
Calibration Date		8/1/2006	Source Location			#13		
Initial Activity		396100	Scintillator Location			BLC Geometry		
Current Activity		141456	Material			Beryllium		
Slope [mV/MeV]			1,972.16	σ-slope [mV/MeV]				23.02
Intercept [mV]			14.43	σ-Intercept [mV]				67.72
R^2			1.000	σ-Linear Fit (Std. Dev.) [mV]				4.48
Disc (mV)	Time (Sec.)	Total Counts	$\frac{Counts}{Sec.}$	$\frac{BG}{Sec.}$	$\frac{Net\ Cts.}{Sec.}$	$\frac{(C-B)}{A_o}$	MeV Calc.	Disc. Error %
50	1	23146	23146.00	5325.00	17821.00	1.26E-01	0.034	173.44
100	1	18185	18185.00	3328.60	14856.40	1.05E-01	0.053	55.74
200	1	12881	12881.00	567.15	12313.85	8.71E-02	0.095	8.36
300	1	10554	10554.00	258.80	10295.20	7.28E-02	0.145	7.19
400	2	18184	9092.00	217.44	8874.56	6.27E-02	0.195	5.48
500	2	15820	7910.00	189.37	7720.63	5.46E-02	0.245	4.49
600	2	13751	6875.50	171.03	6704.47	4.74E-02	0.297	3.81
700	2	11936	5968.00	152.75	5815.25	4.11E-02	0.350	3.61
800	5	26151	5230.20	134.61	5095.59	3.60E-02	0.398	2.43
900	5	22326	4465.20	119.17	4346.03	3.07E-02	0.453	2.82
1000	5	19617	3923.40	105.75	3817.65	2.70E-02	0.497	2.24

Cs-137 Source		Scintillator Thickness (mm)	10 pieces/0.3175 mm
Collected Data	7/21/14	Detector Bias (-kV)	2.1
Calibration Date	3/1/1994	Source Location	#13

Initial Activity		392570	Scintillator Location			BLC Geometry		
Current Activity		245013	Material			Beryllium		
Slope [mV/MeV]			1957.83	σ-slope [mV/MeV]				8.48
Intercept [mV]			-71.57	σ-Intercept [mV]				25.99
R^2			0.987	σ-Linear Fit (Std. Dev.) [mV]				24.90
Disc (mV)	Time (Sec.)	Total Counts	$\frac{Counts}{Sec.}$	$\frac{BG}{Sec.}$	$\frac{Net\ Cts.}{Sec.}$	$\frac{(C-B)}{A_o}$	MeV Calc.	Disc. Error %
50	5	64543	12908.60	845.60	12063.00	4.92E-02	0.033	10.52
100	5	48408	9681.60	525.75	9155.85	3.74E-02	0.063	6.47
150	5	38537	7707.40	367.83	7339.57	3.00E-02	0.093	4.17
200	5	31851	6370.20	298.13	6072.07	2.48E-02	0.124	4.19
250	5	26964	5392.80	264.10	5128.70	2.09E-02	0.152	3.55
300	5	23001	4600.20	246.50	4353.70	1.78E-02	0.183	3.06
350	5	19819	3963.80	225.20	3738.60	1.53E-02	0.211	2.51
400	5	16775	3355.00	211.42	3143.58	1.28E-02	0.242	2.22
450	5	14345	2869.00	197.82	2671.18	1.09E-02	0.271	2.12
500	10	24436	2443.60	187.72	2255.88	9.21E-03	0.299	1.46
550	10	20441	2044.10	177.45	1866.65	7.62E-03	0.329	1.46
600	10	17083	1708.30	166.32	1541.98	6.29E-03	0.356	1.40
700	10	11415	1141.50	148.44	993.06	4.05E-03	0.406	1.35
800	20	15431	771.55	131.94	639.61	2.61E-03	0.440	0.88
900	30	14645	488.17	117.81	370.36	1.51E-03	0.470	1.05
1000	30	9455	315.17	104.39	210.78	8.60E-04	0.490	0.70

Spatial, BLC geometry –10 0.3175 mm layers

Co-60 Source			Scintillator Thickness (mm)			10 pieces/0.3175 mm		
Collected Data		4/17/14	Detector Bias (-kV)			1.8		
Calibration Date		8/1/2006	Source Location			#1		
Initial Activity		396100	Scintillator Location			BLC Geometry		
Current Activity		143612	Material			Beryllium		
Slope [mV/MeV]			434.04	σ-slope [mV/MeV]				5.77
Intercept [mV]			-22.88	σ-Intercept [mV]				8.66
R^2			0.999	σ-Linear Fit (Std. Dev.) [mV]				10.30
Disc (mV)	Time (Sec.)	Total Counts	$\frac{Counts}{Sec.}$	$\frac{BG}{Sec.}$	$\frac{Net\ Cts.}{Sec.}$	$\frac{(C-B)}{A_o}$	MeV Calc.	Disc. Error %
50	1	9061	9061.00	418.87	8642.13	6.02E-02	0.110	9.10
100	2	11441	5720.50	181.55	5538.95	3.86E-02	0.260	5.47
150	3	11844	3948.00	132.19	3815.81	2.66E-02	0.395	3.32
200	4	10694	2673.50	94.36	2579.14	1.80E-02	0.526	2.56
250	5	8786	1757.20	66.13	1691.08	1.18E-02	0.649	1.91

300	10	10945	1094.50	44.96	1049.54	7.31E-03	0.765	1.74
350	20	12918	645.90	30.01	615.89	4.29E-03	0.862	1.57
400	30	10903	363.43	20.67	342.77	2.39E-03	0.939	1.28
450	40	8140	203.50	14.54	188.96	1.32E-03	1.004	1.61
500	60	5935	98.92	10.11	88.80	6.18E-04	1.069	1.71
550	100	4723	47.23	7.68	39.55	2.75E-04	1.115	3.32
600	300	7000	23.33	5.99	17.34	1.21E-04	1.148	1.62
650	300	3492	11.64	5.37	6.27	4.36E-05	1.198	4.46
700	300	2477	8.26	4.40	3.86	2.69E-05	1.218	34.88
750	300	1791	5.97	4.35	1.62	1.13E-05	1.240	92.88
800	300	1521	5.07	4.12	0.95	6.59E-06	1.246	85.16

Co-60 Source			Scintillator Thickness (mm)				10 pieces/0.3175 mm	
Collected Data		4/17/14	Detector Bias (-kV)				1.8	
Calibration Date		8/1/2006	Source Location				#3	
Initial Activity		396100	Scintillator Location				BLC Geometry	
Current Activity		143612	Material				Beryllium	
Slope [mV/MeV]			425.18	σ-slope [mV/MeV]				5.34
Intercept [mV]			-11.12	σ-Intercept [mV]				7.84
R^2			0.999	σ-Linear Fit (Std. Dev.) [mV]				7.55
Disc (mV)	Time (Sec.)	Total Counts	$\frac{Counts}{Sec.}$	$\frac{BG}{Sec.}$	$\frac{Net\ Cts.}{Sec.}$	$\frac{(C-B)}{A_o}$	MeV Calc.	Disc. Error %
50	1	11064	11064.00	418.87	10645.13	7.41E-02	0.091	6.82
100	2	13420	6710.00	181.55	6528.45	4.55E-02	0.247	5.23
150	3	14340	4780.00	132.19	4647.81	3.24E-02	0.371	3.36
200	4	12917	3229.25	94.36	3134.89	2.18E-02	0.504	2.69
250	5	10659	2131.80	66.13	2065.68	1.44E-02	0.631	1.92
300	10	13321	1332.10	44.96	1287.14	8.96E-03	0.749	1.38
350	20	15345	767.25	30.01	737.24	5.13E-03	0.854	1.44
400	20	8074	403.70	20.67	383.03	2.67E-03	0.941	1.10
450	40	8208	205.20	14.54	190.66	1.33E-03	1.015	1.47
500	60	6058	100.97	10.11	90.85	6.33E-04	1.075	1.47
550	100	4601	46.01	7.68	38.33	2.67E-04	1.124	2.82
600	300	6886	22.95	5.99	16.96	1.18E-04	1.156	3.31
650	300	3838	12.79	5.37	7.42	5.17E-05	1.197	3.80

Co-60 Source		Scintillator Thickness (mm)	10 pieces/0.3175 mm
Collected Data	4/17/14	Detector Bias (-kV)	1.8
Calibration Date	8/1/2006	Source Location	#5
Initial Activity	396100	Scintillator Location	BLC Geometry
Current Activity	143612	Material	Beryllium

Slope [mV/MeV]			400.43	σ-slope [mV/MeV]				5.85
Intercept [mV]			-20.37	σ-Intercept [mV]				9.03
R^2			0.999	σ-Linear Fit (Std. Dev.) [mV]				9.73
Disc (mV)	Time (Sec.)	Total Counts	$\frac{Counts}{Sec.}$	$\frac{BG}{Sec.}$	$\frac{Net\ Cts.}{Sec.}$	$\frac{(C-B)}{A_o}$	MeV Calc.	Disc. Error %
50	1	9113	9113.00	418.87	8694.13	6.05E-02	0.107	8.10
100	2	10829	5414.50	181.55	5232.95	3.64E-02	0.280	4.74
150	3	10703	3567.67	132.19	3435.48	2.39E-02	0.429	3.13
200	4	9213	2303.25	94.36	2208.89	1.54E-02	0.571	2.42
250	5	7089	1417.80	66.13	1351.68	9.41E-03	0.703	2.31
300	10	8569	856.90	44.96	811.94	5.65E-03	0.811	1.88
350	20	9839	491.95	30.01	461.94	3.22E-03	0.900	1.25
400	30	7826	260.87	20.67	240.20	1.67E-03	0.974	1.40
450	40	5128	128.20	14.54	113.66	7.91E-04	1.044	1.39
500	100	6171	61.71	10.11	51.60	3.59E-04	1.096	1.43
550	200	5807	29.04	7.68	21.36	1.49E-04	1.141	2.08
600	300	4485	14.95	5.99	8.96	6.24E-05	1.181	4.31
650	300	2904	9.68	5.37	4.31	3.00E-05	1.206	23.98
700	300	1987	6.62	4.40	2.23	1.55E-05	1.228	45.35
750	300	1727	5.76	4.35	1.40	9.77E-06	1.237	65.57
800	300	1508	5.03	4.12	0.90	6.29E-06	1.243	59.92

Co-60 Source			Scintillator Thickness (mm)			10 pieces/0.3175 mm		
Collected Data		4/17/14	Detector Bias (-kV)			1.8		
Calibration Date		8/1/2006	Source Location			#11		
Initial Activity		396100	Scintillator Location			BLC Geometry		
Current Activity		143612	Material			Beryllium		
Slope [mV/MeV]			390.57	σ-slope [mV/MeV]				5.69
Intercept [mV]			-23.28	σ-Intercept [mV]				8.55
R^2			0.999	σ-Linear Fit (Std. Dev.) [mV]				8.73
Disc (mV)	Time (Sec.)	Total Counts	$\frac{Counts}{Sec.}$	$\frac{BG}{Sec.}$	$\frac{Net\ Cts.}{Sec.}$	$\frac{(C-B)}{A_o}$	MeV Calc.	Disc. Error %
50	1	10005	10005.00	418.87	9586.13	6.67E-02	0.133	7.80
100	2	12271	6135.50	181.55	5953.95	4.15E-02	0.299	4.49
150	3	12151	4050.33	132.19	3918.14	2.73E-02	0.447	3.02
200	4	10573	2643.25	94.36	2548.89	1.77E-02	0.583	2.10
250	5	7866	1573.20	66.13	1507.08	1.05E-02	0.720	1.80
300	10	8753	875.30	44.96	830.34	5.78E-03	0.839	1.51
350	20	9746	487.30	30.01	457.29	3.18E-03	0.924	1.34
400	30	7282	242.73	20.67	222.07	1.55E-03	0.998	1.14
450	100	11493	114.93	14.54	100.39	6.99E-04	1.067	1.63

500	200	10345	51.73	10.11	41.61	2.90E-04	1.120	2.70
550	300	7612	25.37	7.68	17.70	1.23E-04	1.155	4.08
600	300	4117	13.72	5.99	7.73	5.38E-05	1.192	3.37
650	300	2625	8.75	5.37	3.38	2.35E-05	1.219	25.44
700	300	1938	6.46	4.40	2.06	1.44E-05	1.233	28.70
750	300	1637	5.46	4.35	1.10	7.68E-06	1.243	110.58
800	300	1502	5.01	4.12	0.88	6.15E-06	1.245	102.78

Co-60 Source			Scintillator Thickness (mm)				10 pieces/0.3175 mm	
Collected Data		4/17/14	Detector Bias (-kV)				1.8	
Calibration Date		8/1/2006	Source Location				#13	
Initial Activity		396100	Scintillator Location				BLC Geometry	
Current Activity		143612	Material				Beryllium	
Slope [mV/MeV]			381.73	σ-slope [mV/MeV]				4.94
Intercept [mV]			-7.25	σ-Intercept [mV]				7.07
R^2			0.999	σ-Linear Fit (Std. Dev.) [mV]				6.72
Disc (mV)	Time (Sec.)	Total Counts	$\frac{Counts}{Sec.}$	$\frac{BG}{Sec.}$	$\frac{Net\ Cts.}{Sec.}$	$\frac{(C-B)}{A_o}$	MeV Calc.	Disc. Error %
50	1	11838	11838.00	418.87	11419.13	7.95E-02	0.120	8.20
100	2	15215	7607.50	181.55	7425.95	5.17E-02	0.265	4.65
150	3	15551	5183.67	132.19	5051.48	3.52E-02	0.406	2.84
200	4	13381	3345.25	94.36	3250.89	2.26E-02	0.553	2.00
250	5	10181	2036.20	66.13	1970.08	1.37E-02	0.694	1.48
300	10	11786	1178.60	44.96	1133.64	7.89E-03	0.815	1.14
350	20	12416	620.80	30.01	590.79	4.11E-03	0.917	0.92
400	30	9352	311.73	20.67	291.07	2.03E-03	0.994	0.74
450	100	14900	149.00	14.54	134.46	9.36E-04	1.064	0.80
500	200	13695	68.48	10.11	58.36	4.06E-04	1.115	0.99
550	300	9567	31.89	7.68	24.21	1.69E-04	1.152	1.50
600	300	5016	16.72	5.99	10.73	7.47E-05	1.188	1.45
650	300	3025	10.08	5.37	4.71	3.28E-05	1.212	8.32
700	300	2214	7.38	4.40	2.98	2.08E-05	1.229	7.43
750	300	1741	5.80	4.35	1.45	1.01E-05	1.243	16.54
800	300	1496	4.99	4.12	0.86	6.01E-06	1.249	15.21

Co-60 Source		Scintillator Thickness (mm)	10 pieces/0.3175 mm
Collected Data	4/17/14	Detector Bias (-kV)	1.8
Calibration Date	8/1/2006	Source Location	#15
Initial Activity	396100	Scintillator Location	BLC Geometry

Current Activity		143612	Material					Beryllium
Slope [mV/MeV]			365.54	σ-slope [mV/MeV]				3.61
Intercept [mV]			-8.08	σ-Intercept [mV]				5.76
R^2			0.998	σ-Linear Fit (Std. Dev.) [mV]				10.51
Disc (mV)	Time (Sec.)	Total Counts	$\frac{Counts}{Sec.}$	$\frac{BG}{Sec.}$	$\frac{Net\ Cts.}{Sec.}$	$\frac{(C-B)}{A_o}$	MeV Calc.	Disc. Error %
50	1	9941	9941.00	418.87	9522.13	6.63E-02	0.135	7.91
100	2	12329	6164.50	181.55	5982.95	4.17E-02	0.296	4.32
150	3	12043	4014.33	132.19	3882.14	2.70E-02	0.450	2.91
200	4	10208	2552.00	94.36	2457.64	1.71E-02	0.593	2.05
250	5	7481	1496.20	66.13	1430.08	9.96E-03	0.734	1.76
300	10	8367	836.70	44.96	791.74	5.51E-03	0.848	1.43
350	20	9060	453.00	30.01	422.99	2.95E-03	0.936	1.19
400	30	6635	221.17	20.67	200.50	1.40E-03	1.017	1.54
450	100	10450	104.50	14.54	89.96	6.26E-04	1.081	1.46
500	200	9524	47.62	10.11	37.51	2.61E-04	1.128	2.47
550	300	6884	22.95	7.68	15.27	1.06E-04	1.165	3.77
600	300	3825	12.75	5.99	6.76	4.71E-05	1.199	3.02
650	300	2514	8.38	5.37	3.01	2.09E-05	1.228	28.46
700	300	1824	6.08	4.40	1.68	1.17E-05	1.239	53.14
750	300	1628	5.43	4.35	1.07	7.47E-06	1.244	109.75
800	300	1478	4.93	4.12	0.80	5.59E-06	1.247	102.21

Co-60 Source			Scintillator Thickness (mm)					10 pieces/0.3175 mm
Collected Data		4/17/14	Detector Bias (-kV)					1.8
Calibration Date		8/1/2006	Source Location					#21
Initial Activity		396100	Scintillator Location					BLC Geometry
Current Activity		143612	Material					Beryllium
Slope [mV/MeV]			366.88	σ-slope [mV/MeV]				3.86
Intercept [mV]			-7.92	σ-Intercept [mV]				6.13
R^2			0.999	σ-Linear Fit (Std. Dev.) [mV]				9.22
Disc (mV)	Time (Sec.)	Total Counts	$\frac{Counts}{Sec.}$	$\frac{BG}{Sec.}$	$\frac{Net\ Cts.}{Sec.}$	$\frac{(C-B)}{A_o}$	MeV Calc.	Disc. Error %
50	1	8440	8440.00	418.87	8021.13	5.59E-02	0.139	8.57
100	3	16014	5338.00	181.55	5156.45	3.59E-02	0.295	4.70
150	3	10915	3638.33	132.19	3506.14	2.44E-02	0.434	2.91
200	5	11329	2265.80	94.36	2171.44	1.51E-02	0.587	2.08
250	10	13361	1336.10	66.13	1269.98	8.84E-03	0.727	1.66
300	20	14804	740.20	44.96	695.24	4.84E-03	0.844	1.36
350	20	7821	391.05	30.01	361.04	2.51E-03	0.933	1.32
400	40	7842	196.05	20.67	175.38	1.22E-03	1.008	1.70

450	90	8278	91.98	14.54	77.44	5.39E-04	1.077	1.56
500	200	8070	40.35	10.11	30.24	2.11E-04	1.131	1.96
550	300	5622	18.74	7.68	11.06	7.70E-05	1.175	5.12
600	300	3112	10.37	5.99	4.38	3.05E-05	1.200	3.37
650	300	2132	7.11	5.37	1.73	1.21E-05	1.232	26.28
700	300	1573	5.24	4.40	0.85	5.90E-06	1.244	22.70

Co-60 Source			Scintillator Thickness (mm)			10 pieces/0.3175 mm		
Collected Data		4/17/14	Detector Bias (-kV)			1.8		
Calibration Date		8/1/2006	Source Location			#23		
Initial Activity		396100	Scintillator Location			BLC Geometry		
Current Activity		143612	Material			Beryllium		
Slope [mV/MeV]			367.45	σ-slope [mV/MeV]				3.81
Intercept [mV]			-3.54	σ-Intercept [mV]				6.08
R^2			0.999	σ-Linear Fit (Std. Dev.) [mV]				7.71
Disc (mV)	Time (Sec.)	Total Counts	$\frac{Counts}{Sec.}$	$\frac{BG}{Sec.}$	$\frac{Net\ Cts.}{Sec.}$	$\frac{(C-B)}{A_o}$	MeV Calc.	Disc. Error %
50	1	9886	9886.00	418.87	9467.13	6.59E-02	0.130	8.66
100	2	12719	6359.50	181.55	6177.95	4.30E-02	0.278	4.61
150	3	12610	4203.33	132.19	4071.14	2.83E-02	0.429	3.09
200	4	10903	2725.75	94.36	2631.39	1.83E-02	0.570	2.27
250	5	8235	1647.00	66.13	1580.88	1.10E-02	0.708	1.80
300	10	8888	888.80	44.96	843.84	5.88E-03	0.838	1.44
350	20	9415	470.75	30.01	440.74	3.07E-03	0.929	1.22
400	40	9120	228.00	20.67	207.33	1.44E-03	1.011	1.53
450	100	10481	104.81	14.54	90.27	6.29E-04	1.080	1.44
500	200	9352	46.76	10.11	36.65	2.55E-04	1.130	2.02
550	300	6552	21.84	7.68	14.16	9.86E-05	1.173	3.80
600	300	3531	11.77	5.99	5.78	4.02E-05	1.203	12.49
650	300	2262	7.54	5.37	2.17	1.51E-05	1.236	31.81
700	300	1680	5.60	4.40	1.20	8.38E-06	1.245	28.29

Co-60 Source			Scintillator Thickness (mm)			10 pieces/0.3175 mm		
Collected Data		4/17/14	Detector Bias (-kV)			1.8		
Calibration Date		8/1/2006	Source Location			#25		
Initial Activity		396100	Scintillator Location			BLC Geometry		
Current Activity		143612	Material			Beryllium		
Slope [mV/MeV]			360.88	σ-slope [mV/MeV]				3.74
Intercept [mV]			-6.70	σ-Intercept [mV]				5.77
R^2			0.999	σ-Linear Fit (Std. Dev.) [mV]				10.24

Disc (mV)	Time (Sec.)	Total Counts	$\frac{Counts}{Sec.}$	$\frac{BG}{Sec.}$	$\frac{Net\ Cts.}{Sec.}$	$\frac{(C-B)}{A_o}$	MeV Calc.	Disc. Error %
50	1	8693	8693.00	418.87	8274.13	5.76E-02	0.130	7.93
100	2	10503	5251.50	181.55	5069.95	3.53E-02	0.301	5.26
150	3	10408	3469.33	132.19	3337.14	2.32E-02	0.451	2.96
200	5	11027	2205.40	94.36	2111.04	1.47E-02	0.596	2.08
250	10	12996	1299.60	66.13	1233.48	8.59E-03	0.735	1.53
300	20	13802	690.10	44.96	645.14	4.49E-03	0.861	1.65
350	30	10702	356.73	30.01	326.72	2.28E-03	0.946	1.13
400	50	8619	172.38	20.67	151.71	1.06E-03	1.030	1.44
450	100	7963	79.63	14.54	65.09	4.53E-04	1.090	1.46
500	300	10727	35.76	10.11	25.64	1.79E-04	1.139	1.94
550	300	5233	17.44	7.68	9.77	6.80E-05	1.181	4.04
600	300	2941	9.80	5.99	3.81	2.66E-05	1.210	11.83
650	300	2028	6.76	5.37	1.39	9.66E-06	1.240	29.54
700	300	1528	5.09	4.40	0.70	4.85E-06	1.248	26.47

Single Layer Geometry – 3.175 mm scintillator

Co-60 Source		Scintillator Thickness (mm)	0.3175
Collected Data	7/28/14	Detector Bias (-kV)	1.8
Calibration Date	8/1/2006	Source Location	#13
Initial Activity	396100	Scintillator Location	On axis
Current Activity	138431	Material	Beryllium
Slope [mV/MeV]	424.55	σ-slope [mV/MeV]	4.71
Intercept [mV]	-3.70	σ-Intercept [mV]	6.29
R^2	0.998	σ-Linear Fit (Std. Dev.) [mV]	4.88

Disc (mV)	Time (Sec.)	Total Counts	$\frac{Counts}{Sec.}$	$\frac{BG}{Sec.}$	$\frac{Net\ Cts.}{Sec.}$	$\frac{(C-B)}{A_o}$	MeV Calc.	Disc. Error %
50	10	11897	1189.70	45.34	1144.36	8.27E-03	0.100	6.67
100	20	14891	744.55	26.65	717.90	5.19E-03	0.235	5.00
150	20	10455	522.75	20.75	502.00	3.63E-03	0.355	3.68
200	30	10704	356.80	16.07	340.73	2.46E-03	0.479	2.36
250	40	9150	228.75	12.11	216.64	1.56E-03	0.607	1.94
300	60	8064	134.40	8.38	126.02	9.10E-04	0.731	1.35
350	100	7177	71.77	5.74	66.03	4.77E-04	0.843	1.06
400	300	9850	32.83	4.30	28.53	2.06E-04	0.941	0.65

Cs-137 Source		Scintillator Thickness (mm)	0.3175
Collected Data	7/28/14	Detector Bias (-kV)	1.8

Calibration Date	3/1/1994	Source Location	#13
Initial Activity	392570	Scintillator Location	On axis
Current Activity	244905	Material	Beryllium
Slope [mV/MeV]	420.07	σ-slope [mV/MeV]	3.05
Intercept [mV]	-6.66	σ-Intercept [mV]	8.79
R^2	0.993	σ-Linear Fit (Std. Dev.) [mV]	6.80

Disc (mV)	Time (Sec.)	Total Counts	$\frac{Counts}{Sec.}$	$\frac{BG}{Sec.}$	$\frac{Net\ Cts.}{Sec.}$	$\frac{(C-B)}{A_o}$	MeV Calc.	Disc. Error %
50	20	11771	588.55	45.34	543.21	2.22E-03	0.128	4.67
100	40	10500	262.50	26.65	235.85	9.63E-04	0.260	2.64
150	100	10731	107.31	20.75	86.56	3.53E-04	0.388	1.50
200	300	9757	32.52	16.07	16.45	6.72E-05	0.478	1.15

Co-60 Source		Scintillator Thickness (mm)	0.3175
Collected Data	7/28/14	Detector Bias (-kV)	1.9
Calibration Date	8/1/2006	Source Location	#13
Initial Activity	396100	Scintillator Location	On axis
Current Activity	138431	Material	Beryllium
Slope [mV/MeV]	741.24	σ-slope [mV/MeV]	7.39
Intercept [mV]	9.20	σ-Intercept [mV]	12.14
R^2	0.984	σ-Linear Fit (Std. Dev.) [mV]	28.20

Disc (mV)	Time (Sec.)	Total Counts	$\frac{Counts}{Sec.}$	$\frac{BG}{Sec.}$	$\frac{Net\ Cts.}{Sec.}$	$\frac{(C-B)}{A_o}$	MeV Calc.	Disc. Error %
50	10	18011	1801.10	131.03	1670.07	1.21E-02	0.043	5.75
100	10	10835	1083.50	37.23	1046.27	7.56E-03	0.123	7.48
150	10	8519	851.90	29.34	822.56	5.94E-03	0.191	6.11
200	20	14025	701.25	25.45	675.80	4.88E-03	0.255	5.12
300	30	14274	475.80	19.16	456.64	3.30E-03	0.386	1.86
400	40	9143	228.58	14.36	214.22	1.55E-03	0.610	4.64
500	50	8843	176.86	10.25	166.61	1.20E-03	0.673	1.63
600	100	9422	94.22	6.70	87.52	6.32E-04	0.798	1.08
700	200	8193	40.97	4.38	36.59	2.64E-04	0.918	1.22
800	300	5055	16.85	2.76	14.09	1.02E-04	1.007	1.23

Cs-137 Source		Scintillator Thickness (mm)	0.3175
Collected Data	7/28/14	Detector Bias (-kV)	1.9
Calibration Date	3/1/1994	Source Location	#13
Initial Activity	392570	Scintillator Location	On axis
Current Activity	244905	Material	Beryllium
Slope [mV/MeV]	702.90	σ-slope [mV/MeV]	5.79
Intercept [mV]	0.90	σ-Intercept [mV]	22.16

R^2			1.000	σ-Linear Fit (Std. Dev.) [mV]				2.04
Disc (mV)	Time (Sec.)	Total Counts	$\frac{Counts}{Sec.}$	$\frac{BG}{Sec.}$	$\frac{Net\ Cts.}{Sec.}$	$\frac{(C-B)}{A_o}$	MeV Calc.	Disc. Error %
50	10	10043	1004.30	131.03	873.27	3.57E-03	0.067	7.03
100	20	10747	537.35	37.23	500.12	2.04E-03	0.140	3.75
150	30	10367	345.57	29.34	316.23	1.29E-03	0.213	3.03
200	40	8970	224.25	25.45	198.80	8.12E-04	0.286	2.20
300	100	7504	75.04	19.16	55.88	2.28E-04	0.423	1.78
400	300	6833	22.78	14.36	8.42	3.44E-05	0.492	1.35

Co-60 Source		Scintillator Thickness (mm)	0.3175
Collected Data	7/28/14	Detector Bias (-kV)	2.0
Calibration Date	8/1/2006	Source Location	#13
Initial Activity	396100	Scintillator Location	On axis
Current Activity	138431	Material	Beryllium

Slope [mV/MeV]	1284.09	σ-slope [mV/MeV]	11.70
Intercept [mV]	21.55	σ-Intercept [mV]	22.08
R^2	1.000	σ-Linear Fit (Std. Dev.) [mV]	5.76

Disc (mV)	Time (Sec.)	Total Counts	$\frac{Counts}{Sec.}$	$\frac{BG}{Sec.}$	$\frac{Net\ Cts.}{Sec.}$	$\frac{(C-B)}{A_o}$	MeV Calc.	Disc. Error %
50	10	24724	2472.40	264.97	2207.43	1.59E-02	0.022	9.85
100	10	15547	1554.70	86.77	1467.93	1.06E-02	0.052	9.08
200	10	10045	1004.50	32.36	972.14	7.02E-03	0.142	6.56
300	10	7776	777.60	26.90	750.70	5.42E-03	0.221	6.48
400	20	12710	635.50	23.43	612.07	4.42E-03	0.289	3.59
500	20	9946	497.30	20.87	476.43	3.44E-03	0.373	3.30
600	30	11782	392.73	17.82	374.91	2.71E-03	0.448	2.48
700	40	12308	307.70	15.36	292.34	2.11E-03	0.525	1.81
800	40	8934	223.35	12.21	211.14	1.53E-03	0.614	1.99
900	50	8380	167.60	10.28	157.32	1.14E-03	0.686	1.37
1000	100	11508	115.08	7.55	107.53	7.77E-04	0.761	1.12

Cs-137 Source		Scintillator Thickness (mm)	0.3175
Collected Data	7/28/14	Detector Bias (-kV)	2.0
Calibration Date	3/1/1994	Source Location	#13
Initial Activity	392570	Scintillator Location	On axis
Current Activity	244905	Material	Beryllium

Slope [mV/MeV]	1241.79	σ-slope [mV/MeV]	11.88
Intercept [mV]	0.71	σ-Intercept [mV]	38.20
R^2	0.993	σ-Linear Fit (Std. Dev.) [mV]	15.66

Disc (mV)	Time (Sec.)	Total Counts	$\frac{Counts}{Sec.}$	$\frac{BG}{Sec.}$	$\frac{Net\ Cts.}{Sec.}$	$\frac{(C-B)}{A_o}$	MeV Calc.	Disc. Error %
50	10	14536	1453.60	264.97	1188.63	4.85E-03	0.044	6.12
100	10	8360	836.00	86.77	749.23	3.06E-03	0.085	6.99
200	20	9569	478.45	32.36	446.09	1.82E-03	0.156	4.01
300	30	8698	289.93	26.90	263.03	1.07E-03	0.243	2.46
400	60	10447	174.12	23.43	150.69	6.15E-04	0.325	1.72
500	100	9301	93.01	20.87	72.14	2.95E-04	0.404	1.49
600	200	8742	43.71	17.82	25.89	1.06E-04	0.462	2.72
700	300	6783	22.61	15.36	7.25	2.96E-05	0.494	1.67

Co-60 Source		Scintillator Thickness (mm)	0.3175
Collected Data	7/28/14	Detector Bias (-kV)	2.1
Calibration Date	8/1/2006	Source Location	#13
Initial Activity	396100	Scintillator Location	On axis
Current Activity	138431	Material	Beryllium
Slope [mV/MeV]	2217.72	σ-slope [mV/MeV]	24.70
Intercept [mV]	23.55	σ-Intercept [mV]	80.28
R^2	0.999	σ-Linear Fit (Std. Dev.) [mV]	6.64

Disc (mV)	Time (Sec.)	Total Counts	$\frac{Counts}{Sec.}$	$\frac{BG}{Sec.}$	$\frac{Net\ Cts.}{Sec.}$	$\frac{(C-B)}{A_o}$	MeV Calc.	Disc. Error %
50	10	30603	3060.30	389.56	2670.74	1.93E-02	0.004	11.97
100	10	21120	2112.00	174.88	1937.12	1.40E-02	0.033	7.50
200	10	13265	1326.50	47.66	1278.84	9.24E-03	0.080	7.75
300	10	10669	1066.90	34.38	1032.52	7.46E-03	0.127	7.61
400	10	9138	913.80	29.60	884.20	6.39E-03	0.169	6.63
500	20	15881	794.05	27.15	766.90	5.54E-03	0.213	5.51
600	20	13956	697.80	24.49	673.31	4.86E-03	0.256	3.98
700	20	11962	598.10	22.97	575.13	4.15E-03	0.310	4.47
800	20	10586	529.30	20.57	508.73	3.67E-03	0.351	3.46
900	20	9313	465.65	18.77	446.88	3.23E-03	0.393	2.66
1000	30	12011	400.37	17.58	382.79	2.77E-03	0.442	2.15

Cs-137 Source		Scintillator Thickness (mm)	0.3175
Collected Data	7/28/14	Detector Bias (-kV)	2.1
Calibration Date	3/1/1994	Source Location	#13
Initial Activity	392570	Scintillator Location	On axis
Current Activity	244905	Material	Beryllium
Slope [mV/MeV]	2161.48	σ-slope [mV/MeV]	13.30
Intercept [mV]	-20.20	σ-Intercept [mV]	41.57
R^2	0.997	σ-Linear Fit (Std. Dev.) [mV]	15.32

Disc (mV)	Time (Sec.)	Total Counts	$\frac{Counts}{Sec.}$	$\frac{BG}{Sec.}$	$\frac{Net\ Cts.}{Sec.}$	$\frac{(C-B)}{A_o}$	MeV Calc.	Disc. Error %
50	5	9254	1850.80	389.56	1461.24	5.97E-03	0.035	13.45
100	10	12219	1221.90	174.88	1047.02	4.28E-03	0.049	5.79
200	20	14221	711.05	47.66	663.39	2.71E-03	0.097	4.13
300	20	10108	505.40	34.38	471.02	1.92E-03	0.148	4.04
400	30	11746	391.53	29.60	361.93	1.48E-03	0.191	2.78
500	40	11764	294.10	27.15	266.95	1.09E-03	0.241	2.37
600	50	11078	221.56	24.49	197.07	8.05E-04	0.287	1.77
700	60	9591	159.85	22.97	136.88	5.59E-04	0.337	1.50
800	80	8863	110.79	20.57	90.22	3.68E-04	0.384	1.26
900	100	7281	72.81	18.77	54.04	2.21E-04	0.425	1.20
1000	200	9311	46.56	17.58	28.98	1.18E-04	0.456	1.71

BLC geometry – 10 0.5 mm layers

Co-60 Source		Scintillator Thickness (mm)	10 pieces/0.5 mm
Collected Data	6/10/14	Detector Bias (-kV)	1.8
Calibration Date	8/1/2006	Source Location	#13
Initial Activity	396100	Scintillator Location	BLC Geometry
Current Activity	140846	Material	Beryllium
Slope [mV/MeV]	290.55	σ-slope [mV/MeV]	2.71
Intercept [mV]	-14.98	σ-Intercept [mV]	7.05
R^2	0.925	σ-Linear Fit (Std. Dev.) [mV]	28.70

Disc (mV)	Time (Sec.)	Total Counts	$\frac{Counts}{Sec.}$	$\frac{BG}{Sec.}$	$\frac{Net\ Cts.}{Sec.}$	$\frac{(C-B)}{A_o}$	MeV Calc.	Disc. Error %
50	10	12496	1249.60	67.93	1181.67	8.39E-03	0.215	3.15
100	20	4292	214.60	16.61	197.99	1.41E-03	0.421	2.35
150	100	4957	49.57	7.16	42.41	3.01E-04	0.581	2.03
200	200	2927	14.64	3.78	10.86	7.71E-05	0.705	3.41
250	300	1607	5.36	2.32	3.04	2.16E-05	0.809	3.94
300	300	694	2.31	1.73	0.58	4.14E-06	0.922	5.32

Co-60 Source		Scintillator Thickness (mm)	10 pieces/0.5 mm
Collected Data	6/10/14	Detector Bias (-kV)	1.9
Calibration Date	8/1/2006	Source Location	#13
Initial Activity	396100	Scintillator Location	BLC Geometry
Current Activity	140846	Material	Beryllium
Slope [mV/MeV]	556.81	σ-slope [mV/MeV]	3.89
Intercept [mV]	-43.28	σ-Intercept [mV]	9.03

R^2			0.948	σ-Linear Fit (Std. Dev.) [mV]				33.39
Disc (mV)	Time (Sec.)	Total Counts	$\frac{Counts}{Sec.}$	$\frac{BG}{Sec.}$	$\frac{Net\ Cts.}{Sec.}$	$\frac{(C-B)}{A_o}$	MeV Calc.	Disc. Error %
50	5	14719	2943.80	208.47	2735.33	1.94E-02	0.118	3.98
100	10	9629	962.90	55.39	907.51	6.44E-03	0.246	2.27
150	20	7504	375.20	25.55	349.65	2.48E-03	0.357	2.16
200	50	8018	160.36	13.92	146.44	1.04E-03	0.451	1.39
250	100	7086	70.86	8.76	62.10	4.41E-04	0.542	1.49
300	200	6857	34.29	5.56	28.73	2.04E-04	0.619	2.02
350	300	5548	18.49	4.21	14.28	1.01E-04	0.684	1.85
400	300	2944	9.81	3.00	6.81	4.84E-05	0.746	1.99
450	300	1733	5.78	2.65	3.13	2.22E-05	0.806	4.96
500	300	1025	3.42	1.84	1.58	1.12E-05	0.853	5.65

Co-60 Source		Scintillator Thickness (mm)	10 pieces/0.5 mm
Collected Data	6/10/14	Detector Bias (-kV)	2.0
Calibration Date	8/1/2006	Source Location	#13
Initial Activity	396100	Scintillator Location	BLC Geometry
Current Activity	140846	Material	Beryllium

Slope [mV/MeV]			905.72	σ-slope [mV/MeV]				3.23
Intercept [mV]			-44.02	σ-Intercept [mV]				8.64
R^2			0.959	σ-Linear Fit (Std. Dev.) [mV]				45.15
Disc (mV)	Time (Sec.)	Total Counts	$\frac{Counts}{Sec.}$	$\frac{BG}{Sec.}$	$\frac{Net\ Cts.}{Sec.}$	$\frac{(C-B)}{A_o}$	MeV Calc.	Disc. Error %
50	2	9374	4687.00	392.20	4294.80	3.05E-02	0.054	7.30
100	5	11800	2360.00	155.44	2204.56	1.57E-02	0.141	2.98
150	10	12670	1267.00	69.76	1197.24	8.50E-03	0.213	2.51
200	20	14614	730.70	42.40	688.30	4.89E-03	0.280	1.86
250	30	13040	434.67	26.74	407.93	2.90E-03	0.340	1.54
300	40	10628	265.70	19.87	245.83	1.75E-03	0.396	1.47
350	60	10217	170.28	14.19	156.09	1.11E-03	0.445	1.23
400	80	8437	105.46	11.05	94.41	6.70E-04	0.497	1.25
450	100	6762	67.62	8.42	59.20	4.20E-04	0.546	1.23
500	200	8617	43.09	6.67	36.42	2.59E-04	0.594	1.50
550	300	9196	30.65	5.53	25.12	1.78E-04	0.632	1.45
600	300	6095	20.32	4.17	16.15	1.15E-04	0.673	2.11
700	300	3084	10.28	3.09	7.19	5.10E-05	0.742	2.45
800	300	1705	5.68	2.19	3.49	2.48E-05	0.798	2.23

Co-60 Source			Scintillator Thickness (mm)				10 pieces/0.5 mm	
Collected Data		6/10/14	Detector Bias (-kV)				2.1	
Calibration Date		8/1/2006	Source Location				#13	
Initial Activity		396100	Scintillator Location				BLC Geometry	
Current Activity		140846	Material				Beryllium	
Slope [mV/MeV]			1459.61	σ-slope [mV/MeV]				4.99
Intercept [mV]			-58.79	σ-Intercept [mV]				15.98
R^2			0.985	σ-Linear Fit (Std. Dev.) [mV]				33.47
Disc (mV)	Time (Sec.)	Total Counts	$\frac{Counts}{Sec.}$	$\frac{BG}{Sec.}$	$\frac{Net\ Cts.}{Sec.}$	$\frac{(C-B)}{A_o}$	MeV Calc.	Disc. Error %
50	2	11643	5821.50	534.95	5286.55	3.75E-02	0.033	9.58
100	3	11780	3926.67	284.24	3642.43	2.59E-02	0.081	5.06
150	4	10400	2600.00	155.33	2444.67	1.74E-02	0.131	3.30
200	5	8892	1778.40	95.59	1682.81	1.19E-02	0.173	3.20
250	10	12960	1296.00	66.74	1229.26	8.73E-03	0.210	2.42
300	20	18584	929.20	49.61	879.59	6.25E-03	0.249	1.62
350	20	13413	670.65	39.32	631.33	4.48E-03	0.289	1.74
400	20	10062	503.10	29.82	473.28	3.36E-03	0.323	1.60
450	30	10957	365.23	24.33	340.90	2.42E-03	0.360	1.77
500	40	11041	276.03	19.58	256.45	1.82E-03	0.392	1.36
550	50	10468	209.36	15.72	193.64	1.37E-03	0.423	1.44
600	60	9468	157.80	14.27	143.53	1.02E-03	0.453	1.79
700	100	9232	92.32	9.76	82.56	5.86E-04	0.512	1.66
800	100	5501	55.01	6.81	48.20	3.42E-04	0.568	1.85
900	100	3496	34.96	5.54	29.42	2.09E-04	0.616	1.96
1000	100	2217	22.17	4.61	17.56	1.25E-04	0.666	1.88

Single Layer Geometry – 0.5 mm scintillator

Co-60 Source			Scintillator Thickness (mm)				0.5	
Collected Data		7/29/14	Detector Bias (-kV)				2.0	
Calibration Date		8/1/2006	Source Location				#13	
Initial Activity		396100	Scintillator Location				On axis	
Current Activity		138381	Material				Beryllium	
Slope [mV/MeV]			779.60	σ-slope [mV/MeV]				7.14
Intercept [mV]			-6.57	σ-Intercept [mV]				23.85
R^2			0.994	σ-Linear Fit (Std. Dev.) [mV]				7.10
Disc (mV)	Time (Sec.)	Total Counts	$\frac{Counts}{Sec.}$	$\frac{BG}{Sec.}$	$\frac{Net\ Cts.}{Sec.}$	$\frac{(C-B)}{A_o}$	MeV Calc.	Disc. Error %
50	10	9684	968.40	236.57	731.83	5.29E-03	#N/A	#N/A
100	30	10203	340.10	60.54	279.56	2.02E-03	0.103	3.29

150	100	13063	130.63	14.42	116.21	8.40E-04	0.197	2.21
200	100	6676	66.76	6.94	59.82	4.32E-04	0.274	2.63
250	200	7390	36.95	4.26	32.69	2.36E-04	0.339	2.53
300	300	6726	22.42	2.50	19.92	1.44E-04	0.391	2.11
350	300	4037	13.46	2.22	11.24	8.12E-05	0.450	1.78

Cs-137 Source			Scintillator Thickness (mm)					0.5
Collected Data		7/29/14	Detector Bias (-kV)					2.0
Calibration Date		3/1/1994	Source Location					#13
Initial Activity		392570	Scintillator Location					On axis
Current Activity		244889	Material					Beryllium
Slope [mV/MeV]			794.34	σ-slope [mV/MeV]				9.82
Intercept [mV]			-25.26	σ-Intercept [mV]				42.60
R^2			0.997	σ-Linear Fit (Std. Dev.) [mV]				2.31
Disc (mV)	Time (Sec.)	Total Counts	$\frac{Counts}{Sec.}$	$\frac{BG}{Sec.}$	$\frac{Net\ Cts.}{Sec.}$	$\frac{(C-B)}{A_o}$	MeV Calc.	Disc. Error %
50	30	11738	391.27	217.24	174.03	7.11E-04	0.061	7.39
75	50	11581	231.62	124.68	106.94	4.37E-04	0.110	5.37
100	80	10232	127.90	60.54	67.36	2.75E-04	0.155	4.87
125	100	7423	74.23	28.25	45.98	1.88E-04	0.191	3.07
150	200	9081	45.41	14.42	30.99	1.27E-04	0.224	3.11
175	300	8762	29.21	8.74	20.47	8.36E-05	0.251	1.94
200	300	6011	20.04	6.94	13.10	5.35E-05	0.283	2.02

Co-60 Source			Scintillator Thickness (mm)					0.5
Collected Data		7/29/14	Detector Bias (-kV)					2.1
Calibration Date		8/1/2006	Source Location					#13
Initial Activity		396100	Scintillator Location					On axis
Current Activity		138381	Material					Beryllium
Slope [mV/MeV]			1275.84	σ-slope [mV/MeV]				10.20
Intercept [mV]			-4.44	σ-Intercept [mV]				39.67
R^2			0.996	σ-Linear Fit (Std. Dev.) [mV]				7.26
Disc (mV)	Time (Sec.)	Total Counts	$\frac{Counts}{Sec.}$	$\frac{BG}{Sec.}$	$\frac{Net\ Cts.}{Sec.}$	$\frac{(C-B)}{A_o}$	MeV Calc.	Disc. Error %
50	10	13711	1371.10	353.66	1017.44	7.35E-03	#N/A	#N/A
100	20	13829	691.45	145.95	545.50	3.94E-03	0.029	3.26
150	30	10300	343.33	55.80	287.53	2.08E-03	0.100	2.84
200	50	9514	190.28	21.27	169.01	1.22E-03	0.154	3.51
250	100	12422	124.22	10.91	113.31	8.19E-04	0.200	2.13
300	100	8477	84.77	7.46	77.31	5.59E-04	0.245	2.30
350	200	12127	60.64	5.50	55.14	3.98E-04	0.283	2.28

400	200	8811	44.06	4.49	39.57	2.86E-04	0.318	2.75
450	300	9610	32.03	3.54	28.49	2.06E-04	0.351	2.95
500	300	6885	22.95	2.74	20.21	1.46E-04	0.389	1.77

Cs-137 Source			Scintillator Thickness (mm)					0.5
Collected Data		7/29/14	Detector Bias (-kV)					2.1
Calibration Date		3/1/1994	Source Location					#13
Initial Activity		392570	Scintillator Location					On axis
Current Activity		244889	Material					Beryllium
Slope [mV/MeV]			1306.96	σ-slope [mV/MeV]				10.25
Intercept [mV]			-32.21	σ-Intercept [mV]				50.47
R^2			0.995	σ-Linear Fit (Std. Dev.) [mV]				5.00
Disc (mV)	Time (Sec.)	Total Counts	$\frac{Counts}{Sec.}$	$\frac{BG}{Sec.}$	$\frac{Net\ Cts.}{Sec.}$	$\frac{(C-B)}{A_o}$	MeV Calc.	Disc. Error %
50	20	11911	595.55	353.66	241.89	9.88E-04	0.042	7.75
75	30	11953	398.43	233.29	165.14	6.74E-04	0.067	10.26
100	40	11107	277.68	145.95	131.73	5.38E-04	0.090	5.40
125	50	9573	191.46	89.98	101.48	4.14E-04	0.116	6.41
150	80	11138	139.23	55.80	83.43	3.41E-04	0.136	3.52
175	100	9953	99.53	34.51	65.02	2.66E-04	0.159	3.96
200	100	7336	73.36	21.27	52.09	2.13E-04	0.181	2.90
225	200	10984	54.92	14.98	39.94	1.63E-04	0.201	4.00
250	200	8777	43.89	10.91	32.98	1.35E-04	0.219	2.90
275	300	10391	34.64	8.70	25.94	1.06E-04	0.237	2.29
300	300	8201	27.34	7.46	19.88	8.12E-05	0.253	3.65
350	300	5341	17.80	5.50	12.30	5.02E-05	0.287	2.13

BLC geometry – 10 0.25 mm layers

Co-60 Source			Scintillator Thickness (mm)					10 pieces/0.25 mm
Collected Data		6/11/14	Detector Bias (-kV)					1.8
Calibration Date		8/1/2006	Source Location					#13
Initial Activity		396100	Scintillator Location					BLC Geometry
Current Activity		140795	Material					Beryllium
Slope [mV/MeV]			204.00	σ-slope [mV/MeV]				1.29
Intercept [mV]			-5.86	σ-Intercept [mV]				5.11
R^2			0.913	σ-Linear Fit (Std. Dev.) [mV]				15.39
Disc (mV)	Time (Sec.)	Total Counts	$\frac{Counts}{Sec.}$	$\frac{BG}{Sec.}$	$\frac{Net\ Cts.}{Sec.}$	$\frac{(C-B)}{A_o}$	MeV Calc.	Disc. Error %
25	10	10076	1007.60	162.00	845.60	6.01E-03	0.143	3.02

50	50	7266	145.32	19.67	125.65	8.92E-04	0.299	2.10
75	100	3716	37.16	5.60	31.56	2.24E-04	0.408	3.40
100	100	1318	13.18	2.54	10.64	7.56E-05	0.492	3.25
125	200	1155	5.78	1.81	3.97	2.82E-05	0.565	5.10
150	300	888	2.96	1.41	1.55	1.10E-05	0.641	3.42

Cs-137 Source			Scintillator Thickness (mm)			10 pieces/0.25 mm		
Collected Data		7/18/14	Detector Bias (-kV)			1.8		
Calibration Date		3/1/1994	Source Location			#13		
Initial Activity		392570	Scintillator Location			BLC Geometry		
Current Activity		245060	Material			Beryllium		
Slope [mV/MeV]			257.90	σ-slope [mV/MeV]				2.74
Intercept [mV]			-17.75	σ-Intercept [mV]				12.00
R^2			0.922	σ-Linear Fit (Std. Dev.) [mV]				11.06
Disc (mV)	Time (Sec.)	Total Counts	$\frac{Counts}{Sec.}$	$\frac{BG}{Sec.}$	$\frac{Net\ Cts.}{Sec.}$	$\frac{(C-B)}{A_o}$	MeV Calc.	Disc. Error %
25	20	8115	405.75	162.00	243.75	9.95E-04	0.161	4.46
50	200	10122	50.61	19.67	30.94	1.26E-04	0.279	2.94
75	300	3314	11.05	5.60	5.45	2.22E-05	0.355	8.32
100	300	1276	4.25	2.54	1.71	6.99E-06	0.399	3.93

Co-60 Source			Scintillator Thickness (mm)			10 pieces/0.25 mm		
Collected Data		6/11/14	Detector Bias (-kV)			1.9		
Calibration Date		8/1/2006	Source Location			#13		
Initial Activity		396100	Scintillator Location			BLC Geometry		
Current Activity		140795	Material			Beryllium		
Slope [mV/MeV]			367.94	σ-slope [mV/MeV]				2.48
Intercept [mV]			-16.22	σ-Intercept [mV]				8.76
R^2			0.942	σ-Linear Fit (Std. Dev.) [mV]				14.20
Disc (mV)	Time (Sec.)	Total Counts	$\frac{Counts}{Sec.}$	$\frac{BG}{Sec.}$	$\frac{Net\ Cts.}{Sec.}$	$\frac{(C-B)}{A_o}$	MeV Calc.	Disc. Error %
25	10	22075	2207.50	344.93	1862.57	1.32E-02	0.084	3.74
50	10	7156	715.60	110.28	605.32	4.30E-03	0.172	2.65
75	30	7274	242.47	32.66	209.81	1.49E-03	0.258	2.29
100	60	5771	96.18	12.77	83.41	5.92E-04	0.335	2.12
125	100	4828	48.28	7.20	41.08	2.92E-04	0.390	2.10
150	100	2612	26.12	4.36	21.76	1.55E-04	0.438	2.73
175	200	3065	15.33	2.49	12.84	9.12E-05	0.478	2.96
200	200	1949	9.75	2.15	7.60	5.39E-05	0.517	3.59

Cs-137 Source			Scintillator Thickness (mm)			10 pieces/0.25 mm		
Collected Data		7/18/14	Detector Bias (-kV)			1.9		
Calibration Date		3/1/1994	Source Location			#13		
Initial Activity		392570	Scintillator Location			BLC Geometry		
Current Activity		245060	Material			Beryllium		
Slope [mV/MeV]			463.90	σ-slope [mV/MeV]				4.16
Intercept [mV]			-37.01	σ-Intercept [mV]				17.27
R^2			0.970	σ-Linear Fit (Std. Dev.) [mV]				7.84
Disc (mV)	Time (Sec.)	Total Counts	$\frac{Counts}{Sec.}$	$\frac{BG}{Sec.}$	$\frac{Net\ Cts.}{Sec.}$	$\frac{(C-B)}{A_o}$	MeV Calc.	Disc. Error %
25	10	9250	925.00	344.93	580.07	2.37E-03	0.101	5.66
50	40	11184	279.60	110.28	169.32	6.91E-04	0.185	2.73
75	100	8808	88.08	32.66	55.42	2.26E-04	0.246	2.09
100	200	6447	32.24	12.77	19.47	7.94E-05	0.298	2.19
125	300	4435	14.78	7.20	7.58	3.09E-05	0.344	3.44
150	300	2428	8.09	4.36	3.73	1.52E-05	0.375	4.25

Co-60 Source			Scintillator Thickness (mm)			10 pieces/0.25 mm		
Collected Data		6/11/14	Detector Bias (-kV)			2.0		
Calibration Date		8/1/2006	Source Location			#13		
Initial Activity		396100	Scintillator Location			BLC Geometry		
Current Activity		140795	Material			Beryllium		
Slope [mV/MeV]			582.37	σ-slope [mV/MeV]				2.92
Intercept [mV]			-16.08	σ-Intercept [mV]				11.95
R^2			0.942	σ-Linear Fit (Std. Dev.) [mV]				19.84
Disc (mV)	Time (Sec.)	Total Counts	$\frac{Counts}{Sec.}$	$\frac{BG}{Sec.}$	$\frac{Net\ Cts.}{Sec.}$	$\frac{(C-B)}{A_o}$	MeV Calc.	Disc. Error %
25	10	34816	3481.60	505.40	2976.20	2.11E-02	0.049	5.96
50	10	17351	1735.10	270.06	1465.04	1.04E-02	0.097	2.58
75	10	9034	903.40	138.10	765.30	5.44E-03	0.149	2.11
100	20	9293	464.65	66.79	397.86	2.83E-03	0.204	2.33
125	30	7567	252.23	31.60	220.63	1.57E-03	0.252	2.28
150	60	8802	146.70	16.38	130.32	9.26E-04	0.297	1.55
175	100	9211	92.11	10.38	81.73	5.80E-04	0.337	1.88
200	100	6265	62.65	7.09	55.56	3.95E-04	0.367	2.76
250	100	3254	32.54	4.34	28.20	2.00E-04	0.418	2.81
300	100	1724	17.24	3.27	13.97	9.92E-05	0.471	2.55

Cs-137 Source		Scintillator Thickness (mm)	10 pieces/0.25 mm
Collected Data	7/18/14	Detector Bias (-kV)	2.0
Calibration Date	3/1/1994	Source Location	#13

Initial Activity		392570	Scintillator Location			BLC Geometry		
Current Activity		245060	Material			Beryllium		
Slope [mV/MeV]			727.85	σ-slope [mV/MeV]				3.89
Intercept [mV]			-47.67	σ-Intercept [mV]				17.91
R^2			0.957	σ-Linear Fit (Std. Dev.) [mV]				14.96
Disc (mV)	Time (Sec.)	Total Counts	$\frac{Counts}{Sec.}$	$\frac{BG}{Sec.}$	$\frac{Net\ Cts.}{Sec.}$	$\frac{(C-B)}{A_o}$	MeV Calc.	Disc. Error %
25	10	15540	1554.00	505.40	1048.60	4.28E-03	0.063	8.63
50	20	13523	676.15	270.06	406.09	1.66E-03	0.129	4.53
75	30	10655	355.17	138.10	217.07	8.86E-04	0.170	3.31
100	50	8814	176.28	66.79	109.49	4.47E-04	0.208	3.08
125	100	9199	91.99	31.60	60.39	2.46E-04	0.242	1.74
150	200	9601	48.01	16.38	31.63	1.29E-04	0.278	2.84
175	300	8769	29.23	10.38	18.85	7.69E-05	0.299	1.94
200	300	5687	18.96	7.09	11.87	4.84E-05	0.326	3.75
250	300	2744	9.15	4.34	4.81	1.96E-05	0.363	4.70

Co-60 Source			Scintillator Thickness (mm)			10 pieces/0.25 mm		
Collected Data		6/11/14	Detector Bias (-kV)			2.1		
Calibration Date		8/1/2006	Source Location			#13		
Initial Activity		396100	Scintillator Location			BLC Geometry		
Current Activity		140795	Material			Beryllium		
Slope [mV/MeV]			987.51	σ-slope [mV/MeV]				3.98
Intercept [mV]			-37.80	σ-Intercept [mV]				18.31
R^2			0.900	σ-Linear Fit (Std. Dev.) [mV]				53.93
Disc (mV)	Time (Sec.)	Total Counts	$\frac{Counts}{Sec.}$	$\frac{BG}{Sec.}$	$\frac{Net\ Cts.}{Sec.}$	$\frac{(C-B)}{A_o}$	MeV Calc.	Disc. Error %
25	2	12801	6400.50	1179.10	5221.40	3.71E-02	#N/A	#N/A
50	4	11529	2882.25	424.35	2457.90	1.75E-02	0.065	5.34
75	6	10880	1813.33	271.98	1541.36	1.09E-02	0.094	2.64
100	8	9323	1165.38	167.35	998.03	7.09E-03	0.130	2.80
125	10	7842	784.20	102.51	681.69	4.84E-03	0.160	2.42
150	20	10330	516.50	63.24	453.26	3.22E-03	0.194	1.64
175	40	14002	350.05	39.08	310.97	2.21E-03	0.227	1.91
200	50	12372	247.44	25.14	222.30	1.58E-03	0.251	2.55
250	60	8443	140.72	12.89	127.83	9.08E-04	0.298	1.67
300	80	6711	83.89	8.49	75.40	5.36E-04	0.342	1.99
350	100	5527	55.27	5.96	49.31	3.50E-04	0.377	2.51
400	100	3764	37.64	4.85	32.79	2.33E-04	0.405	3.60
500	100	1838	18.38	2.90	15.48	1.10E-04	0.462	4.16
600	100	1003	10.03	1.97	8.06	5.72E-05	0.512	4.18

Cs-137 Source			Scintillator Thickness (mm)					10 pieces/0.25 mm
Collected Data		7/18/14	Detector Bias (-kV)					2.1
Calibration Date		3/1/1994	Source Location					#13
Initial Activity		392570	Scintillator Location					BLC Geometry
Current Activity		245060	Material					Beryllium
Slope [mV/MeV]			1139.10	σ-slope [mV/MeV]				5.70
Intercept [mV]			-71.88	σ-Intercept [mV]				27.42
R^2			0.990	σ-Linear Fit (Std. Dev.) [mV]				9.39
Disc (mV)	Time (Sec.)	Total Counts	$\frac{Counts}{Sec.}$	$\frac{BG}{Sec.}$	$\frac{Net\ Cts.}{Sec.}$	$\frac{(C-B)}{A_o}$	MeV Calc.	Disc. Error %
25	5	27892	5578.40	1179.10	4399.30	1.80E-02	#N/A	#N/A
50	10	11881	1188.10	424.35	763.75	3.12E-03	0.086	7.18
75	20	14583	729.15	271.98	457.18	1.87E-03	0.121	4.50
100	30	13831	461.03	167.35	293.68	1.20E-03	0.148	2.53
125	40	11953	298.83	102.51	196.31	8.01E-04	0.176	2.81
150	50	9849	196.98	63.24	133.74	5.46E-04	0.196	1.78
175	80	10309	128.86	39.08	89.78	3.66E-04	0.222	2.40
200	100	8763	87.63	25.14	62.49	2.55E-04	0.241	2.10
250	200	9025	45.13	12.89	32.24	1.32E-04	0.277	1.29
300	300	4900	16.33	8.49	7.84	3.20E-05	0.342	4.39
350	300	3243	10.81	5.96	4.85	1.98E-05	0.362	6.67

Single Layer Geometry – 0.25 mm scintillator

Co-60 Source			Scintillator Thickness (mm)					0.25
Collected Data		7/30/14	Detector Bias (-kV)					2.0
Calibration Date		8/1/2006	Source Location					#13
Initial Activity		396100	Scintillator Location					On axis
Current Activity		138331	Material					Beryllium
Slope [mV/MeV]			494.38	σ-slope [mV/MeV]				8.04
Intercept [mV]			33.85	σ-Intercept [mV]				36.07
R^2			0.988	σ-Linear Fit (Std. Dev.) [mV]				4.38
Disc (mV)	Time (Sec.)	Total Counts	$\frac{Counts}{Sec.}$	$\frac{BG}{Sec.}$	$\frac{Net\ Cts.}{Sec.}$	$\frac{(C-B)}{A_o}$	MeV Calc.	Disc. Error %
50	20	13107	655.35	216.45	438.90	3.17E-03	0.012	4.05
75	30	10052	335.07	112.97	222.10	1.61E-03	0.066	2.90
100	60	9181	153.02	48.02	105.00	7.59E-04	0.114	2.09
125	200	12910	64.55	19.04	45.51	3.29E-04	0.183	1.74
150	300	8647	28.82	7.58	21.24	1.54E-04	0.241	2.10

175	300	4678	15.59	3.75	11.84	8.56E-05	0.286	2.78
200	300	2936	9.79	2.60	7.19	5.20E-05	0.325	3.33

Cs-137 Source			Scintillator Thickness (mm)					0.25
Collected Data		7/30/14	Detector Bias (-kV)					2.0
Calibration Date		3/1/1994	Source Location					#13
Initial Activity		392570	Scintillator Location					On axis
Current Activity		244874	Material					Beryllium
Slope [mV/MeV]			1002.27	σ-slope [mV/MeV]				38.46
Intercept [mV]			-100.18	σ-Intercept [mV]				167.49
R^2			0.999	σ-Linear Fit (Std. Dev.) [mV]				1.07
Disc (mV)	Time (Sec.)	Total Counts	$\frac{Counts}{Sec.}$	$\frac{BG}{Sec.}$	$\frac{Net\ Cts.}{Sec.}$	$\frac{(C-B)}{A_o}$	MeV Calc.	Disc. Error %
50	40	10348	258.70	216.45	42.25	1.72E-04	0.120	12.88
75	80	10463	130.79	112.97	17.82	7.27E-05	0.175	16.64
100	100	5835	58.35	48.02	10.33	4.22E-05	0.201	12.62
125	300	7948	26.49	19.04	7.45	3.04E-05	0.224	6.93
150	300	3538	11.79	7.58	4.21	1.72E-05	0.250	4.10

Co-60 Source			Scintillator Thickness (mm)					0.25
Collected Data		7/30/14	Detector Bias (-kV)					2.1
Calibration Date		8/1/2006	Source Location					#13
Initial Activity		396100	Scintillator Location					On axis
Current Activity		138331	Material					Beryllium
Slope [mV/MeV]			776.22	σ-slope [mV/MeV]				14.37
Intercept [mV]			45.32	σ-Intercept [mV]				71.10
R^2			0.954	σ-Linear Fit (Std. Dev.) [mV]				11.93
Disc (mV)	Time (Sec.)	Total Counts	$\frac{Counts}{Sec.}$	$\frac{BG}{Sec.}$	$\frac{Net\ Cts.}{Sec.}$	$\frac{(C-B)}{A_o}$	MeV Calc.	Disc. Error %
50	10	10284	1028.40	334.48	693.92	5.02E-03	#N/A	#N/A
75	20	13071	653.55	213.16	440.39	3.18E-03	0.012	3.65
100	30	11953	398.43	127.24	271.19	1.96E-03	0.049	2.22
125	50	12029	240.58	76.58	164.00	1.19E-03	0.086	2.10
150	70	9896	141.37	40.17	101.20	7.32E-04	0.118	1.84
175	100	7872	78.72	21.86	56.86	4.11E-04	0.164	2.27
200	200	9318	46.59	12.27	34.32	2.48E-04	0.201	1.66
225	300	8902	29.67	6.95	22.72	1.64E-04	0.236	2.43
250	300	6200	20.67	4.55	16.12	1.17E-04	0.261	4.42
300	300	3554	11.85	2.69	9.16	6.62E-05	0.302	5.23

Cs-137 Source		Scintillator Thickness (mm)	0.25
Collected Data	7/30/14	Detector Bias (-kV)	2.1
Calibration Date	3/1/1994	Source Location	#13
Initial Activity	392570	Scintillator Location	On axis
Current Activity	244874	Material	Beryllium

Slope [mV/MeV]	1153.41	σ-slope [mV/MeV]	15.92
Intercept [mV]	-65.65	σ-Intercept [mV]	80.83
R^2	0.952	σ-Linear Fit (Std. Dev.) [mV]	11.49

Disc (mV)	Time (Sec.)	Total Counts	$\frac{Counts}{Sec.}$	$\frac{BG}{Sec.}$	$\frac{Net\ Cts.}{Sec.}$	$\frac{(C-B)}{A_o}$	MeV Calc.	Disc. Error %
50	20	8839	441.95	334.48	107.47	4.39E-04	0.056	9.49
75	50	12953	259.06	213.16	45.90	1.87E-04	0.114	13.59
100	80	12531	156.64	127.24	29.40	1.20E-04	0.143	5.68
125	100	9147	91.47	76.58	14.89	6.08E-05	0.185	44.92
150	200	10763	53.82	40.17	13.65	5.57E-05	0.189	5.92
175	300	9341	31.14	21.86	9.28	3.79E-05	0.209	6.91
200	300	5651	18.84	12.27	6.57	2.68E-05	0.231	4.87
225	300	2592	8.64	4.55	4.09	1.67E-05	0.251	3.36

Appendix B MCNP Results

Detector #1

Proof of Concept – Case 1 (Beryllium/Beryllium)

Co-60 Source				
Scintillator Thickness (mm)			1	
Scintillator Location			on axis	
Source Location			Center	
Material			Beryllium/Beryllium	
Energy (MeV)	$\frac{dN}{dE}\left(\frac{cts}{bin}\right)$	$\sigma\left[\frac{dN}{dE}\right]$	$N\left(Br\sum\frac{dN}{dE}\right)$	$\sigma[N]$
0.000	1.67E-05	2.58E-06		
0.001	3.98E-01	3.18E-04	2.09E-02	6.45E-05
0.051	1.43E-03	2.40E-05	1.80E-02	5.99E-05
0.101	1.14E-03	2.15E-05	1.57E-02	5.59E-05
0.151	9.92E-04	1.98E-05	1.37E-02	5.23E-05
0.201	1.10E-03	2.09E-05	1.15E-02	4.79E-05
0.251	1.18E-03	2.17E-05	9.16E-03	4.27E-05
0.301	1.01E-03	2.00E-05	7.14E-03	3.78E-05
0.351	8.10E-04	1.80E-05	5.52E-03	3.32E-05
0.401	6.64E-04	1.63E-05	4.19E-03	2.89E-05
0.451	5.08E-04	1.42E-05	3.18E-03	2.52E-05
0.501	3.89E-04	1.24E-05	2.40E-03	2.19E-05
0.551	3.08E-04	1.11E-05	1.78E-03	1.89E-05
0.601	2.39E-04	9.76E-06	1.31E-03	1.62E-05
0.651	1.84E-04	8.59E-06	9.37E-04	1.37E-05
0.701	1.36E-04	7.37E-06	6.67E-04	1.15E-05
0.751	9.88E-05	6.28E-06	4.69E-04	9.68E-06
0.800	7.52E-05	5.49E-06	3.19E-04	7.98E-06
0.850	5.50E-05	4.68E-06	2.09E-04	6.46E-06
0.900	3.98E-05	3.99E-06	1.29E-04	5.08E-06
0.950	2.97E-05	3.44E-06	7.00E-05	3.74E-06
1.000	1.53E-05	2.47E-06	3.94E-05	2.81E-06
1.050	9.90E-06	1.99E-06	1.96E-05	1.98E-06
1.100	7.60E-06	1.74E-06	4.40E-06	9.37E-07
1.150	2.10E-06	9.16E-07		

Cs-137 Source				
Scintillator Thickness (mm)			1	
Scintillator Location			on axis	
Source Location			Center	
Material			Beryllium/beryllium	
Energy (MeV)	$\frac{dN}{dE}\left(\frac{cts}{bin}\right)$	$\sigma\left[\frac{dN}{dE}\right]$	$N\left(Br\sum\frac{dN}{dE}\right)$	$\sigma[N]$
0.000	4.60E-06	6.78E-07		
0.001	4.01E-01	1.61E-04	9.30E-03	2.92E-05
0.051	3.16E-03	1.77E-05	6.19E-03	2.38E-05
0.101	1.56E-03	1.24E-05	4.76E-03	2.09E-05
0.151	1.14E-03	1.06E-05	3.71E-03	1.85E-05
0.201	9.57E-04	9.76E-06	2.83E-03	1.61E-05
0.251	8.14E-04	9.04E-06	2.08E-03	1.38E-05
0.301	6.85E-04	8.29E-06	1.45E-03	1.15E-05
0.351	5.73E-04	7.56E-06	9.21E-04	9.20E-06
0.401	4.45E-04	6.67E-06	5.12E-04	6.86E-06
0.451	3.62E-04	6.01E-06	1.79E-04	4.06E-06
0.501	1.86E-04	4.32E-06	7.91E-06	8.53E-07
0.551	8.00E-06	8.94E-07	5.52E-07	2.25E-07
0.601	5.00E-07	2.24E-07	9.20E-08	9.20E-08
0.651	1.00E-07	1.00E-07	0.00E+00	0.00E+00
0.701	0.00E+00	0.00E+00	0.00E+00	0.00E+00
0.751	0.00E+00	0.00E+00		

Na-22 Source				
Scintillator Thickness (mm)			1	
Scintillator Location			on axis	
Source Location			Center	
Material			Beryllium/Beryllium	
Energy (MeV)	$\frac{dN}{dE}\left(\frac{cts}{bin}\right)$	$\sigma\left[\frac{dN}{dE}\right]$	$N\left(Br\sum\frac{dN}{dE}\right)$	$\sigma[N]$
0.000	1.85E-05	4.13E-06		
0.001	3.97E-01	4.77E-04	2.70E-02	6.41E-05
0.051	1.39E-03	1.18E-05	2.05E-02	5.50E-05
0.101	1.11E-03	1.05E-05	1.61E-02	4.80E-05
0.151	9.45E-04	9.72E-06	1.28E-02	4.22E-05
0.201	1.07E-03	1.03E-05	9.94E-03	3.66E-05
0.251	1.21E-03	1.10E-05	7.23E-03	3.07E-05
0.301	1.03E-03	1.02E-05	4.81E-03	2.41E-05

0.351	8.09E-04	8.97E-06	2.84E-03	1.70E-05
0.401	6.68E-04	8.16E-06	2.14E-03	1.46E-05
0.451	5.22E-04	7.22E-06	1.61E-03	1.27E-05
0.501	3.92E-04	6.26E-06	1.22E-03	1.10E-05
0.551	3.04E-04	5.51E-06	9.16E-04	9.56E-06
0.601	2.40E-04	4.89E-06	6.76E-04	8.22E-06
0.651	1.85E-04	4.29E-06	4.91E-04	7.01E-06
0.701	1.37E-04	3.70E-06	3.55E-04	5.95E-06
0.750	1.00E-04	3.16E-06	2.55E-04	5.05E-06
0.800	7.63E-05	2.76E-06	1.78E-04	4.22E-06
0.850	5.99E-05	2.45E-06	1.19E-04	3.44E-06
0.900	4.39E-05	2.09E-06	7.48E-05	2.73E-06
0.950	3.11E-05	1.76E-06	4.37E-05	2.09E-06
1.000	2.49E-05	1.58E-06	1.88E-05	1.37E-06
1.050	1.88E-05	1.37E-06		

Proof of Concept – Case 2 (Beryllium/Polypropylene)

Co-60 Source						
Scintillator Thickness (mm)					1	
Scintillator Location					on axis	
Source Location					Center	
Material					Beryllium/Polypropylene	
Energy (MeV)	$\frac{d\gamma}{dE}\left(\frac{cts}{bin}\right)$	$\sigma_\gamma\left[\frac{dN}{dE}\right]$	$\frac{d\beta}{dE}\left(\frac{cts}{bin}\right)$	$\sigma_\beta\left[\frac{dN}{dE}\right]$	$N\left(Br\sum\frac{dN}{dE}\right)$	$\sigma[N]$
0.000	2.37E-05	3.08E-06	0.00E+00	0.00E+00		
0.001	4.70E-01	2.82E-04	1.33E-03	1.15E-05	3.10E-02	7.86E-05
0.051	1.73E-03	2.62E-05	9.77E-05	3.13E-06	2.75E-02	7.40E-05
0.101	1.53E-03	2.47E-05	3.30E-06	5.75E-07	2.44E-02	6.98E-05
0.151	1.39E-03	2.36E-05	4.50E-06	6.71E-07	2.16E-02	6.57E-05
0.201	1.53E-03	2.48E-05	9.70E-06	9.85E-07	1.86E-02	6.08E-05
0.251	1.76E-03	2.63E-05	1.52E-05	1.23E-06	1.51E-02	5.48E-05
0.301	1.53E-03	2.47E-05	1.30E-05	1.14E-06	1.20E-02	4.89E-05
0.351	1.27E-03	2.25E-05	9.60E-06	9.80E-07	9.44E-03	4.34E-05
0.401	1.05E-03	2.04E-05	1.05E-05	1.02E-06	7.33E-03	3.83E-05
0.451	8.41E-04	1.83E-05	8.00E-06	8.94E-07	5.64E-03	3.36E-05
0.501	6.54E-04	1.62E-05	6.00E-06	7.75E-07	4.33E-03	2.94E-05
0.551	5.13E-04	1.43E-05	4.30E-06	6.56E-07	3.30E-03	2.57E-05
0.601	4.08E-04	1.28E-05	4.40E-06	6.64E-07	2.48E-03	2.22E-05
0.651	3.08E-04	1.11E-05	1.80E-06	4.24E-07	1.86E-03	1.93E-05

0.701	2.43E-04	9.87E-06	1.10E-06	3.32E-07	1.37E-03	1.66E-05
0.751	1.90E-04	8.72E-06	9.00E-07	3.00E-07	9.93E-04	1.41E-05
0.800	1.46E-04	7.66E-06	3.00E-07	1.73E-07	7.01E-04	1.18E-05
0.850	1.11E-04	6.66E-06	1.00E-07	1.00E-07	4.79E-04	9.78E-06
0.900	9.02E-05	6.00E-06			2.99E-04	7.72E-06
0.950	6.77E-05	5.20E-06			1.63E-04	5.71E-06
1.000	3.42E-05	3.70E-06			9.49E-05	4.36E-06
1.050	2.34E-05	3.06E-06			4.82E-05	3.10E-06
1.100	1.76E-05	2.65E-06			1.30E-05	1.61E-06
1.150	5.80E-06	1.52E-06			1.40E-06	5.29E-07
1.200	4.00E-07	4.00E-07			6.00E-07	3.46E-07
1.250	2.00E-07	2.83E-07			2.00E-07	2.00E-07
1.300	1.00E-07	2.00E-07			0.00E+00	0.00E+00
1.350	0.00E+00	0.00E+00			0.00E+00	0.00E+00
1.400	0.00E+00	0.00E+00				

Cl-36 Source				
Scintillator Thickness (mm)			1	
Scintillator Location			on axis	
Source Location			Center	
Material			Beryllium/Polypropylene	
Energy (MeV)	$\frac{dN}{dE}\left(\frac{cts}{bin}\right)$	$\sigma\left[\frac{dN}{dE}\right]$	$N\left(Br\sum\frac{dN}{dE}\right)$	$\sigma[N]$
0.000	3.19E-04	5.53E-06		
0.001	1.93E-04	4.31E-06	6.26E-01	2.41E-04
0.051	5.33E-02	6.80E-05	5.73E-01	2.31E-04
0.101	6.87E-02	8.09E-05	5.06E-01	2.16E-04
0.151	7.13E-02	7.69E-05	4.36E-01	2.02E-04
0.201	7.46E-02	8.05E-05	3.63E-01	1.85E-04
0.251	7.80E-02	8.42E-05	2.86E-01	1.65E-04
0.301	7.92E-02	8.54E-05	2.09E-01	1.41E-04
0.351	6.89E-02	8.11E-05	1.41E-01	1.16E-04
0.401	5.43E-02	6.93E-05	8.79E-02	9.27E-05
0.451	3.90E-02	6.13E-05	4.96E-02	6.96E-05
0.501	2.49E-02	4.88E-05	2.52E-02	4.97E-05
0.551	1.45E-02	3.71E-05	1.09E-02	3.31E-05
0.601	7.38E-03	2.68E-05	3.69E-03	1.94E-05
0.651	2.98E-03	1.73E-05	7.69E-04	8.84E-06
0.701	7.54E-04	8.67E-06	2.94E-05	1.73E-06
0.751	3.00E-05	1.73E-06		

Sr-90 Source				
Scintillator Thickness (mm)			1	
Scintillator Location			on axis	
Source Location			Center	
Material			Beryllium/Polypropylene	
Energy (MeV)	$\frac{dN}{dE}\left(\frac{cts}{bin}\right)$	$\sigma\left[\frac{dN}{dE}\right]$	$N\left(Br\sum\frac{dN}{dE}\right)$	$\sigma[N]$
0.000	6.28E-03	5.02E-05		
0.001	6.43E-03	7.08E-05	1.21E+00	6.70E-04
0.050	4.09E-02	1.72E-04	1.13E+00	6.48E-04
0.099	5.14E-02	1.95E-04	1.03E+00	6.18E-04
0.148	5.18E-02	1.97E-04	9.22E-01	5.85E-04
0.197	7.33E-02	2.35E-04	7.75E-01	5.36E-04
0.246	8.01E-02	2.40E-04	6.15E-01	4.79E-04
0.295	7.13E-02	2.28E-04	4.72E-01	4.22E-04
0.344	5.70E-02	2.05E-04	3.58E-01	3.68E-04
0.392	4.29E-02	1.80E-04	2.72E-01	3.21E-04
0.441	3.06E-02	1.53E-04	2.11E-01	2.83E-04
0.490	2.08E-02	1.25E-04	1.70E-01	2.54E-04
0.539	1.49E-02	1.07E-04	1.40E-01	2.30E-04
0.588	1.16E-02	9.51E-05	1.17E-01	2.09E-04
0.637	9.71E-03	8.55E-05	9.73E-02	1.91E-04
0.686	8.10E-03	7.94E-05	8.11E-02	1.74E-04
0.735	6.84E-03	7.25E-05	6.74E-02	1.58E-04
0.784	5.68E-03	6.59E-05	5.60E-02	1.43E-04
0.833	4.76E-03	6.00E-05	4.65E-02	1.30E-04
0.882	3.99E-03	5.50E-05	3.85E-02	1.18E-04
0.931	3.32E-03	5.05E-05	3.19E-02	1.07E-04
0.980	2.74E-03	4.61E-05	2.64E-02	9.64E-05
1.029	2.30E-03	4.19E-05	2.18E-02	8.68E-05
1.078	1.91E-03	3.83E-05	1.80E-02	7.79E-05
1.127	1.57E-03	3.49E-05	1.48E-02	6.97E-05
1.176	1.29E-03	3.16E-05	1.22E-02	6.21E-05
1.224	1.02E-03	2.80E-05	1.02E-02	5.54E-05
1.273	8.64E-04	2.57E-05	8.45E-03	4.91E-05
1.322	6.84E-04	2.30E-05	7.08E-03	4.33E-05
1.371	5.61E-04	2.08E-05	5.96E-03	3.80E-05
1.420	4.28E-04	1.82E-05	5.10E-03	3.34E-05
1.469	3.49E-04	1.64E-05	4.41E-03	2.91E-05
2.301	1.10E-03	9.50E-05		

Proof of Concept – Case 3 (Polypropylene/Polypropylene)

Co-60 Source						
Scintillator Thickness (mm)						1
Scintillator Location						on axis
Source Location						Center
Material						Polypropylene/Polypropylene
Energy (MeV)	$\frac{d\gamma}{dE}\left(\frac{cts}{bin}\right)$	$\sigma_\gamma\left[\frac{dN}{dE}\right]$	$\frac{d\beta}{dE}\left(\frac{cts}{bin}\right)$	$\sigma_\beta\left[\frac{dN}{dE}\right]$	$N\left(Br\sum\frac{dN}{dE}\right)$	$\sigma[N]$
0.000	2.19E-05	2.96E-06	0.00E+00	0.00E+00		
0.001	4.69E-01	2.81E-04	1.33E-03	1.15E-05	3.08E-02	7.81E-05
0.051	1.64E-03	2.56E-05	9.77E-05	3.13E-06	2.74E-02	7.38E-05
0.101	1.47E-03	2.41E-05	3.30E-06	5.75E-07	2.45E-02	6.97E-05
0.151	1.34E-03	2.30E-05	4.50E-06	6.71E-07	2.18E-02	6.58E-05
0.201	1.51E-03	2.44E-05	9.70E-06	9.85E-07	1.88E-02	6.11E-05
0.251	1.73E-03	2.63E-05	1.52E-05	1.23E-06	1.53E-02	5.51E-05
0.301	1.54E-03	2.46E-05	1.30E-05	1.14E-06	1.22E-02	4.93E-05
0.351	1.26E-03	2.24E-05	9.60E-06	9.80E-07	9.67E-03	4.39E-05
0.401	1.06E-03	2.05E-05	1.05E-05	1.02E-06	7.55E-03	3.88E-05
0.451	8.51E-04	1.84E-05	8.00E-06	8.94E-07	5.84E-03	3.41E-05
0.501	6.67E-04	1.63E-05	6.00E-06	7.75E-07	4.50E-03	3.00E-05
0.551	5.21E-04	1.45E-05	4.30E-06	6.56E-07	3.45E-03	2.63E-05
0.601	4.23E-04	1.30E-05	4.40E-06	6.64E-07	2.60E-03	2.28E-05
0.651	3.42E-04	1.17E-05	1.80E-06	4.24E-07	1.92E-03	1.96E-05
0.701	2.50E-04	1.00E-05	1.10E-06	3.32E-07	1.42E-03	1.68E-05
0.751	1.97E-04	8.86E-06	9.00E-07	3.00E-07	1.02E-03	1.43E-05
0.801	1.53E-04	7.80E-06	3.00E-07	1.73E-07	7.16E-04	1.20E-05
0.851	1.17E-04	6.85E-06	1.00E-07	1.00E-07	4.81E-04	9.80E-06
0.901	8.49E-05	5.82E-06			3.12E-04	7.89E-06
0.951	6.98E-05	5.27E-06			1.72E-04	5.86E-06
1.001	3.56E-05	3.77E-06			1.01E-04	4.49E-06
1.051	2.43E-05	3.11E-06			5.24E-05	3.24E-06
1.101	1.98E-05	2.81E-06			1.28E-05	1.60E-06
1.151	6.00E-06	1.55E-06			7.99E-07	4.00E-07
1.201	3.00E-07	3.46E-07			2.00E-07	2.00E-07
1.251	1.00E-07	2.00E-07				

Sr-90 Source				
Scintillator Thickness (mm)			1	
Scintillator Location			on axis	
Source Location			Center	
Material			Polypropylene/Polypropylene	
Energy (MeV)	$\frac{dN}{dE}\left(\frac{cts}{bin}\right)$	$\sigma\left[\frac{dN}{dE}\right]$	$N\left(Br\sum\frac{dN}{dE}\right)$	$\sigma[N]$
0.000	6.29E-03	5.03E-05		
0.001	6.47E-03	5.04E-05	1.21E+00	4.83E-04
0.050	4.09E-02	1.23E-04	1.13E+00	4.68E-04
0.099	5.14E-02	1.44E-04	1.02E+00	4.45E-04
0.148	5.18E-02	1.45E-04	9.20E-01	4.21E-04
0.197	7.28E-02	1.60E-04	7.74E-01	3.89E-04
0.246	7.91E-02	1.74E-04	6.16E-01	3.48E-04
0.295	7.03E-02	1.69E-04	4.75E-01	3.04E-04
0.344	5.62E-02	1.46E-04	3.63E-01	2.67E-04
0.392	4.26E-02	1.28E-04	2.78E-01	2.34E-04
0.441	3.05E-02	1.10E-04	2.17E-01	2.07E-04
0.490	2.10E-02	9.25E-05	1.75E-01	1.85E-04
0.539	1.52E-02	7.59E-05	1.44E-01	1.69E-04
0.588	1.20E-02	6.93E-05	1.20E-01	1.54E-04
0.637	1.00E-02	6.21E-05	1.00E-01	1.41E-04
0.686	8.41E-03	5.72E-05	8.34E-02	1.29E-04
0.735	7.12E-03	5.27E-05	6.91E-02	1.17E-04
0.784	5.99E-03	4.91E-05	5.72E-02	1.07E-04
0.833	5.03E-03	4.42E-05	4.71E-02	9.69E-05
0.882	4.20E-03	4.11E-05	3.87E-02	8.77E-05
0.931	3.53E-03	3.75E-05	3.16E-02	7.94E-05
0.980	2.94E-03	3.41E-05	2.58E-02	7.17E-05
1.029	2.44E-03	3.13E-05	2.09E-02	6.45E-05
1.078	2.03E-03	2.84E-05	1.68E-02	5.79E-05
1.127	1.67E-03	2.57E-05	1.35E-02	5.19E-05
1.176	1.38E-03	2.35E-05	1.07E-02	4.63E-05
1.224	1.10E-03	2.10E-05	8.52E-03	4.12E-05
1.273	9.17E-04	1.91E-05	6.69E-03	3.66E-05
1.322	7.37E-04	1.71E-05	5.21E-03	3.23E-05
1.371	5.95E-04	1.55E-05	4.03E-03	2.84E-05
1.420	4.59E-04	1.36E-05	3.11E-03	2.49E-05
1.469	3.75E-04	1.22E-05	2.36E-03	2.17E-05
2.301	1.55E-03	8.25E-05		

Pb-210 Source						
Scintillator Thickness (mm)					1.0	
Scintillator Location					on axis	
Source Location					Center	
Material					Polypropylene/Polypropylene	
Energy (MeV)	$\frac{d\gamma}{dE}\left(\frac{cts}{bin}\right)$	$\sigma_\gamma\left[\frac{dN}{dE}\right]$	$\frac{d\beta}{dE}\left(\frac{cts}{bin}\right)$	$\sigma_\beta\left[\frac{dN}{dE}\right]$	$N\left(Br\sum\frac{dN}{dE}\right)$	$\sigma[N]$
0.000	2.45E-01	1.47E-04	2.30E-03	1.52E-05		
0.001	5.93E-03	2.43E-05	4.16E-05	2.04E-06	5.19E-01	1.60E-04
0.051	7.31E-02	8.04E-05	7.01E-03	2.66E-05	4.65E-01	1.55E-04
0.101	2.00E-07	1.41E-07	1.21E-02	3.51E-05	4.24E-01	1.28E-04
0.151			1.52E-02	3.81E-05	3.69E-01	1.22E-04
0.201			1.99E-02	4.39E-05	2.98E-01	1.14E-04
0.251			2.58E-02	4.90E-05	2.29E-01	1.03E-04
0.301			2.50E-02	5.01E-05	1.71E-01	9.03E-05
0.351			2.12E-02	4.46E-05	1.24E-01	7.85E-05
0.401			1.72E-02	4.14E-05	8.69E-02	6.68E-05
0.451			1.34E-02	3.61E-05	6.04E-02	5.62E-05
0.501			9.66E-03	3.09E-05	4.13E-02	4.69E-05
0.551			6.92E-03	2.63E-05	2.77E-02	3.88E-05
0.601			4.96E-03	2.23E-05	1.82E-02	3.18E-05
0.651			3.46E-03	1.87E-05	1.15E-02	2.57E-05
0.701			2.45E-03	1.57E-05	7.03E-03	2.04E-05
0.751			1.63E-03	1.27E-05	4.14E-03	1.59E-05
0.801			1.05E-03	1.02E-05	2.27E-03	1.22E-05
0.851			6.78E-04	8.20E-06	1.16E-03	9.09E-06
0.901			4.06E-04	6.37E-06	5.46E-04	6.49E-06
0.951			2.24E-04	4.72E-06	2.27E-04	4.46E-06
1.001			1.16E-04	3.41E-06	8.15E-05	2.87E-06
1.051			5.28E-05	2.30E-06	2.09E-05	1.72E-06
1.101			2.21E-05	1.49E-06	5.77E-06	8.72E-07
1.151			5.50E-06	7.41E-07	1.37E-06	4.58E-07
1.201			1.60E-06	4.00E-07		

Cl-36 Source				
Scintillator Thickness (mm)			1.0	
Scintillator Location			on axis	
Source Location			Center	
Material			Polypropylene/polypropylene	
Energy (MeV)	$\frac{dN}{dE}\left(\frac{cts}{bin}\right)$	$\sigma\left[\frac{dN}{dE}\right]$	$N\left(Br\sum\frac{dN}{dE}\right)$	$\sigma[N]$

0.000	3.35E-03	1.80E-05		
0.001	1.93E-04	4.32E-06	6.26E-01	2.41E-04
0.051	5.33E-02	6.80E-05	5.73E-01	2.31E-04
0.101	6.87E-02	8.09E-05	5.06E-01	2.16E-04
0.151	7.13E-02	7.69E-05	4.36E-01	2.02E-04
0.201	7.45E-02	8.04E-05	3.63E-01	1.85E-04
0.251	7.77E-02	8.39E-05	2.87E-01	1.65E-04
0.301	7.88E-02	8.50E-05	2.09E-01	1.42E-04
0.351	6.87E-02	8.09E-05	1.42E-01	1.16E-04
0.401	5.45E-02	6.95E-05	8.86E-02	9.32E-05
0.451	3.93E-02	6.16E-05	5.01E-02	6.99E-05
0.501	2.51E-02	4.92E-05	2.54E-02	4.97E-05
0.551	1.47E-02	3.75E-05	1.10E-02	3.26E-05
0.601	7.46E-03	2.63E-05	3.72E-03	1.93E-05
0.651	3.00E-03	1.71E-05	7.74E-04	8.90E-06
0.701	7.58E-04	8.72E-06	3.05E-05	1.76E-06
0.751	3.11E-05	1.76E-06		

Proof of Concept – Case 4 (Mylar Wrap)

Sr-90 Source				
Scintillator Thickness (mm)			1	
Scintillator Location			on axis	
Source Location			Center	
Material			Mylar Wrap	
Energy (MeV)	$\frac{dN}{dE}\left(\frac{cts}{bin}\right)$	$\sigma\left[\frac{dN}{dE}\right]$	$N\left(Br\sum\frac{dN}{dE}\right)$	$\sigma[N]$
0.000	6.75E-03	1.63E-04		
0.001	1.03E-04	2.03E-05	1.09E+00	1.44E-03
0.051	2.38E-02	3.05E-04	1.05E+00	1.41E-03
0.101	4.11E-02	3.95E-04	9.64E-01	1.36E-03
0.151	4.77E-02	4.29E-04	8.68E-01	1.29E-03
0.201	7.19E-02	5.18E-04	7.25E-01	1.18E-03
0.251	7.73E-02	5.41E-04	5.70E-01	1.05E-03
0.301	6.71E-02	4.96E-04	4.36E-01	9.20E-04
0.351	5.23E-02	4.49E-04	3.31E-01	8.02E-04
0.401	3.93E-02	3.85E-04	2.53E-01	7.04E-04
0.451	2.72E-02	3.26E-04	1.99E-01	6.24E-04
0.501	1.86E-02	2.71E-04	1.61E-01	5.62E-04
0.551	1.38E-02	2.34E-04	1.34E-01	5.11E-04

0.601	1.12E-02	2.10E-04	1.12E-01	4.66E-04
0.651	9.32E-03	1.92E-04	9.30E-02	4.25E-04
0.701	7.79E-03	1.76E-04	7.74E-02	3.87E-04
0.751	6.62E-03	1.62E-04	6.41E-02	3.51E-04
0.801	5.55E-03	1.49E-04	5.30E-02	3.18E-04
0.851	4.63E-03	1.36E-04	4.38E-02	2.88E-04
0.901	3.76E-03	1.23E-04	3.63E-02	2.60E-04
0.951	3.20E-03	1.13E-04	2.99E-02	2.34E-04
1.001	2.61E-03	1.02E-04	2.46E-02	2.11E-04
1.051	2.19E-03	9.34E-05	2.03E-02	1.89E-04
1.101	1.74E-03	8.34E-05	1.68E-02	1.70E-04
1.151	1.45E-03	7.62E-05	1.39E-02	1.51E-04
1.201	1.23E-03	6.99E-05	1.14E-02	1.34E-04
1.251	9.40E-04	6.13E-05	9.56E-03	1.20E-04
1.301	7.95E-04	5.64E-05	7.97E-03	1.05E-04
1.351	6.46E-04	5.08E-05	6.68E-03	9.23E-05
1.401	5.11E-04	4.52E-05	5.66E-03	8.05E-05
1.451	4.16E-04	4.08E-05	4.82E-03	6.94E-05
2.301	1.21E-03	2.20E-04		

¼ and ½ mm Scintillator

Co-60 Source						
Scintillator Thickness (mm)						0.25
Scintillator Location						on axis
Source Location						Center
Material						Polypropylene/Polypropylene
Energy (MeV)	$\frac{d\gamma}{dE}\left(\frac{cts}{bin}\right)$	$\sigma_\gamma\left[\frac{dN}{dE}\right]$	$\frac{d\beta}{dE}\left(\frac{cts}{bin}\right)$	$\sigma_\beta\left[\frac{dN}{dE}\right]$	$N\left(Br\sum\frac{dN}{dE}\right)$	$\sigma[N]$
0.000	4.73E-05	1.19E-05	1.80E-06	4.24E-07		
0.001	4.60E-01	8.27E-04	1.53E-03	1.24E-05	1.76E-02	3.36E-04
0.051	1.73E-03	1.62E-04	7.66E-05	2.77E-06	1.41E-02	2.95E-04
0.101	3.22E-03	2.02E-04	7.54E-05	2.74E-06	7.56E-03	2.15E-04
0.151	1.41E-03	1.32E-04	2.17E-05	1.47E-06	4.72E-03	1.69E-04
0.201	8.46E-04	1.01E-04	1.46E-05	1.21E-06	3.01E-03	1.36E-04
0.251	6.21E-04	8.69E-05	8.20E-06	9.05E-07	1.76E-03	1.04E-04
0.301	3.40E-04	6.48E-05	5.80E-06	7.62E-07	1.08E-03	8.18E-05
0.351	2.18E-04	5.17E-05	3.40E-06	5.83E-07	6.40E-04	6.34E-05
0.401	1.27E-04	3.97E-05	2.10E-06	4.58E-07	3.84E-04	4.94E-05
0.451	7.28E-05	2.96E-05	1.40E-06	3.74E-07	2.37E-04	3.95E-05

0.501	5.03E-05	2.56E-05	8.00E-07	2.83E-07	1.36E-04	3.01E-05
0.551	2.85E-05	1.86E-05	4.00E-07	2.00E-07	7.84E-05	2.37E-05
0.601	1.50E-05	1.55E-05	3.00E-07	1.73E-07	4.81E-05	1.79E-05
0.651	6.75E-06	9.54E-06	0.00E+00	0.00E+00	3.46E-05	1.52E-05
0.701	8.25E-06	1.03E-05	1.00E-07	1.00E-07	1.80E-05	1.11E-05
0.751	6.75E-06	1.08E-05			4.50E-06	2.60E-06
0.801	1.50E-06	2.12E-06			1.50E-06	1.50E-06
0.851	0.00E+00	0.00E+00				

Sr-90 Source				
Scintillator Thickness (mm)			0.25	
Scintillator Location			on axis	
Source Location			Center	
Material			Polypropylene/polypropylene	
Energy (MeV)	$\frac{dN}{dE}\left(\frac{cts}{bin}\right)$	$\sigma\left[\frac{dN}{dE}\right]$	$N\left(Br\sum\frac{dN}{dE}\right)$	$\sigma[N]$
0.000	6.81E-03	5.18E-05		
0.001	1.27E-04	7.14E-06	1.17E+00	4.47E-04
0.051	8.37E-02	1.67E-04	1.00E+00	4.14E-04
0.101	2.05E-01	2.46E-04	5.91E-01	3.33E-04
0.151	1.16E-01	2.09E-04	3.59E-01	2.59E-04
0.201	7.18E-02	1.58E-04	2.15E-01	2.06E-04
0.251	4.18E-02	1.25E-04	1.32E-01	1.63E-04
0.301	2.53E-02	1.01E-04	8.12E-02	1.28E-04
0.351	1.51E-02	7.85E-05	5.10E-02	1.01E-04
0.401	9.02E-03	5.95E-05	3.30E-02	8.10E-05
0.451	5.59E-03	4.69E-05	2.18E-02	6.61E-05
0.501	3.56E-03	3.78E-05	1.47E-02	5.42E-05
0.551	2.37E-03	3.08E-05	9.95E-03	4.46E-05
0.601	1.60E-03	2.52E-05	6.76E-03	3.68E-05
0.651	1.09E-03	2.10E-05	4.58E-03	3.02E-05
0.701	7.43E-04	1.72E-05	3.09E-03	2.48E-05
0.751	5.08E-04	1.42E-05	2.08E-03	2.04E-05
0.801	3.38E-04	1.16E-05	1.40E-03	1.67E-05
0.851	2.39E-04	9.77E-06	9.20E-04	1.35E-05
0.901	1.58E-04	7.95E-06	6.05E-04	1.10E-05
0.951	1.04E-04	6.45E-06	3.98E-04	8.87E-06
1.001	6.91E-05	5.25E-06	2.59E-04	7.15E-06
1.051	4.17E-05	4.09E-06	1.76E-04	5.87E-06
1.101	3.07E-05	3.51E-06	1.15E-04	4.71E-06
1.151	1.96E-05	2.80E-06	7.54E-05	3.79E-06

1.201	1.24E-05	2.23E-06	5.06E-05	3.07E-06
1.251	8.90E-06	1.89E-06	3.28E-05	2.42E-06
1.301	5.40E-06	1.47E-06	2.20E-05	1.92E-06
1.351	3.30E-06	1.15E-06	1.54E-05	1.54E-06
1.401	2.80E-06	1.06E-06	9.80E-06	1.11E-06
1.451	1.30E-06	7.21E-07	7.20E-06	8.48E-07
2.301	1.80E-06	1.97E-06		

Co-60 Source						
Scintillator Thickness (mm)						0.50
Scintillator Location						on axis
Source Location						Center
Material						Polypropylene/Polypropylene
Energy (MeV)	$\frac{d\gamma}{dE}\left(\frac{cts}{bin}\right)$	$\sigma_\gamma\left[\frac{dN}{dE}\right]$	$\frac{d\beta}{dE}\left(\frac{cts}{bin}\right)$	$\sigma_\beta\left[\frac{dN}{dE}\right]$	$N\left(Br\sum\frac{dN}{dE}\right)$	$\sigma[N]$
0.000	3.14E-05	3.54E-06	5.00E-07	2.24E-07		
0.001	4.73E-01	2.84E-04	1.50E-03	1.23E-05	2.34E-02	6.83E-05
0.051	1.29E-03	2.28E-05	7.05E-05	2.66E-06	2.07E-02	6.43E-05
0.101	1.74E-03	2.64E-05	3.17E-05	1.78E-06	1.72E-02	5.86E-05
0.151	2.55E-03	3.21E-05	5.62E-05	2.37E-06	1.21E-02	4.90E-05
0.201	1.68E-03	2.59E-05	2.32E-05	1.52E-06	8.70E-03	4.16E-05
0.251	1.19E-03	2.17E-05	1.69E-05	1.30E-06	6.30E-03	3.55E-05
0.301	8.94E-04	1.89E-05	1.26E-05	1.12E-06	4.50E-03	3.00E-05
0.351	6.50E-04	1.61E-05	1.05E-05	1.02E-06	3.19E-03	2.52E-05
0.401	4.77E-04	1.38E-05	7.40E-06	8.60E-07	2.23E-03	2.11E-05
0.451	3.36E-04	1.16E-05	5.10E-06	7.14E-07	1.55E-03	1.76E-05
0.501	2.41E-04	9.82E-06	4.90E-06	7.00E-07	1.07E-03	1.46E-05
0.551	1.70E-04	8.24E-06	2.40E-06	4.90E-07	7.25E-04	1.20E-05
0.601	1.20E-04	6.91E-06	1.60E-06	4.00E-07	4.84E-04	9.83E-06
0.651	8.25E-05	5.74E-06	6.00E-07	2.45E-07	3.19E-04	7.97E-06
0.701	5.68E-05	4.77E-06	1.10E-06	3.32E-07	2.04E-04	6.38E-06
0.751	3.63E-05	3.81E-06	2.00E-07	1.41E-07	1.31E-04	5.12E-06
0.801	2.42E-05	3.11E-06	2.00E-07	1.41E-07	8.26E-05	4.06E-06
0.851	1.85E-05	2.72E-06	1.00E-07	1.00E-07	4.56E-05	3.02E-06
0.901	1.00E-05	2.00E-06			2.56E-05	2.26E-06
0.951	6.30E-06	1.59E-06			1.30E-05	1.61E-06
1.001	3.60E-06	1.20E-06			5.80E-06	1.08E-06
1.051	1.50E-06	7.74E-07			2.80E-06	7.48E-07
1.101	1.20E-06	6.92E-07			4.00E-07	2.83E-07
1.151	2.00E-07	2.83E-07			0.00E+00	0.00E+00
1.201	0.00E+00	0.00E+00				

Sr-90 Source				
Scintillator Thickness (mm)			0.50	
Scintillator Location			on axis	
Source Location			Center	
Material			Polypropylene/polypropylene	
Energy (MeV)	$\frac{dN}{dE}\left(\frac{cts}{bin}\right)$	$\sigma\left[\frac{dN}{dE}\right]$	$N\left(Br\sum\frac{dN}{dE}\right)$	$\sigma[N]$
0.000	6.65E-03	8.90E-05		
0.001	1.25E-04	1.23E-05	1.17E+00	8.05E-04
0.051	3.64E-02	2.04E-04	1.10E+00	7.78E-04
0.101	8.69E-02	3.13E-04	9.26E-01	7.13E-04
0.151	1.29E-01	3.60E-04	6.68E-01	6.15E-04
0.201	1.00E-01	3.21E-04	4.68E-01	5.24E-04
0.251	7.28E-02	2.91E-04	3.22E-01	4.36E-04
0.301	5.10E-02	2.45E-04	2.20E-01	3.61E-04
0.351	3.31E-02	1.99E-04	1.54E-01	3.01E-04
0.401	2.14E-02	1.58E-04	1.11E-01	2.57E-04
0.451	1.43E-02	1.29E-04	8.24E-02	2.22E-04
0.501	9.90E-03	1.09E-04	6.26E-02	1.93E-04
0.551	7.29E-03	9.33E-05	4.81E-02	1.69E-04
0.601	5.52E-03	8.18E-05	3.70E-02	1.48E-04
0.651	4.34E-03	7.20E-05	2.83E-02	1.30E-04
0.701	3.29E-03	6.26E-05	2.17E-02	1.14E-04
0.751	2.56E-03	5.52E-05	1.66E-02	9.93E-05
0.801	1.97E-03	4.86E-05	1.27E-02	8.66E-05
0.851	1.54E-03	4.30E-05	9.61E-03	7.52E-05
0.901	1.19E-03	3.79E-05	7.23E-03	6.49E-05
0.951	8.91E-04	3.26E-05	5.45E-03	5.61E-05
1.001	6.85E-04	2.86E-05	4.08E-03	4.83E-05
1.051	5.07E-04	2.47E-05	3.06E-03	4.15E-05
1.101	3.85E-04	2.15E-05	2.29E-03	3.55E-05
1.151	2.85E-04	1.85E-05	1.72E-03	3.03E-05
1.201	2.10E-04	1.59E-05	1.30E-03	2.58E-05
1.251	1.65E-04	1.41E-05	9.72E-04	2.17E-05
1.301	1.19E-04	1.19E-05	7.35E-04	1.81E-05
1.351	7.56E-05	9.53E-06	5.83E-04	1.54E-05
1.401	5.28E-05	7.97E-06	4.78E-04	1.31E-05
1.451	4.86E-05	7.64E-06	3.81E-04	1.07E-05
2.301	9.51E-05	3.16E-05		

Co-60 Source				
Scintillator Thickness (mm)				0.50
Scintillator Location				on axis
Source Location				Center
Material				Beryllium/Beryllium
Energy (MeV)	$\frac{dN}{dE}\left(\frac{cts}{bin}\right)$	$\sigma\left[\frac{dN}{dE}\right]$	$N\left(Br\sum\frac{dN}{dE}\right)$	$\sigma[N]$
0.000	2.16E-05	1.47E-06		
0.001	4.00E-01	1.60E-04	1.55E-02	2.79E-05
0.051	1.08E-03	1.04E-05	1.34E-02	2.59E-05
0.101	1.30E-03	1.15E-05	1.08E-02	2.32E-05
0.151	1.78E-03	1.33E-05	7.23E-03	1.90E-05
0.201	1.13E-03	1.07E-05	4.97E-03	1.58E-05
0.251	7.58E-04	8.71E-06	3.45E-03	1.31E-05
0.301	5.40E-04	7.34E-06	2.37E-03	1.09E-05
0.351	3.85E-04	6.20E-06	1.60E-03	8.96E-06
0.401	2.66E-04	5.16E-06	1.07E-03	7.33E-06
0.451	1.83E-04	4.29E-06	7.06E-04	5.94E-06
0.501	1.23E-04	3.50E-06	4.60E-04	4.80E-06
0.551	7.86E-05	2.81E-06	3.03E-04	3.89E-06
0.601	5.43E-05	2.33E-06	1.94E-04	3.12E-06
0.651	3.56E-05	1.89E-06	1.23E-04	2.48E-06
0.701	2.29E-05	1.51E-06	7.73E-05	1.97E-06
0.751	1.48E-05	1.22E-06	4.78E-05	1.55E-06
0.800	9.10E-06	9.54E-07	2.96E-05	1.22E-06
0.850	6.10E-06	7.81E-07	1.74E-05	9.33E-07
0.900	4.30E-06	6.56E-07	8.79E-06	6.63E-07
0.950	2.80E-06	5.29E-07	3.20E-06	4.00E-07
1.000	1.00E-06	3.16E-07	1.20E-06	2.45E-07
1.050	4.00E-07	2.00E-07	4.00E-07	1.41E-07
1.100	2.00E-07	1.41E-07		

Co-60 Source				
Scintillator Thickness (mm)				0.25
Scintillator Location				on axis
Source Location				Center
Material				Beryllium/Beryllium
Energy (MeV)	$\frac{dN}{dE}\left(\frac{cts}{bin}\right)$	$\sigma\left[\frac{dN}{dE}\right]$	$N\left(Br\sum\frac{dN}{dE}\right)$	$\sigma[N]$
0.000	3.42E-05	3.70E-06		
0.001	4.01E-01	3.21E-04	1.28E-02	5.06E-05

0.051	1.48E-03	2.43E-05	9.82E-03	4.44E-05
0.101	2.47E-03	3.16E-05	4.88E-03	3.12E-05
0.151	9.95E-04	1.99E-05	2.89E-03	2.41E-05
0.201	5.93E-04	1.54E-05	1.70E-03	1.85E-05
0.251	3.51E-04	1.19E-05	1.00E-03	1.41E-05
0.301	2.14E-04	9.25E-06	5.74E-04	1.07E-05
0.351	1.23E-04	7.02E-06	3.28E-04	8.09E-06
0.401	7.25E-05	5.38E-06	1.83E-04	6.05E-06
0.451	3.92E-05	3.96E-06	1.05E-04	4.57E-06
0.501	2.42E-05	3.11E-06	5.62E-05	3.35E-06
0.551	1.41E-05	2.37E-06	2.80E-05	2.37E-06
0.601	7.10E-06	1.68E-06	1.38E-05	1.66E-06
0.651	3.20E-06	1.13E-06	7.39E-06	1.22E-06
0.701	2.40E-06	9.79E-07	2.60E-06	7.21E-07
0.751	6.00E-07	4.89E-07	1.40E-06	5.29E-07
0.800	3.00E-07	3.46E-07	7.99E-07	4.00E-07
0.850	1.00E-07	2.00E-07	6.00E-07	3.46E-07
0.900	2.00E-07	2.83E-07	2.00E-07	2.00E-07
0.950	1.00E-07	2.00E-07		

Source Location – Case 1(Beryllium/Beryllium)

Co-60 Source				
Scintillator Thickness (mm)			1	
Scintillator Location			on axis	
Source Location			Top	
Material			Beryllium/Beryllium	
Energy (MeV)	$\frac{dN}{dE}\left(\frac{cts}{bin}\right)$	$\sigma\left[\frac{dN}{dE}\right]$	$N\left(Br\sum\frac{dN}{dE}\right)$	$\sigma[N]$
0.000	1.44E-05	2.40E-06		
0.001	3.82E-01	3.06E-04	1.95E-02	6.23E-05
0.051	1.32E-03	2.29E-05	1.68E-02	5.79E-05
0.101	1.06E-03	2.05E-05	1.47E-02	5.42E-05
0.151	9.19E-04	1.91E-05	1.28E-02	5.07E-05
0.201	1.04E-03	2.04E-05	1.08E-02	4.64E-05
0.251	1.11E-03	2.11E-05	8.54E-03	4.13E-05
0.301	9.61E-04	1.96E-05	6.62E-03	3.64E-05
0.351	7.60E-04	1.75E-05	5.11E-03	3.19E-05
0.401	6.22E-04	1.58E-05	3.86E-03	2.78E-05
0.451	4.76E-04	1.38E-05	2.91E-03	2.41E-05

0.501	3.62E-04	1.20E-05	2.19E-03	2.09E-05
0.551	2.86E-04	1.07E-05	1.62E-03	1.80E-05
0.601	2.21E-04	9.40E-06	1.18E-03	1.53E-05
0.651	1.68E-04	8.18E-06	8.42E-04	1.30E-05
0.701	1.22E-04	6.97E-06	5.98E-04	1.09E-05
0.751	8.92E-05	5.97E-06	4.20E-04	9.16E-06
0.800	6.75E-05	5.19E-06	2.85E-04	7.54E-06
0.850	5.01E-05	4.48E-06	1.85E-04	6.07E-06
0.900	3.70E-05	3.85E-06	1.11E-04	4.70E-06
0.950	2.60E-05	3.22E-06	5.88E-05	3.42E-06
1.000	1.22E-05	2.21E-06	3.44E-05	2.62E-06
1.050	8.90E-06	1.89E-06	1.66E-05	1.81E-06
1.100	6.10E-06	1.56E-06	4.40E-06	9.21E-07
1.150	2.10E-06	9.16E-07	2.00E-07	1.00E-07
1.200	0.00E+00	0.00E+00	2.00E-07	1.00E-07
1.250	0.00E+00	0.00E+00	2.00E-07	1.00E-07
1.300	0.00E+00	0.00E+00	2.00E-07	1.00E-07
1.350	0.00E+00	0.00E+00	2.00E-07	1.00E-07
1.400	1.00E-07	1.00E-07		

Co-60 Source				
Scintillator Thickness (mm)			1	
Scintillator Location			on axis	
Source Location			Bottom	
Material			Beryllium/Beryllium	
Energy (MeV)	$\frac{dN}{dE}\left(\frac{cts}{bin}\right)$	$\sigma\left[\frac{dN}{dE}\right]$	$N\left(Br\sum\frac{dN}{dE}\right)$	$\sigma[N]$
0.000	1.63E-05	2.55E-06		
0.001	3.83E-01	3.06E-04	1.95E-02	6.24E-05
0.051	1.27E-03	2.26E-05	1.69E-02	5.81E-05
0.101	9.99E-04	2.00E-05	1.49E-02	5.46E-05
0.151	8.87E-04	1.88E-05	1.31E-02	5.12E-05
0.201	9.13E-04	1.92E-05	1.13E-02	4.75E-05
0.251	1.07E-03	2.07E-05	9.16E-03	4.27E-05
0.301	9.52E-04	1.94E-05	7.26E-03	3.81E-05
0.351	7.80E-04	1.76E-05	5.70E-03	3.38E-05
0.401	6.33E-04	1.59E-05	4.43E-03	2.98E-05
0.451	5.11E-04	1.43E-05	3.41E-03	2.61E-05
0.501	3.91E-04	1.25E-05	2.63E-03	2.29E-05
0.551	3.14E-04	1.12E-05	2.00E-03	2.00E-05
0.601	2.49E-04	9.95E-06	1.51E-03	1.73E-05

0.651	1.96E-04	8.84E-06	1.11E-03	1.49E-05
0.701	1.47E-04	7.66E-06	8.21E-04	1.28E-05
0.751	1.13E-04	6.71E-06	5.96E-04	1.09E-05
0.800	8.08E-05	5.68E-06	4.34E-04	9.32E-06
0.850	6.54E-05	5.11E-06	3.04E-04	7.79E-06
0.900	4.84E-05	4.40E-06	2.07E-04	6.42E-06
0.950	3.65E-05	3.82E-06	1.34E-04	5.17E-06
1.000	2.62E-05	3.24E-06	8.15E-05	4.03E-06
1.050	1.89E-05	2.75E-06	4.38E-05	2.95E-06
1.100	9.20E-06	1.92E-06	2.54E-05	2.24E-06
1.150	7.00E-06	1.67E-06	1.14E-05	1.50E-06
1.200	5.40E-06	1.47E-06	6.00E-07	2.83E-07
1.250	2.00E-07	2.83E-07	2.00E-07	0.00E+00
1.300	0.00E+00	0.00E+00	2.00E-07	0.00E+00
1.350	0.00E+00	0.00E+00	2.00E-07	0.00E+00
1.400	0.00E+00	0.00E+00		

Source Location – Case 2(Beryllium/Polypropylene)

Cl-36 Source				
Scintillator Thickness (mm)			1	
Scintillator Location			on axis	
Source Location			Top	
Material			Beryllium/Polypropylene	
Energy (MeV)	$\frac{dN}{dE}\left(\frac{cts}{bin}\right)$	$\sigma\left[\frac{dN}{dE}\right]$	$N\left(Br\sum\frac{dN}{dE}\right)$	$\sigma[N]$
0.000	3.19E-04	5.54E-06		
0.001	1.92E-04	4.29E-06	6.26E-01	2.41E-04
0.051	5.33E-02	6.80E-05	5.73E-01	2.31E-04
0.101	6.88E-02	8.09E-05	5.06E-01	2.16E-04
0.151	7.13E-02	7.69E-05	4.36E-01	2.02E-04
0.201	7.46E-02	8.05E-05	3.63E-01	1.85E-04
0.251	7.80E-02	8.42E-05	2.86E-01	1.65E-04
0.301	7.92E-02	8.54E-05	2.09E-01	1.41E-04
0.351	6.89E-02	8.11E-05	1.41E-01	1.16E-04
0.401	5.43E-02	6.93E-05	8.79E-02	9.27E-05
0.451	3.90E-02	6.13E-05	4.96E-02	6.95E-05
0.501	2.49E-02	4.88E-05	2.52E-02	4.96E-05
0.551	1.45E-02	3.71E-05	1.09E-02	3.29E-05
0.601	7.38E-03	2.68E-05	3.69E-03	1.91E-05

0.651	2.98E-03	1.70E-05	7.69E-04	8.68E-06
0.701	7.54E-04	8.51E-06	2.94E-05	1.70E-06
0.751	3.00E-05	1.70E-06		

Cl-36 Source				
Scintillator Thickness (mm)			1	
Scintillator Location			on axis	
Source Location			Bottom	
Material			Beryllium/Polypropylene	
Energy (MeV)	$\frac{dN}{dE}\left(\frac{cts}{bin}\right)$	$\sigma\left[\frac{dN}{dE}\right]$	$N\left(Br\sum\frac{dN}{dE}\right)$	$\sigma[N]$
0.000	3.19E-04	5.54E-06		
0.001	3.50E-03	1.82E-05	6.26E-01	2.41E-04
0.051	5.33E-02	6.80E-05	5.74E-01	2.31E-04
0.101	6.87E-02	8.09E-05	5.06E-01	2.16E-04
0.151	7.13E-02	7.69E-05	4.37E-01	2.02E-04
0.201	7.46E-02	8.05E-05	3.63E-01	1.85E-04
0.251	7.80E-02	8.42E-05	2.87E-01	1.65E-04
0.301	7.92E-02	8.54E-05	2.09E-01	1.41E-04
0.351	6.89E-02	8.11E-05	1.42E-01	1.16E-04
0.401	5.43E-02	6.93E-05	8.83E-02	9.29E-05
0.451	3.90E-02	6.13E-05	5.00E-02	6.99E-05
0.501	2.49E-02	4.88E-05	2.57E-02	5.00E-05
0.551	1.45E-02	3.71E-05	1.14E-02	3.36E-05
0.601	7.38E-03	2.68E-05	4.15E-03	2.02E-05
0.651	2.98E-03	1.70E-05	1.23E-03	1.11E-05
0.701	7.54E-04	8.51E-06	4.87E-04	7.07E-06
0.751	2.98E-05	1.73E-06		

Source Location – Case 3(Polypropylene/Polypropylene)

Sr-90 Source				
Scintillator Thickness (mm)			1	
Scintillator Location			on axis	
Source Location			Bottom	
Material			Polypropylene/Polypropylene	
Energy (MeV)	$\frac{dN}{dE}\left(\frac{cts}{bin}\right)$	$\sigma\left[\frac{dN}{dE}\right]$	$N\left(Br\sum\frac{dN}{dE}\right)$	$\sigma[N]$
0.000	9.80E-04	1.98E-05		
0.001	6.33E-03	6.97E-05	1.21E+00	6.69E-04

0.050	4.09E-02	1.72E-04	1.13E+00	6.47E-04
0.099	5.14E-02	1.95E-04	1.02E+00	6.16E-04
0.148	5.18E-02	1.97E-04	9.20E-01	5.84E-04
0.197	7.28E-02	2.33E-04	7.74E-01	5.36E-04
0.246	7.91E-02	2.37E-04	6.16E-01	4.80E-04
0.295	7.02E-02	2.25E-04	4.75E-01	4.24E-04
0.344	5.64E-02	2.03E-04	3.62E-01	3.73E-04
0.392	4.26E-02	1.79E-04	2.77E-01	3.27E-04
0.441	3.05E-02	1.53E-04	2.16E-01	2.89E-04
0.490	2.10E-02	1.26E-04	1.74E-01	2.60E-04
0.539	1.51E-02	1.09E-04	1.44E-01	2.36E-04
0.588	1.19E-02	9.55E-05	1.20E-01	2.16E-04
0.637	1.01E-02	8.84E-05	1.00E-01	1.97E-04
0.686	8.46E-03	8.12E-05	8.31E-02	1.80E-04
0.735	7.15E-03	7.44E-05	6.88E-02	1.63E-04
0.784	6.02E-03	6.86E-05	5.68E-02	1.48E-04
0.833	4.99E-03	6.19E-05	4.68E-02	1.35E-04
0.882	4.17E-03	5.68E-05	3.85E-02	1.22E-04
0.931	3.52E-03	5.21E-05	3.14E-02	1.11E-04
0.980	2.91E-03	4.77E-05	2.56E-02	9.99E-05
1.029	2.45E-03	4.35E-05	2.07E-02	8.99E-05
1.078	2.03E-03	3.98E-05	1.66E-02	8.06E-05
1.127	1.66E-03	3.59E-05	1.33E-02	7.22E-05
1.176	1.36E-03	3.26E-05	1.06E-02	6.44E-05
1.224	1.09E-03	2.93E-05	8.41E-03	5.73E-05
1.273	9.18E-04	2.68E-05	6.57E-03	5.06E-05
1.322	7.27E-04	2.38E-05	5.12E-03	4.47E-05
1.371	5.86E-04	2.13E-05	3.95E-03	3.92E-05
1.420	4.46E-04	1.87E-05	3.05E-03	3.45E-05
1.469	3.73E-04	1.71E-05	2.31E-03	3.00E-05
2.301	1.15E-03	9.70E-05		

Sr-90 Source				
Scintillator Thickness (mm)			1	
Scintillator Location			on axis	
Source Location			Top	
Material			Polypropylene/Polypropylene	
Energy (MeV)	$\frac{dN}{dE}\left(\frac{cts}{bin}\right)$	$\sigma\left[\frac{dN}{dE}\right]$	$N\left(Br\sum\frac{dN}{dE}\right)$	$\sigma[N]$
0.000	9.78E-04	2.80E-05		
0.001	6.30E-03	7.05E-05	1.13E+00	6.48E-04

0.050	4.09E-02	1.80E-04	1.02E+00	6.18E-04
0.099	5.14E-02	1.95E-04	9.20E-01	5.86E-04
0.148	5.18E-02	1.97E-04	7.74E-01	5.38E-04
0.197	7.29E-02	2.33E-04	6.16E-01	4.83E-04
0.246	7.91E-02	2.37E-04	4.75E-01	4.27E-04
0.295	7.03E-02	2.25E-04	3.62E-01	3.76E-04
0.344	5.64E-02	2.03E-04	2.77E-01	3.30E-04
0.392	4.26E-02	1.79E-04	2.16E-01	2.93E-04
0.441	3.06E-02	1.53E-04	1.74E-01	2.63E-04
0.490	2.10E-02	1.30E-04	1.44E-01	2.39E-04
0.539	1.51E-02	1.09E-04	1.20E-01	2.18E-04
0.588	1.19E-02	9.78E-05	1.00E-01	1.99E-04
0.637	1.01E-02	8.85E-05	8.30E-02	1.82E-04
0.686	8.46E-03	8.12E-05	6.87E-02	1.65E-04
0.735	7.15E-03	7.58E-05	5.67E-02	1.50E-04
0.784	6.02E-03	6.86E-05	4.67E-02	1.36E-04
0.833	5.00E-03	6.30E-05	3.84E-02	1.24E-04
0.882	4.18E-03	5.76E-05	3.13E-02	1.12E-04
0.931	3.52E-03	5.28E-05	2.55E-02	1.01E-04
0.980	2.92E-03	4.84E-05	2.06E-02	9.06E-05
1.029	2.44E-03	4.43E-05	1.66E-02	8.13E-05
1.078	2.03E-03	4.01E-05	1.33E-02	7.27E-05
1.127	1.65E-03	3.63E-05	1.06E-02	6.49E-05
1.176	1.35E-03	3.28E-05	8.37E-03	5.79E-05
1.224	1.09E-03	2.94E-05	6.55E-03	5.12E-05
1.273	9.12E-04	2.70E-05	5.11E-03	4.52E-05
1.322	7.20E-04	2.40E-05	3.93E-03	3.97E-05
1.371	5.87E-04	2.16E-05	3.04E-03	3.49E-05
1.420	4.46E-04	1.89E-05	2.30E-03	3.03E-05
1.469	3.73E-04	1.73E-05	1.13E+00	6.48E-04
2.301	1.15E-03	9.86E-05		

Source Location – Case 4(Mylar Wrap)

Sr-90 Source				
Scintillator Thickness (mm)			1	
Scintillator Location			on axis	
Source Location			Top	
Material			Mylar Wrap	
Energy	$\frac{dN}{dE}\left(\frac{cts}{bin}\right)$	$\sigma\left[\frac{dN}{dE}\right]$	$N\left(Br\sum\frac{dN}{dE}\right)$	$\sigma[N]$

(MeV)				
0.000	6.60E-03	1.62E-04		
0.001	1.03E-04	2.03E-05	1.09E+00	1.44E-03
0.051	2.38E-02	3.05E-04	1.04E+00	1.41E-03
0.101	4.11E-02	3.95E-04	9.61E-01	1.36E-03
0.151	4.77E-02	4.29E-04	8.66E-01	1.29E-03
0.201	7.19E-02	5.18E-04	7.22E-01	1.18E-03
0.251	7.73E-02	5.41E-04	5.68E-01	1.05E-03
0.301	6.71E-02	4.96E-04	4.33E-01	9.20E-04
0.351	5.23E-02	4.50E-04	3.29E-01	8.02E-04
0.401	3.93E-02	3.85E-04	2.50E-01	7.04E-04
0.451	2.72E-02	3.26E-04	1.96E-01	6.24E-04
0.501	1.86E-02	2.71E-04	1.59E-01	5.62E-04
0.551	1.38E-02	2.34E-04	1.31E-01	5.11E-04
0.601	1.12E-02	2.10E-04	1.09E-01	4.66E-04
0.651	9.34E-03	1.92E-04	9.03E-02	4.24E-04
0.701	7.79E-03	1.76E-04	7.48E-02	3.86E-04
0.751	6.63E-03	1.62E-04	6.15E-02	3.50E-04
0.801	5.54E-03	1.49E-04	5.04E-02	3.17E-04
0.851	4.64E-03	1.35E-04	4.11E-02	2.87E-04
0.901	3.74E-03	1.22E-04	3.36E-02	2.59E-04
0.951	3.19E-03	1.13E-04	2.73E-02	2.34E-04
1.001	2.60E-03	1.02E-04	2.21E-02	2.10E-04
1.051	2.19E-03	9.36E-05	1.77E-02	1.88E-04
1.101	1.73E-03	8.31E-05	1.42E-02	1.69E-04
1.151	1.44E-03	7.60E-05	1.14E-02	1.51E-04
1.201	1.23E-03	7.03E-05	8.89E-03	1.33E-04
1.251	9.37E-04	6.13E-05	7.02E-03	1.19E-04
1.301	7.93E-04	5.63E-05	5.43E-03	1.04E-04
1.351	6.32E-04	5.03E-05	4.17E-03	9.13E-05
1.401	5.01E-04	4.48E-05	3.17E-03	7.96E-05
1.451	4.12E-04	4.06E-05	2.34E-03	6.85E-05
2.301	1.17E-03	2.17E-04		

Sr-90 Source				
Scintillator Thickness (mm)			1	
Scintillator Location			on axis	
Source Location			Bottom	
Material			Mylar Wrap	
Energy (MeV)	$\frac{dN}{dE}\left(\frac{cts}{bin}\right)$	$\sigma\left[\frac{dN}{dE}\right]$	$N\left(Br\sum\frac{dN}{dE}\right)$	$\sigma[N]$

0.000	6.60E-03	6.07E-05		
0.001	1.05E-04	1.62E-04	1.09E+00	1.44E-03
0.051	2.38E-02	2.05E-05	1.05E+00	1.41E-03
0.101	4.11E-02	3.05E-04	9.64E-01	1.36E-03
0.151	4.77E-02	3.95E-04	8.68E-01	1.29E-03
0.201	7.19E-02	4.29E-04	7.25E-01	1.18E-03
0.251	7.73E-02	5.18E-04	5.70E-01	1.05E-03
0.301	6.71E-02	5.41E-04	4.36E-01	9.20E-04
0.351	5.23E-02	4.96E-04	3.31E-01	8.02E-04
0.401	3.93E-02	4.50E-04	2.53E-01	7.04E-04
0.451	2.72E-02	3.85E-04	1.98E-01	6.24E-04
0.501	1.86E-02	3.26E-04	1.61E-01	5.62E-04
0.551	1.38E-02	2.71E-04	1.34E-01	5.11E-04
0.601	1.12E-02	2.34E-04	1.11E-01	4.66E-04
0.651	9.34E-03	2.10E-04	9.27E-02	4.24E-04
0.701	7.78E-03	1.92E-04	7.71E-02	3.86E-04
0.751	6.63E-03	1.76E-04	6.38E-02	3.50E-04
0.801	5.54E-03	1.62E-04	5.28E-02	3.17E-04
0.851	4.64E-03	1.48E-04	4.35E-02	2.87E-04
0.901	3.75E-03	1.35E-04	3.60E-02	2.59E-04
0.951	3.20E-03	1.22E-04	2.96E-02	2.33E-04
1.001	2.60E-03	1.13E-04	2.44E-02	2.10E-04
1.051	2.18E-03	1.02E-04	2.00E-02	1.88E-04
1.101	1.74E-03	9.32E-05	1.66E-02	1.69E-04
1.151	1.44E-03	8.34E-05	1.37E-02	1.51E-04
1.201	1.22E-03	7.59E-05	1.13E-02	1.33E-04
1.251	9.34E-04	6.98E-05	9.38E-03	1.19E-04
1.301	7.90E-04	6.11E-05	7.80E-03	1.04E-04
1.351	6.36E-04	5.62E-05	6.53E-03	9.14E-05
1.401	5.03E-04	5.04E-05	5.53E-03	7.96E-05
1.451	4.09E-04	4.49E-05	4.71E-03	6.86E-05
2.301	1.18E-03	2.17E-04		

Source Location – ¼ and ½ mm Scintillator

Sr-90 Source	
Scintillator Thickness (mm)	0.25
Scintillator Location	on axis
Source Location	Top
Material	Polypropylene/polypropylene

Energy (MeV)	$\frac{dN}{dE}\left(\frac{cts}{bin}\right)$	$\sigma\left[\frac{dN}{dE}\right]$	$N\left(Br\sum\frac{dN}{dE}\right)$	$\sigma[N]$
0.000	6.67E-03	5.20E-05		
0.001	1.27E-04	7.13E-06	1.17E+00	4.47E-04
0.051	8.38E-02	1.68E-04	1.00E+00	4.14E-04
0.101	2.05E-01	2.46E-04	5.91E-01	3.33E-04
0.151	1.16E-01	2.09E-04	3.59E-01	2.59E-04
0.201	7.18E-02	1.58E-04	2.15E-01	2.05E-04
0.251	4.18E-02	1.25E-04	1.32E-01	1.63E-04
0.301	2.53E-02	1.01E-04	8.11E-02	1.27E-04
0.351	1.51E-02	7.85E-05	5.09E-02	1.00E-04
0.401	9.01E-03	5.95E-05	3.29E-02	8.09E-05
0.451	5.58E-03	4.69E-05	2.17E-02	6.59E-05
0.501	3.56E-03	3.77E-05	1.46E-02	5.40E-05
0.551	2.36E-03	3.07E-05	9.90E-03	4.44E-05
0.601	1.59E-03	2.51E-05	6.72E-03	3.67E-05
0.651	1.09E-03	2.09E-05	4.54E-03	3.01E-05
0.701	7.40E-04	1.72E-05	3.06E-03	2.47E-05
0.751	5.04E-04	1.42E-05	2.05E-03	2.02E-05
0.801	3.36E-04	1.16E-05	1.38E-03	1.66E-05
0.851	2.36E-04	9.74E-06	9.06E-04	1.35E-05
0.901	1.57E-04	7.91E-06	5.92E-04	1.09E-05
0.951	1.03E-04	6.42E-06	3.87E-04	8.80E-06
1.001	6.87E-05	5.25E-06	2.49E-04	7.06E-06
1.051	4.13E-05	4.06E-06	1.67E-04	5.77E-06
1.101	3.02E-05	3.47E-06	1.06E-04	4.61E-06
1.151	1.85E-05	2.72E-06	6.92E-05	3.72E-06
1.201	1.21E-05	2.20E-06	4.50E-05	3.00E-06
1.251	8.70E-06	1.87E-06	2.76E-05	2.35E-06
1.301	5.10E-06	1.43E-06	1.74E-05	1.87E-06
1.351	3.20E-06	1.13E-06	1.10E-05	1.48E-06
1.401	2.60E-06	1.02E-06	5.80E-06	1.08E-06
1.451	1.20E-06	6.93E-07	3.40E-06	8.25E-07
2.301	1.60E-06	1.72E-06		

Sr-90 Source	
Scintillator Thickness (mm)	0.25
Scintillator Location	on axis
Source Location	Bottom
Material	Polypropylene/polypropylene

Energy (MeV)	$\frac{dN}{dE}\left(\frac{cts}{bin}\right)$	$\sigma\left[\frac{dN}{dE}\right]$	$N\left(Br\sum\frac{dN}{dE}\right)$	$\sigma[N]$
0.000	0.007	5.20E-05		
0.001	0.000	7.11E-06	1.17E+00	4.47E-04
0.051	0.084	1.67E-04	1.00E+00	4.14E-04
0.101	0.205	2.46E-04	5.91E-01	3.33E-04
0.151	0.116	2.09E-04	3.59E-01	2.59E-04
0.201	0.072	1.58E-04	2.15E-01	2.06E-04
0.251	0.042	1.25E-04	1.32E-01	1.63E-04
0.301	0.025	1.01E-04	8.11E-02	1.27E-04
0.351	0.015	7.85E-05	5.09E-02	1.00E-04
0.401	0.009	5.95E-05	3.29E-02	8.09E-05
0.451	0.006	4.69E-05	2.17E-02	6.59E-05
0.501	0.004	3.77E-05	1.46E-02	5.41E-05
0.551	0.002	3.07E-05	9.91E-03	4.45E-05
0.601	0.002	2.51E-05	6.72E-03	3.67E-05
0.651	0.001	2.09E-05	4.54E-03	3.01E-05
0.701	0.001	1.72E-05	3.06E-03	2.48E-05
0.751	0.001	1.42E-05	2.05E-03	2.03E-05
0.801	0.000	1.16E-05	1.38E-03	1.66E-05
0.851	0.000	9.77E-06	9.02E-04	1.34E-05
0.901	0.000	7.90E-06	5.90E-04	1.09E-05
0.951	0.000	6.40E-06	3.85E-04	8.78E-06
1.001	0.000	5.23E-06	2.49E-04	7.05E-06
1.051	4.06E-05	4.03E-06	1.67E-04	5.79E-06
1.101	3.01E-05	3.47E-06	1.07E-04	4.63E-06
1.151	1.91E-05	2.77E-06	6.90E-05	3.71E-06
1.201	1.20E-05	2.19E-06	4.50E-05	3.00E-06
1.251	8.40E-06	1.83E-06	2.82E-05	2.37E-06
1.301	5.10E-06	1.43E-06	1.80E-05	1.90E-06
1.351	3.20E-06	1.13E-06	1.16E-05	1.52E-06
1.401	2.90E-06	1.08E-06	5.80E-06	1.08E-06
1.451	1.30E-06	7.21E-07	3.20E-06	8.00E-07
2.301	1.60E-06	1.72E-06		

Sr-90 Source	
Scintillator Thickness (mm)	0.50
Scintillator Location	on axis
Source Location	Top
Material	Polypropylene/polypropylene

Energy (MeV)	$\frac{dN}{dE}\left(\frac{cts}{bin}\right)$	$\sigma\left[\frac{dN}{dE}\right]$	$N\left(Br\sum\frac{dN}{dE}\right)$	$\sigma[N]$
0.000	6.53E-03	7.18E-05		
0.001	1.26E-04	1.00E-05	1.17E+00	6.61E-04
0.051	3.64E-02	1.67E-04	1.10E+00	6.40E-04
0.101	8.68E-02	2.61E-04	9.26E-01	5.84E-04
0.151	1.29E-01	3.09E-04	6.69E-01	4.96E-04
0.201	1.01E-01	2.62E-04	4.68E-01	4.21E-04
0.251	7.28E-02	2.33E-04	3.22E-01	3.51E-04
0.301	5.11E-02	1.94E-04	2.20E-01	2.93E-04
0.351	3.30E-02	1.59E-04	1.54E-01	2.46E-04
0.401	2.14E-02	1.28E-04	1.11E-01	2.10E-04
0.451	1.43E-02	1.06E-04	8.24E-02	1.81E-04
0.501	9.94E-03	8.94E-05	6.25E-02	1.58E-04
0.551	7.26E-03	7.56E-05	4.80E-02	1.38E-04
0.601	5.56E-03	6.67E-05	3.69E-02	1.21E-04
0.651	4.34E-03	5.90E-05	2.82E-02	1.06E-04
0.701	3.29E-03	5.14E-05	2.16E-02	9.25E-05
0.751	2.57E-03	4.53E-05	1.65E-02	8.07E-05
0.801	1.96E-03	3.96E-05	1.25E-02	7.03E-05
0.851	1.52E-03	3.50E-05	9.49E-03	6.09E-05
0.901	1.17E-03	3.05E-05	7.14E-03	5.28E-05
0.951	8.81E-04	2.66E-05	5.38E-03	4.56E-05
1.001	6.82E-04	2.33E-05	4.02E-03	3.91E-05
1.051	4.99E-04	2.00E-05	3.02E-03	3.37E-05
1.101	3.89E-04	1.77E-05	2.24E-03	2.87E-05
1.151	2.80E-04	1.50E-05	1.68E-03	2.45E-05
1.201	2.08E-04	1.29E-05	1.27E-03	2.08E-05
1.251	1.63E-04	1.14E-05	9.41E-04	1.74E-05
1.301	1.10E-04	9.38E-06	7.22E-04	1.46E-05
1.351	7.42E-05	7.70E-06	5.73E-04	1.24E-05
1.401	5.46E-05	6.61E-06	4.64E-04	1.05E-05
1.451	4.48E-05	5.99E-06	3.74E-04	8.65E-06
2.301	9.36E-05	2.53E-05		

Sr-90 Source	
Scintillator Thickness (mm)	0.50
Scintillator Location	on axis
Source Location	Bottom
Material	Polypropylene/polypropylene

Energy (MeV)	$\frac{dN}{dE}\left(\frac{cts}{bin}\right)$	$\sigma\left[\frac{dN}{dE}\right]$	$N\left(Br\sum\frac{dN}{dE}\right)$	$\sigma[N]$
0.000	6.52E-03	7.17E-05		
0.001	1.24E-04	9.98E-06	1.17E+00	6.61E-04
0.051	3.64E-02	1.67E-04	1.10E+00	6.40E-04
0.101	8.68E-02	2.61E-04	9.26E-01	5.84E-04
0.151	1.29E-01	3.09E-04	6.69E-01	4.96E-04
0.201	1.01E-01	2.62E-04	4.68E-01	4.21E-04
0.251	7.28E-02	2.33E-04	3.22E-01	3.51E-04
0.301	5.11E-02	1.94E-04	2.20E-01	2.93E-04
0.351	3.30E-02	1.59E-04	1.54E-01	2.46E-04
0.401	2.14E-02	1.28E-04	1.11E-01	2.10E-04
0.451	1.43E-02	1.06E-04	8.24E-02	1.81E-04
0.501	9.94E-03	8.95E-05	6.25E-02	1.58E-04
0.551	7.27E-03	7.56E-05	4.80E-02	1.38E-04
0.601	5.56E-03	6.67E-05	3.69E-02	1.21E-04
0.651	4.34E-03	5.90E-05	2.82E-02	1.06E-04
0.701	3.30E-03	5.14E-05	2.16E-02	9.26E-05
0.751	2.58E-03	4.54E-05	1.65E-02	8.07E-05
0.801	1.96E-03	3.96E-05	1.25E-02	7.03E-05
0.851	1.52E-03	3.50E-05	9.50E-03	6.10E-05
0.901	1.17E-03	3.07E-05	7.16E-03	5.27E-05
0.951	8.83E-04	2.65E-05	5.39E-03	4.56E-05
1.001	6.82E-04	2.33E-05	4.03E-03	3.92E-05
1.051	5.01E-04	2.00E-05	3.03E-03	3.37E-05
1.101	3.87E-04	1.76E-05	2.25E-03	2.87E-05
1.151	2.85E-04	1.51E-05	1.68E-03	2.44E-05
1.201	2.08E-04	1.29E-05	1.27E-03	2.08E-05
1.251	1.61E-04	1.13E-05	9.46E-04	1.74E-05
1.301	1.10E-04	9.38E-06	7.26E-04	1.47E-05
1.351	7.54E-05	7.77E-06	5.76E-04	1.25E-05
1.401	5.60E-05	6.70E-06	4.64E-04	1.05E-05
1.451	4.38E-05	5.92E-06	3.76E-04	8.67E-06
2.301	9.40E-05	2.52E-05		

View Factor

Co-60 Source	
Scintillator Thickness (mm)	1
Scintillator Location	2 mm off axis

Source Location						Center
Material						Polypropylene/Polypropylene
Energy (MeV)	$\frac{d\gamma}{dE}\left(\frac{cts}{bin}\right)$	$\sigma_\gamma\left[\frac{dN}{dE}\right]$	$\frac{d\beta}{dE}\left(\frac{cts}{bin}\right)$	$\sigma_\beta\left[\frac{dN}{dE}\right]$	$N\left(Br\sum\frac{dN}{dE}\right)$	$\sigma[N]$
0.000	2.16E-05	2.94E-06	0.00E+00	0.00E+00		
0.001	4.70E-01	2.82E-04	1.33E-03	1.15E-05	3.07E-02	7.79E-05
0.051	1.71E-03	2.59E-05	9.77E-05	3.13E-06	2.72E-02	7.34E-05
0.101	1.52E-03	2.46E-05	3.30E-06	5.75E-07	2.41E-02	6.91E-05
0.151	1.37E-03	2.32E-05	4.50E-06	6.71E-07	2.14E-02	6.51E-05
0.201	1.50E-03	2.44E-05	9.70E-06	9.85E-07	1.84E-02	6.03E-05
0.251	1.71E-03	2.59E-05	1.52E-05	1.23E-06	1.50E-02	5.45E-05
0.301	1.51E-03	2.44E-05	1.30E-05	1.14E-06	1.19E-02	4.87E-05
0.351	1.25E-03	2.23E-05	9.60E-06	9.80E-07	9.42E-03	4.33E-05
0.401	1.03E-03	2.03E-05	1.05E-05	1.02E-06	7.34E-03	3.83E-05
0.451	8.29E-04	1.82E-05	8.00E-06	8.94E-07	5.68E-03	3.36E-05
0.501	6.58E-04	1.62E-05	6.00E-06	7.75E-07	4.36E-03	2.95E-05
0.551	5.16E-04	1.43E-05	4.30E-06	6.56E-07	3.32E-03	2.57E-05
0.601	4.03E-04	1.27E-05	4.40E-06	6.64E-07	2.51E-03	2.24E-05
0.651	3.23E-04	1.14E-05	1.80E-06	4.24E-07	1.86E-03	1.93E-05
0.701	2.47E-04	9.92E-06	1.10E-06	3.32E-07	1.37E-03	1.65E-05
0.751	1.85E-04	8.59E-06	9.00E-07	3.00E-07	9.98E-04	1.41E-05
0.801	1.46E-04	7.65E-06	3.00E-07	1.73E-07	7.05E-04	1.19E-05
0.851	1.13E-04	6.72E-06	1.00E-07	1.00E-07	4.80E-04	9.79E-06
0.901	9.42E-05	6.14E-06			2.91E-04	7.63E-06
0.951	6.60E-05	5.13E-06			1.59E-04	5.65E-06
1.001	3.63E-05	3.81E-06			8.69E-05	4.17E-06
1.051	1.91E-05	2.76E-06			4.88E-05	3.12E-06
1.101	1.80E-05	2.68E-06			1.28E-05	1.60E-06
1.151	5.60E-06	1.50E-06			1.60E-06	5.65E-07
1.201	3.00E-07	3.46E-07			9.99E-07	4.47E-07
1.251	4.00E-07	4.00E-07			2.00E-07	2.00E-07
1.301	1.00E-07	2.00E-07				

Co-60 Source						
Scintillator Thickness (mm)						1
Scintillator Location						4 mm off axis
Source Location						Center
Material						Polypropylene/Polypropylene
Energy (MeV)	$\frac{d\gamma}{dE}\left(\frac{cts}{bin}\right)$	$\sigma_\gamma\left[\frac{dN}{dE}\right]$	$\frac{d\beta}{dE}\left(\frac{cts}{bin}\right)$	$\sigma_\beta\left[\frac{dN}{dE}\right]$	$N\left(Br\sum\frac{dN}{dE}\right)$	$\sigma[N]$
0.000	2.30E-05	3.03E-06	0.00E+00	0.00E+00		

0.001	4.69E-01	2.81E-04	1.33E-03	1.15E-05	3.09E-02	7.83E-05
0.051	1.66E-03	2.58E-05	9.77E-05	3.13E-06	2.74E-02	7.38E-05
0.101	1.48E-03	2.42E-05	3.30E-06	5.75E-07	2.45E-02	6.97E-05
0.151	1.34E-03	2.31E-05	4.50E-06	6.71E-07	2.18E-02	6.58E-05
0.201	1.51E-03	2.44E-05	9.70E-06	9.85E-07	1.88E-02	6.11E-05
0.251	1.73E-03	2.63E-05	1.52E-05	1.23E-06	1.53E-02	5.51E-05
0.301	1.54E-03	2.46E-05	1.30E-05	1.14E-06	1.22E-02	4.93E-05
0.351	1.26E-03	2.24E-05	9.60E-06	9.80E-07	9.70E-03	4.40E-05
0.401	1.06E-03	2.05E-05	1.05E-05	1.02E-06	7.57E-03	3.88E-05
0.451	8.56E-04	1.85E-05	8.00E-06	8.94E-07	5.85E-03	3.42E-05
0.501	6.70E-04	1.63E-05	6.00E-06	7.75E-07	4.51E-03	3.00E-05
0.551	5.18E-04	1.44E-05	4.30E-06	6.56E-07	3.47E-03	2.63E-05
0.601	4.26E-04	1.30E-05	4.40E-06	6.64E-07	2.61E-03	2.28E-05
0.651	3.42E-04	1.17E-05	1.80E-06	4.24E-07	1.93E-03	1.96E-05
0.701	2.53E-04	1.01E-05	1.10E-06	3.32E-07	1.42E-03	1.68E-05
0.751	2.01E-04	8.96E-06	9.00E-07	3.00E-07	1.02E-03	1.43E-05
0.801	1.52E-04	7.80E-06	3.00E-07	1.73E-07	7.13E-04	1.19E-05
0.851	1.18E-04	6.86E-06	1.00E-07	1.00E-07	4.78E-04	9.77E-06
0.901	8.29E-05	5.75E-06			3.12E-04	7.90E-06
0.951	7.11E-05	5.33E-06			1.70E-04	5.83E-06
1.001	3.73E-05	3.86E-06			9.53E-05	4.36E-06
1.051	2.31E-05	3.04E-06			4.92E-05	3.13E-06
1.101	1.82E-05	2.70E-06			1.28E-05	1.60E-06
1.151	6.00E-06	1.55E-06			7.99E-07	4.00E-07
1.201	3.00E-07	3.46E-07			2.00E-07	2.00E-07
1.251	1.00E-07	2.00E-07				

Co-60 Source						
Scintillator Thickness (mm)				1		
Scintillator Location				6 mm off axis		
Source Location				Center		
Material				Polypropylene/Polypropylene		
Energy (MeV)	$\frac{d\gamma}{dE}\left(\frac{cts}{bin}\right)$	$\sigma_\gamma\left[\frac{dN}{dE}\right]$	$\frac{d\beta}{dE}\left(\frac{cts}{bin}\right)$	$\sigma_\beta\left[\frac{dN}{dE}\right]$	$N\left(Br\sum\frac{dN}{dE}\right)$	$\sigma[N]$
0.000	2.22E-05	2.98E-06	0.00E+00	0.00E+00		
0.001	4.69E-01	2.81E-04	1.33E-03	1.15E-05	3.09E-02	7.84E-05
0.051	1.67E-03	2.57E-05	9.77E-05	3.13E-06	2.75E-02	7.40E-05
0.101	1.48E-03	2.42E-05	3.30E-06	5.75E-07	2.45E-02	7.00E-05
0.151	1.35E-03	2.31E-05	4.50E-06	6.71E-07	2.18E-02	6.60E-05
0.201	1.50E-03	2.46E-05	9.70E-06	9.85E-07	1.88E-02	6.13E-05
0.251	1.74E-03	2.64E-05	1.52E-05	1.23E-06	1.53E-02	5.53E-05

0.301	1.54E-03	2.49E-05	1.30E-05	1.14E-06	1.22E-02	4.93E-05
0.351	1.26E-03	2.23E-05	9.60E-06	9.80E-07	9.69E-03	4.40E-05
0.401	1.06E-03	2.05E-05	1.05E-05	1.02E-06	7.58E-03	3.89E-05
0.451	8.63E-04	1.86E-05	8.00E-06	8.94E-07	5.84E-03	3.42E-05
0.501	6.66E-04	1.64E-05	6.00E-06	7.75E-07	4.51E-03	3.00E-05
0.551	5.19E-04	1.44E-05	4.30E-06	6.56E-07	3.46E-03	2.63E-05
0.601	4.26E-04	1.30E-05	4.40E-06	6.64E-07	2.61E-03	2.28E-05
0.651	3.42E-04	1.17E-05	1.80E-06	4.24E-07	1.92E-03	1.96E-05
0.701	2.54E-04	1.01E-05	1.10E-06	3.32E-07	1.41E-03	1.68E-05
0.751	2.03E-04	9.00E-06	9.00E-07	3.00E-07	1.01E-03	1.42E-05
0.801	1.51E-04	7.78E-06	3.00E-07	1.73E-07	7.05E-04	1.19E-05
0.851	1.16E-04	6.80E-06	1.00E-07	1.00E-07	4.73E-04	9.72E-06
0.901	8.19E-05	5.71E-06			3.10E-04	7.86E-06
0.951	7.13E-05	5.33E-06			1.67E-04	5.78E-06
1.001	3.64E-05	3.81E-06			9.45E-05	4.35E-06
1.051	2.33E-05	3.05E-06			4.80E-05	3.10E-06
1.101	1.81E-05	2.69E-06			1.18E-05	1.54E-06
1.151	5.40E-06	1.47E-06			9.99E-07	4.47E-07
1.201	4.00E-07	4.00E-07			2.00E-07	2.00E-07
1.251	1.00E-07	2.00E-07				

Co-60 Source						
Scintillator Thickness (mm)				1		
Scintillator Location				8 mm off axis		
Source Location				Center		
Material				Polypropylene/Polypropylene		
Energy (MeV)	$\frac{d\gamma}{dE}\left(\frac{cts}{bin}\right)$	$\sigma_\gamma\left[\frac{dN}{dE}\right]$	$\frac{d\beta}{dE}\left(\frac{cts}{bin}\right)$	$\sigma_\beta\left[\frac{dN}{dE}\right]$	$N\left(Br\sum\frac{dN}{dE}\right)$	$\sigma[N]$
0.000	2.02E-05	2.84E-06	0.00E+00	0.00E+00		
0.001	4.68E-01	2.81E-04	1.33E-03	1.15E-05	3.10E-02	7.86E-05
0.051	1.69E-03	2.61E-05	9.77E-05	3.13E-06	2.75E-02	7.41E-05
0.101	1.51E-03	2.44E-05	3.30E-06	5.75E-07	2.45E-02	7.00E-05
0.151	1.36E-03	2.34E-05	4.50E-06	6.71E-07	2.18E-02	6.59E-05
0.201	1.53E-03	2.47E-05	9.70E-06	9.85E-07	1.87E-02	6.11E-05
0.251	1.74E-03	2.64E-05	1.52E-05	1.23E-06	1.52E-02	5.51E-05
0.301	1.52E-03	2.46E-05	1.30E-05	1.14E-06	1.22E-02	4.93E-05
0.351	1.26E-03	2.24E-05	9.60E-06	9.80E-07	9.64E-03	4.39E-05
0.401	1.06E-03	2.05E-05	1.05E-05	1.02E-06	7.51E-03	3.88E-05
0.451	8.48E-04	1.85E-05	8.00E-06	8.94E-07	5.81E-03	3.41E-05
0.501	6.77E-04	1.65E-05	6.00E-06	7.75E-07	4.45E-03	2.98E-05
0.551	5.28E-04	1.46E-05	4.30E-06	6.56E-07	3.39E-03	2.60E-05

0.601	4.17E-04	1.29E-05	4.40E-06	6.64E-07	2.56E-03	2.26E-05
0.651	3.29E-04	1.14E-05	1.80E-06	4.24E-07	1.90E-03	1.95E-05
0.701	2.55E-04	1.01E-05	1.10E-06	3.32E-07	1.39E-03	1.67E-05
0.751	1.94E-04	8.82E-06	9.00E-07	3.00E-07	9.98E-04	1.41E-05
0.801	1.48E-04	7.70E-06	3.00E-07	1.73E-07	7.02E-04	1.18E-05
0.851	1.12E-04	6.69E-06	1.00E-07	1.00E-07	4.78E-04	9.77E-06
0.901	8.48E-05	5.81E-06			3.09E-04	7.85E-06
0.951	6.98E-05	5.27E-06			1.69E-04	5.81E-06
1.001	3.76E-05	3.88E-06			9.39E-05	4.33E-06
1.051	2.30E-05	3.03E-06			4.80E-05	3.09E-06
1.101	1.70E-05	2.61E-06			1.40E-05	1.66E-06
1.151	6.20E-06	1.57E-06			1.60E-06	5.38E-07
1.201	4.00E-07	4.00E-07			7.99E-07	3.60E-07
1.251	3.00E-07	3.46E-07			2.00E-07	1.00E-07
1.301	0.00E+00	0.00E+00			2.00E-07	1.00E-07
1.351	0.00E+00	0.00E+00			2.00E-07	1.00E-07
1.401	1.00E-07	1.00E-07				

BLC Geometry

Co-60 Source				
Scintillator Thickness (mm)			4 pieces/1.0	
Scintillator Location			BLC Geometry	
Source Location			Center	
Material			Beryllium/polypropylene	
Energy (MeV)	$\frac{dN}{dE}\left(\frac{cts}{bin}\right)$	$\sigma\left[\frac{dN}{dE}\right]$	$N\left(Br\sum\frac{dN}{dE}\right)$	$\sigma[N]$
0.000	5.72E-05	4.78E-06		
0.001	4.53E-01	2.72E-04	7.18E-02	1.20E-04
0.051	4.56E-03	4.29E-05	6.24E-02	1.12E-04
0.101	3.75E-03	3.89E-05	5.49E-02	1.05E-04
0.151	3.31E-03	3.64E-05	4.83E-02	9.82E-05
0.201	3.73E-03	3.87E-05	4.08E-02	9.02E-05
0.251	4.14E-03	4.05E-05	3.25E-02	8.06E-05
0.301	3.48E-03	3.76E-05	2.55E-02	7.13E-05
0.351	2.82E-03	3.33E-05	1.99E-02	6.30E-05
0.401	2.31E-03	3.05E-05	1.53E-02	5.51E-05
0.451	1.81E-03	2.68E-05	1.16E-02	4.82E-05
0.501	1.42E-03	2.39E-05	8.76E-03	4.18E-05
0.551	1.09E-03	2.08E-05	6.58E-03	3.62E-05

0.601	8.46E-04	1.84E-05	4.88E-03	3.12E-05
0.651	6.55E-04	1.61E-05	3.57E-03	2.67E-05
0.701	4.91E-04	1.40E-05	2.59E-03	2.27E-05
0.751	3.71E-04	1.22E-05	1.84E-03	1.92E-05
0.801	2.83E-04	1.06E-05	1.27E-03	1.59E-05
0.851	2.14E-04	9.22E-06	8.46E-04	1.30E-05
0.901	1.60E-04	7.98E-06	5.26E-04	1.02E-05
0.951	1.20E-04	6.91E-06	2.86E-04	7.56E-06
1.001	6.34E-05	5.03E-06	1.59E-04	5.64E-06
1.051	3.82E-05	3.91E-06	8.29E-05	4.07E-06
1.101	2.95E-05	3.43E-06	2.40E-05	2.19E-06
1.151	9.80E-06	1.98E-06	4.40E-06	9.37E-07
1.201	1.60E-06	7.99E-07	1.20E-06	4.90E-07
1.251	4.00E-07	4.00E-07	4.00E-07	2.83E-07
1.301	2.00E-07	2.83E-07	0.00E+00	0.00E+00
1.351	0.00E+00	0.00E+00		

Co-60 Source				
Scintillator Thickness (mm)			4 pieces/1.0	
Scintillator Location			BLC Geometry	
Source Location			Top	
Material			Beryllium/polypropylene	
Energy (MeV)	$\frac{dN}{dE}\left(\frac{cts}{bin}\right)$	$\sigma\left[\frac{dN}{dE}\right]$	$N\left(Br\sum\frac{dN}{dE}\right)$	$\sigma[N]$
0.000	5.36E-05	4.63E-06		
0.001	4.48E-01	3.58E-04	6.69E-02	1.15E-04
0.051	4.24E-03	4.07E-05	5.81E-02	1.07E-04
0.101	3.48E-03	3.69E-05	5.12E-02	1.01E-04
0.151	3.10E-03	3.53E-05	4.50E-02	9.45E-05
0.201	3.53E-03	3.73E-05	3.79E-02	8.68E-05
0.251	3.90E-03	3.97E-05	3.01E-02	7.72E-05
0.301	3.24E-03	3.57E-05	2.36E-02	6.85E-05
0.351	2.62E-03	3.24E-05	1.83E-02	6.03E-05
0.401	2.14E-03	2.91E-05	1.40E-02	5.28E-05
0.451	1.67E-03	2.57E-05	1.07E-02	4.61E-05
0.501	1.31E-03	2.28E-05	8.04E-03	4.00E-05
0.551	1.01E-03	2.00E-05	6.01E-03	3.46E-05
0.601	7.74E-04	1.76E-05	4.46E-03	2.98E-05
0.651	6.09E-04	1.56E-05	3.24E-03	2.54E-05
0.701	4.54E-04	1.34E-05	2.33E-03	2.16E-05
0.751	3.44E-04	1.17E-05	1.64E-03	1.81E-05

0.801	2.57E-04	1.01E-05	1.13E-03	1.50E-05
0.851	1.96E-04	8.83E-06	7.35E-04	1.21E-05
0.901	1.35E-04	7.34E-06	4.65E-04	9.64E-06
0.951	1.08E-04	6.55E-06	2.50E-04	7.06E-06
1.001	5.37E-05	4.64E-06	1.42E-04	5.33E-06
1.051	3.51E-05	3.75E-06	7.17E-05	3.79E-06
1.101	2.41E-05	3.10E-06	2.36E-05	2.17E-06
1.151	9.20E-06	1.92E-06	5.20E-06	1.02E-06
1.201	2.10E-06	9.16E-07	9.99E-07	4.47E-07
1.251	3.00E-07	3.46E-07	4.00E-07	2.83E-07
1.301	2.00E-07	2.83E-07	0.00E+00	0.00E+00
1.351	0.00E+00	0.00E+00		

Co-60 Source				
Scintillator Thickness (mm)			4 pieces/1.0	
Scintillator Location			BLC Geometry	
Source Location			Bottom	
Material			Beryllium/polypropylene	
Energy (MeV)	$\frac{dN}{dE}\left(\frac{cts}{bin}\right)$	$\sigma\left[\frac{dN}{dE}\right]$	$N\left(Br\sum\frac{dN}{dE}\right)$	$\sigma[N]$
0.000	5.08E-05	4.51E-06		
0.001	4.48E-01	3.58E-04	6.69E-02	1.15E-04
0.051	4.25E-03	4.08E-05	5.81E-02	1.07E-04
0.101	3.52E-03	3.72E-05	5.11E-02	1.01E-04
0.151	3.09E-03	3.52E-05	4.49E-02	9.45E-05
0.201	3.49E-03	3.70E-05	3.79E-02	8.69E-05
0.251	3.89E-03	3.97E-05	3.01E-02	7.73E-05
0.301	3.25E-03	3.57E-05	2.36E-02	6.85E-05
0.351	2.62E-03	3.25E-05	1.83E-02	6.03E-05
0.401	2.15E-03	2.92E-05	1.40E-02	5.28E-05
0.451	1.67E-03	2.57E-05	1.07E-02	4.61E-05
0.501	1.32E-03	2.30E-05	8.00E-03	3.99E-05
0.551	1.00E-03	2.00E-05	5.99E-03	3.45E-05
0.601	7.80E-04	1.76E-05	4.43E-03	2.97E-05
0.651	5.99E-04	1.54E-05	3.23E-03	2.54E-05
0.701	4.56E-04	1.35E-05	2.32E-03	2.15E-05
0.751	3.32E-04	1.15E-05	1.65E-03	1.81E-05
0.801	2.60E-04	1.02E-05	1.13E-03	1.50E-05
0.851	1.93E-04	8.80E-06	7.42E-04	1.22E-05
0.901	1.39E-04	7.43E-06	4.64E-04	9.64E-06
0.951	1.06E-04	6.53E-06	2.51E-04	7.08E-06

1.001	5.65E-05	4.75E-06	1.38E-04	5.25E-06
1.051	3.38E-05	3.67E-06	7.02E-05	3.75E-06
1.101	2.46E-05	3.14E-06	2.10E-05	2.05E-06
1.151	8.70E-06	1.86E-06	3.60E-06	7.19E-13
1.201	1.20E-06	6.92E-07	1.20E-06	2.40E-13
1.251	4.00E-07	4.00E-07	4.00E-07	7.99E-14
1.301	2.00E-07	2.83E-07	0.00E+00	0.00E+00
1.351	0.00E+00	0.00E+00		

Geometric Uncertainties

Sr-90 Point Source				
Scintillator Thickness (mm)			1	
Scintillator Location			on axis	
Source Location			Center	
Material			Polypropylene/polypropylene	
Energy (MeV)	$\frac{dN}{dE}\left(\frac{cts}{bin}\right)$	$\sigma\left[\frac{dN}{dE}\right]$	$N\left(Br\sum\frac{dN}{dE}\right)$	$\sigma[N]$
0.000	6.29E-03	5.03E-05		
0.001	5.59E-03	1.55E-04	1.32E+00	1.65E-03
0.050	4.48E-02	4.30E-04	1.23E+00	1.59E-03
0.099	5.66E-02	4.87E-04	1.11E+00	1.51E-03
0.148	5.68E-02	4.89E-04	1.00E+00	1.43E-03
0.197	7.82E-02	5.63E-04	8.43E-01	1.32E-03
0.246	8.46E-02	5.75E-04	6.74E-01	1.18E-03
0.295	7.59E-02	5.46E-04	5.23E-01	1.05E-03
0.344	6.13E-02	5.02E-04	4.00E-01	9.22E-04
0.392	4.68E-02	4.40E-04	3.06E-01	8.10E-04
0.441	3.32E-02	3.72E-04	2.40E-01	7.20E-04
0.490	2.30E-02	3.12E-04	1.94E-01	6.48E-04
0.539	1.65E-02	2.68E-04	1.61E-01	5.90E-04
0.588	1.32E-02	2.38E-04	1.35E-01	5.40E-04
0.637	1.09E-02	2.17E-04	1.13E-01	4.95E-04
0.686	9.37E-03	2.01E-04	9.40E-02	4.53E-04
0.735	7.78E-03	1.84E-04	7.84E-02	4.14E-04
0.784	6.78E-03	1.72E-04	6.48E-02	3.76E-04
0.833	5.55E-03	1.56E-04	5.37E-02	3.42E-04
0.882	4.66E-03	1.43E-04	4.44E-02	3.11E-04
0.931	4.05E-03	1.33E-04	3.63E-02	2.82E-04
0.980	3.41E-03	1.22E-04	2.95E-02	2.54E-04

1.029	2.81E-03	1.11E-04	2.39E-02	2.28E-04
1.078	2.26E-03	9.95E-05	1.93E-02	2.06E-04
1.127	1.82E-03	8.94E-05	1.57E-02	1.85E-04
1.176	1.65E-03	8.50E-05	1.24E-02	1.64E-04
1.224	1.30E-03	7.53E-05	9.78E-03	1.46E-04
1.273	1.05E-03	6.78E-05	7.68E-03	1.29E-04
1.322	8.47E-04	6.08E-05	5.98E-03	1.14E-04
1.371	6.65E-04	5.39E-05	4.65E-03	1.01E-04
1.420	5.45E-04	4.89E-05	3.56E-03	8.82E-05
1.469	4.04E-04	4.20E-05		
2.301	1.38E-03	2.54E-04		

Sr-90 Source with Mylar Window Doubled				
Scintillator Thickness (mm)			1	
Scintillator Location			on axis	
Source Location			Center	
Material			Polypropylene/polypropylene	
Energy (MeV)	$\frac{dN}{dE}\left(\frac{cts}{bin}\right)$	$\sigma\left[\frac{dN}{dE}\right]$	$N\left(Br\sum\frac{dN}{dE}\right)$	$\sigma[N]$
0.000	6.29E-03	5.03E-05		
0.001	6.27E-03	2.46E-04	1.23E+00	2.37E-03
0.050	4.48E-02	6.45E-04	1.14E+00	2.28E-03
0.099	5.56E-02	7.11E-04	1.03E+00	2.17E-03
0.148	5.52E-02	7.07E-04	9.16E-01	2.05E-03
0.197	7.39E-02	8.12E-04	7.68E-01	1.88E-03
0.246	7.93E-02	8.41E-04	6.10E-01	1.68E-03
0.295	6.94E-02	7.91E-04	4.71E-01	1.49E-03
0.344	5.54E-02	7.10E-04	3.60E-01	1.31E-03
0.392	4.24E-02	6.28E-04	2.75E-01	1.15E-03
0.441	3.04E-02	5.35E-04	2.14E-01	1.01E-03
0.490	2.07E-02	4.42E-04	1.73E-01	9.11E-04
0.539	1.53E-02	3.82E-04	1.42E-01	8.27E-04
0.588	1.18E-02	3.36E-04	1.19E-01	7.56E-04
0.637	1.01E-02	3.11E-04	9.84E-02	6.89E-04
0.686	8.39E-03	2.83E-04	8.17E-02	6.28E-04
0.735	7.20E-03	2.64E-04	6.73E-02	5.69E-04
0.784	6.01E-03	2.40E-04	5.52E-02	5.16E-04
0.833	4.96E-03	2.18E-04	4.53E-02	4.68E-04
0.882	4.05E-03	1.98E-04	3.72E-02	4.24E-04
0.931	3.43E-03	1.82E-04	3.04E-02	3.83E-04
0.980	2.84E-03	1.66E-04	2.47E-02	3.45E-04

1.029	2.42E-03	1.53E-04	1.99E-02	3.10E-04
1.078	1.94E-03	1.37E-04	1.60E-02	2.78E-04
1.127	1.53E-03	1.22E-04	1.29E-02	2.50E-04
1.176	1.29E-03	1.12E-04	1.03E-02	2.24E-04
1.224	9.99E-04	9.83E-05	8.33E-03	2.01E-04
1.273	9.34E-04	9.51E-05	6.46E-03	1.77E-04
1.322	7.21E-04	8.35E-05	5.02E-03	1.56E-04
1.371	5.83E-04	7.51E-05	3.85E-03	1.36E-04
1.420	4.02E-04	6.23E-05	3.05E-03	1.21E-04
1.469	3.92E-04	6.16E-05	2.27E-03	1.05E-04
2.301	1.13E-03	3.35E-04		

Sr-90 Source with Scintillator + 10%				
Scintillator Thickness (mm)			1.1	
Scintillator Location			on axis	
Source Location			Center	
Material			Polypropylene/polypropylene	
Energy (MeV)	$\frac{dN}{dE}\left(\frac{cts}{bin}\right)$	$\sigma\left[\frac{dN}{dE}\right]$	$N\left(Br\sum\frac{dN}{dE}\right)$	$\sigma[N]$
0.000	6.29E-03	5.03E-05		
0.001	6.43E-03	5.02E-05	1.21E+00	4.83E-04
0.050	4.09E-02	1.23E-04	1.13E+00	4.67E-04
0.099	5.13E-02	1.44E-04	1.02E+00	4.45E-04
0.148	5.08E-02	1.42E-04	9.22E-01	4.21E-04
0.197	6.18E-02	1.48E-04	7.98E-01	3.94E-04
0.246	7.40E-02	1.63E-04	6.50E-01	3.59E-04
0.295	7.00E-02	1.68E-04	5.10E-01	3.17E-04
0.344	5.74E-02	1.49E-04	3.96E-01	2.80E-04
0.392	4.43E-02	1.33E-04	3.07E-01	2.46E-04
0.441	3.28E-02	1.11E-04	2.41E-01	2.20E-04
0.490	2.31E-02	9.69E-05	1.95E-01	1.97E-04
0.539	1.66E-02	7.96E-05	1.62E-01	1.80E-04
0.588	1.30E-02	7.29E-05	1.36E-01	1.65E-04
0.637	1.09E-02	6.56E-05	1.14E-01	1.51E-04
0.686	9.22E-03	6.09E-05	9.57E-02	1.39E-04
0.735	7.85E-03	5.65E-05	8.00E-02	1.27E-04
0.784	6.64E-03	5.18E-05	6.67E-02	1.15E-04
0.833	5.61E-03	4.71E-05	5.55E-02	1.05E-04
0.882	4.76E-03	4.38E-05	4.60E-02	9.58E-05
0.931	4.05E-03	4.05E-05	3.79E-02	8.68E-05
0.980	3.38E-03	3.65E-05	3.11E-02	7.88E-05

1.029	2.85E-03	3.36E-05	2.54E-02	7.13E-05
1.078	2.39E-03	3.10E-05	2.06E-02	6.42E-05
1.127	1.97E-03	2.80E-05	1.67E-02	5.77E-05
1.176	1.64E-03	2.56E-05	1.34E-02	5.17E-05
1.224	1.32E-03	2.30E-05	1.08E-02	4.63E-05
1.273	1.10E-03	2.09E-05	8.56E-03	4.13E-05
1.322	9.01E-04	1.89E-05	6.76E-03	3.67E-05
1.371	7.48E-04	1.74E-05	5.26E-03	3.24E-05
1.420	5.79E-04	1.52E-05	4.10E-03	2.86E-05
1.469	4.66E-04	1.36E-05	3.17E-03	2.51E-05
2.301	1.58E-03	8.52E-05		

Sr-90 Source with Scintillator - 10%				
Scintillator Thickness (mm)			0.9	
Scintillator Location			on axis	
Source Location			Center	
Material			Polypropylene/polypropylene	
Energy (MeV)	$\frac{dN}{dE}\left(\frac{cts}{bin}\right)$	$\sigma\left[\frac{dN}{dE}\right]$	$N\left(Br\sum\frac{dN}{dE}\right)$	$\sigma[N]$
0.000	6.29E-03	5.03E-05		
0.001	6.49E-03	5.32E-05	1.21E+00	4.97E-04
0.050	4.09E-02	1.31E-04	1.13E+00	4.79E-04
0.099	5.14E-02	1.44E-04	1.02E+00	4.57E-04
0.148	5.69E-02	1.48E-04	9.09E-01	4.33E-04
0.197	8.48E-02	1.86E-04	7.39E-01	3.90E-04
0.246	8.19E-02	1.80E-04	5.76E-01	3.46E-04
0.295	6.95E-02	1.67E-04	4.37E-01	3.04E-04
0.344	5.47E-02	1.53E-04	3.27E-01	2.62E-04
0.392	4.01E-02	1.28E-04	2.47E-01	2.29E-04
0.441	2.77E-02	1.05E-04	1.92E-01	2.03E-04
0.490	1.91E-02	9.15E-05	1.54E-01	1.81E-04
0.539	1.38E-02	7.70E-05	1.26E-01	1.64E-04
0.588	1.09E-02	6.74E-05	1.04E-01	1.50E-04
0.637	9.08E-03	6.18E-05	8.62E-02	1.36E-04
0.686	7.58E-03	5.76E-05	7.10E-02	1.24E-04
0.735	6.37E-03	5.22E-05	5.83E-02	1.12E-04
0.784	5.26E-03	4.74E-05	4.78E-02	1.02E-04
0.833	4.38E-03	4.38E-05	3.90E-02	9.17E-05
0.882	3.64E-03	3.93E-05	3.17E-02	8.28E-05
0.931	3.04E-03	3.64E-05	2.56E-02	7.44E-05
0.980	2.48E-03	3.27E-05	2.07E-02	6.68E-05

1.029	2.04E-03	2.97E-05	1.66E-02	5.98E-05
1.078	1.68E-03	2.69E-05	1.32E-02	5.34E-05
1.127	1.35E-03	2.40E-05	1.06E-02	4.78E-05
1.176	1.13E-03	2.22E-05	8.29E-03	4.23E-05
1.224	8.80E-04	1.95E-05	6.53E-03	3.75E-05
1.273	7.36E-04	1.78E-05	5.06E-03	3.30E-05
1.322	5.69E-04	1.57E-05	3.92E-03	2.90E-05
1.371	4.65E-04	1.41E-05	2.99E-03	2.54E-05
1.420	3.61E-04	1.25E-05	2.27E-03	2.21E-05
1.469	2.79E-04	1.10E-05	1.71E-03	1.92E-05
2.301	8.54E-04	6.12E-05		

Detector #2

BLC Geometry – 10 3.175 mm layers

Co-60 Source				
Scintillator Thickness (mm)			10 pieces/3.175	
Scintillator Location			BLC Geometry	
Source Location			#1 or #5	
Material			Beryllium	
Energy (MeV)	$\frac{dN}{dE}\left(\frac{cts}{bin}\right)$	$\sigma\left[\frac{dN}{dE}\right]$	$N\left(Br\sum\frac{dN}{dE}\right)$	$\sigma[N]$
0.000	3.20E-05	5.66E-06		
0.001	3.28E-01	4.59E-04	1.16E-01	3.38E-04
0.051	3.90E-02	1.95E-04	7.65E-02	2.76E-04
0.101	1.47E-02	1.21E-04	6.18E-02	2.48E-04
0.151	9.43E-03	9.71E-05	5.24E-02	2.28E-04
0.201	7.08E-03	8.36E-05	4.53E-02	2.12E-04
0.251	5.87E-03	7.63E-05	3.95E-02	1.98E-04
0.301	5.12E-03	7.11E-05	3.44E-02	1.85E-04
0.351	4.32E-03	6.56E-05	3.00E-02	1.73E-04
0.401	3.94E-03	6.27E-05	2.61E-02	1.61E-04
0.451	3.51E-03	5.93E-05	2.26E-02	1.50E-04
0.501	3.17E-03	5.62E-05	1.94E-02	1.39E-04
0.551	2.93E-03	5.41E-05	1.65E-02	1.28E-04
0.601	2.51E-03	4.99E-05	1.40E-02	1.18E-04
0.651	2.30E-03	4.78E-05	1.17E-02	1.08E-04
0.701	2.05E-03	4.53E-05	9.65E-03	9.81E-05
0.751	1.88E-03	4.33E-05	7.77E-03	8.80E-05
0.801	1.69E-03	4.11E-05	6.08E-03	7.79E-05

0.851	1.49E-03	3.85E-05	4.59E-03	6.77E-05
0.901	1.35E-03	3.66E-05	3.25E-03	5.70E-05
0.951	1.13E-03	3.36E-05	2.12E-03	4.60E-05
1.001	7.64E-04	2.77E-05	1.35E-03	3.68E-05
1.051	5.82E-04	2.41E-05	7.72E-04	2.78E-05
1.101	4.31E-04	2.08E-05	3.42E-04	1.85E-05
1.151	2.36E-04	1.54E-05	1.06E-04	1.03E-05
1.201	6.70E-05	8.19E-06	3.90E-05	6.24E-06
1.251	3.60E-05	6.00E-06	3.00E-06	1.73E-06
1.301	1.00E-06	1.00E-06	2.00E-06	1.41E-06
1.351	2.00E-06	1.41E-06		

Co-60 Source				
Scintillator Thickness (mm)			10 pieces/3.175	
Scintillator Location			BLC Geometry	
Source Location			#3	
Material			Beryllium	
Energy (MeV)	$\frac{dN}{dE}\left(\frac{cts}{bin}\right)$	$\sigma\left[\frac{dN}{dE}\right]$	$N\left(Br\sum\frac{dN}{dE}\right)$	$\sigma[N]$
0.000	4.50E-05	6.71E-06		
0.001	3.48E-01	4.88E-04	1.33E-01	3.62E-04
0.051	4.58E-02	2.11E-04	8.78E-02	2.95E-04
0.101	1.73E-02	1.29E-04	7.05E-02	2.65E-04
0.151	1.09E-02	1.04E-04	5.96E-02	2.44E-04
0.201	8.05E-03	8.93E-05	5.16E-02	2.27E-04
0.251	6.64E-03	8.10E-05	4.49E-02	2.12E-04
0.301	5.75E-03	7.59E-05	3.92E-02	1.98E-04
0.351	4.99E-03	7.04E-05	3.42E-02	1.85E-04
0.401	4.50E-03	6.70E-05	2.97E-02	1.72E-04
0.451	4.07E-03	6.35E-05	2.56E-02	1.60E-04
0.501	3.61E-03	6.00E-05	2.20E-02	1.48E-04
0.551	3.26E-03	5.70E-05	1.88E-02	1.37E-04
0.601	2.84E-03	5.31E-05	1.59E-02	1.26E-04
0.651	2.58E-03	5.08E-05	1.33E-02	1.15E-04
0.701	2.34E-03	4.84E-05	1.10E-02	1.05E-04
0.751	2.14E-03	4.61E-05	8.87E-03	9.42E-05
0.801	1.91E-03	4.38E-05	6.96E-03	8.34E-05
0.851	1.72E-03	4.15E-05	5.24E-03	7.24E-05
0.901	1.53E-03	3.91E-05	3.71E-03	6.09E-05
0.951	1.30E-03	3.61E-05	2.41E-03	4.91E-05
1.001	8.97E-04	3.00E-05	1.51E-03	3.89E-05

1.051	6.53E-04	2.55E-05	8.60E-04	2.93E-05
1.101	4.77E-04	2.18E-05	3.84E-04	1.96E-05
1.151	2.57E-04	1.60E-05	1.27E-04	1.13E-05
1.201	8.20E-05	9.05E-06	4.50E-05	6.71E-06
1.251	4.40E-05	6.64E-06		

Co-60 Source				
Scintillator Thickness (mm)			10 pieces/3.175	
Scintillator Location			BLC Geometry	
Source Location			#11 or #15	
Material			Beryllium	
Energy (MeV)	$\frac{dN}{dE}\left(\frac{cts}{bin}\right)$	$\sigma\left[\frac{dN}{dE}\right]$	$N\left(Br\sum\frac{dN}{dE}\right)$	$\sigma[N]$
0.000	4.70E-05	6.86E-06		
0.001	3.70E-01	4.81E-04	1.42E-01	3.72E-04
0.051	4.93E-02	2.17E-04	9.24E-02	3.02E-04
0.101	1.85E-02	1.35E-04	7.39E-02	2.71E-04
0.151	1.13E-02	1.05E-04	6.26E-02	2.49E-04
0.201	8.48E-03	9.16E-05	5.41E-02	2.32E-04
0.251	6.97E-03	8.29E-05	4.72E-02	2.17E-04
0.301	6.02E-03	7.71E-05	4.12E-02	2.02E-04
0.351	5.25E-03	7.24E-05	3.59E-02	1.89E-04
0.401	4.71E-03	6.83E-05	3.12E-02	1.76E-04
0.451	4.32E-03	6.57E-05	2.69E-02	1.64E-04
0.501	3.80E-03	6.16E-05	2.31E-02	1.52E-04
0.551	3.36E-03	5.78E-05	1.97E-02	1.40E-04
0.601	3.15E-03	5.61E-05	1.66E-02	1.29E-04
0.651	2.73E-03	5.21E-05	1.39E-02	1.18E-04
0.701	2.51E-03	5.00E-05	1.14E-02	1.06E-04
0.751	2.28E-03	4.76E-05	9.08E-03	9.52E-05
0.801	1.93E-03	4.39E-05	7.15E-03	8.45E-05
0.851	1.79E-03	4.23E-05	5.36E-03	7.32E-05
0.901	1.54E-03	3.93E-05	3.82E-03	6.17E-05
0.951	1.41E-03	3.75E-05	2.41E-03	4.91E-05
1.001	9.25E-04	3.04E-05	1.49E-03	3.85E-05
1.051	6.40E-04	2.53E-05	8.47E-04	2.91E-05
1.101	4.58E-04	2.14E-05	3.90E-04	1.97E-05
1.151	2.59E-04	1.61E-05	1.31E-04	1.14E-05
1.201	9.50E-05	9.75E-06	3.60E-05	6.00E-06
1.251	3.40E-05	5.83E-06	2.00E-06	1.41E-06
1.301	2.00E-06	1.41E-06		

Co-60 Source				
Scintillator Thickness (mm)			10 pieces/3.175	
Scintillator Location			BLC Geometry	
Source Location			#13	
Material			Beryllium	
Energy (MeV)	$\frac{dN}{dE}\left(\frac{cts}{bin}\right)$	$\sigma\left[\frac{dN}{dE}\right]$	$N\left(Br\sum\frac{dN}{dE}\right)$	$\sigma[N]$
0.000	5.14E-05	2.27E-06		
0.001	3.95E-01	1.58E-04	1.65E-01	1.27E-04
0.051	5.89E-02	7.66E-05	1.06E-01	1.02E-04
0.101	2.16E-02	4.53E-05	8.45E-02	9.12E-05
0.151	1.32E-02	3.57E-05	7.13E-02	8.40E-05
0.201	9.77E-03	3.13E-05	6.15E-02	7.80E-05
0.251	7.94E-03	2.78E-05	5.36E-02	7.28E-05
0.301	6.78E-03	2.58E-05	4.68E-02	6.81E-05
0.351	5.91E-03	2.42E-05	4.09E-02	6.37E-05
0.401	5.28E-03	2.27E-05	3.57E-02	5.95E-05
0.451	4.76E-03	2.19E-05	3.09E-02	5.54E-05
0.501	4.26E-03	2.04E-05	2.67E-02	5.15E-05
0.551	3.86E-03	1.97E-05	2.28E-02	4.76E-05
0.601	3.50E-03	1.85E-05	1.93E-02	4.38E-05
0.651	3.16E-03	1.77E-05	1.62E-02	4.01E-05
0.701	2.87E-03	1.69E-05	1.33E-02	3.63E-05
0.751	2.56E-03	1.59E-05	1.07E-02	3.27E-05
0.801	2.28E-03	1.50E-05	8.45E-03	2.90E-05
0.851	2.04E-03	1.43E-05	6.42E-03	2.53E-05
0.901	1.79E-03	1.35E-05	4.62E-03	2.14E-05
0.951	1.62E-03	1.26E-05	3.00E-03	1.73E-05
1.001	1.13E-03	1.06E-05	1.87E-03	1.37E-05
1.051	7.82E-04	8.84E-06	1.09E-03	1.04E-05
1.101	5.91E-04	7.68E-06	5.02E-04	7.09E-06
1.151	3.31E-04	5.76E-06	1.71E-04	4.14E-06
1.201	1.30E-04	3.61E-06	4.12E-05	2.03E-06
1.251	3.69E-05	1.92E-06	4.30E-06	6.55E-07
1.301	2.70E-06	5.19E-07	1.60E-06	4.00E-07
1.351	1.20E-06	3.46E-07	4.00E-07	2.00E-07
1.401	4.00E-07	2.00E-07		

Co-60 Source	
Scintillator Thickness (mm)	10 pieces/3.175

Scintillator Location			BLC Geometry	
Source Location			#21 or #25	
Material			Beryllium	
Energy (MeV)	$\frac{dN}{dE}\left(\frac{cts}{bin}\right)$	$\sigma\left[\frac{dN}{dE}\right]$	$N\left(Br\sum\frac{dN}{dE}\right)$	$\sigma[N]$
0.000	3.90E-05	6.24E-06		
0.001	3.35E-01	4.69E-04	1.19E-01	3.41E-04
0.051	4.00E-02	1.96E-04	7.86E-02	2.79E-04
0.101	1.54E-02	1.23E-04	6.32E-02	2.51E-04
0.151	9.58E-03	9.77E-05	5.36E-02	2.31E-04
0.201	7.16E-03	8.45E-05	4.64E-02	2.15E-04
0.251	6.03E-03	7.72E-05	4.04E-02	2.01E-04
0.301	5.14E-03	7.15E-05	3.53E-02	1.88E-04
0.351	4.45E-03	6.68E-05	3.08E-02	1.75E-04
0.401	4.05E-03	6.35E-05	2.68E-02	1.63E-04
0.451	3.63E-03	6.03E-05	2.31E-02	1.52E-04
0.501	3.30E-03	5.74E-05	1.99E-02	1.41E-04
0.551	2.85E-03	5.32E-05	1.70E-02	1.30E-04
0.601	2.65E-03	5.14E-05	1.44E-02	1.20E-04
0.651	2.33E-03	4.81E-05	1.20E-02	1.10E-04
0.701	2.18E-03	4.66E-05	9.86E-03	9.92E-05
0.751	1.98E-03	4.45E-05	7.88E-03	8.87E-05
0.801	1.72E-03	4.13E-05	6.17E-03	7.85E-05
0.851	1.55E-03	3.93E-05	4.62E-03	6.80E-05
0.901	1.33E-03	3.65E-05	3.29E-03	5.73E-05
0.951	1.22E-03	3.49E-05	2.07E-03	4.55E-05
1.001	7.69E-04	2.77E-05	1.30E-03	3.61E-05
1.051	5.53E-04	2.35E-05	7.51E-04	2.74E-05
1.101	4.09E-04	2.02E-05	3.43E-04	1.85E-05
1.151	2.19E-04	1.48E-05	1.24E-04	1.11E-05
1.201	9.60E-05	9.80E-06	2.80E-05	5.29E-06
1.251	2.60E-05	5.10E-06	2.00E-06	1.41E-06
1.301	2.00E-06	1.41E-06		

Co-60 Source				
Scintillator Thickness (mm)			10 pieces/3.175	
Scintillator Location			BLC Geometry	
Source Location			#23	
Material			Beryllium	
Energy (MeV)	$\frac{dN}{dE}\left(\frac{cts}{bin}\right)$	$\sigma\left[\frac{dN}{dE}\right]$	$N\left(Br\sum\frac{dN}{dE}\right)$	$\sigma[N]$

0.000	4.00E-05	6.32E-06		
0.001	3.56E-01	4.63E-04	1.38E-01	3.68E-04
0.051	4.77E-02	2.14E-04	9.04E-02	2.99E-04
0.101	1.80E-02	1.33E-04	7.24E-02	2.68E-04
0.151	1.12E-02	1.05E-04	6.13E-02	2.47E-04
0.201	8.25E-03	9.08E-05	5.30E-02	2.30E-04
0.251	6.86E-03	8.23E-05	4.62E-02	2.14E-04
0.301	5.89E-03	7.65E-05	4.03E-02	2.00E-04
0.351	5.11E-03	7.15E-05	3.52E-02	1.87E-04
0.401	4.57E-03	6.76E-05	3.06E-02	1.75E-04
0.451	4.12E-03	6.39E-05	2.65E-02	1.63E-04
0.501	3.74E-03	6.10E-05	2.28E-02	1.51E-04
0.551	3.29E-03	5.73E-05	1.95E-02	1.39E-04
0.601	2.97E-03	5.43E-05	1.65E-02	1.28E-04
0.651	2.67E-03	5.16E-05	1.38E-02	1.18E-04
0.701	2.52E-03	5.02E-05	1.13E-02	1.06E-04
0.751	2.22E-03	4.71E-05	9.09E-03	9.53E-05
0.801	1.93E-03	4.39E-05	7.16E-03	8.46E-05
0.851	1.72E-03	4.15E-05	5.44E-03	7.37E-05
0.901	1.59E-03	3.99E-05	3.85E-03	6.20E-05
0.951	1.39E-03	3.73E-05	2.46E-03	4.96E-05
1.001	8.90E-04	2.98E-05	1.57E-03	3.96E-05
1.051	6.43E-04	2.53E-05	9.30E-04	3.05E-05
1.101	5.15E-04	2.27E-05	4.16E-04	2.04E-05
1.151	2.74E-04	1.65E-05	1.42E-04	1.19E-05
1.201	1.00E-04	1.00E-05	4.20E-05	6.48E-06
1.251	3.80E-05	6.16E-06	4.00E-06	2.00E-06
1.301	3.00E-06	1.73E-06		

Cs-137 Source				
Scintillator Thickness (mm)			10 pieces/3.175	
Scintillator Location			BLC Geometry	
Source Location			#13	
Material			Beryllium	
Energy (MeV)	$\frac{dN}{dE}\left(\frac{cts}{bin}\right)$	$\sigma\left[\frac{dN}{dE}\right]$	$N\left(Br\sum\frac{dN}{dE}\right)$	$\sigma[N]$
0.000	1.31E-05	1.34E-06		
0.001	3.07E-01	1.84E-04	6.50E-02	6.41E-05
0.051	5.40E-02	8.64E-05	4.02E-02	5.03E-05
0.101	2.62E-02	6.02E-05	2.81E-02	4.21E-05
0.151	1.55E-02	4.65E-05	2.10E-02	3.62E-05

0.201	1.09E-02	3.80E-05	1.60E-02	3.17E-05
0.251	8.32E-03	3.41E-05	1.22E-02	2.76E-05
0.301	6.74E-03	3.03E-05	9.07E-03	2.38E-05
0.351	5.60E-03	2.74E-05	6.50E-03	2.02E-05
0.401	4.84E-03	2.57E-05	4.27E-03	1.64E-05
0.451	4.65E-03	2.51E-05	2.13E-03	1.16E-05
0.501	3.54E-03	2.19E-05	5.06E-04	5.68E-06
0.551	9.32E-04	1.14E-05	7.73E-05	2.21E-06
0.601	1.60E-04	4.69E-06	3.86E-06	4.95E-07
0.651	5.92E-06	9.03E-07	1.14E-06	2.69E-07
0.701	2.48E-06	5.84E-07		

BLC Geometry – 10 0.5 mm layers

Co-60 Source				
Scintillator Thickness (mm)			10 pieces/0.50	
Scintillator Location			BLC Geometry	
Source Location			#13	
Material			Beryllium	
Energy (MeV)	$\frac{dN}{dE}\left(\frac{cts}{bin}\right)$	$\sigma\left[\frac{dN}{dE}\right]$	$N\left(Br\sum\frac{dN}{dE}\right)$	$\sigma[N]$
0.000	8.88E-05	2.98E-06		
0.001	4.50E-01	1.35E-04	4.94E-02	7.00E-05
0.051	1.83E-02	4.20E-05	3.11E-02	5.60E-05
0.101	8.81E-03	2.99E-05	2.23E-02	4.73E-05
0.151	8.25E-03	2.89E-05	1.40E-02	3.74E-05
0.201	4.78E-03	2.20E-05	9.26E-03	3.03E-05
0.251	3.14E-03	1.76E-05	6.13E-03	2.47E-05
0.301	2.14E-03	1.46E-05	3.99E-03	1.99E-05
0.351	1.41E-03	1.18E-05	2.59E-03	1.61E-05
0.401	9.39E-04	9.67E-06	1.65E-03	1.29E-05
0.451	6.14E-04	7.86E-06	1.03E-03	1.02E-05
0.501	3.92E-04	6.28E-06	6.42E-04	8.01E-06
0.551	2.46E-04	4.97E-06	3.97E-04	6.29E-06
0.601	1.60E-04	3.99E-06	2.37E-04	4.87E-06
0.651	9.42E-05	3.07E-06	1.43E-04	3.78E-06
0.701	6.37E-05	2.52E-06	7.95E-05	2.82E-06
0.751	3.45E-05	1.86E-06	4.51E-05	2.12E-06
0.801	2.17E-05	1.47E-06	2.34E-05	1.53E-06
0.851	1.20E-05	1.10E-06	1.14E-05	1.07E-06

0.901	5.90E-06	7.68E-07	5.50E-06	7.41E-07
0.951	3.20E-06	5.66E-07	2.30E-06	4.79E-07
1.001	1.00E-06	3.16E-07	1.30E-06	3.60E-07
1.051	1.10E-06	3.32E-07	2.00E-07	1.41E-07
1.101	2.00E-07	1.41E-07		

BLC Geometry – 10 0.25 mm layers

Co-60 Source				
Scintillator Thickness (mm)			10 pieces/0.25	
Scintillator Location			BLC Geometry	
Source Location			#13	
Material			Beryllium	
Energy (MeV)	$\frac{dN}{dE}\left(\frac{cts}{bin}\right)$	$\sigma\left[\frac{dN}{dE}\right]$	$N\left(Br\sum\frac{dN}{dE}\right)$	$\sigma[N]$
0.000	1.33E-04	3.65E-06		
0.001	4.58E-01	1.37E-04	3.54E-02	5.95E-05
0.051	1.49E-02	3.87E-05	2.05E-02	4.52E-05
0.101	1.10E-02	3.31E-05	9.50E-03	3.09E-05
0.151	4.21E-03	2.06E-05	5.29E-03	2.30E-05
0.201	2.39E-03	1.55E-05	2.90E-03	1.70E-05
0.251	1.32E-03	1.15E-05	1.59E-03	1.26E-05
0.301	7.24E-04	8.47E-06	8.62E-04	9.28E-06
0.351	3.96E-04	6.29E-06	4.66E-04	6.83E-06
0.401	2.25E-04	4.75E-06	2.42E-04	4.91E-06
0.451	1.19E-04	3.44E-06	1.23E-04	3.51E-06
0.501	5.87E-05	2.42E-06	6.45E-05	2.54E-06
0.551	3.24E-05	1.80E-06	3.21E-05	1.79E-06
0.601	1.45E-05	1.20E-06	1.76E-05	1.33E-06
0.651	8.30E-06	9.11E-07	9.29E-06	9.64E-07
0.701	5.10E-06	7.14E-07	4.20E-06	6.48E-07
0.751	1.50E-06	3.87E-07	2.70E-06	5.19E-07
0.801	1.60E-06	4.00E-07	1.10E-06	3.31E-07
0.851	7.00E-07	2.65E-07	4.00E-07	2.00E-07
0.901	1.00E-07	1.00E-07	3.00E-07	1.73E-07
0.951	3.00E-07	1.73E-07		

Cs-137 Source	
Scintillator Thickness (mm)	10 pieces/0.25
Scintillator Location	BLC Geometry

Source Location			#13	
Material			Beryllium	
Energy (MeV)	$\frac{dN}{dE}\left(\frac{cts}{bin}\right)$	$\sigma\left[\frac{dN}{dE}\right]$	$N\left(Br\sum\frac{dN}{dE}\right)$	$\sigma[N]$
0.000	2.13E-05	1.46E-06		
0.001	4.29E-01	1.72E-04	1.15E-02	2.28E-05
0.051	1.44E-02	3.75E-05	4.86E-03	1.50E-05
0.101	5.46E-03	2.35E-05	2.35E-03	1.04E-05
0.151	2.66E-03	1.62E-05	1.12E-03	7.18E-06
0.201	1.38E-03	1.17E-05	4.87E-04	4.74E-06
0.251	6.31E-04	7.96E-06	1.97E-04	3.01E-06
0.301	2.69E-04	5.20E-06	7.27E-05	1.83E-06
0.351	1.07E-04	3.27E-06	2.36E-05	1.04E-06
0.401	3.80E-05	1.95E-06	6.16E-06	5.32E-07
0.451	1.16E-05	1.08E-06	8.28E-07	1.95E-07
0.501	1.60E-06	4.00E-07	9.20E-08	6.50E-08
0.551	2.00E-07	1.41E-07		

Single Layer Geometry – 3.175 mm

Co-60 Source				
Scintillator Thickness (mm)			3.175	
Scintillator Location			On axis	
Source Location			#13	
Material			Beryllium	
Energy (MeV)	$\frac{dN}{dE}\left(\frac{cts}{bin}\right)$	$\sigma\left[\frac{dN}{dE}\right]$	$N\left(Br\sum\frac{dN}{dE}\right)$	$\sigma[N]$
0.000	6.80E-06	8.25E-07		
0.001	3.11E-01	1.55E-04	1.99E-02	4.46E-05
0.051	9.26E-03	3.06E-05	1.06E-02	3.25E-05
0.101	2.43E-03	1.56E-05	8.20E-03	2.86E-05
0.151	1.43E-03	1.19E-05	6.77E-03	2.60E-05
0.201	1.03E-03	1.01E-05	5.74E-03	2.39E-05
0.251	8.05E-04	8.93E-06	4.93E-03	2.22E-05
0.301	6.78E-04	8.20E-06	4.26E-03	2.06E-05
0.351	5.87E-04	7.68E-06	3.67E-03	1.91E-05
0.401	5.29E-04	7.25E-06	3.14E-03	1.77E-05
0.451	4.56E-04	6.75E-06	2.68E-03	1.64E-05
0.501	4.00E-04	6.33E-06	2.28E-03	1.51E-05
0.551	3.63E-04	6.03E-06	1.92E-03	1.39E-05
0.601	3.24E-04	5.69E-06	1.60E-03	1.26E-05

0.651	2.81E-04	5.31E-06	1.32E-03	1.15E-05
0.701	2.62E-04	5.13E-06	1.06E-03	1.03E-05
0.751	2.40E-04	4.90E-06	8.16E-04	9.03E-06
0.801	1.98E-04	4.45E-06	6.18E-04	7.86E-06
0.851	1.70E-04	4.12E-06	4.49E-04	6.69E-06
0.901	1.44E-04	3.79E-06	3.05E-04	5.52E-06
0.951	1.23E-04	3.50E-06	1.82E-04	4.27E-06
1.001	7.51E-05	2.74E-06	1.07E-04	3.27E-06
1.051	4.55E-05	2.13E-06	6.16E-05	2.48E-06
1.101	3.91E-05	1.98E-06	2.25E-05	1.50E-06
1.151	1.88E-05	1.37E-06	3.70E-06	6.08E-07
1.201	3.00E-06	5.48E-07	7.00E-07	2.64E-07
1.251	7.00E-07	2.65E-07		

Cs-137 Source				
Scintillator Thickness (mm)				3.175
Scintillator Location				On axis
Source Location				#13
Material				Beryllium
Energy (MeV)	$\frac{dN}{dE}\left(\frac{cts}{bin}\right)$	$\sigma\left[\frac{dN}{dE}\right]$	$N\left(Br\sum\frac{dN}{dE}\right)$	$\sigma[N]$
0.000	1.80E-06	4.24E-07		
0.001	2.77E-01	1.39E-04	9.96E-03	2.15E-05
0.051	1.30E-02	3.63E-05	4.00E-03	1.35E-05
0.101	3.02E-03	1.72E-05	2.61E-03	1.09E-05
0.151	1.60E-03	1.26E-05	1.87E-03	9.27E-06
0.201	1.08E-03	1.03E-05	1.38E-03	7.96E-06
0.251	7.87E-04	8.89E-06	1.02E-03	6.83E-06
0.301	6.37E-04	7.96E-06	7.24E-04	5.76E-06
0.351	4.96E-04	7.04E-06	4.96E-04	4.77E-06
0.401	4.15E-04	6.43E-06	3.05E-04	3.74E-06
0.451	3.80E-04	6.15E-06	1.31E-04	2.45E-06
0.501	2.54E-04	5.04E-06	1.36E-05	7.91E-07
0.551	2.74E-05	1.65E-06	1.01E-06	2.16E-07
0.601	2.00E-06	4.47E-07	9.20E-08	6.50E-08
0.651	1.00E-07	1.00E-07	4.60E-08	4.60E-08
0.701	1.00E-07	1.00E-07		

Single Layer Geometry – 0.50 mm

Co-60 Source				
Scintillator Thickness (mm)				0.50
Scintillator Location				On axis
Source Location				#13
Material				Beryllium
Energy (MeV)	$\frac{dN}{dE}\left(\frac{cts}{bin}\right)$	$\sigma\left[\frac{dN}{dE}\right]$	$N\left(Br\sum\frac{dN}{dE}\right)$	$\sigma[N]$
0.000	9.40E-06	9.69E-07		
0.001	3.19E-01	1.59E-04	5.08E-03	2.25E-05
0.051	2.07E-03	1.43E-05	3.02E-03	1.73E-05
0.101	9.60E-04	9.79E-06	2.06E-03	1.43E-05
0.151	8.06E-04	8.94E-06	1.25E-03	1.12E-05
0.201	4.45E-04	6.68E-06	8.07E-04	8.97E-06
0.251	2.85E-04	5.32E-06	5.22E-04	7.22E-06
0.301	1.94E-04	4.39E-06	3.29E-04	5.73E-06
0.351	1.23E-04	3.50E-06	2.06E-04	4.54E-06
0.401	7.85E-05	2.80E-06	1.28E-04	3.57E-06
0.451	4.72E-05	2.17E-06	8.04E-05	2.83E-06
0.501	3.29E-05	1.81E-06	4.76E-05	2.18E-06
0.551	1.83E-05	1.35E-06	2.93E-05	1.71E-06
0.601	1.29E-05	1.14E-06	1.64E-05	1.28E-06
0.651	7.30E-06	8.54E-07	9.09E-06	9.53E-07
0.701	4.50E-06	6.71E-07	4.60E-06	6.78E-07
0.751	2.00E-06	4.47E-07	2.60E-06	5.10E-07
0.801	1.20E-06	3.46E-07	1.40E-06	3.74E-07
0.851	8.00E-07	2.83E-07	6.00E-07	2.45E-07
0.901	3.00E-07	1.73E-07	3.00E-07	1.73E-07
0.951	3.00E-07	1.73E-07		

Cs-137 Source				
Scintillator Thickness (mm)				0.50
Scintillator Location				On axis
Source Location				#13
Material				Beryllium
Energy (MeV)	$\frac{dN}{dE}\left(\frac{cts}{bin}\right)$	$\sigma\left[\frac{dN}{dE}\right]$	$N\left(Br\sum\frac{dN}{dE}\right)$	$\sigma[N]$
0.000	1.20E-06	3.46E-07		
0.001	2.88E-01	1.44E-04	2.00E-03	9.56E-06
0.051	2.67E-03	1.63E-05	7.71E-04	5.95E-06

0.101	6.55E-04	8.12E-06	4.70E-04	4.64E-06
0.151	4.04E-04	6.34E-06	2.84E-04	3.61E-06
0.201	2.62E-04	5.11E-06	1.63E-04	2.74E-06
0.251	1.75E-04	4.18E-06	8.31E-05	1.95E-06
0.301	1.00E-04	3.16E-06	3.71E-05	1.30E-06
0.351	4.78E-05	2.18E-06	1.51E-05	8.33E-07
0.401	2.14E-05	1.46E-06	5.24E-06	4.91E-07
0.451	1.01E-05	1.00E-06	5.98E-07	1.66E-07
0.501	1.30E-06	3.60E-07		

Single Layer Geometry – 0.25 mm

Co-60 Source				
Scintillator Thickness (mm)			0.25	
Scintillator Location			On axis	
Source Location			#13	
Material			Beryllium	
Energy (MeV)	$\frac{dN}{dE}\left(\frac{cts}{bin}\right)$	$\sigma\left[\frac{dN}{dE}\right]$	$N\left(Br\sum\frac{dN}{dE}\right)$	$\sigma[N]$
0.000	1.45E-05	1.20E-06		
0.001	3.20E-01	1.60E-04	3.55E-03	1.88E-05
0.051	1.64E-03	1.28E-05	1.91E-03	1.38E-05
0.101	1.05E-03	1.03E-05	8.66E-04	9.30E-06
0.151	3.96E-04	6.29E-06	4.70E-04	6.86E-06
0.201	2.23E-04	4.72E-06	2.48E-04	4.97E-06
0.251	1.19E-04	3.44E-06	1.29E-04	3.59E-06
0.301	6.21E-05	2.49E-06	6.70E-05	2.59E-06
0.351	3.12E-05	1.77E-06	3.58E-05	1.89E-06
0.401	1.53E-05	1.24E-06	2.05E-05	1.43E-06
0.451	1.05E-05	1.02E-06	9.99E-06	9.99E-07
0.501	4.60E-06	6.78E-07	5.40E-06	7.34E-07
0.551	3.20E-06	5.66E-07	2.20E-06	4.69E-07
0.601	1.30E-06	3.60E-07	8.99E-07	3.00E-07
0.651	7.00E-07	2.65E-07	2.00E-07	1.41E-07
0.701	1.00E-07	1.00E-07		

Cs-137 Source	
Scintillator Thickness (mm)	0.25
Scintillator Location	On axis
Source Location	#13

Material			Beryllium	
Energy (MeV)	$\frac{dN}{dE}\left(\frac{cts}{bin}\right)$	$\sigma\left[\frac{dN}{dE}\right]$	$N\left(Br\sum\frac{dN}{dE}\right)$	$\sigma[N]$
0.00E+00	1.80E-06	4.24E-07		
1.00E-03	2.89E-01	1.45E-04	1.16E-03	7.28E-06
5.10E-02	1.51E-03	1.23E-05	4.61E-04	4.61E-06
1.01E-01	5.33E-04	7.30E-06	2.16E-04	3.16E-06
1.51E-01	2.50E-04	5.00E-06	1.01E-04	2.16E-06
2.01E-01	1.30E-04	3.61E-06	4.17E-05	1.38E-06
2.51E-01	5.45E-05	2.33E-06	1.66E-05	8.75E-07
3.01E-01	2.37E-05	1.54E-06	5.75E-06	5.14E-07
3.51E-01	8.70E-06	9.33E-07	1.75E-06	2.83E-07
4.01E-01	3.20E-06	5.66E-07	2.76E-07	1.13E-07
4.51E-01	3.00E-07	1.73E-07	1.38E-07	7.96E-08
5.01E-01	3.00E-07	1.73E-07		

Appendix C Sample MCNP Inputs

Detector # 1

Na-22 Gamma Source, Case 1 Geometry

```
Na-22 source
c    *** Cell Cards ***
20   300   -1.0600     -10    11             $ Polystyrene
30   200   -1.4000    -1                     $ surface of source
90   600   -0.9000     -11 1 18 19 20        $ polypropylene spacers
100  500   -8.0300     -13  12               $ detector housing
110    0               -12  10  14           $ void inside housing
120  700   -2.2300     -14 15                $ pmt
130    0               -15                   $ inside of pmt
140  500   -8.0300     -16  17               $ base housing
150    0               -17                   $ void in base
160    0                16  13               $ void outside detector
170  800   -1.848      -18
180  800   -1.848      -20
200  100   -1.0320     -19

c    *** Surface Cards ***
1   rcc    -0.3175 0 0 .3175 0 0 1.27                    $ outside radius of source
10  rcc    0.3675  0  -3.5675 0 0 6.8175 2.1075          $ polystyrene holder
11  rpp   -0.57875 1.31375 -1.50 1.50 -3.25 3.25          $ polypropylene spacers
12  rcc    0.3675  0  -3.5675 0 0  11.5825   2.1075       $ inside of detector housing
13  rcc    0.3675  0  -3.8850 0 0  11.9000   2.425        $ outside of detector housing
14  rcc    0.3675  0   8.015  0 0  -4.6      1.875        $ outside of pmt
15  rcc    0.3675  0   8.015  0 0  -4.2825   1.5575       $ inside of pmt
```

```
16  rcc    0.3675  0   8.015  0 0   6.5      4.55         $ outside of base
17  rcc    0.3675  0   8.3325 0 0   5.865    4.235        $ inside of base
18  rpp    0  0.3175  -1.50 1.50 -3.25  3.25             $ beryllium layer
19  rpp    0.3175 0.4175 -1.50 1.50 -3.25  3.25          $ scintillator layer
20  rpp    0.4175 0.7350 -1.50 1.50 -3.25  3.25               $ beryllium layer

mode   e p
imp:e 1 8r 0 1 1 1
imp:p 1 8r 0 1 1 1
sdef par=2 x=-0.15875 y=0 z=0  axs=1 0 0  rad=d3 erg=1.274537
si3   0     0.15
sp3   0     1
m100 6000    0.47           $ scintillator
     1001    0.53
     estep 11
m200 6000   -0.625017       $ mylar
     8016   -0.333024
     1001   -0.041959
     estep 12
m300 6000   -0.856289       $ polyethylene
     1000   -0.143711
     estep 12
m400 13027   1               $ aluminum
     estep 6
m500 6000   -0.0008          $ Stainless Steel 304
     25000  -0.0200
     24000  -0.1900
     28000  -0.1000
     14000  -0.0075
     15000  -0.00045
     16000  -0.0003
     7000   -0.0010
```

```
     26000  -0.67995
     estep 10
m600 6000   -.922582       $ polystyrene
     1000   -.077418
     estep 6
m700 5010   -0.007973       $ borosilicate glass rho=2.23 g/cc
     5011   -0.032091
     8016   -0.539562
     11023  -0.028191
     13027  -0.011644
     14000  -0.377220
     19000  -0.003321
m800 4009    1
f8:e,p   200
e8    0  0.001  25i  1.3001
prdmp 1e15 1e15 1e15
nps 1e7
```

Na-22 Positron Source, Case 1 Geometry

```
Na-22 source
c    *** Cell Cards ***
20   300   -1.0600     -10    11 18 19 20    $ Polystyrene
30   200   -1.4000    -1                     $ surface of source
90   600   -0.9000     -11 1   18 19 20      $ polypropylene spacers
100  500   -8.0300     -13  12               $ detector housing
110    0               -12  10  14           $ void inside housing
120  700   -2.2300     -14 15                $ pmt
130    0               -15                   $ inside of pmt
140  500   -8.0300     -16  17               $ base housing
```

```
150    0                -17                    $ void in base
160    0                 16  13                $ void outside detector
170  800   -1.848      -18                    $ beryllium
180  800   -1.848      -20                    $ beryllium
200  100   -1.0320     -19                    $ scintillator

c    *** Surface Cards ***
1   rcc    -0.3175  0  0  .3175  0  0  1.27                $ outside radius of source
10  rcc    0.3675  0  -3.5675  0 0  6.8175  2.1075         $ polystyrene holder
11  rpp   -0.57875  1.31375  -1.50  1.50  -3.25  3.25    $ polypropylene spacers
12  rcc    0.3675  0  -3.5675 0 0  11.5825   2.1075      $ inside of detector housing
13  rcc    0.3675  0  -3.8850 0 0  11.9000   2.425       $ outside of detector housing
14  rcc    0.3675  0   8.015  0 0  -4.6      1.875       $ outside of pmt
15  rcc    0.3675  0   8.015  0 0  -4.2825   1.5575      $ inside of pmt
16  rcc    0.3675  0   8.015  0 0   6.5      4.55        $ outside of base
17  rcc    0.3675  0   8.3325 0 0   5.865    4.235       $ inside of base
18  rpp    0  0.3175  -1.50 1.50 -3.25  3.25             $ beryllium layer
19  rpp    0.3175 0.4175 -1.50 1.50 -3.25  3.25          $ scintillator layer
20  rpp    0.4175 0.7350 -1.50 1.50 -3.25  3.25          $ beryllium layer

mode   e p
imp:e 1 8r 0 1 1 1
imp:p 1 8r 0 1 1 1
c *** -3 is a positron particle identifier ***
sdef par=-3 x=-0.15875 y=0 z=0  erg=d1  rad=d4
c *** Positron energy distribution ***
si1   A 0 0.0910 0.1820 0.2730 0.3640 0.4550 0.5460 0.6370 0.7280 0.8190
      0.9101 1.0011 1.0921 1.1831 1.2741 1.3651 1.4561 1.5471 1.6381 1.7291
      1.8201
c *** probability distribution ***
sp1   0 1.46E-01 2.75E-01 2.71E-01 1.96E-01 9.46E-02 1.67E-02 4.85E-05
      4.84E-05 4.92E-05 4.92E-05 4.84E-05 4.67E-05 4.41E-05 4.05E-05
```

```
      3.58E-05 2.99E-05 2.27E-05 1.47E-05 6.92E-06 1.14E-06
si4   0     .15
sp4   0     1
m100 6000    0.47           $ scintillator
     1001    0.53
     estep 11
m200 6000   -0.625017       $ mylar
     8016   -0.333024
     1001   -0.041959
     estep 12
m300 6000   -0.856289       $ polyethylene
     1000   -0.143711
     estep 12
m400 13027   1                 $ aluminum
     estep 6
m500 6000   -0.0008            $ Stainless Steel 304
     25000  -0.0200
     24000  -0.1900
     28000  -0.1000
     14000  -0.0075
     15000  -0.00045
     16000  -0.0003
     7000   -0.0010
     26000  -0.67995
     estep 10
m600 6000   -.922582           $ polystyrene
     1000   -.077418
     estep 6
m700 5010   -0.007973          $ borosilicate glass rho=2.23 g/cc
     5011   -0.032091
     8016   -0.539562
     11023  -0.028191
```

```
     13027  -0.011644
     14000  -0.377220
     19000  -0.003321
m800 4009    1
f8:e,p   200
e8    0  0.001  39i  2.001
prdmp 1e15 1e15 1e15
nps 1e7
```

Cs-137 gamma source, case 1 geometry

```
Cs-137 source
c    *** Cell Cards ***
20   300   -1.0600     -10    11                                $ Polystyrene
30   200   -1.4000    -1                                        $ surface of source
90   600   -0.9000     -11 1   18 19 20                         $ polypropylene spacers
100  500   -8.0300     -13  12                                  $ detector housing
110    0               -12  10  14                              $ void inside housing
120  700   -2.2300     -14 15                                   $ pmt
130    0               -15                                      $ inside of pmt
140  500   -8.0300     -16  17                                  $ base housing
150    0               -17                                      $ void in base
160    0                16  13                                  $ void outside detector
170  800   -1.848      -18                                      $ beryllium
180  800   -1.848      -20                                      $ beryllium
200  100   -1.0320     -19                                      $ scintillator

c    *** Surface Cards ***
1   rcc    -0.3175  0  0  .3175  0  0  1.27                $ outside radius of source
10  rcc    0.3675  0  -3.5675  0 0  6.8175  2.1075         $ polystyrene holder
11  rpp   -0.57875  1.31375  -1.50  1.50  -3.25  3.25      $ polypropylene spacers
12  rcc    0.3675  0  -3.5675 0 0  11.5825   2.1075        $ inside of detector housing
```

```
13  rcc    0.3675  0  -3.8850 0 0  11.9000   2.425          $ outside of detector housing
14  rcc    0.3675  0   8.015  0 0  -4.6      1.875          $ outside of pmt
15  rcc    0.3675  0   8.015  0 0  -4.2825   1.5575         $ inside of pmt
16  rcc    0.3675  0   8.015  0 0   6.5      4.55           $ outside of base
17  rcc    0.3675  0   8.3325 0 0   5.865    4.235          $ inside of base
18  rpp    0  0.3175  -1.50 1.50 -3.25  3.25                $ beryllium layer
19  rpp    0.3175 0.4175 -1.50 1.50 -3.25  3.25             $ scintillator layer
20  rpp    0.4175 0.7350 -1.50 1.50 -3.25  3.25             $ beryllium layer

mode   e p
imp:e 1 8r 0 1 1 1
imp:p 1 8r 0 1 1 1
sdef par=2 x=-0.15875 y=0 z=0  axs=1 0 0 ext = 0 rad=d5 erg=d3
c *** Gamma Energies ***
si3  L  .031817  .032194  .036304  .036378  .037255 .661657
c *** Gamma Branching Ratios ***
sp3  D  1.99 3.64 0.348  0.672  0.213  85.1
si5   0     0.15
sp5   0     1
m100 6000    0.47           $ scintillator
     1001    0.53
     estep 11
m200 6000   -0.625017       $ mylar
     8016   -0.333024
     1001   -0.041959
     estep 12
m300 6000   -0.856289       $ polyethylene
     1000   -0.143711
     estep 12
m400 13027   1              $ aluminum
     estep 6
m500 6000   -0.0008         $ Stainless Steel 304
     25000  -0.0200
     24000  -0.1900
```

```
     28000  -0.1000
     14000  -0.0075
     15000  -0.00045
     16000  -0.0003
     7000   -0.0010
     26000  -0.67995
     estep 10
m600 6000   -.922582        $ polystyrene
     1000   -.077418
     estep 6
m700 5010   -0.007973       $ borosilicate glass rho=2.23 g/cc
     5011   -0.032091
     8016   -0.539562
     11023  -0.028191
     13027  -0.011644
     14000  -0.377220
     19000  -0.003321
m800 4009    1
f8:e,p   200
e8    0  0.001  14i  0.751
prdmp 1e15 1e15 1e15
nps 1e7
```

Cl-36 beta source, case 2 geometry

```
Cl-36 source
c    *** Cell Cards ***
10   100   -1.0320     -9                        $ Scint layer
20   300   -1.0600    -10  9   11  13            $ Polystyrene
30   400   -2.7000    -1  3 -4  5                $ surface of source
40     0              -3  -4  5                  $ void next to scintillator
50   200   -1.4000    -2  -5  6                  $ Mylar window
60   500   -8.0300    -2  -6  7                  $ Stainless Steel backer
```

```
70   400   -2.7000    -2  -7  8                  $ aluminum plug
80   400   -2.7000    -1   2  -5  8              $ aluminum ring
90   600   -0.9000     -11 1  9 13               $ polypropylene spacers
100  500   -8.0300     -12  10                   $ detector housing
110    0               12                        $ void outside poly
120  700   -1.848     -13                        $ beryllium

c    *** Surface Cards ***
1   rcc    -0.3175  0  0  .3175  0  0  1.27      $ outside radius of source
2   cx     1.19                                  $ radius of active region
3   cx     1.02                                  $ inner radius of aluminum ring
4   px     0                                     $ surface of source next to scintillator
5   px    -0.08                                  $ void between scintillator and mylar
6   px    -0.080641                              $ surface of mylar
7   px    -0.10604                               $ surface of ss 304 backing
8   px    -0.3175                                $ surface of aluminum plug
9   rpp    0  0.10  -1.50  1.50  -3.25  3.25     $ scintillator cell
10  rcc    0.05  0  -3.25  0 0  6.5  2           $ polystyrene holder
11  rpp   -0.89625  0.99625  -1.50  1.50  -3.25  3.25    $ polypropylene spacers
12  rcc    0.05  0  -3.5675 0 0  6.8175   2.3175
13  rpp    0.10  0.4175  -1.50  1.50  -3.25  3.25

mode   e p
imp:e 1 9r 0  1
imp:p 1 9r 0  1
sdef par=3 pos= -0.08064001  0  0 axs= 1 0 0 ext= 0 rad=d4 erg=d1
c *** Beta Energy Spectrum ***
si1  A 0 0.0355 0.0709 0.1064 0.1419 0.1774 0.2129 0.2483 0.2838 0.3193 0.3547
       0.3902 0.4257 0.4612 0.4966 0.5321 0.5676 0.6031 0.6386 0.6740 0.7095
C *** Beta Energy Probability ***
sp1    0 5.230E-02 5.812E-02 6.261E-02 6.577E-02 6.798E-02 6.936E-02 6.996E-02
       6.975E-02 6.867E-02 6.657E-02 6.341E-02 5.902E-02 5.337E-02 4.650E-02
       3.857E-02 2.986E-02 2.083E-02 1.222E-02 5.229E-03 8.469E-04
si4    0 1.02
```

```
sp4    0  1
m100 6000    0.47           $ scintillator
     1001    0.53
     estep 11
m200 6000   -0.625017       $ mylar
     8016   -0.333024
     1001   -0.041959
     estep 1228
m300 6000   -0.856289       $ polypropylene
     1000   -0.143711
     estep 6
m400 13027   1              $ aluminum
     estep 6
m500 6000   -0.0008         $ Stainless Steel 304
     25000  -0.0200
     24000  -0.1900
     28000  -0.1000
     14000  -0.0075
     15000  -0.00045
     16000  -0.0003
     7000   -0.0010
     26000  -0.67995
     estep 10
m600 6000   -.922582        $ polystyrene
     1000   -.077418
     estep  6
m700 4009   1
f8:e,p   10
e8    0  0.00001 0.001  14i  0.751
prdmp 1e15 1e15 1e15
nps 1e7
```

Pb-210 beta source, case 3 geometry

```
Pb210 source w/ Bi210 in equilibrium
c    *** Cell Cards ***
10   100   -1.0320     -9             $ Scint layer
20   300   -1.0600    -10  9  11      $ Polystyrene
30   400   -2.7000    -1  3 -4  5     $ surface of source
40     0              -3  -4  5       $ void next to scintillator
50   400   -2.7000    -2  -5  6       $ Mylar window
60   500   -8.0300    -2  -6  7       $ Stainless Steel backer
70   400   -2.7000    -2  -7  8       $ aluminum plug
80   400   -2.7000    -1   2  -5  8   $ aluminum ring
90   600   -0.9000     -11 1  9       $ polypropylene spacers
100  500   -8.0300     -12  10        $ detector housing
110    0               12             $ void outside poly

c    *** Surface Cards ***
1   rcc    -0.3175  0  0  .3175  0  0  1.27         $ outside radius of source
2   cx     1.19                                     $ radius of active region
3   cx     1.02                                     $ inner radius of aluminum ring
4   px     0                                        $ surface of source next to scintillator
5   px    -0.08                                     $ void between scintillator and mylar
6   px    -0.082541                                 $ surface of mylar
7   px    -0.10794                                  $ surface of ss 304 backing
8   px    -0.3175                                   $ surface of aluminum plug
9   rpp    0  0.100  -1.50  1.50  -3.25  3.25       $ scintillator cell
10  rcc    0.250  0  -3.25  0 0  6.5  2             $ polystyrene holder
11  rpp   -0.95  1.05  -1.50  1.50  -3.25  3.25     $ polypropylene spacers
12  rcc    0.250  0  -3.5675 0 0  6.8175   2.3175

mode   e p
imp:e 1 9r 0
```

```
imp:p 1 9r 0
sdef par=3 pos= -0.08254001  0  0 axs= 1 0 0 ext= 0 rad=d4 erg=d1
si1  s 2  3  5
c *** Pb-210 beta, Bi-210 beta and Pb-210 CE branching ratios ***
sp1    100 100 74.58
c *** Pb-210 beta energy spectrum ***
si2  A 0 0.0032 0.0063 0.0095 0.0126 0.0158 0.0189 0.0221 0.0252 0.0284 0.0315
       0.0347 0.0378 0.041 0.0441 0.0473 0.0504 0.0536 0.0567 0.0599 0.063
c *** Pb-210 probability distribution ***
sp2    0 4.02E-01 2.60E-01 1.50E-01 7.26E-02 2.85E-02 1.59E-02 1.38E-02 1.19E-02
       1.02E-02 8.58E-03 7.08E-03 5.72E-03 4.49E-03 3.41E-03 2.46E-03 1.66E-03
       1.02E-03 5.28E-04 1.93E-04 3.13E-05
c *** Bi-210 beta energy spectrum ***
si3  A 0 0.0581 0.1162 0.1742 0.2323 0.2904 0.3484 0.4065 0.4646 0.5227 0.5807
       0.6388 0.6969 0.7550 0.8131 0.8711 0.9292 0.9873 1.0454 1.1034 1.1615
c *** Bi-210 probability distribution ***
sp3    0 7.59E-02 7.96E-02 8.20E-02 8.29E-02 8.25E-02 8.06E-02 7.75E-02 7.32E-02
       6.79E-02 6.17E-02 5.48E-02 4.74E-02 3.97E-02 3.20E-02 2.45E-02 1.75E-02
       1.12E-02 6.16E-03 2.33E-03 4.22E-04
si4    0 1.1
sp4    0 1
c *** Pb-210 Conversion electrons ***
si5  L .0301515  .0425399
sp5  D  60.3  14.28
m100 6000    0.47           $ scintillator
     1001    0.53
     estep 6
m200 6000   -0.625017       $ mylar
     8016   -0.333024
     1001   -0.041959
     estep 625
m300 6000   -0.856289       $ polyethylene
```

```
     1000   -0.143711
     estep 3
m400 13027   1               $ aluminum
     estep 3
m500 6000   -0.0008          $ Stainless Steel 304
     25000      -0.0200
     24000  -0.1900
     28000  -0.1000
     14000  -0.0075
     15000  -0.00045
     16000  -0.0003
     7000   -0.0010
     26000  -0.67995
     estep 5
m600 6000   -.922582        $ polystyrene
     1000   -.077418
     estep 6
f8:e,p   10
e8    0  0.00001 0.001  24i  1.251
prdmp 1e15 1e15 1e15
nps 1e7
```

Pb-210 gamma source, case 3 geometry

```
Pb210 source w/ Bi210 in equilibrium
c    *** Cell Cards ***
10   100   -1.0320     -9             $ Scint layer
20   300   -1.0600    -10  9  11      $ Polystyrene
30   400   -2.7000    -1  3 -4  5     $ surface of source
40     0              -3  -4  5       $ void next to scintillator
50   400   -2.7000    -2  -5  6       $ Mylar window
```

```
60   500   -8.0300    -2  -6  7       $ Stainless Steel backer
70   400   -2.7000    -2  -7  8       $ aluminum plug
80   400   -2.7000    -1   2  -5  8   $ aluminum ring
90   600   -0.9000     -11 1  9       $ polypropylene spacers
100  500   -8.0300     -12  10        $ detector housing
110    0               12             $ void outside poly

c    *** Surface Cards ***
1   rcc    -0.3175  0  0  .3175  0  0  1.27        $ outside radius of source
2   cx     1.19                                    $ radius of active region
3   cx     1.02                                    $ inner radius of aluminum ring
4   px     0                                       $ surface of source next to scintillator
5   px    -0.08                                    $ void between scintillator and mylar
6   px    -0.082541                                $ surface of mylar
7   px    -0.10794                                 $ surface of ss 304 backing
8   px    -0.3175                                  $ surface of aluminum plug
9   rpp    0  0.100  -1.50  1.50  -3.25  3.25      $ scintillator cell
10  rcc    0.250  0  -3.25  0 0  6.5  2            $ polystyrene holder
11  rpp   -0.95  1.05  -1.50  1.50  -3.25  3.25    $ polypropylene spacers
12  rcc    0.250  0  -3.5675 0 0  6.8175   2.3175

mode   e p
imp:e 1 9r 0
imp:p 1 9r 0
sdef par=2 pos= -0.08254001  0  0 axs= 1 0 0 ext= 0 rad=d4 erg=d1
c *** x-ray energies ***
si1  L  .0108  .046539
c *** x-ray branching ratios ***
sp1  D   23.6  4.25
si4    0 1.1
sp4    0 1
m100 6000    0.47                $ scintillator
```

```
     1001    0.53
     estep 6
m200 6000   -0.625017       $ mylar
     8016   -0.333024
     1001   -0.041959
     estep 625
m300 6000   -0.856289       $ polyethylene
     1000   -0.143711
     estep 3
m400 13027   1              $ aluminum
     estep 3
m500 6000   -0.0008         $ Stainless Steel 304
     25000      -0.0200
     24000  -0.1900
     28000  -0.1000
     14000  -0.0075
     15000  -0.00045
     16000  -0.0003
     7000   -0.0010
     26000  -0.67995
     estep 5
m600 6000   -.922582        $ polystyrene
     1000   -.077418
     estep 6
f8:e,p   10
e8    0  0.00001 0.001  24i  1.251
prdmp 1e15 1e15 1e15
nps 1e7
```

Sr-90 beta source in top location, case 4 geometry

```
Sr90 source
c    *** Cell Cards ***
1    100   -1.0320    -9             $ Scint layer
20   300   -1.0600    -10  9  11     $ Polystyrene
30   400   -2.7000    -1  3 -4  5    $ surface of source
40     0              -3  -4  5      $ void next to scintillator
50   200   -1.4000    -2  -5  6      $ Mylar window
60   500   -8.0300    -2  -6  7      $ Stainless Steel backer
70   400   -2.7000    -2  -7  8      $ aluminum plug
80   400   -2.7000    -1   2  -5  8  $ aluminum ring
90   600   -0.9000     -11 1  18     $ polypropylene spacers
100  500   -8.0300     -13  12       $ detector housing
110    0               -12  10  14   $ void inside housing
120  700   -2.2300     -14 15        $ pmt
130    0               -15           $ inside of pmt
140  500   -8.0300     -16  17       $ base housing
150    0               -17           $ void in base
160    0                16  13       $ void outside detector
170  200   -1.4      -18  9          $ mylar

c    *** Surface Cards ***
1   rcc    -0.3175  0  1.88  .3175  0  0  1.27            $ outside radius of source
2   c/x     0 1.88 1.19                                   $ radius of active region
3   c/x     0 1.88 1.02                                   $ inner radius of aluminum ring
4   px     0                                              $ surface of source next to scintillator
5   px    -0.08                                           $ void between scintillator and mylar
6   px    -0.08064287                                          $ surface of mylar
7   px    -0.10604                                             $ surface of ss 304 backing
8   px    -0.3175                                              $ surface of aluminum plug
9   rpp     0.00192861  0.10192861  -1.50  1.50  -3.25  3.25   $ scintillator cell
```

```
10  rcc    0.0135  0  -3.5675  0 0  6.8175  2.1075            $ polystyrene holder
11  rpp   -0.93275  0.95975  -1.50  1.50  -3.25  3.25         $ polypropylene spacers
12  rcc    0.0135  0  -3.5675 0 0  11.5825   2.1075           $ inside of detector housing
13  rcc    0.0135  0  -3.8850 0 0  11.9000   2.425             $ outside of detector housing
14  rcc    0.0135  0   8.015  0 0  -4.6      1.875             $ outside of pmt
15  rcc    0.0135  0   8.015  0 0  -4.2825   1.5575            $ inside of pmt
16  rcc    0.0135  0   8.015  0 0   6.5      4.55              $ outside of base
17  rcc    0.0135  0   8.3325 0 0   5.865    4.235             $ inside of base
18  rpp    0     0.10385722  -1.50 1.50 -3.25   3.25           $ mylar

mode   e p
imp:e 1 14r 0 1
imp:p 1 14r 0 1
sdef par=3 pos= -0.08064286  0  1.88  erg=d1 axs= 1 0 0 ext= 0 rad=d4
si1  s 2    3
sp1    1    1                                        $ sr-90 and yr-90
c *** Sr-90 beta energy spectrum ***
si2  A 0 0.0273 0.0546 0.0819 0.1092 0.1365 0.1638 0.1911 0.2184 0.2457 0.2730
     0.3003 0.3276 0.3549 0.3822 0.4095 0.4368 0.4641 0.4914 0.5187 0.5460
c *** Sr-90 probability distribution ***
sp2  0 7.79E-02 7.60E-02 7.50E-02 7.40E-02 7.30E-02 7.17E-02 7.01E-02 6.80E-02
     6.53E-02 6.19E-02 5.78E-02 5.27E-02 4.68E-02 4.01E-02 3.27E-02 2.48E-02
     1.71E-02 9.75E-03 4.28E-03 1.01E-03
c *** Y-90 beta energy spectrum ***
si3  A 0 0.1142 0.2284 0.3426 0.4568 0.5710 0.6852 0.7994 0.9136 1.0278
     1.1420 1.2562 1.3704 1.4846 1.5988 1.7130 1.8272 1.9414 2.0556
     2.1698 2.2840
c *** Y-90 probability distribution ***
sp3  0 4.26E-02 5.18E-02 5.94E-02 6.50E-02 6.87E-02 7.08E-02 7.17E-02 7.15E-02
     7.04E-02 6.85E-02 6.57E-02 6.19E-02 5.69E-02 5.07E-02 4.30E-02 3.42E-02
     2.46E-02 1.50E-02 6.43E-03 1.13E-03
si4    0 1.1
```

```
sp4    0  1
m100 6000    0.47           $ scintillator
     1001    0.53
     estep 11
m200 6000   -0.625017       $ mylar
     8016   -0.333024
     1001   -0.041959
     estep 1228
m300 6000   -0.856289       $ polypropylene
     1000   -0.143711
     estep 6
m400 13027   1              $ aluminum
     estep 6
m500 6000   -0.0008          $ Stainless Steel 304
     25000  -0.0200
     24000  -0.1900
     28000  -0.1000
     14000  -0.0075
     15000  -0.00045
     16000  -0.0003
     7000   -0.0010
     26000  -0.67995
     estep 10
m600 6000   -.922582         $ polystyrene
     1000   -.077418
     estep  6
m700 4009   1
f8:e,p   1
e8    0   0.00001 0.001  45i  2.301
prdmp 1e15 1e15 1e15
nps 1e6
```

Co-60 gamma source, case 3 geometry, ¼ mm scintillator

```
Co60 source
c    *** Cell Cards ***
10   100   -1.0320     -9                $ Scint layer
20   300   -1.0600     -10  9  11        $ Polystyrene
30   200   -1.4000    -1                 $ surface of source
90   600   -0.9000     -11 1  9          $ polypropylene spacers
100  500   -8.0300     -13  12           $ detector housing
110    0               -12  10  14       $ void inside housing
120  700   -2.2300     -14 15            $ pmt
130    0               -15               $ inside of pmt
140  500   -8.0300     -16  17           $ base housing
150    0               -17               $ void in base
160    0                16  13           $ void outside detector

c    *** Surface Cards ***
1   rcc    -0.3175  0  0  .3175  0  0  1.27              $ outside radius of source
9   rpp     0  0.025  -1.50  1.50  -3.25  3.25           $ scintillator cell
10  rcc    0.0125  0  -3.5675  0 0  6.8175  2.1075       $ polystyrene holder
11  rpp   -0.93375  0.95875  -1.50  1.50  -3.25  3.25    $ polypropylene spacers
12  rcc    0.0125  0  -3.5675 0 0  11.5825   2.1075      $ inside of detector housing
13  rcc    0.0125  0  -3.8850 0 0  11.9000   2.425       $ outside of detector housing
14  rcc    0.0125  0   8.015  0 0  -4.6      1.875       $ outside of pmt
15  rcc    0.0125  0   8.015  0 0  -4.2825   1.5575      $ inside of pmt
16  rcc    0.0125  0   8.015  0 0   6.5      4.55        $ outside of base
17  rcc    0.0125  0   8.3325 0 0   5.865    4.235       $ inside of base

mode   e p
imp:e 1 9r 0 1
imp:p 1 9r 0 1
sdef par=2 x=-0.15875 y=0 z=0  axs=1 0 0 rad=d3 erg=d1
```

```
c *** gamma energies ***
si1  L .007461  .007478  .008265  .34714  .82610  1.173228  1.332492  2.15857
c *** gamma branching ratios ***
sp1  D .00322  .0063  .001151  .0075  .0076  99.85  99.9826  .00120
si3   0     0.15
sp3   0     1
m100 6000    0.47           $ scintillator
     1001    0.53
     estep 11
m200 6000   -0.625017       $ mylar
     8016   -0.333024
     1001   -0.041959
     estep 12
m300 6000   -0.856289       $ polyethylene
     1000   -0.143711
     estep 12
m400 82000    1             $ lead
m500 6000   -0.0008          $ Stainless Steel 304
     25000  -0.0200
     24000  -0.1900
     28000  -0.1000
     14000  -0.0075
     15000  -0.00045
     16000  -0.0003
     7000   -0.0010
     26000  -0.67995
     estep 10
m600 6000   -.922582        $ polystyrene
     1000   -.077418
     estep 6
m700 5010   -0.007973       $ borosilicate glass rho=2.23 g/cc
     5011   -0.032091
```

```
     8016   -0.539562
     11023  -0.028191
     13027  -0.011644
     14000  -0.377220
     19000  -0.003321
m800 4009    1
f8:e,p   10
e8    0  0.001  27i  1.401
prdmp 1e15 1e15 1e15
nps 1e7
```

Co-60 beta source, case 3 geometry, ¼ mm scintillator

```
Co60 source
c    *** Cell Cards ***
10   100   -1.0320     -9                $ Scint layer
20   300   -1.0600     -10  9  11        $ Polystyrene
30   200   -1.4000    -1                 $ surface of source
90   600   -0.9000     -11 1  9          $ polypropylene spacers
100  500   -8.0300     -13  12           $ detector housing
110    0               -12  10  14       $ void inside housing
120  700   -2.2300     -14 15            $ pmt
130    0               -15               $ inside of pmt
140  500   -8.0300     -16  17           $ base housing
150    0               -17               $ void in base
160    0                16  13           $ void outside detector

c    *** Surface Cards ***
1   rcc    -0.3175  0  0  .3175  0  0  1.27              $ outside radius of source
9   rpp     0  0.025  -1.50  1.50  -3.25  3.25          $ scintillator cell
10  rcc    0.0125  0  -3.5675  0 0  6.8175  2.1075       $ polystyrene holder
```

```
11  rpp   -0.93375  0.95875  -1.50  1.50  -3.25  3.25    $ polypropylene spacers
12  rcc    0.0125  0  -3.5675 0 0  11.5825   2.1075      $ inside of detector housing
13  rcc    0.0125  0  -3.8850 0 0  11.9000   2.425       $ outside of detector housing
14  rcc    0.0125  0   8.015  0 0  -4.6      1.875       $ outside of pmt
15  rcc    0.0125  0   8.015  0 0  -4.2825   1.5575      $ inside of pmt
16  rcc    0.0125  0   8.015  0 0   6.5      4.55        $ outside of base
17  rcc    0.0125  0   8.3325 0 0   5.865    4.235       $ inside of base

mode   e p
imp:e 1 9r 0
imp:p 1 9r 0
sdef par=3 x=-0.15875 y=0 z=0  erg=d3  rad=d4
si3   S  1  2
sp3      1  2.8921e-4
c *** Conversion electrons ***
si2   L 1.164895  1.172220  1.324159  1.331484
c *** Branching ratios ***
sp2   D .01498  .001463  .01137  .001108
c *** beta energy spectrum ***
si1   A 0.0746 0.1491 0.2237 0.2982 0.3728 0.4473 0.5219 0.5964 0.6710 0.7455
       0.8201 0.8947 0.9692 1.0438 1.1183 1.1929 1.2674 1.3420 1.4165 1.4911
c *** probability distribution ***
sp1    4.45E-01 3.30E-01 1.78E-01 4.58E-02 6.36E-04 5.99E-05 5.96E-05 5.77E-05
       5.54E-05 5.40E-05 5.23E-05 4.99E-05 4.66E-05 4.24E-05 3.71E-05 3.06E-05
       2.31E-05 1.47E-05 6.66E-06 1.57E-06
si4   0     .15
sp4   0     1
m100 6000    0.47           $ scintillator
     1001    0.53
     estep 11
m200 6000   -0.625017       $ mylar
     8016   -0.333024
```

```
     1001   -0.041959
     estep 12
m300 6000   -0.856289       $ polyethylene
     1000   -0.143711
     estep 12
m400 13027   1              $ aluminum
     estep 6
m500 6000   -0.0008         $ Stainless Steel 304
     25000  -0.0200
     24000  -0.1900
     28000  -0.1000
     14000  -0.0075
     15000  -0.00045
     16000  -0.0003
     7000   -0.0010
     26000  -0.67995
     estep 10
m600 6000   -.922582        $ polystyrene
     1000   -.077418
     estep 6
m700 5010   -0.007973       $ borosilicate glass rho=2.23 g/cc
     5011   -0.032091
     8016   -0.539562
     11023  -0.028191
     13027  -0.011644
     14000  -0.377220
     19000  -0.003321
m800 4009    1
f8:e,p   10
e8    0  0.001  27i  1.401
prdmp 1e15 1e15 1e15
nps 1e7
```

Sr-90 beta source, case 3 geometry, ½ mm scintillator, bottom location

```
Sr90 source
c    *** Cell Cards ***
1    100   -1.0320    -9              $ Scint layer
20   300   -1.0600    -10  9  11      $ Polystyrene
30   400   -2.7000    -1  3 -4  5     $ surface of source
40     0              -3  -4  5       $ void next to scintillator
50   200   -1.4000    -2  -5  6       $ Mylar window
60   500   -8.0300    -2  -6  7       $ Stainless Steel backer
70   400   -2.7000    -2  -7  8       $ aluminum plug
80   400   -2.7000    -1   2  -5  8   $ aluminum ring
90   600   -0.9000     -11 1  18      $ polypropylene spacers
100  500   -8.0300     -13  12        $ detector housing
110    0               -12  10  14    $ void inside housing
120  700   -2.2300     -14 15         $ pmt
130    0               -15            $ inside of pmt
140  500   -8.0300     -16  17        $ base housing
150    0               -17            $ void in base
160    0                16  13        $ void outside detector
170  100   -1.032      -18  9         $ paper spacer

c    *** Surface Cards ***
1   rcc    -0.3175  0  -1.88  .3175  0  0  1.27     $ outside radius of source
2   c/x     0 -1.88 1.19                             $ radius of active region
3   c/x     0 -1.88 1.02                             $ inner radius of aluminum ring
4   px     0                                         $ surface of source next to scintillator
5   px    -0.08                                      $ void between scintillator and mylar
6   px    -0.08064287                                $ surface of mylar
7   px    -0.10604                                   $ surface of ss 304 backing
8   px    -0.3175                                    $ surface of aluminum plug
9   rpp     0.00064287  0.05064287  -1.50  1.50  -3.25  3.25     $ scintillator cell
```

```
10  rcc    0.0135  0  -3.5675  0 0  6.8175  2.1075              $ polystyrene holder
11  rpp   -0.93275  0.95975  -1.50  1.50  -3.25  3.25           $ polypropylene spacers
12  rcc    0.0135  0  -3.5675 0 0  11.5825   2.1075             $ inside of detector housing
13  rcc    0.0135  0  -3.8850 0 0  11.9000   2.425              $ outside of detector housing
14  rcc    0.0135  0   8.015  0 0  -4.6      1.875              $ outside of pmt
15  rcc    0.0135  0   8.015  0 0  -4.2825   1.5575             $ inside of pmt
16  rcc    0.0135  0   8.015  0 0   6.5      4.55               $ outside of base
17  rcc    0.0135  0   8.3325 0 0   5.865    4.235              $ inside of base
18  rpp    0     0.05128574  -1.50 1.50 -3.25   3.25            $ paper spacer

mode   e p
imp:e 1 14r 0 1
imp:p 1 14r 0 1
sdef par=3 pos= -0.08064286  0  -1.88  erg=d1 axs= 1 0 0 ext= 0 rad=d4
si1  s 2    3
sp1    1    1                                        $ sr-90 and yr-90
c *** Sr-90 beta energy spectrum ***
si2  A 0 0.0273 0.0546 0.0819 0.1092 0.1365 0.1638 0.1911 0.2184 0.2457 0.2730
     0.3003 0.3276 0.3549 0.3822 0.4095 0.4368 0.4641 0.4914 0.5187 0.5460
c *** Sr-90 probability distribution ***
sp2  0 7.79E-02 7.60E-02 7.50E-02 7.40E-02 7.30E-02 7.17E-02 7.01E-02 6.80E-02
     6.53E-02 6.19E-02 5.78E-02 5.27E-02 4.68E-02 4.01E-02 3.27E-02 2.48E-02
     1.71E-02 9.75E-03 4.28E-03 1.01E-03
c *** Y-90 beta energy spectrum ***
si3  A 0 0.1142 0.2284 0.3426 0.4568 0.5710 0.6852 0.7994 0.9136 1.0278
     1.1420 1.2562 1.3704 1.4846 1.5988 1.7130 1.8272 1.9414 2.0556
     2.1698 2.2840
c *** Y-90 probability distribution ***
sp3  0 4.26E-02 5.18E-02 5.94E-02 6.50E-02 6.87E-02 7.08E-02 7.17E-02 7.15E-02
     7.04E-02 6.85E-02 6.57E-02 6.19E-02 5.69E-02 5.07E-02 4.30E-02 3.42E-02
     2.46E-02 1.50E-02 6.43E-03 1.13E-03
si4    0 1.1
```

```
sp4    0  1
m100 6000    0.47           $ scintillator
     1001    0.53
     estep 11
m200 6000   -0.625017       $ mylar
     8016   -0.333024
     1001   -0.041959
     estep 1228
m300 6000   -0.856289       $ polypropylene
     1000   -0.143711
     estep 6
m400 13027   1              $ aluminum
     estep 6
m500 6000   -0.0008         $ Stainless Steel 304
     25000  -0.0200
     24000  -0.1900
     28000  -0.1000
     14000  -0.0075
     15000  -0.00045
     16000  -0.0003
     7000   -0.0010
     26000  -0.67995
     estep 10
m600 6000   -.922582       $ polystyrene
     1000   -.077418
     estep  6
m700 4009   1
f8:e,p   1
e8    0   0.00001 0.001  45i  2.301
prdmp 1e15 1e15 1e15
nps 5e6
```

Co-60 gamma source, BLC Geometry

```
Co60 source
c    *** Cell Cards ***
10   100   -1.0320     -9                                $ Scint layer
20   300   -1.0600     -10   11                         $ Polystyrene
30   200   -1.4000    -1                                 $ surface of source
90   600   -0.9000     -11   9 19 21 23 18 20 22 1       $ polypropylene spacers
100  500   -8.0300     -13  12                           $ detector housing
110    0               -12  10  14                       $ void inside housing
120  700   -2.2300     -14 15                            $ pmt
130    0               -15                               $ inside of pmt
140  500   -8.0300     -16  17                           $ base housing
150    0               -17                               $ void in base
160    0                16  13  -24                      $ void outside detector
170  100   -1.032      -19       $ scintillator
180  100   -1.032      -21       $ scintillator
190  100   -1.032      -23       $ scintillator
200  800   -1.848      -18       $ beryllium
210  800   -1.848      -20       $ beryllium
220  800   -1.848      -22       $ beryllium
230    0                24

c    *** Surface Cards ***
1   rcc    -0.3175  0  0  0.3175  0  0   1.27              $ outside radius of source
9   rpp     0  0.10  -1.50  1.50  -3.25  3.25              $ scintillator cell
10  rcc    0.67625  0  -3.5675  0 0  6.8175  2.1075        $ polystyrene holder
11  rpp   -0.32  1.5725  -1.50  1.50  -3.25  3.25          $ polypropylene spacers
12  rcc    0.67625  0  -3.5675 0 0  11.5825   2.1075       $ inside of detector housing
13  rcc    0.67625  0  -3.8850 0 0  11.9000   2.425        $ outside of detector housing
14  rcc    0.67625  0   8.015  0 0  -4.6      1.875        $ outside of pmt
15  rcc    0.67625  0   8.015  0 0  -4.2825   1.5575       $ inside of pmt
```

```
16  rcc    0.67625  0   8.015  0 0   6.5      4.55          $ outside of base
17  rcc    0.67625  0   8.3325 0 0   5.865    4.235         $ inside of base
18  rpp    0.10   0.4175 -1.50 1.50 -3.25  3.25             $ layers
19  rpp    0.4175 0.5175 -1.50 1.50 -3.25  3.25
20  rpp    0.5175 0.8350 -1.50 1.50 -3.25  3.25
21  rpp    0.8350 0.9350 -1.50 1.50 -3.25  3.25
22  rpp    0.9350 1.2525 -1.50 1.50 -3.25  3.25
23  rpp    1.2525 1.3525 -1.50 1.50 -3.25  3.25
24  rcc    0.67625  0  -4.25  0  0  19.0  5.00

mode   e p
imp:e 1 16r  0
imp:p 1 16r  0
sdef par=2 x=-0.15875 y=0 z=0  axs=1 0 0 rad=d3 erg=d1
c *** gamma energies ***
si1  L .007461  .007478  .008265  .34714  .82610  1.173228  1.332492  2.15857
c *** gamma branching ratios ***
sp1  D .00322  .0063  .001151  .0075  .0076  99.85  99.9826  .00120
si3   0     0.15
sp3   0     1
m100 6000    0.47           $ scintillator
     1001    0.53
     estep 11
m200 6000   -0.625017       $ mylar
     8016   -0.333024
     1001   -0.041959
     estep 12
m300 6000   -0.856289       $ polyethylene
     1000   -0.143711
     estep 12
m400 13027   1              $ aluminum
     estep 6
```

```
m500 6000   -0.0008          $ Stainless Steel 304
     25000  -0.0200
     24000  -0.1900
     28000  -0.1000
     14000  -0.0075
     15000  -0.00045
     16000  -0.0003
     7000   -0.0010
     26000  -0.67995
     estep 10
m600 6000   -.922582         $ polystyrene
     1000   -.077418
     estep 6
m700 5010   -0.007973        $ borosilicate glass rho=2.23 g/cc
     5011   -0.032091
     8016   -0.539562
     11023  -0.028191
     13027  -0.011644
     14000  -0.377220
     19000  -0.003321
m800 4009    1
f8:e,p   10 170 180 190 t
e8    0  0.001  27i  1.401
f4:p  10 170 180 190
prdmp 1e15 1e15 1e15
nps 1e6
```

Detector #2

Co-60 gamma source, BLC geometry, 3.175 mm scintillator

```
c    *** Detector Cell Cards ***
1   400  -8.03     -2  1                                  $ Housing
2   200  -8.03     -1  -3                                 $ SS Layer
3   600  -0.178    -1  3  -4                              $ Cardboard
4   100  -1.848    -1  4  -5                              $ Beryllium
5   200  -1.032    -1  5  -6                              $ scintillator
6   100  -1.848    -1  6  -7                              $ Beryllium
7   200  -1.032    -1  7  -8                              $ scintillator
8   100  -1.848    -1  8  -9                              $ Beryllium
9   200  -1.032    -1  9  -10                             $ scintillator
10   100  -1.848    -1  10 -11                            $ Beryllium
11   200  -1.032    -1  11 -12                            $ scintillator
12   100  -1.848    -1  12 -13                            $ Beryllium
13   200  -1.032    -1  13 -14                            $ scintillator
14   100  -1.848    -1  14 -15                            $ Beryllium
15   200  -1.032    -1  15 -16                            $ scintillator
16   100  -1.848    -1  16 -17                            $ Beryllium
17   200  -1.032    -1  17 -18                            $ scintillator
18   100  -1.848    -1  18 -19                            $ Beryllium
19   200  -1.032    -1  19 -20                            $ scintillator
20   100  -1.848    -1  20 -21                            $ Beryllium
21   200  -1.032    -1  21 -22                            $ scintillator
22   100  -1.848    -1  22 -23                            $ Beryllium
23   200  -1.032    -1  23 -24                            $ scintillator
24   100  -1.848    -1  24 -25                            $ Beryllium
25   600  -0.178    -1  25 -26                            $ Cardboard
26   400  -8.03     -1 26                                 $ SS Layer
```

```
27   400  -8.03    -27  28                                $ flange
28   400  -8.03    -28 29                                 $ PMT wall
29     0           -29                                    $ void in PMT
30   500  -1.4     -30
31     0            1 27 28 30

c    *** Detector Surface Cards ***
1     rpp -8.89  8.89  0  14.9225  -8.255   7.9375            $ outside detector surface
2     rpp -7.9375  7.9375  0.635 14.2875  -7.9375  7.9375     $ inside detector surface
3     py   1.11125
4     py 2.38125
5     py 3.01625
6     py 3.33375
7     py 3.96875
8     py 4.28625
9     py 4.92125
10    py 5.23875
11    py 5.87375
12    py 6.19125
13    py 6.82625
14    py 7.14375
15    py 7.77875
16    py 8.09625
17    py 8.73125
18    py 9.04875
19    py 9.68375
20    py 10.00125
21    py 10.63625
22    py 10.95375
23    py 11.58875
24    py 11.90625
25    py 12.54125
```

```
26    py   13.81125
27    rpp -8.89  8.89  -.9525 15.875   7.9375  8.5725              $ flange
28    rcc  0  7.46125  7.9375  0  0  33.3375   8.4138              $ outside of PMT
29    rcc  0  7.46125  7.9375  0  0  33.0200    8.0963             $ inside of PMT
30    rcc  0  0  0  0 -0.3175 0 1.27                               $ source

mode   e p
imp:e 1 27r 0 1 0
imp:p 1 27r 0 1 0
sdef par=2 x= 0 y = -0.15875 z=0  axs=0 1 0 ext=0 rad=d3 erg=d1 vec=0 1 0
     dir = d4
c *** gamma energies ***
si1  L .007461  .007478  .008265  .34714  .82610  1.173228  1.332492  2.15857
c *** gamma branching ratios ***
sp1  D .00322  .0063  .001151  .0075  .0076  99.85  99.9826  .00120
si3   0     0.15
sp3   0     1
si4   0   1
sp4   0   1
m100 4009 1                  $ Beryllium rho=1.848 g/cc
m200 6000  0.47              $ BC-404, rho=1.032 g/cc
     1001  0.53
m300 13027 1                 $ Aluminum, rho=2.7 g/cc
m400 6000   -0.0008          $ Stainless Steel 304 rho=8.03 g/cc
     25055      -0.0200
     24000  -0.1900
     28000  -0.1000
     14000  -0.0075
     15031  -0.00045
     16000  -0.0003
     7014   -0.0010
     26000  -0.67995
```

```
m500 6000   -0.625017        $ mylar
     8016   -0.333024
     1001   -0.041959
m600 6000   -0.50            $ cardboard from 1984 forestry pub.
     8016   -0.44
     1001   -0.06
f8:e,p  5 7 9 11 13 15 17 19 21 23 t
e8    0  0.001  27i  1.401
prdmp 1e15 1e15 1e15
nps 1e7
```

Cs-137 gamma source, single layer geometry, ¼ mm scintillator

```
c    *** Detector Cell Cards ***
10   400  -8.03    -2 1                        $ Housing
11   200  -8.03    -1 -3                       $ SS Layer
14   600  -0.178    -1 3 -4                    $ Cardboard
15   100  -1.848     -1 4 -5                   $ Beryllium
16   200  -1.032    -1 5 -6                    $ scintillator
17   100  -1.848    -1 6 -7                    $ Beryllium
18   600  -0.178    -1 7 -8                    $ Cardboard
19   400  -8.03     -1 8                       $ SS Layer
20   400  -8.03    -9  10                      $ flange
21   400  -8.03    -10 11                      $ PMT wall
22     0           -11                         $ void in PMT
23   500  -1.4     -12                         $ source
50     0            1 9 10 12

c    *** Detector Surface Cards ***
1     rpp -8.89  8.89  0  14.9225  -8.255   7.9375            $ outside detector surface
```

```
2     rpp -7.9375  7.9375  0.635 14.2875  -7.9375  7.9375     $ inside detector surface
3     py   1.11125
4     py   4.27375
5     py   7.44875
6     py   7.47375
7     py   11.28375
8     py   13.81125
9     rpp -8.89  8.89  -.9525 15.875   7.9375  8.5725          $ flange
10    rcc  0  7.46125  7.9375  0  0  33.3375   8.4138          $ outside of PMT
11    rcc  0  7.46125  7.9375  0  0  33.0200    8.0963         $ inside of PMT
12    rcc  0  0  0  0 -0.00677 0 1.27                          $ source

mode   e p
imp:e 1 9r 0 1 0
imp:p 1 9r 0 1 0
sdef par=2 x= 0 y = -0.003385 z=0  axs=0 1 0 ext=0 rad=d3 erg=d1 vec=0 1 0
     dir = d4
c *** gamma energies ***
si1  L  .031817  .032194  .036304  .036378  .037255 .661657
c *** branching ratios ***
sp1  D  1.99 3.64 0.348  0.672  0.213  85.1
si3   0     0.15
sp3   0     1
si4   0   1
sp4   0   1
m100 4009 1                    $ Beryllium rho=1.848 g/cc
m200 6000  0.47                $ BC-404, rho=1.032 g/cc
     1001  0.53
m300 13027 1                   $ Aluminum, rho=2.7 g/cc
m400 6000   -0.0008            $ Stainless Steel 304 rho=8.03 g/cc
     25055      -0.0200
     24000  -0.1900
```

```
     28000  -0.1000
     14000  -0.0075
     15031  -0.00045
     16000  -0.0003
     7014   -0.0010
     26000  -0.67995
m500 6000   -0.625017          $ mylar
     8016   -0.333024
     1001   -0.041959
m600 6000   -0.50              $ cardboard from 1984 forestry pub.
     8016   -0.44
     1001   -0.06
f8:e,p   16
e8    0  0.001  27i  1.401
prdmp 1e15 1e15 1e15
nps 1e7
```

Neutron Source, Validation Experiment, BLC Geometry, 3.175 mm scintillator

```
Big Beryllium Detector with target chamber and stand
c    *** Detector Cell Cards ***
101   400  -8.03     -101  102                    $ Housing
102   400  -8.03     -102  -103                   $ SS Layer
103   600  -0.178    -102  103  -104              $ Cardboard
104   100  -1.848    -102  104  -105              $ Beryllium
105   200  -1.032    -102  105  -106              $ scintillator
106   100  -1.848    -102  106  -107              $ Beryllium
107   200  -1.032    -102  107  -108              $ scintillator
108   100  -1.848    -102  108  -109              $ Beryllium
109   200  -1.032    -102  109  -110              $ scintillator
110   100  -1.848    -102  110 -111               $ Beryllium
111   200  -1.032    -102  111 -112               $ scintillator
```

```
112   100  -1.848    -102  112 -113                $ Beryllium
113   200  -1.032    -102  113 -114                $ scintillator
114   100  -1.848    -102  114 -115                $ Beryllium
115   200  -1.032    -102  115 -116                $ scintillator
116   100  -1.848    -102  116 -117                $ Beryllium
117   200  -1.032    -102  117 -118                $ scintillator
118   100  -1.848    -102  118 -119                $ Beryllium
119   200  -1.032    -102  119 -120                $ scintillator
120   100  -1.848    -102  120 -121                $ Beryllium
121   200  -1.032    -102  121 -122                $ scintillator
122   100  -1.848    -102  122 -123                $ Beryllium
123   200  -1.032    -102  123 -124                $ scintillator
124   100  -1.848    -102  124 -125                $ Beryllium
125   600  -0.178    -102  125 -126                $ Cardboard
126   400  -8.03     -102 126                      $ SS Layer
127   400  -8.03    -127  128                      $ flange
128   400  -8.03    -128 129                       $ PMT wall
129     0           -129                           $ void in PMT
c   *** Top Stand Cell Cards ***
20   400  -8.03     10  -13  14  -15  -16  17            $ Top plate
21   400  -8.03     10  -13  14  -15  -21  22            $ Bottom plate
22   400  -8.03     10  -11  14  -15  -17  18            $ Top hinge (1)
23   400  -8.03     12  -13  14  -15  -17  18            $ Top hinge (2)
24   400  -8.03     10  -11  14  -15  -20  21            $ Bottom hinge (1)
25   400  -8.03     12  -13  14  -15  -20  21            $ Bottom hinge (2)
26   400  -8.03     11  -12  -17  19  -23  24            $ Front support-top
27   400  -8.03     11  -12  -19  21  -25  26            $ Front support-bot
28   400  -8.03    -27   28  -38  -18  19  31            $ Side support-front-top
29   400  -8.03    -29   30  -38  -19  20  31            $ Side support-front-bottom
30   400  -8.03     32  -33  -38  -18  19  31            $ Side support-front-top
31   400  -8.03     34  -35  -38  -19  20  31            $ Side support-front-bottom
32   400  -8.03    -36                                   $ front bolt
33   400  -8.03    -37                                   $ back bolt
34    0          -10 -16 22 14 -15 -47                   $ void left
```

```
35    0           13 -16 22 14 -15 39 -47                 $ void right
36    0          -14 -16 22 -47                           $ void front
37    0           15 -16 22 41 42 -47                     $ void back
38    0           16 101 127 128 -47                      $ void top
39    0          -22 40 41 42 43 44 45 46 -47             $ void bottom
40    0           (14 -31 10 -11 -18 20 36 37):(-38 31 -32 -34 10 36 37)  $ void left
41    0           (14 -31 12 -13 -18 20 36 37):(-38 31 27 29 -13 36 37)   $ void right
42    0           (11 -12 14 -17 19 -24):(11 -12 14 -19 21 -26)           $ void center front
43    0           (11 -12 -31 23 -17 19 36):(11 -12 -31 25 -19 21 36)     $ void center
44    0 (31 -38 -19 21 -12 11 -30 35  37):(-17 19 31 -38 -12 11 -28 33 37)  $ void center back
45    0 38 -15 37 11 -12 -17 21:38 -15 10 -11 -18 20 37:38 -15 12 -13 -18 20 37 $ void back
46   300 -2.7  -39                                        $ knob
c    *** Plate below lower stand cell cards ***
47   300 -2.7  -40                                        $ plate
48   300 -2.7  -41                                        $ knob spacer
49   300 -2.7  -42                                        $ knob
c    *** Stand Base plate cell cards ***
50   300 -2.7  -43                                        $ base plate
51   300 -2.7  -44                                        $ knob spacer
52   300 -2.7  -45                                        $ knob
53   300 -2.7  -46                                        $ pole
c    *** Target chamber cell cards ***
54   300 -2.7  -50  51 56 58 60                           $ vacuum chamber outer wall
55     0        -51 62                                    $ Vacuum chamber
56   300 -2.7   -52                                       $ Upper flange
57   400  -8.03   -53                                     $ Upper hardware
58   300 -2.7   -54                                       $ Lower chamber dial
59   300 -2.7   -55                                       $ Sample holder
60     0        -57 51                                    $ Inside beam line
61   300 -2.7   -56 57 51                                 $ beam line tube
62   300 -2.7   -58 59 56 51                              $ 165 SBD
63     0         -59 56 51                                $ 165 SBD inside
64   300 -2.7    -60 61 51                                $ 110 SBD
65     0         -61 51                                   $ 110 SBD inside
```

```
66   300 -2.7    -62                                        $ Target holder
68    0          50 52 53 54 55 56 58 60 -64
69    0          64 47 -65                                  $ Inside room
70   500 -2.31   65 -66                                     $ Concrete
71     0         66

c    *** Detector Surface Cards ***
101   1  rpp -8.89  8.89  0  14.9225  -8.255   7.9375            $ outside detector surface
102   1  rpp -7.9375  7.9375  0.635 14.2875  -7.9375  7.9375     $ inside detector surface
103   1  py   1.11125
104   1  py 2.38125
105   1  py 3.01625
106   1  py 3.33375
107   1  py 3.96875
108   1  py 4.28625
109   1  py 4.92125
110   1 py 5.23875
111   1 py 5.87375
112   1 py 6.19125
113   1 py 6.82625
114   1 py 7.14375
115   1 py 7.77875
116   1 py 8.09625
117   1 py 8.73125
118   1 py 9.04875
119   1 py 9.68375
120   1 py 10.00125
121   1 py 10.63625
122   1 py 10.95375
123   1 py 11.58875
124   1 py 11.90625
125   1 py 12.54125
126   1 py   13.81125
127   1 rpp -8.89  8.89  -.9525 15.875   7.9375  8.5725              $ flange
```

```
128   1 rcc  0  7.46125  7.9375  0  0  33.3375   8.4138              $ outside of PMT
129   1 rcc  0  7.46125  7.9375  0  0  33.0200    8.0963             $ inside of PMT
c    *** Top Stand Surface Cards ***  built at origin, translation 2 moves origin
10   2 px   -8.25
11   2 px   -7.2975
12   2 px    7.2975
13   2 px    8.25
14   2 py  -12.065
15   2 py   12.065
16   2 pz    5.5563
17   2 pz    4.6038
18   2 pz    3.0163
19   2 pz    0
20   2 pz   -3.0163
21   2 pz   -4.6038
22   2 pz   -5.5563
23   2 p     0      0.819  -0.574  -5.9363
24   2 p     0      0.819  -0.574  -6.5508
25   2 p     0      0.819   0.574  -5.9363
26   2 p     0      0.819   0.574  -6.5508
27   2 p    0.819  0       -0.574  5.0254
28   2 p    0.819  0       -0.574  4.2453
29   2 p    0.819  0       0.574   5.0254
30   2 p    0.819  0       0.574   4.2453
31   2 py   -3.5
32   2 p    0.819  0        0.574   -5.0254
33   2 p    0.819  0        0.574   -4.2453
34   2 p    0.819  0        -0.574  -5.0254
35   2 p    0.819  0        -0.574  -4.2453
36   2 rcc  -8.2500 -6.6500   0  16.5  0  0  0.4763
37   2 rcc  -8.2500 11.5887   0  16.5  0  0  0.4763
38   2 py   11.1124
39   2 rcc  8.25   -6.6500    0  1.905  0  0  1.905
c    *** Plate below lower stand surface cards ***
```

```
40   2 box  -6.99 -10.795 -5.5563 15.24 0 0 0 22.86 0 0 0 -3.81
41   2 rcc   0.6300 12.0650  -3.6663  0 1.9050 0  1.905
42   2 rcc   0.6300 13.9700  -3.6663  0 0.9525 0  3.4925
c    *** Base plate of stand surface cards ***
43   2 box  -24.77 -10.795 -9.3663  33.02 0 0 0 22.86 0 0 0 -7.9375
44   2 rcc   8.2500  0.6350  -13.3350   1.9050 0  0  1.905
45   2 rcc   10.1550  0.6350  -13.3350  0.9525 0  0  3.4925
c    *** Tripod base pole ***
46   2 rcc  0  0  -17.3038  0  0  -143.8274  1.5875
47   2 rpp  -30 30 -14.8 25 -161.1312 60
c    *** Target chamber ***
50   rcc  0  0  15.24  0  0  -30.4800  7.6200
51   rcc  0  0  15.23  0  0  -29.5275  6.6675
52   rcc  0  0  15.24  0  0    1.9050  9.5250
53   rcc  0  0  17.145 0  0   25.4000  4.4450
54   rcc  0  0 -15.240 0  0   -6.4770  4.1275
55   box  1.27 1.27 -21.717 -40.64 0 0 0 -2.54 0 0 0 -2.54
56   rcc  0  0  0  -38.12  0  0  2.5400
57   rcc  0  0  0  -38.12  0  0  2.2225
58   rcc  0  0  0  -36.82  -9.866  0  2.54
59   rcc  0  0  0  -36.82  -9.866  0  2.2225
60   rcc  0  0  0  0 -38.12  0  2.5400
61   rcc  0  0  0  0 -38.12  0  2.2225
62   box  -1.27 -1.27 15.23 2.54 0 0 0 2.54 0 0 0 -13.66
64   rpp  -50  14.5 -39 10.25 -25 44
c    *** room dimensions
65   rpp -51 175.26  -51 175.26 -175.26  65
66   rpp -51 220.98  -51 220.98 -220.98  65

mode   n p
imp:n 1 78r 0
imp:p 1 78r 0
sdef pos= 0 0 0 vec=1 0 0 dir=d3 erg= fdir d4
c *** Neutron Angular Dependence ***
```

```
si3  A -1  -0.866 -0.500 0  0.500 0.866 1
c *** Angular Probability Distribution ***
sp3  1.01  1.02  1.04  1.06  1.09 1.11  1.12
c *** Energy Dependence from Angular Distribution ***
ds4  2.071 2.123 2.273 2.496 2.741 2.935 3.009
*tr1 0  12.065 1  0 90 90 90 0 90 90 90 0  1
*tr2 0  25.4026  -14.1288   0 90 90 90 0 90 90 90 0  1
m100 4009 1                 $ Beryllium rho=1.848 g/cc
m200 6000  0.47             $ BC-404, rho=1.032 g/cc
     1001  0.53
m300 13027 1                $ Aluminum, rho=2.7 g/cc
m400 6000   -0.0008         $ Stainless Steel 304 rho=8.03 g/cc
     25055      -0.0200
     24000  -0.1900
     28000  -0.1000
     14000  -0.0075
     15031  -0.00045
     16000  -0.0003
     7014   -0.0010
     26000  -0.67995
m500 1001   -0.00453        $ Concrete (LANL Mix from DANT) rho=2.25 g/cc
     8016   -0.51260
     14000  -0.36036
     13027  -0.03555
     11023  -0.01527
     20000  -0.05791
     26000  -0.01378
m600 6000   -0.50           $ cardboard from 1984 forestry pub.
     8016   -0.44
     1001   -0.06
f4:n      104 106 108 110 112 114 116 118 120 122 124 t
c *** Calculation of He-6 nuclei produced ***
fm4    -1 100 107
nps   1e8
```

```
prdmp 9e9  9e9  9e9
```

He-6 beta source, Validation Experiment, BLC Geometry, 3.175 mm scintillator

```
c    *** Detector Cell Cards ***
1   400  -8.03     -2  1                    $ Housing
2   400  -8.03     -1  -3                   $ SS Layer
3   600  -0.178    -1  3  -4                $ Cardboard
4   100  -1.848    -1  4  -5                $ Beryllium
5   200  -1.032    -1  5  -6                $ scintillator
6   100  -1.848    -1  6  -7                $ Beryllium
7   200  -1.032    -1  7  -8                $ scintillator
8   100  -1.848    -1  8  -9                $ Beryllium
9   200  -1.032    -1  9  -10               $ scintillator
10   100  -1.848    -1  10 -11              $ Beryllium
11   200  -1.032    -1  11 -12              $ scintillator
12   100  -1.848    -1  12 -13              $ Beryllium
13   200  -1.032    -1  13 -14              $ scintillator
14   100  -1.848    -1  14 -15              $ Beryllium
15   200  -1.032    -1  15 -16              $ scintillator
16   100  -1.848    -1  16 -17              $ Beryllium
17   200  -1.032    -1  17 -18              $ scintillator
18   100  -1.848    -1  18 -19              $ Beryllium
19   200  -1.032    -1  19 -20              $ scintillator
20   100  -1.848    -1  20 -21              $ Beryllium
21   200  -1.032    -1  21 -22              $ scintillator
22   100  -1.848    -1  22 -23              $ Beryllium
23   200  -1.032    -1  23 -24              $ scintillator
24   100  -1.848    -1  24 -25              $ Beryllium
25   600  -0.178    -1  25 -26              $ Cardboard
26   400  -8.03     -1 26                   $ SS Layer
```

```
27   400  -8.03    -27  28                  $ flange
28   400  -8.03    -28 29                   $ PMT wall
29     0           -29                      $ void in PMT
31     0            1 27 28 -30
32     0            30

c    *** Detector Surface Cards ***
1     rpp -8.89  8.89  0  14.9225  -8.255   7.9375            $ outside detector surface
2     rpp -7.9375  7.9375  0.635 14.2875  -7.9375  7.9375     $ inside detector surface
3     py   1.11125
4     py 2.38125
5     py 3.01625
6     py 3.33375
7     py 3.96875
8     py 4.28625
9     py 4.92125
10    py 5.23875
11    py 5.87375
12    py 6.19125
13    py 6.82625
14    py 7.14375
15    py 7.77875
16    py 8.09625
17    py 8.73125
18    py 9.04875
19    py 9.68375
20    py 10.00125
21    py 10.63625
22    py 10.95375
23    py 11.58875
24    py 11.90625
25    py 12.54125
```

```
26    py   13.81125
27    rpp -8.89  8.89  -.9525 15.875   7.9375  8.5725            $ flange
28    rcc  0  7.46125  7.9375  0  0  33.3375   8.4138            $ outside of PMT
29    rcc  0  7.46125  7.9375  0  0  33.0200    8.0963           $ inside of PMT
30  rpp -15 15 -25 25 -10 50

mode   p e
imp:p 1 27r 0 1 0
imp:e 1 27r 0 1 0
sdef par=3 x=d2 y =d3 z=d4  erg=d1
c *** He-6 beta energy spectrum ***
si1   L 0 0.2852 0.3667 0.4414 0.5161 0.5840 0.6520 0.7267 0.8014 0.8761
      0.9576 1.0323 1.1070 1.1749 1.2564 1.3311 1.4805 1.5552 1.6299
      1.7046 1.7793 1.8540 1.9219 2.0034 2.0713 2.1460 2.2207 2.2954
      2.3633 2.4448 2.5127 2.5874 2.6689 2.7436 2.8115 2.8795 2.9542
      3.0289 3.1104 3.1783 3.2530 3.3209 3.4024 3.4703
C *** Probability Distribution ***
sp1   0 0.01340 0.01720 0.02014 0.02239 0.02429 0.02584 0.02731 0.02878
      0.02999 0.03094 0.03189 0.03267 0.03362 0.03405 0.03457 0.03509
      0.03518 0.03492 0.03492 0.03440 0.03319 0.03241 0.03129 0.02982
      0.02809 0.02679 0.02498 0.02316 0.02092 0.01919 0.01711 0.01513
      0.01305 0.01098 0.00916 0.00717 0.00553 0.00415 0.00285 0.00190
      0.00112 0.00069 0.00026
C *** starting location uniform distribution within layer ***
si2   -7.9375 7.9375
sp2   0 1
si3   s 5 6 7 8 9 10 11 12 13 14 15
c *** starting location distributed by layer, from first calculation ***
sp3   3.11 2.38 1.82 1.39 1.07 .826 .640 .498 .389 .304 .240
C *** starting location uniform distribution within layer ***
si4   -7.9375 7.9375
sp4   0 1
```

```
si5   2.38125 3.01625
sp5   0 1
si6   3.33375 3.96875
sp6   0 1
si7   4.28625 4.92125
sp7   0 1
si8   5.23875 5.87375
sp8   0 1
si9   6.19125 6.82625
sp9   0 1
si10  7.14375 7.77875
sp10  0 1
si11  8.09625 8.73125
sp11  0 1
si12  9.04875 9.68375
sp12  0 1
si13  10.00125 10.63625
sp13  0 1
si14  10.95375 11.58875
sp14  0 1
si15  11.90625 12.54125
sp15  0 1
m100 4009 1                  $ Beryllium rho=1.848 g/cc
m200 6000  0.47              $ BC-404, rho=1.032 g/cc
     1001  0.53
m300 13027 1                 $ Aluminum, rho=2.7 g/cc
m400 6000   -0.0008          $ Stainless Steel 304 rho=8.03 g/cc
     25055      -0.0200
     24000  -0.1900
     28000  -0.1000
     14000  -0.0075
     15031  -0.00045
```

```
     16000  -0.0003
     7014   -0.0010
     26000  -0.67995
m500 6000   -0.625017        $ mylar
     8016   -0.333024
     1001   -0.041959
m600 6000   -0.50            $ cardboard from 1984 forestry pub.
     8016   -0.44
     1001   -0.06
f8:e,p  5 7 9 11 13 15 17 19 21 23 t
e8    0  0.001  27i  1.4 1.9 2.4 2.9 3.5
prdmp 1e15 1e15 1e15
nps 1e6
```

Validation Experiment, Neutron Fluence at Average Detector Solid Angle

```
Big Beryllium Detector
c    *** Detector Cell Cards ***
101   0    -101  102                    $ Housing
102   0    -102  -103                   $ SS Layer
103   0    -102  103  -104              $ Cardboard
104   0    -102  104  -105              $ Beryllium
105   0    -102  105  -106              $ scintillator
106   0    -102  106  -107              $ Beryllium
107   0    -102  107  -108              $ scintillator
108   0    -102  108  -109              $ Beryllium
109   0    -102  109  -110              $ scintillator
110   0    -102  110 -111               $ Beryllium
111   0    -102  111 -112               $ scintillator
112   0    -102  112 -113               $ Beryllium
113   0    -102  113 -114               $ scintillator
```

```
114   0    -102  114 -115                $ Beryllium
115   0    -102  115 -116                $ scintillator
116   0    -102  116 -117                $ Beryllium
117   0    -102  117 -118                $ scintillator
118   0    -102  118 -119                $ Beryllium
119   0    -102  119 -120                $ scintillator
120   0    -102  120 -121                $ Beryllium
121   0    -102  121 -122                $ scintillator
122   0    -102  122 -123                $ Beryllium
123   0    -102  123 -124                $ scintillator
124   0    -102  124 -125                $ Beryllium
125   0    -102  125 -126                $ Cardboard
126   0     -102 126                     $ SS Layer
127   0    -127  128                     $ flange
128   0    -128 129                      $ PMT wall
129     0           -129                 $ void in PMT
c   *** Top Stand Cell Cards ***
20   400  -8.03     10  -13  14  -15  -16  17            $ Top plate
21   400  -8.03     10  -13  14  -15  -21  22            $ Bottom plate
22   400  -8.03     10  -11  14  -15  -17  18            $ Top hinge (1)
23   400  -8.03     12  -13  14  -15  -17  18            $ Top hinge (2)
24   400  -8.03     10  -11  14  -15  -20  21            $ Bottom hinge (1)
25   400  -8.03     12  -13  14  -15  -20  21            $ Bottom hinge (2)
26   400  -8.03     11  -12  -17  19  -23  24            $ Front support-top
27   400  -8.03     11  -12  -19  21  -25  26            $ Front support-bot
28   400  -8.03    -27   28  -38  -18  19  31            $ Side support-front-top
29   400  -8.03    -29   30  -38  -19  20  31            $ Side support-front-bottom
30   400  -8.03     32  -33  -38  -18  19  31            $ Side support-front-top
31   400  -8.03     34  -35  -38  -19  20  31            $ Side support-front-bottom
32   400  -8.03    -36                                   $ front bolt
33   400  -8.03    -37                                   $ back bolt
34    0          -10 -16 22 14 -15 -47                   $ void left
```

```
35    0           13 -16 22 14 -15 39 -47                 $ void right
36    0          -14 -16 22 -47                           $ void front
37    0           15 -16 22 41 42 -47                     $ void back
38    0           16 101 127 128 -47                      $ void top
39    0          -22 40 41 42 43 44 45 46 -47             $ void bottom
40    0           (14 -31 10 -11 -18 20 36 37):(-38 31 -32 -34 10 36 37)  $ void left
41    0           (14 -31 12 -13 -18 20 36 37):(-38 31 27 29 -13 36 37)   $ void right
42    0           (11 -12 14 -17 19 -24):(11 -12 14 -19 21 -26)           $ void center front
43    0           (11 -12 -31 23 -17 19 36):(11 -12 -31 25 -19 21 36)     $ void center
44    0 (31 -38 -19 21 -12 11 -30 35  37):(-17 19 31 -38 -12 11 -28 33 37) $ void center back
45    0 38 -15 37 11 -12 -17 21:38 -15 10 -11 -18 20 37:38 -15 12 -13 -18 20 37 $ void back
46   300 -2.7  -39                                        $ knob
c    *** Plate below lower stand cell cards ***
47   300 -2.7  -40                                        $ plate
48   300 -2.7  -41                                        $ knob spacer
49   300 -2.7  -42                                        $ knob
c    *** Stand Base plate cell cards ***
50   300 -2.7  -43                                        $ base plate
51   300 -2.7  -44                                        $ knob spacer
52   300 -2.7  -45                                        $ knob
53   300 -2.7  -46                                        $ pole
c    *** Target chamber cell cards ***
54   300 -2.7  -50  51 56 58 60                           $ vacuum chamber outer wall
55     0        -51 62                                    $ Vacuum chamber
56   300 -2.7   -52                                       $ Upper flange
57   400  -8.03   -53                                     $ Upper hardware
58   300 -2.7   -54                                       $ Lower chamber dial
59   300 -2.7   -55                                       $ Sample holder
60     0        -57 51                                    $ Inside beam line
61   300 -2.7   -56 57 51                                 $ beam line tube
62   300 -2.7   -58 59 56 51                              $ 165 SBD
63     0         -59 56 51                                $ 165 SBD inside
```

```
64   300 -2.7    -60 61 51                                  $ 110 SBD
65     0         -61 51                                     $ 110 SBD inside
66   300 -2.7    -62                                        $ Target holder
68    0          50 52 53 54 55 56 58 60 -64
69    0          64 47 -65                                  $ Inside room
70   500 -2.31   65 -66                                     $ Concrete
71     0         66

c    *** Detector Surface Cards ***
101   1  rpp -8.89  8.89  0  14.9225  -8.255   7.9375            $ outside detector surface
102   1  rpp -7.9375  7.9375  0.635 14.2875  -7.9375  7.9375     $ inside detector surface
103   1  py   1.11125
104   1  py 2.38125
105   1  py 3.01625
106   1  py 3.33375
107   1  py 3.96875
108   1  py 4.28625
109   1  py 4.92125
110   1 py 5.23875
111   1 py 5.87375
112   1 py 6.19125
113   1 py 6.82625
114   1 py 7.14375
115   1 py 7.77875
116   1 py 8.09625
117   1 py 8.73125
118   1 py 9.04875
119   1 py 9.68375
120   1 py 10.00125
121   1 py 10.63625
122   1 py 10.95375
123   1 py 11.58875
```

```
124   1 py 11.90625
125   1 py 12.54125
126   1 py   13.81125
127   1 rpp -8.89  8.89  -.9525 15.875   7.9375  8.5725            $ flange
128   1 rcc  0  7.46125  7.9375  0  0  33.3375   8.4138            $ outside of PMT
129   1 rcc  0  7.46125  7.9375  0  0  33.0200    8.0963           $ inside of PMT
c    *** Top Stand Surface Cards ***  built at origin, translation 2 moves origin
10   2 px   -8.25
11   2 px   -7.2975
12   2 px    7.2975
13   2 px    8.25
14   2 py  -12.065
15   2 py   12.065
16   2 pz    5.5563
17   2 pz    4.6038
18   2 pz    3.0163
19   2 pz    0
20   2 pz   -3.0163
21   2 pz   -4.6038
22   2 pz   -5.5563
23   2 p     0      0.819  -0.574  -5.9363
24   2 p     0      0.819  -0.574  -6.5508
25   2 p     0      0.819   0.574  -5.9363
26   2 p     0      0.819   0.574  -6.5508
27   2 p    0.819  0       -0.574  5.0254
28   2 p    0.819  0       -0.574  4.2453
29   2 p    0.819  0       0.574   5.0254
30   2 p    0.819  0       0.574   4.2453
31   2 py   -3.5
32   2 p    0.819  0        0.574   -5.0254
33   2 p    0.819  0        0.574   -4.2453
34   2 p    0.819  0        -0.574  -5.0254
```

```
35   2 p    0.819  0        -0.574  -4.2453
36   2 rcc  -8.2500 -6.6500   0  16.5  0  0  0.4763
37   2 rcc  -8.2500 11.5887   0  16.5  0  0  0.4763
38   2 py   11.1124
39   2 rcc  8.25   -6.6500    0  1.905  0  0  1.905
c    *** Plate below lower stand surface cards ***
40   2 box  -6.99 -10.795 -5.5563 15.24 0 0 0 22.86 0 0 0 -3.81
41   2 rcc   0.6300 12.0650  -3.6663  0 1.9050 0  1.905
42   2 rcc   0.6300 13.9700  -3.6663  0 0.9525 0  3.4925
c    *** Base plate of stand surface cards ***
43   2 box  -24.77 -10.795 -9.3663  33.02 0 0 0 22.86 0 0 0 -7.9375
44   2 rcc   8.2500  0.6350  -13.3350   1.9050 0  0  1.905
45   2 rcc   10.1550  0.6350  -13.3350  0.9525 0  0  3.4925
c    *** Tripod base pole ***
46   2 rcc  0  0  -17.3038  0  0  -143.8274  1.5875
47   2 rpp  -30 30 -14.8 25 -161.1312 60
c    *** Target chamber ***
50   rcc  0  0  15.24  0  0  -30.4800  7.6200
51   rcc  0  0  15.23  0  0  -29.5275  6.6675
52   rcc  0  0  15.24  0  0    1.9050  9.5250
53   rcc  0  0  17.145 0  0   25.4000  4.4450
54   rcc  0  0 -15.240 0  0   -6.4770  4.1275
55   box  1.27 1.27 -21.717 -40.64 0 0 0 -2.54 0 0 0 -2.54
56   rcc  0  0  0  -38.12  0  0  2.5400
57   rcc  0  0  0  -38.12  0  0  2.2225
58   rcc  0  0  0  -36.82  -9.866  0  2.54
59   rcc  0  0  0  -36.82  -9.866  0  2.2225
60   rcc  0  0  0  0 -38.12  0  2.5400
61   rcc  0  0  0  0 -38.12  0  2.2225
62   box  -1.27 -1.27 15.23 2.54 0 0 0 2.54 0 0 0 -13.66
64   rpp  -50  14.5 -39 10.25 -25 44
c    *** room dimensions
```

```
65   rpp -51 175.26  -51 175.26 -175.26  65
66   rpp -51 220.98  -51 220.98 -220.98  65

mode   n p
imp:n 1 78r 0
imp:p 1 78r 0
sdef pos= 0 0 0 vec=1 0 0 dir=d3 erg= fdir d4
c *** Neutron Angular Dependence ***
si3  A -1  -0.866 -0.500 0  0.500 0.866 1
c *** Angular Probability Distribution ***
sp3  1.01  1.02  1.04  1.06  1.09 1.11  1.12
c *** Energy Dependence from Angular Distribution ***
ds4  2.071 2.123 2.273 2.496 2.741 2.935 3.009
*tr1 0  12.065 1  0 90 90 90 0 90 90 90 0  1
*tr2 0  25.4026  -14.1288   0 90 90 90 0 90 90 90 0  1
m100 4009 1                  $ Beryllium rho=1.848 g/cc
m200 6000  0.47              $ BC-404, rho=1.032 g/cc
     1001  0.53
m300 13027 1                 $ Aluminum, rho=2.7 g/cc
m400 6000   -0.0008          $ Stainless Steel 304 rho=8.03 g/cc
     25055      -0.0200
     24000  -0.1900
     28000  -0.1000
     14000  -0.0075
     15031  -0.00045
     16000  -0.0003
     7014   -0.0010
     26000  -0.67995
m500 1001   -0.00453         $ Concrete (LANL Mix from DANT) rho=2.25 g/cc
     8016   -0.51260
     14000  -0.36036
     13027  -0.03555
```

```
     11023  -0.01527
     20000  -0.05791
     26000  -0.01378
m600 6000   -0.50            $ cardboard from 1984 forestry pub.
     8016   -0.44
     1001   -0.06
f4:n      104 106 108 110 112 114 116 118 120 122 124 t
nps   1e8
prdmp 9e9  9e9  9e9
```

Appendix D Sample MCNP Output Files

Detector #1

Co-60 gamma source, BLC geometry

```
Co60 source
c    *** Cell Cards ***
10   100   -1.0320     -9                  $ Scint layer
20   300   -1.0600     -10   11            $ Polystyrene
30   200   -1.4000    -1                   $ surface of source
90   600   -0.9000     -11   9 19 21 23 18 20 22 1      $ polypropylene spacers
100  500   -8.0300     -13  12                          $ detector housing
110    0               -12  10  14                      $ void inside housing
120  700   -2.2300     -14 15                           $ pmt
130    0               -15                              $ inside of pmt
140  500   -8.0300     -16  17                          $ base housing
150    0               -17                              $ void in base
160    0                16  13  -24                     $ void outside detector
170  100   -1.032      -19
180  100   -1.032      -21
190  100   -1.032      -23
200  800   -1.848      -18
210  800   -1.848      -20
220  800   -1.848      -22
230    0                24

c    *** Surface Cards ***
1   rcc    -0.3175  0  0  0.3175  0  0   1.27           $ outside radius of s
9   rpp     0  0.10  -1.50  1.50  -3.25  3.25           $ scintillator cell
10  rcc    0.67625  0  -3.5675  0 0  6.8175  2.1075     $ polystyrene holder
11  rpp   -0.32  1.5725  -1.50  1.50  -3.25  3.25       $ polypropylene spacers
12  rcc    0.67625  0  -3.5675 0 0  11.5825   2.1075    $ inside of detector
13  rcc    0.67625  0  -3.8850 0 0  11.9000   2.425     $ outside of detecto
14  rcc    0.67625  0   8.015  0 0  -4.6      1.875     $ outside of pmt
15  rcc    0.67625  0   8.015  0 0  -4.2825   1.5575    $ inside of pmt
```

```
      31-       16  rcc    0.67625  0   8.015  0 0   6.5      4.55      $ outside of base
      32-       17  rcc    0.67625  0   8.3325 0 0   5.865    4.235     $ inside of base
      33-       18  rpp    0.10   0.4175 -1.50 1.50 -3.25  3.25
      34-       19  rpp    0.4175 0.5175 -1.50 1.50 -3.25  3.25
      35-       20  rpp    0.5175 0.8350 -1.50 1.50 -3.25  3.25
      36-       21  rpp    0.8350 0.9350 -1.50 1.50 -3.25  3.25
      37-       22  rpp    0.9350 1.2525 -1.50 1.50 -3.25  3.25
      38-       23  rpp    1.2525 1.3525 -1.50 1.50 -3.25  3.25
      39-       24  rcc    0.67625  0  -4.25  0  0  19.0  5.00
      40-
      41-       mode   e p
      42-       imp:e 1 16r  0
      43-       imp:p 1 16r  0
      44-       sdef par=2 x=-0.15875 y=0 z=0  axs=1 0 0 rad=d3 erg=d1
      45-       si1  L .007461  .007478  .008265  .34714  .82610  1.173228  1.332492  2.15857
      46-       sp1  D .00322  .0063  .001151  .0075  .0076  99.85  99.9826  .00120
      47-       si3   0     0.15
      48-       sp3   0     1
      49-       m100 6000    0.47           $ scintillator
      50-            1001    0.53
      51-            estep 11
      52-       m200 6000   -0.625017       $ mylar
      53-            8016   -0.333024
      54-            1001   -0.041959
      55-            estep 12
      56-       m300 6000   -0.856289       $ polyethylene
      57-            1000   -0.143711
      58-            estep 12
      59-       m400 13027   1              $ aluminum
warning.  material      400 is not used in the problem.
      60-            estep 6
      61-       m500 6000   -0.0008         $ Stainless Steel 304
      62-            25000  -0.0200
      63-            24000  -0.1900
      64-            28000  -0.1000
      65-            14000  -0.0075
      66-            15000  -0.00045
      67-            16000  -0.0003
```

```
        68-            7000   -0.0010
        69-            26000  -0.67995
        70-            estep 10
        71-       m600 6000   -.922582        $ polystyrene
        72-            1000   -.077418
        73-            estep 6
        74-       m700 5010   -0.007973       $ borosilicate glass rho=2.23 g/cc
        75-            5011   -0.032091
        76-            8016   -0.539562
        77-            11023  -0.028191
        78-            13027  -0.011644
        79-            14000  -0.377220
        80-            19000  -0.003321
        81-       m800 4009    1
        82-       f8:e,p   10 170 180 190 t
        83-       e8    0  0.001  27i  1.401
        84-       prdmp 1e15 1e15 1e15
        85-       nps 1e7
  warning.  source variable rad is sampled uniformly.
1cells
print table 60
```

	cell	mat	atom density	gram density	volume	mass	pieces	photon importance	electron importance
1	10	100	1.00573E-01	1.03200E+00	1.95000E+00	2.01240E+00	0	1.0000E+00	1.0000E+00
2	20	300	1.36518E-01	1.06000E+00	0.00000E+00	0.00000E+00	0	1.0000E+00	1.0000E+00
3	30	200	9.65255E-02	1.40000E+00	1.60880E+00	2.25231E+00	1	1.0000E+00	1.0000E+00
4	90	600	8.32577E-02	9.00000E-01	0.00000E+00	0.00000E+00	0	1.0000E+00	1.0000E+00
5	100	500	8.86197E-02	8.03000E+00	5.82298E+01	4.67585E+02	1	1.0000E+00	1.0000E+00
6	110	0	0.00000E+00	0.00000E+00	1.56833E+01	0.00000E+00	1	1.0000E+00	1.0000E+00
7	120	700	7.06619E-02	2.23000E+00	1.81690E+01	4.05168E+01	1	1.0000E+00	1.0000E+00
8	130	0	0.00000E+00	0.00000E+00	3.26365E+01	0.00000E+00	1	1.0000E+00	1.0000E+00
9	140	500	8.86197E-02	8.03000E+00	9.22879E+01	7.41072E+02	1	1.0000E+00	1.0000E+00
10	150	0	0.00000E+00	0.00000E+00	3.30464E+02	0.00000E+00	1	1.0000E+00	1.0000E+00
11	160	0	0.00000E+00	0.00000E+00	8.49657E+02	0.00000E+00	1	1.0000E+00	1.0000E+00
12	170	100	1.00573E-01	1.03200E+00	1.95000E+00	2.01240E+00	0	1.0000E+00	1.0000E+00

```
      13      180      100  1.00573E-01 1.03200E+00 1.95000E+00 2.01240E+00  0  1.0000E+00 1.0000E+00
      14      190      100  1.00573E-01 1.03200E+00 1.95000E+00 2.01240E+00  0  1.0000E+00 1.0000E+00
      15      200      800  1.23485E-01 1.84800E+00 6.19125E+00 1.14414E+01  0  1.0000E+00 1.0000E+00
      16      210      800  1.23485E-01 1.84800E+00 6.19125E+00 1.14414E+01  0  1.0000E+00 1.0000E+00
      17      220      800  1.23485E-01 1.84800E+00 6.19125E+00 1.14414E+01  0  1.0000E+00 1.0000E+00
      18      230        0  0.00000E+00 0.00000E+00 0.00000E+00 0.00000E+00  0  0.0000E+00 0.0000E+00

 total                                                1.42511E+03 1.29380E+03

    minimum source weight = 1.0000E+00    maximum source weight = 1.0000E+00

 ***************************************************
 * Random Number Generator  =                    1 *
 * Random Number Seed       =       19073486328125 *
 * Random Number Multiplier =       19073486328125 *
 * Random Number Adder      =                    0 *
 * Random Number Bits Used  =                   48 *
 * Random Number Stride     =               152917 *
 ***************************************************

         2 warning messages so far.
1cross-section tables
print table 100

     table    length

                        tables from file mcplib04

   1000.04p    1898  ENDF/B-VI Release 8 Photoatomic Data for 1-H              mat 100      02/07/03
   4000.04p    2363  ENDF/B-VI Release 8 Photoatomic Data for 4-BE             mat 400      02/07/03
   5000.04p    3116  ENDF/B-VI Release 8 Photoatomic Data for 5-B              mat 500      02/07/03
   6000.04p    3152  ENDF/B-VI Release 8 Photoatomic Data for 6-C              mat 600      02/07/03
   7000.04p    3194  ENDF/B-VI Release 8 Photoatomic Data for 7-N              mat 700      02/07/03
   8000.04p    3272  ENDF/B-VI Release 8 Photoatomic Data for 8-O              mat 800      02/07/03
  11000.04p    3995  ENDF/B-VI Release 8 Photoatomic Data for 11-NA            mat1100      02/07/03
  13000.04p    4846  ENDF/B-VI Release 8 Photoatomic Data for 13-AL            mat1300      02/07/03
  14000.04p    4792  ENDF/B-VI Release 8 Photoatomic Data for 14-SI            mat1400      02/07/03
  15000.04p    4498  ENDF/B-VI Release 8 Photoatomic Data for 15-P             mat1500      02/07/03
```

```
  16000.04p    4654  ENDF/B-VI Release 8 Photoatomic Data for 16-S              mat1600      02/07/03
  19000.04p    5047  ENDF/B-VI Release 8 Photoatomic Data for 19-K              mat1900      02/07/03
  24000.04p    5682  ENDF/B-VI Release 8 Photoatomic Data for 24-CR             mat2400      02/07/03
  25000.04p    5598  ENDF/B-VI Release 8 Photoatomic Data for 25-MN             mat2500      02/07/03
  26000.04p    5718  ENDF/B-VI Release 8 Photoatomic Data for 26-FE             mat2600      02/07/03
  28000.04p    5826  ENDF/B-VI Release 8 Photoatomic Data for 28-NI             mat2800      02/07/03

  total       67651

 maximum photon energy set to  100.0 mev (maximum electron energy)

                        tables from file el03

   1000.03e    2329   6/6/98
   4000.03e    2331   6/6/98
   5000.03e    2331   6/6/98
   6000.03e    2333   6/6/98
   7000.03e    2333   6/6/98
   8000.03e    2333   6/6/98
  11000.03e    2337   6/6/98
  13000.03e    2337   6/6/98
  14000.03e    2339   6/6/98
  15000.03e    2339   6/6/98
  16000.03e    2339   6/6/98
  19000.03e    2343   6/6/98
  24000.03e    2345   6/6/98
  25000.03e    2345   6/6/98
  26000.03e    2345   6/6/98
  28000.03e    2347   6/6/98

  warning.  material      800 has been set to a conductor.


*****************************************************************************************************************
************

 dump no.    1 on file runtpe     nps =           0     coll =              0     ctm =        0.00   nrn =
0
```

```
         3 warning messages so far.
 warning.  tally not scored beyond last energy bin.
 nps =     7905479     nrn =               71873 tal =    8     erg = 1.4140E+00
1problem summary

      run terminated when    10000000  particle histories were done.
+
06/23/14 05:50:35
      Co60 source                                                                    probid =
06/23/14 05:04:48
0
 photon creation     tracks      weight        energy  photon loss         tracks      weight        energy
                                 (per source particle)                   (per source particle)

 source            10000000    1.0000E+00    1.2528E+00    escape  9781973    9.7820E-01    1.0312E+00
                                                           energy cutoff     0    0.            1.6924E-05
                                                           time cutoff       0    0.            0.
 weight window      0    0.            0.                  weight window     0    0.            0.
 cell importance    0    0.            0.                  cell importance   0    0.            0.
 weight cutoff      0    0.            0.                  weight cutoff     0    0.            0.
 e or t importance  0    0.            0.                  e or t importance 0    0.            0.
 dxtran             0    0.            0.                  dxtran            0    0.            0.
 forced collisions  0    0.            0.                  forced collisions 0    0.            0.
 exp. transform     0    0.            0.                  exp. transform    0    0.            0.
 from neutrons      0    0.            0.                  compton scatter   0    0.            2.1752E-01
 bremsstrahlung 592011   5.9201E-02    1.7822E-03          capture       932066   9.3207E-02    5.8362E-03
 p-annihilation   5516   5.5160E-04   2.8187E-04           pair production 2765   2.7650E-04    3.6200E-04
 photonuclear            0    0.            0.             photonuclear abs         0    0.            0.
 electron x-rays      57129    5.7129E-03    4.2915E-05
 1st fluorescence     62148    6.2148E-03    3.9676E-05
 2nd fluorescence         0    0.            0.
     total         10716804    1.0717E+00    1.2549E+00              total         10716804    1.0717E+00
1.2549E+00

   number of photons banked                   654656        average time of (shakes)              cutoffs
   photon tracks per source particle      1.0717E+00          escape            2.1402E-02          tco
1.0000E+33
```

```
   photon collisions per source particle  6.3031E-01          capture           1.5375E-02          eco
1.0000E-03
   total photon collisions                   6303126          capture or escape 2.0877E-02          wc1
0.0000E+00
                                                              any termination   2.0875E-02          wc2
0.0000E+00
0
 electron creation   tracks      weight        energy            electron loss       tracks      weight
energy
                     (per source particle)                       (per source particle)

 source   0    0.            0.                              escape        57891  5.7891E-03  3.1690E-03
energy cutoff 205206835    2.0521E+01    2.0298E-02          time cutoff       0  0.          0.
 weight window        0    0.            0.                  weight window     0  0.          0.
 cell importance      0    0.            0.                  cell importance   0  0.          0.
 weight cutoff        0    0.            0.                  weight cutoff     0  0.          0.
 e or t importance    0    0.            0.                  e or t importance 0  0.          0.
 pair production   5515    5.5150E-04    7.9414E-05          scattering        0  0.          2.7731E-01
 compton recoil 5227128    5.2271E-01    2.1752E-01          bremsstrahlung    0  0.          1.7822E-03
 photo-electric  900157    9.0016E-02    5.7025E-03          p-annihilation 2752  2.7520E-04  2.7251E-07
 photon auger     89901    8.9901E-03    6.7907E-05
 electron auger  102372    1.0237E-02    7.7183E-05
 knock-on     198942405    1.9894E+01    7.9116E-02
     total    205267478    2.0527E+01    3.0256E-01          total     205267478  2.0527E+01  3.0256E-01

   number of electrons banked              205267478                                                cutoffs
   electron tracks per source particle    2.0527E+01                                                  tco
1.0000E+33
   electron sub-steps per source particle 2.7908E+03                                                  eco
1.0000E-03
   total electron sub-steps              27908268192                                                  wc1
0.0000E+00
                                                                                                      wc2
0.0000E+00

 computer time so far in this run  2237.61 minutes           maximum number ever in bank       151
 computer time in mcrun            2237.52 minutes           bank overflows to backup file       0
 source particles per minute            4.4692E+03
```

```
 random numbers generated             125633919264            most random numbers used was      205579 in
history     1621300

  warning.   random number stride   152917 exceeded      246 times.

 range of sampled source weights = 1.0000E+00 to 1.0000E+00

 number of histories processed by each thread
     1432621     1429248     1427443     1430460     1424344     1429861     1426023

1tally        8        nps =    10000000
           tally type 8    pulse height distribution.                   units   number
           tally for  photons   electrons

 cell  10      *** Contribution from Layer 1 ***
      energy
    0.0000E+00   2.23000E-05 0.0670
    1.0000E-03   4.71712E-01 0.0003
    5.1000E-02   1.79630E-03 0.0075
    1.0100E-01   1.54460E-03 0.0080
    1.5100E-01   1.38990E-03 0.0085
    2.0100E-01   1.53740E-03 0.0081
    2.5100E-01   1.76950E-03 0.0075
    3.0100E-01   1.54180E-03 0.0080
    3.5100E-01   1.25890E-03 0.0089
    4.0100E-01   1.04780E-03 0.0098
    4.5100E-01   8.18700E-04 0.0110
    5.0100E-01   6.65200E-04 0.0123
    5.5100E-01   5.01000E-04 0.0141
    6.0100E-01   4.02600E-04 0.0158
    6.5100E-01   3.17000E-04 0.0178
    7.0100E-01   2.44900E-04 0.0202
    7.5100E-01   1.88500E-04 0.0230
    8.0100E-01   1.42500E-04 0.0265
    8.5100E-01   1.10600E-04 0.0301
    9.0100E-01   8.94000E-05 0.0334
    9.5100E-01   7.36000E-05 0.0369
    1.0010E+00   3.31000E-05 0.0550
```

```
   1.0510E+00   2.10000E-05 0.0690
   1.1010E+00   1.91000E-05 0.0724
   1.1510E+00   5.60000E-06 0.1336
   1.2010E+00   3.00000E-07 0.5774
   1.2510E+00   2.00000E-07 0.7071
   1.3010E+00   1.00000E-07 1.0000
   1.3510E+00   0.00000E+00 0.0000
   1.4010E+00   0.00000E+00 0.0000
     total      4.87254E-01 0.0003

cell  170           *** Contribution from Layer #2  ***
     energy
   0.0000E+00   1.59000E-05 0.0793
   1.0000E-03   3.77799E-01 0.0004
   5.1000E-02   1.37650E-03 0.0085
   1.0100E-01   1.05150E-03 0.0097
   1.5100E-01   9.19700E-04 0.0104
   2.0100E-01   9.98100E-04 0.0100
   2.5100E-01   1.09370E-03 0.0096
   3.0100E-01   9.01800E-04 0.0105
   3.5100E-01   7.27000E-04 0.0117
   4.0100E-01   5.86400E-04 0.0131
   4.5100E-01   4.66900E-04 0.0146
   5.0100E-01   3.52500E-04 0.0168
   5.5100E-01   2.64900E-04 0.0194
   6.0100E-01   2.02400E-04 0.0222
   6.5100E-01   1.53400E-04 0.0255
   7.0100E-01   1.14300E-04 0.0296
   7.5100E-01   9.13000E-05 0.0331
   8.0100E-01   6.59000E-05 0.0390
   8.5100E-01   4.79000E-05 0.0457
   9.0100E-01   3.20000E-05 0.0559
   9.5100E-01   2.42000E-05 0.0643
   1.0010E+00   1.28000E-05 0.0884
   1.0510E+00   8.60000E-06 0.1078
   1.1010E+00   6.20000E-06 0.1270
   1.1510E+00   2.10000E-06 0.2182
   1.2010E+00   5.00000E-07 0.4472
```

```
   1.2510E+00   0.00000E+00 0.0000
   1.3010E+00   1.00000E-07 1.0000
   1.3510E+00   0.00000E+00 0.0000
   1.4010E+00   0.00000E+00 0.0000
     total      3.87316E-01 0.0004

cell  180          *** Contribution from Layer # 3 ***
     energy
   0.0000E+00   1.05000E-05 0.0976
   1.0000E-03   2.99305E-01 0.0005
   5.1000E-02   1.06170E-03 0.0097
   1.0100E-01   7.72800E-04 0.0114
   1.5100E-01   6.43500E-04 0.0125
   2.0100E-01   7.27800E-04 0.0117
   2.5100E-01   7.79600E-04 0.0113
   3.0100E-01   6.23100E-04 0.0127
   3.5100E-01   4.95500E-04 0.0142
   4.0100E-01   3.90200E-04 0.0160
   4.5100E-01   2.98100E-04 0.0183
   5.0100E-01   2.25400E-04 0.0211
   5.5100E-01   1.72300E-04 0.0241
   6.0100E-01   1.27600E-04 0.0280
   6.5100E-01   1.00600E-04 0.0315
   7.0100E-01   7.21000E-05 0.0372
   7.5100E-01   4.79000E-05 0.0457
   8.0100E-01   3.78000E-05 0.0514
   8.5100E-01   2.91000E-05 0.0586
   9.0100E-01   1.97000E-05 0.0712
   9.5100E-01   1.09000E-05 0.0958
   1.0010E+00   7.20000E-06 0.1179
   1.0510E+00   3.20000E-06 0.1768
   1.1010E+00   2.60000E-06 0.1961
   1.1510E+00   7.00000E-07 0.3780
   1.2010E+00   0.00000E+00 0.0000
   1.2510E+00   1.00000E-07 1.0000
   1.3010E+00   0.00000E+00 0.0000
   1.3510E+00   0.00000E+00 0.0000
   1.4010E+00   0.00000E+00 0.0000
```

```
     total      3.05965E-01 0.0005

cell  190               *** Contribution from Layer # 4 ***
     energy
   0.0000E+00   9.50000E-06 0.1026
   1.0000E-03   2.37707E-01 0.0006
   5.1000E-02   8.40400E-04 0.0109
   1.0100E-01   5.95500E-04 0.0130
   1.5100E-01   4.90300E-04 0.0143
   2.0100E-01   5.64100E-04 0.0133
   2.5100E-01   5.66400E-04 0.0133
   3.0100E-01   4.44600E-04 0.0150
   3.5100E-01   3.48200E-04 0.0169
   4.0100E-01   2.89500E-04 0.0186
   4.5100E-01   2.16400E-04 0.0215
   5.0100E-01   1.68200E-04 0.0244
   5.5100E-01   1.30200E-04 0.0277
   6.0100E-01   9.70000E-05 0.0321
   6.5100E-01   6.87000E-05 0.0382
   7.0100E-01   4.71000E-05 0.0461
   7.5100E-01   3.39000E-05 0.0543
   8.0100E-01   2.64000E-05 0.0615
   8.5100E-01   1.71000E-05 0.0765
   9.0100E-01   1.43000E-05 0.0836
   9.5100E-01   7.50000E-06 0.1155
   1.0010E+00   5.60000E-06 0.1336
   1.0510E+00   2.70000E-06 0.1924
   1.1010E+00   1.10000E-06 0.3015
   1.1510E+00   3.00000E-07 0.5774
   1.2010E+00   1.00000E-07 1.0000
   1.2510E+00   0.00000E+00 0.0000
   1.3010E+00   0.00000E+00 0.0000
   1.3510E+00   0.00000E+00 0.0000
   1.4010E+00   0.00000E+00 0.0000
     total      2.42692E-01 0.0006

cell union total         *** All layers treated as a single unit ***
     energy
```

0.0000E+00	5.72000E-05	0.0418
1.0000E-03	4.52894E-01	0.0003
5.1000E-02	**4.56450E-03**	**0.0047**
1.0100E-01	**3.74600E-03**	**0.0052**
1.5100E-01	**3.31360E-03**	**0.0055**
2.0100E-01	**3.72740E-03**	**0.0052**
2.5100E-01	**4.13520E-03**	**0.0049**
3.0100E-01	**3.48020E-03**	**0.0054**
3.5100E-01	**2.82100E-03**	**0.0059**
4.0100E-01	**2.31460E-03**	**0.0066**
4.5100E-01	**1.81090E-03**	**0.0074**
5.0100E-01	**1.42400E-03**	**0.0084**
5.5100E-01	**1.08660E-03**	**0.0096**
6.0100E-01	**8.46200E-04**	**0.0109**
6.5100E-01	**6.55400E-04**	**0.0123**
7.0100E-01	**4.90800E-04**	**0.0143**
7.5100E-01	**3.71400E-04**	**0.0164**
8.0100E-01	**2.83300E-04**	**0.0188**
8.5100E-01	**2.13600E-04**	**0.0216**
9.0100E-01	**1.59800E-04**	**0.0250**
9.5100E-01	**1.19600E-04**	**0.0289**
1.0010E+00	**6.34000E-05**	**0.0397**
1.0510E+00	**3.82000E-05**	**0.0512**
1.1010E+00	**2.95000E-05**	**0.0582**
1.1510E+00	**9.80000E-06**	**0.1010**
1.2010E+00	**1.60000E-06**	**0.2500**
1.2510E+00	**4.00000E-07**	**0.5000**
1.3010E+00	**2.00000E-07**	**0.7071**
1.3510E+00	**0.00000E+00**	**0.0000**
1.4010E+00	**0.00000E+00**	**0.0000**
total	4.88659E-01	0.0003

==========
==========

```
           results of 10 statistical checks for the estimated answer for the tally fluctuation chart (tfc)
bin of tally        8

 tfc bin     --mean--      ---------relative error---------      ----variance of the variance----      --
figure of merit--     -pdf-
 behavior    behavior      value   decrease   decrease rate      value   decrease   decrease rate
value     behavior     slope

 desired      random       <0.10      yes      1/sqrt(nps)       <0.10      yes        1/nps
constant    random      >3.00
 observed     random        0.00      yes          yes            0.00      yes         yes
constant    random      10.00
 passed?        yes          yes      yes          yes             yes      yes         yes
yes        yes         yes


==========================================================================================================
========================


 this tally meets the statistical criteria used to form confidence intervals: check the tally fluctuation
chart to verify.
 the results in other bins associated with this tally may not meet these statistical criteria.

 ----- estimated confidence intervals:  -----

 estimated asymmetric confidence interval(1,2,3 sigma): 4.8710E-01 to 4.8741E-01; 4.8694E-01 to 4.8757E-01;
4.8678E-01 to 4.8773E-01
 estimated  symmetric confidence interval(1,2,3 sigma): 4.8710E-01 to 4.8741E-01; 4.8694E-01 to 4.8757E-01;
4.8678E-01 to 4.8773E-01

1analysis of the results in the tally fluctuation chart bin (tfc) for tally        8 with nps=    10000000
print table 160


 normed average tally per history  = 4.87254E-01          unnormed average tally per history  = 4.87254E-01
 estimated tally relative error    = 0.0003               estimated variance of the variance  = 0.0000
 relative error from zero tallies  = 0.0003               relative error from nonzero scores  = 0.0000
```

```
 number of nonzero history tallies =     4872538          efficiency for the nonzero tallies  = 0.4873
 history number of largest  tally  =           1          largest  unnormalized history tally = 1.00000E+00
 (largest  tally)/(average tally)  = 2.05232E+00          (largest  tally)/(avg nonzero tally)= 1.00000E+00

 (confidence interval shift)/mean  = 0.0000               shifted confidence interval center  = 4.87254E-01


 if the largest  history score sampled so far were to occur on the next history, the tfc bin quantities
would change as follows:

      estimated quantities           value at nps           value at nps+1
value(nps+1)/value(nps)-1.

      mean                            4.87254E-01            4.87254E-01                    0.000000
      relative error                  3.24395E-04            3.24395E-04                    0.000000
      variance of the variance        2.60114E-10            2.60112E-10                   -0.000008
      shifted center                  4.87254E-01            4.87254E-01                    0.000000
      figure of merit                 4.24704E+03            4.24704E+03                    0.000000

 the 100 largest  history tallies appear to have a  maximum value of about 1.00000E+00
 the large score tail of the empirical history score probability density function appears to have no
unsampled regions.

 fom = (histories/minute)*(f(x) signal-to-noise ratio)**2 = (4.469E+03)*( 9.748E-01)**2 =
(4.469E+03)*(9.503E-01) = 4.247E+03

1    some tally scores were not made for various reasons:

                                   beyond last bin     not in
                   tally      angle   energy   time    user
                      8          0       2       0       0

1status of the statistical checks used to form confidence intervals for the mean for each tally bin


 tally   result of statistical checks for the tfc bin (the first check not passed is listed) and error
magnitude check for all bins
```

8 passed the 10 statistical checks for the tally fluctuation chart bin result
missed all bin error check: 155 tally bins had 15 bins with zeros and 25 bins with relative errors exceeding 0.10

the 10 statistical checks are only for the tally fluctuation chart bin and do not apply to other tally bins.

the tally bins with zeros may or may not be correct: compare the source, cutoffs, multipliers, et cetera with the tally bins.

warning. 1 of the 1 tallies had bins with relative errors greater than recommended.
1tally fluctuation charts

nps	mean	tally error	vov	8 slope	fom
512000	4.8683E-01	0.0014	0.0000	10.0	4393
1024000	4.8704E-01	0.0010	0.0000	10.0	4310
1536000	4.8736E-01	0.0008	0.0000	10.0	4295
2048000	4.8729E-01	0.0007	0.0000	10.0	4279
2560000	4.8714E-01	0.0006	0.0000	10.0	4266
3072000	4.8700E-01	0.0006	0.0000	10.0	4258
3584000	4.8721E-01	0.0005	0.0000	10.0	4260
4096000	4.8713E-01	0.0005	0.0000	10.0	4258
4608000	4.8712E-01	0.0005	0.0000	10.0	4254
5120000	4.8709E-01	0.0005	0.0000	10.0	4252
5632000	4.8712E-01	0.0004	0.0000	10.0	4250
6144000	4.8712E-01	0.0004	0.0000	10.0	4250
6656000	4.8717E-01	0.0004	0.0000	10.0	4250
7168000	4.8717E-01	0.0004	0.0000	10.0	4250
7680000	4.8724E-01	0.0004	0.0000	10.0	4250
8192000	4.8725E-01	0.0004	0.0000	10.0	4249
8704000	4.8724E-01	0.0003	0.0000	10.0	4249
9216000	4.8725E-01	0.0003	0.0000	10.0	4249
9728000	4.8730E-01	0.0003	0.0000	10.0	4248
10000000	4.8725E-01	0.0003	0.0000	10.0	4247

```
************************************************************************************************************
************

 dump no.    2 on file runtpe     nps =    10000000     coll =    27914571318     ctm =     2237.52   nrn =
 125633919264

         6 warning messages so far.


 run terminated when    10000000  particle histories were done.

 computer time = 2237.62 minutes

 mcnp     version 5     09282010                     06/23/14 05:50:35                     probid =
06/23/14 05:04:48
```

Detector #2

Neutron Source, Validation Experiment, BLC Geometry, 3.175 mm scintillator

```
         1-       Big Beryllium Detector
         2-       c    *** Detector Cell Cards ***
         3-       101   400  -8.03     -101  102             $ Housing
         4-       102   400  -8.03     -102  -103            $ SS Layer
         5-       103   600  -0.178    -102  103  -104       $ Cardboard
         6-       104   100  -1.848    -102  104  -105       $ Beryllium
         7-       105   200  -1.032    -102  105  -106       $ scintil
         8-       106   100  -1.848    -102  106  -107       $ Beryllium
         9-       107   200  -1.032    -102  107  -108       $ scintill
        10-       108   100  -1.848    -102  108  -109       $ Beryllium
        11-       109   200  -1.032    -102  109  -110       $ scintill
        12-       110   100  -1.848    -102  110 -111        $ Beryllium
```

```
13-        111   200  -1.032    -102  111 -112        $ scintilla
14-        112   100  -1.848    -102  112 -113        $ Beryllium
15-        113   200  -1.032    -102  113 -114        $ scintilla
16-        114   100  -1.848    -102  114 -115        $ Beryllium
17-        115   200  -1.032    -102  115 -116        $ scintilla
18-        116   100  -1.848    -102  116 -117        $ Beryllium
19-        117   200  -1.032    -102  117 -118        $ scintilla
20-        118   100  -1.848    -102  118 -119        $ Beryllium
21-        119   200  -1.032    -102  119 -120        $ scintilla
22-        120   100  -1.848    -102  120 -121        $ Beryllium
23-        121   200  -1.032    -102  121 -122        $ scintilla
24-        122   100  -1.848    -102  122 -123        $ Beryllium
25-        123   200  -1.032    -102  123 -124        $ scintilla
26-        124   100  -1.848    -102  124 -125        $ Beryllium
27-        125   600  -0.178    -102  125 -126        $ Cardboa
28-        126   400  -8.03     -102 126              $ SS Layer
29-        127   400  -8.03    -127  128              $ flange
30-        128   400  -8.03    -128 129               $ PMT wall
31-        129     0           -129                  $ void in PMT
32-        c   *** Top Stand Cell Cards ***
33-        20   400  -8.03     10  -13  14  -15  -16  17            $ Top plate
34-        21   400  -8.03     10  -13  14  -15  -21  22            $ Bottom plate
35-        22   400  -8.03     10  -11  14  -15  -17  18            $ Top hinge (1)
36-        23   400  -8.03     12  -13  14  -15  -17  18            $ Top hinge (2)
37-        24   400  -8.03     10  -11  14  -15  -20  21            $ Bottom hinge (1)
38-        25   400  -8.03     12  -13  14  -15  -20  21            $ Bottom hinge (2)
39-        26   400  -8.03     11  -12  -17  19  -23  24            $ Front support-top
40-        27   400  -8.03     11  -12  -19  21  -25  26            $ Front support-bot
41-        28   400  -8.03    -27   28  -38  -18  19  31            $ Side support-front-t
42-        29   400  -8.03    -29   30  -38  -19  20  31            $ Side support-front-b
43-        30   400  -8.03     32  -33  -38  -18  19  31            $ Side support-front-t
44-        31   400  -8.03     34  -35  -38  -19  20  31            $ Side support-front-b
45-        32   400  -8.03    -36                                   $ front bolt
46-        33   400  -8.03    -37                                   $ back bolt
```

```
47-       34    0          -10 -16 22 14 -15 -47                    $ void left
48-       35    0           13 -16 22 14 -15 39 -47                 $ void right
49-       36    0          -14 -16 22 -47                           $ void front
50-       37    0           15 -16 22 41 42 -47                     $ void back
51-       38    0           16 101 127 128 -47                      $ void top
52-       39    0          -22 40 41 42 43 44 45 46 -47             $ void bottom
53-       40    0           (14 -31 10 -11 -18 20 36 37):(-38 31 -32 -34 10 36 37)
54-       41    0           (14 -31 12 -13 -18 20 36 37):(-38 31 27 29 -13 36 37)
55-       42    0           (11 -12 14 -17 19 -24):(11 -12 14 -19 21 -26)
56-       43    0           (11 -12 -31 23 -17 19 36):(11 -12 -31 25 -19 21 36)
57-       44    0 (31 -38 -19 21 -12 11 -30 35  37):(-17 19 31 -38 -12 11 -28 33 37)
58-       45    0 38 -15 37 11 -12 -17 21:38 -15 10 -11 -18 20 37:38 -15 12 -13 -18 20 37
59-       46   300 -2.7  -39                                        $ knob
60-       c    *** Plate below lower stand cell cards ***
61-       47   300 -2.7  -40                                        $ plate
62-       48   300 -2.7  -41                                        $ knob spacer
63-       49   300 -2.7  -42                                        $ knob
64-       c    *** Stand Base plate cell cards ***
65-       50   300 -2.7  -43                                        $ base plate
66-       51   300 -2.7  -44                                        $ knob spacer
67-       52   300 -2.7  -45                                        $ knob
68-       53   300 -2.7  -46                                        $ pole
69-       c    *** Target chamber cell cards ***
70-       54   300 -2.7  -50  51 56 58 60                 $ vacuum chamber outer
71-       55     0        -51 62                          $ Vacuum chamber
72-       56   300 -2.7   -52                              $ Upper flange
73-       57   400  -8.03   -53                            $ Upper hardware
74-       58   300 -2.7   -54                              $ Lower chamber dial
75-       59   300 -2.7   -55                              $ Sample holder
76-       60     0        -57 51                          $ Inside beam line
77-       61   300 -2.7   -56 57 51                       $ beam line tube
78-       62   300 -2.7   -58 59 56 51                    $ 165 SBD
79-       63     0         -59 56 51                      $ 165 SBD inside
80-       64   300 -2.7    -60 61 51                      $ 110 SBD
```

```
 81-        65     0          -61 51                          $ 110 SBD inside
 82-        66   300 -2.7     -62                             $ Target holder
 83-        68    0           50 52 53 54 55 56 58 60 -64
 84-        69    0           64 47 -65                       $ Inside room
 85-        70   500 -2.31    65 -66                          $ Concrete
 86-        71     0          66
 87-
 88-        c    *** Detector Surface Cards ***
 89-        101   1  rpp -8.89  8.89  0  14.9225  -8.255   7.9375            $ outside detec
 90-        102   1  rpp -7.9375  7.9375  0.635 14.2875  -7.9375  7.9375     $ inside detect
 91-        103   1  py   1.11125
 92-        104   1  py 2.38125
 93-        105   1  py 3.01625
 94-        106   1  py 3.33375
 95-        107   1  py 3.96875
 96-        108   1  py 4.28625
 97-        109   1  py 4.92125
 98-        110   1 py 5.23875
 99-        111   1 py 5.87375
100-        112   1 py 6.19125
101-        113   1 py 6.82625
102-        114   1 py 7.14375
103-        115   1 py 7.77875
104-        116   1 py 8.09625
105-        117   1 py 8.73125
106-        118   1 py 9.04875
107-        119   1 py 9.68375
108-        120   1 py 10.00125
109-        121   1 py 10.63625
110-        122   1 py 10.95375
111-        123   1 py 11.58875
112-        124   1 py 11.90625
113-        125   1 py 12.54125
114-        126   1 py   13.81125
```

```
115-        127   1 rpp -8.89  8.89  -.9525 15.875   7.9375  8.5725    $ flange
116-        128   1 rcc  0  7.46125  7.9375  0  0  33.3375   8.4138    $ outside o
117-        129   1 rcc  0  7.46125  7.9375  0  0  33.0200    8.0963   $ inside of
118-        c    *** Top Stand Surface Cards ***  built at origin, translation 2 moves origi
119-        10   2 px   -8.25
120-        11   2 px   -7.2975
121-        12   2 px    7.2975
122-        13   2 px    8.25
123-        14   2 py  -12.065
124-        15   2 py   12.065
125-        16   2 pz    5.5563
126-        17   2 pz    4.6038
127-        18   2 pz    3.0163
128-        19   2 pz    0
129-        20   2 pz   -3.0163
130-        21   2 pz   -4.6038
131-        22   2 pz   -5.5563
132-        23   2 p     0      0.819  -0.574  -5.9363
133-        24   2 p     0      0.819  -0.574  -6.5508
134-        25   2 p     0      0.819   0.574  -5.9363
135-        26   2 p     0      0.819   0.574  -6.5508
136-        27   2 p    0.819  0       -0.574  5.0254
137-        28   2 p    0.819  0       -0.574  4.2453
138-        29   2 p    0.819  0       0.574   5.0254
139-        30   2 p    0.819  0       0.574   4.2453
140-        31   2 py   -3.5
141-        32   2 p    0.819  0        0.574   -5.0254
142-        33   2 p    0.819  0        0.574   -4.2453
143-        34   2 p    0.819  0        -0.574  -5.0254
144-        35   2 p    0.819  0        -0.574  -4.2453
145-        36   2 rcc  -8.2500 -6.6500   0  16.5  0  0  0.4763
146-        37   2 rcc  -8.2500 11.5887   0  16.5  0  0  0.4763
147-        38   2 py   11.1124
148-        39   2 rcc  8.25   -6.6500    0  1.905  0  0  1.905
```

```
149-        c    *** Plate below lower stand surface cards ***
150-        40   2 box  -6.99 -10.795 -5.5563 15.24 0 0 0 22.86 0 0 0 -3.81
151-        41   2 rcc   0.6300 12.0650  -3.6663  0 1.9050 0  1.905
152-        42   2 rcc   0.6300 13.9700  -3.6663  0 0.9525 0  3.4925
153-        c    *** Base plate of stand surface cards ***
154-        43   2 box  -24.77 -10.795 -9.3663  33.02 0 0 0 22.86 0 0 0 -7.9375
155-        44   2 rcc   8.2500  0.6350  -13.3350   1.9050 0  0  1.905
156-        45   2 rcc   10.1550  0.6350  -13.3350  0.9525 0  0  3.4925
157-        c    *** Tripod base pole ***
158-        46   2 rcc  0  0  -17.3038  0  0  -143.8274  1.5875
159-        47   2 rpp  -30 30 -14.8 25 -161.1312 60
160-        c    *** Target chamber ***
161-        50   rcc  0  0  15.24  0  0  -30.4800  7.6200
162-        51   rcc  0  0  15.23  0  0  -29.5275  6.6675
163-        52   rcc  0  0  15.24  0  0    1.9050  9.5250
164-        53   rcc  0  0  17.145 0  0   25.4000  4.4450
165-        54   rcc  0  0 -15.240 0  0   -6.4770  4.1275
166-        55   box  1.27 1.27 -21.717 -40.64 0 0 0 -2.54 0 0 0 -2.54
167-        56   rcc  0  0  0  -38.12  0  0  2.5400
168-        57   rcc  0  0  0  -38.12  0  0  2.2225
169-        58   rcc  0  0  0  -36.82  -9.866  0  2.54
170-        59   rcc  0  0  0  -36.82  -9.866  0  2.2225
171-        60   rcc  0  0  0  0 -38.12  0  2.5400
172-        61   rcc  0  0  0  0 -38.12  0  2.2225
173-        62   box  -1.27 -1.27 15.23 2.54 0 0 0 2.54 0 0 0 -13.66
174-        64   rpp  -50  14.5 -39 10.25 -25 44
175-        c    *** room dimensions
176-        65   rpp -51 175.26  -51 175.26 -175.26  65
177-        66   rpp -51 220.98  -51 220.98 -220.98  65
178-
179-        mode   n p
comment.  photonuclear physics may be needed (phys:p).
180-        imp:n 1 78r 0
181-        imp:p 1 78r 0
```

```
182-       sdef pos= 0 0 0 vec=1 0 0 dir=d3 erg= fdir d4
183-       si3  A -1  -0.866 -0.500 0  0.500 0.866 1
184-       sp3  1.01  1.02  1.04  1.06  1.09 1.11  1.12
185-       ds4  2.071 2.123 2.273 2.496 2.741 2.935 3.009
186-       *tr1 0  12.065 1  0 90 90 90 0 90 90 90 0  1
187-       *tr2 0  25.4026  -14.1288   0 90 90 90 0 90 90 90 0  1
188-       m100 4009 1                  $ Beryllium rho=1.848 g/cc
189-       m200 6000  0.47              $ BC-404, rho=1.032 g/cc
190-            1001  0.53
191-       m300 13027 1                 $ Aluminum, rho=2.7 g/cc
192-       m400 6000   -0.0008          $ Stainless Steel 304 rho=8.03 g/cc
193-            25055      -0.0200
194-            24000  -0.1900
195-            28000  -0.1000
196-            14000  -0.0075
197-            15031  -0.00045
198-            16000  -0.0003
199-            7014   -0.0010
200-            26000  -0.67995
201-       m500 1001   -0.00453         $ Concrete (LANL Mix from DANT) rho=2.25 g/cc
202-            8016   -0.51260
203-            14000  -0.36036
204-            13027  -0.03555
205-            11023  -0.01527
206-            20000  -0.05791
207-            26000  -0.01378
208-       m600 6000   -0.50       $ cardboard from 1984 forestry pub.
209-            8016   -0.44
210-            1001   -0.06
211-       f4:n      104 106 108 110 112 114 116 118 120 122 124 t
212-       fm4    -1 100 107
213-       nps   1e8
214-       prdmp 9e9  9e9  9e9
215-
```

```
  warning.  there are only neutron tallies in this problem.

    minimum source weight = 1.0000E+00    maximum source weight = 1.0000E+00

 ***************************************************
 * Random Number Generator  =                    1 *
 * Random Number Seed       =       19073486328125 *
 * Random Number Multiplier =       19073486328125 *
 * Random Number Adder      =                    0 *
 * Random Number Bits Used  =                   48 *
 * Random Number Stride     =               152917 *
 ***************************************************


          1 warning message so far.
1cross-section tables
print table 100

     table    length

                        tables from file endf70a

   1001.70c    5533   1-H -  1 at 293.6K from endf/b-vii.0 njoy99.248     mat 125      03/27/08
   4009.70c  285797   4-Be-  9 at 293.6K from endf/b-vii.0 njoy99.248     mat 425      08/24/07
   6000.70c   55095   6-C -  0 at 293.6K from endf/b-vii.0 njoy99.248     mat 600      08/24/07
   7014.70c  102655   7-N - 14 at 293.6K from endf/b-vii.0 njoy99.248     mat 725      08/24/07
   8016.70c  264123   8-O - 16 at 293.6K from endf/b-vii.0 njoy99.248     mat 825      08/25/07
  11023.70c   62862  11-Na- 23 at 293.6K from endf/b-vii.0 njoy99.248     mat1125      08/25/07
  13027.70c  158468  13-Al- 27 at 293.6K from endf/b-vii.0 njoy99.248     mat1325      08/25/07
  15031.70c   35741  15-P - 31 at 293.6K from endf/b-vii.0 njoy99.248     mat1525      08/25/07

                        tables from file endf60
```

```
14000.60c   98643  14-si-nat from endf/b-vi                            mat1400      11/25/93

                      tables from file actia

16000.62c   98522  16-s-0 at 293.6K from endf/b-vi.8 njoy99.50         mat1600      12/06/01
20000.62c  123189  20-ca-0 at 293.6K from endf-vi.8 njoy99.50          mat2000      12/05/01

                      tables from file rmccs

24000.50c  117261  njoy  (  1324)      79/06/21.
26000.55c  142443  njoy  ( 260)       10/21/82
28000.50c  105647  njoy  (  1328)      79/06/21.

                      tables from file endf70b

25055.70c  250045  25-Mn- 55 at 293.6K from endf/b-vii.0 njoy99.248    mat2525      08/26/07

                      tables from file mcplib04

 1000.04p    1898  ENDF/B-VI Release 8 Photoatomic Data for 1-H        mat 100      02/07/03
 4000.04p    2363  ENDF/B-VI Release 8 Photoatomic Data for 4-BE       mat 400      02/07/03
 6000.04p    3152  ENDF/B-VI Release 8 Photoatomic Data for 6-C        mat 600      02/07/03
 7000.04p    3194  ENDF/B-VI Release 8 Photoatomic Data for 7-N        mat 700      02/07/03
 8000.04p    3272  ENDF/B-VI Release 8 Photoatomic Data for 8-O        mat 800      02/07/03
11000.04p    3995  ENDF/B-VI Release 8 Photoatomic Data for 11-NA      mat1100      02/07/03
13000.04p    4846  ENDF/B-VI Release 8 Photoatomic Data for 13-AL      mat1300      02/07/03
14000.04p    4792  ENDF/B-VI Release 8 Photoatomic Data for 14-SI      mat1400      02/07/03
15000.04p    4498  ENDF/B-VI Release 8 Photoatomic Data for 15-P       mat1500      02/07/03
16000.04p    4654  ENDF/B-VI Release 8 Photoatomic Data for 16-S       mat1600      02/07/03
20000.04p    5013  ENDF/B-VI Release 8 Photoatomic Data for 20-CA      mat2000      02/07/03
24000.04p    5682  ENDF/B-VI Release 8 Photoatomic Data for 24-CR      mat2400      02/07/03
25000.04p    5598  ENDF/B-VI Release 8 Photoatomic Data for 25-MN      mat2500      02/07/03
26000.04p    5718  ENDF/B-VI Release 8 Photoatomic Data for 26-FE      mat2600      02/07/03
28000.04p    5826  ENDF/B-VI Release 8 Photoatomic Data for 28-NI      mat2800      02/07/03
```

```
  total     1970525

 maximum photon energy set to  100.0 mev (maximum electron energy)

                        tables from file el03

   1000.03e    2329   6/6/98
   4000.03e    2331   6/6/98
   6000.03e    2333   6/6/98
   7000.03e    2333   6/6/98
   8000.03e    2333   6/6/98
  11000.03e    2337   6/6/98
  13000.03e    2337   6/6/98
  14000.03e    2339   6/6/98
  15000.03e    2339   6/6/98
  16000.03e    2339   6/6/98
  20000.03e    2343   6/6/98
  24000.03e    2345   6/6/98
  25000.03e    2345   6/6/98
  26000.03e    2345   6/6/98
  28000.03e    2347   6/6/98

  warning.  material      100 has been set to a conductor.

  warning.  material      300 has been set to a conductor.


*************************************************************************************************
*********************

1problem summary

      run terminated when   100000000  particle histories were done.
```

```
+
10/10/14 07:13:46
      Big Beryllium Detector                                probid =  10/10/14 06:47:50
0
 neutron creation tracks  weight   energy   neutron loss   tracks      weight        energy
 (per source particle)                                          (per source particle)
source      100000000  1.0000E+00 2.5196E+00  escape       97016921   9.4371E-01   1.8909E+00
                                               energy cutoff            0    0.          0.
                                               time cutoff              0    0.          0.
 weight window     0  0.         0.           weight window            0    0.          0.
 cell importance   0  0.         0.           cell importance          0    0.          0.
 weight cutoff     0  7.1641E-03 1.0170E-09   weight cutoff      3026637    7.1638E-03  1.0876E-09
 e or t importance 0  0.         0.           e or t importance        0    0.          0.
 dxtran            0  0.         0.           dxtran                   0    0.          0.
 forced collisions 0  0.         0.           forced collisions        0    0.          0.
 exp. transform    0  0.         0.           exp. transform           0    0.          0.
 upscattering      0  0.         2.7251E-08   downscattering           0    0.          6.1788E-01
 photonuclear      0  0.         0.           capture                  0    5.6711E-02  9.9173E-03
 (n,xn)        87118  8.3442E-04 2.0079E-04   loss to (n,xn)       43559    4.1721E-04  1.0367E-03
 prompt fission    0  0.         0.           loss to fission          0    0.          0.
 delayed fission   0  0.         0.
 total     100087118  1.0080E+00 2.5198E+00   total            100087117    1.0080E+00  2.5198E+00

   number of neutrons banked                    43559        average time of (shakes)
cutoffs
   neutron tracks per source particle     1.0009E+00          escape            2.7544E+03
tco   1.0000E+33
   neutron collisions per source particle 1.1973E+01          capture           3.7667E+04
eco   0.0000E+00
   total neutron collisions               1197321078          capture or escape 4.7336E+03
wc1  -5.0000E-01
   net multiplication              1.0004E+00 0.0000          any termination   5.4316E+03
wc2  -2.5000E-01
0
```

```
 photon creation     tracks   weight  energy   photon loss   tracks   weight     energy
 (per source particle)                         (per source particle)
 source                0 0.         0.         escape       10542094    1.0546E-01    1.2011E-01
                                                energy cutoff       0    0.            1.5769E-05
                                                time cutoff         0    0.            0.
 weight window          0 0.         0.         weight window       0    0.            0.
 cell importance        0 0.         0.         cell importance     0    0.            0.
 weight cutoff          0 0.         0.         weight cutoff       0    0.            0.
 e or t importance      0 0.         0.         e or t importance   0    0.            0.
 dxtran                 0 0.         0.         dxtran              0    0.            0.
 forced collisions      0 0.         0.         forced collisions   0    0.            0.
 exp. transform         0 0.         0.         exp. transform      0    0.            0.
 from neutrons   24375752 2.4379E-01 5.2510E-01 compton scatter     0    0.            3.6220E-01
 bremsstrahlung   7281144 7.2826E-02 6.1345E-03 capture      24412727    2.4415E-01    1.4612E-02
 p-annihilation   1722282 1.7225E-02 8.8023E-03 pair production861141    8.6127E-03    4.3206E-02
 photonuclear           0 0.         0.         photonuclear abs    0    0.            0.
 electron x-rays        0 0.         0.
 1st fluorescence 2436786 2.4382E-02 1.1591E-04
 2nd fluorescence       0 0.         0.
 total           35815964 3.5822E-01 5.4015E-01 total        35815962    3.5822E-01    5.4015E-01

number of photons banked                 33379178        average time of (shakes)
cutoffs
   photon tracks per source particle      3.5816E-01          escape            1.1027E+04
tco   1.0000E+33
   photon collisions per source particle  1.7016E+00          capture           2.2979E+04
eco   1.0000E-03
   total photon collisions                 170157066          capture or escape 1.9374E+04
wc1  -5.0000E-01
                                                              any termination   1.9812E+04
wc2  -2.5000E-01

 computer time so far in this run  1235.63 minutes            maximum number ever in bank
17
```

```
 computer time in mcrun            1235.33 minutes            bank overflows to backup file
0
 source particles per minute            8.0950E+04
 random numbers generated              20573167119            most random numbers used was
15283 in history    71021241

 range of sampled source weights = 1.0000E+00 to 1.0000E+00

      2 particles got lost.

 neutron-induced photon production mt loop failed   2 times.

 number of histories processed by each thread
    14342875    14243672    14277774    14326676    14294411    14269229    14245363
1energy distribution of photons produced in neutron collisions

  energy      number of        number       cum number      weight of       weight       cum
weight
 interval      photons        frequency    distribution      photons       frequency
distribution

20.000             0      0.00000E+00    0.00000E+00    0.00000E+00    0.00000E+00    0.00000E+00
15.000             0      0.00000E+00    0.00000E+00    0.00000E+00    0.00000E+00    0.00000E+00
10.000          9574      3.92767E-04    3.92767E-04    9.57335E-05    3.92694E-04    3.92694E-04
 9.000         35021      1.43671E-03    1.82948E-03    3.49077E-04    1.43190E-03    1.82459E-03
 8.000         89640      3.67743E-03    5.50691E-03    8.96706E-04    3.67824E-03    5.50283E-03
 7.000        669179      2.74527E-02    3.29596E-02    6.68988E-03    2.74415E-02    3.29443E-02
    6.000      700699      2.87457E-02    6.17053E-02    7.00842E-03    2.87481E-02    6.16925E-02
    5.000      316312      1.29765E-02    7.46818E-02    3.16976E-03    1.30022E-02    7.46946E-02
    4.000     1587314      6.51186E-02    1.39800E-01    1.58764E-02    6.51243E-02    1.39819E-01
    3.000     1916835      7.86370E-02    2.18437E-01    1.91721E-02    7.86431E-02    2.18462E-01
    2.000     4091449      1.67849E-01    3.86286E-01    4.09216E-02    1.67858E-01    3.86320E-01
    1.000     8654741      3.55055E-01    7.41342E-01    8.65490E-02    3.55019E-01    7.41339E-01
    0.500     4530651      1.85867E-01    9.27209E-01    4.53064E-02    1.85845E-01    9.27184E-01
```

```
    0.100     1077236      4.41929E-02    9.71402E-01    1.07877E-02    4.42505E-02    9.71434E-01
    0.010      611687      2.50941E-02    9.96496E-01    6.11449E-03    2.50813E-02    9.96516E-01
    0.000       85414      3.50406E-03    1.00000E+00    8.49471E-04    3.48448E-03    1.00000E+00

   total       24375752      1.00000E+00                   2.43787E-01    1.00000E+00

1tally        4        nps =   100000000
           tally type 4    track length estimate of particle flux.
           tally for  neutrons

           volumes
                   cell:      104          106          108          110          112          114
116
                         1.60030E+02  1.60030E+02  1.60030E+02  1.60030E+02  1.60030E+02
1.60030E+02  1.60030E+02
                   cell:      118          120          122          124         total
                         1.60030E+02  1.60030E+02  1.60030E+02  1.60030E+02  1.76033E+03
 *** Total Volume of Beryllium ***
 *** He-6 nuclei produced per layer per unit volume
 cell  104
 multiplier bin:  -1.00000E+00       100         107
                 3.10541E-06 0.0004

 cell  106
 multiplier bin:  -1.00000E+00       100         107
                 2.37621E-06 0.0005

 cell  108
 multiplier bin:  -1.00000E+00       100         107
                 1.81506E-06 0.0006

 cell  110
 multiplier bin:  -1.00000E+00       100         107
                 1.39091E-06 0.0006
```

```
cell  112
multiplier bin:  -1.00000E+00       100         107
                1.07037E-06 0.0007

cell  114
multiplier bin:  -1.00000E+00       100         107
                8.26284E-07 0.0008

cell  116
multiplier bin:  -1.00000E+00       100         107
                6.40334E-07 0.0009

cell  118
multiplier bin:  -1.00000E+00       100         107
                4.98128E-07 0.0011

cell  120
multiplier bin:  -1.00000E+00       100         107
                3.89394E-07 0.0012

cell  122
multiplier bin:  -1.00000E+00       100         107
                3.04903E-07 0.0013

cell  124
multiplier bin:  -1.00000E+00       100         107
                2.40318E-07 0.0015

cell union total
multiplier bin:  -1.00000E+00       100         107
                1.15067E-06 0.0005
```

```
=================================================================================================
==================================

           results of 10 statistical checks for the estimated answer for the tally fluctuation
chart (tfc) bin of tally        4

 tfc bin     --mean--      ---------relative error---------      ----variance of the variance----
--figure of merit--     -pdf-
 behavior    behavior      value   decrease   decrease rate      value   decrease   decrease rate
value     behavior     slope

 desired      random       <0.10      yes      1/sqrt(nps)       <0.10      yes        1/nps
constant    random      >3.00
 observed     random        0.00      yes          yes            0.00      yes         yes
decrease   decrease     10.00
 passed?        yes          yes      yes          yes             yes      yes         yes
no         no         yes


=================================================================================================
==================================


 warning.  the tally in the tally fluctuation chart bin did not pass  2 of the 10 statistical
checks.

1analysis of the results in the tally fluctuation chart bin (tfc) for tally        4 with nps=
100000000 print table 160

 normed average tally per history  = 3.10541E-06          unnormed average tally per history  =
4.96959E-04
 estimated tally relative error    = 0.0004               estimated variance of the variance  =
0.0000
```

```
 relative error from zero tallies  = 0.0004               relative error from nonzero scores  =
0.0002

 number of nonzero history tallies =     6740001          efficiency for the nonzero tallies  =
0.0674
 history number of largest  tally  =    55491794          largest  unnormalized history tally =
2.02055E-01
 (largest  tally)/(average tally)  = 4.06582E+02          (largest  tally)/(avg nonzero tally)=
2.74037E+01

 (confidence interval shift)/mean  = 0.0000               shifted confidence interval center  =
3.10541E-06


 if the largest  history score sampled so far were to occur on the next history, the tfc bin
quantities would change as follows:

      estimated quantities           value at nps           value at nps+1
value(nps+1)/value(nps)-1.

      mean                            3.10541E-06            3.10542E-06
0.000004
      relative error                  4.35977E-04            4.35994E-04
0.000039
      variance of the variance        9.08515E-07            9.15844E-07
0.008067
      shifted center                  3.10541E-06            3.10541E-06
0.000000
      figure of merit                 4.25885E+03            4.25851E+03                    -
0.000078

 the estimated slope of the 200 largest  tallies starting at  9.16426E-02 appears to be decreasing
at least exponentially.
```

```
 the large score tail of the empirical history score probability density function appears to have
no unsampled regions.

 fom = (histories/minute)*(f(x) signal-to-noise ratio)**2 = (8.095E+04)*( 2.294E-01)**2 =
(8.095E+04)*(5.261E-02) = 4.259E+03

1unnormed tally density for tally        4          nonzero tally mean(m) = 7.373E-03   nps =
100000000

*******************************************************************************************
*********************

 dump no.    2 on file runtpe     nps =   100000000     coll =     1367478144     ctm =
1235.33   nrn =
 20573167119

 run terminated when   100000000  particle histories were done.

 computer time = 1235.63 minutes
 mcnp     version 5     09282010                     10/10/14 07:13:46                     probid
=  10/10/14 06:47:50
```

He-6 beta source, Validation Experiment, BLC Geometry, 3.175 mm scintillator

```
1-       c    *** Detector Cell Cards ***
2-       1   400  -8.03     -2  1                 $ Housing
3-       2   400  -8.03     -1  -3                $ SS Layer
4-       3   600  -0.178    -1  3  -4             $ Cardboard
5-       4   100  -1.848    -1  4  -5             $ Beryllium
6-       5   200  -1.032    -1  5  -6             $ scintillator
7-       6   100  -1.848    -1  6  -7             $ Beryllium
8-       7   200  -1.032    -1  7  -8             $ scintillator
9-       8   100  -1.848    -1  8  -9             $ Beryllium
```

```
9   200  -1.032    -1  9  -10            $ scintillator
10   100  -1.848    -1  10 -11           $ Beryllium
11   200  -1.032    -1  11 -12           $ scintillator
12   100  -1.848    -1  12 -13           $ Beryllium
13   200  -1.032    -1  13 -14           $ scintillator
14   100  -1.848    -1  14 -15           $ Beryllium
15   200  -1.032    -1  15 -16           $ scintillator
16   100  -1.848    -1  16 -17           $ Beryllium
17   200  -1.032    -1  17 -18           $ scintillator
18   100  -1.848    -1  18 -19           $ Beryllium
19   200  -1.032    -1  19 -20           $ scintillator
20   100  -1.848    -1  20 -21           $ Beryllium
21   200  -1.032    -1  21 -22           $ scintillator
22   100  -1.848    -1  22 -23           $ Beryllium
23   200  -1.032    -1  23 -24           $ scintillator
24   100  -1.848    -1  24 -25           $ Beryllium
25   600  -0.178    -1  25 -26           $ Cardboard
26   400  -8.03     -1 26                $ SS Layer
27   400  -8.03    -27  28               $ flange
28   400  -8.03    -28 29                $ PMT wall
29     0           -29                  $ void in PMT
31     0            1 27 28 -30
32     0            30

c    *** Detector Surface Cards ***
1     rpp -8.89  8.89  0  14.9225  -8.255   7.9375    $ outside detector
2     rpp -7.9375  7.9375  0.635 14.2875  -7.9375  7.9375     $ inside detector
3     py   1.11125
4     py 2.38125
5     py 3.01625
6     py 3.33375
7     py 3.96875
8     py 4.28625
9     py 4.92125
```

```
44-        10    py 5.23875
45-        11    py 5.87375
46-        12    py 6.19125
47-        13    py 6.82625
48-        14    py 7.14375
49-        15    py 7.77875
50-        16    py 8.09625
51-        17    py 8.73125
52-        18    py 9.04875
53-        19    py 9.68375
54-        20    py 10.00125
55-        21    py 10.63625
56-        22    py 10.95375
57-        23    py 11.58875
58-        24    py 11.90625
59-        25    py 12.54125
60-        26    py   13.81125
61-        27    rpp -8.89  8.89  -.9525 15.875   7.9375  8.5725    $ flange
62-        28    rcc  0  7.46125  7.9375  0  0  33.3375   8.4138    $ outside of
63-        29    rcc  0  7.46125  7.9375  0  0  33.0200    8.0963   $ inside of P
64-        30  rpp -15 15 -25 25 -10 50
65-
66-        mode   p e
67-        imp:p 1 27r 0 1 0
68-        imp:e 1 27r 0 1 0
69-        sdef par=3 x=d2 y =d3 z=d4  erg=d1
70-        si1   L 0 0.2852 0.3667 0.4414 0.5161 0.5840 0.6520 0.7267 0.8014 0.8761
71-              0.9576 1.0323 1.1070 1.1749 1.2564 1.3311 1.4805 1.5552 1.6299
72-              1.7046 1.7793 1.8540 1.9219 2.0034 2.0713 2.1460 2.2207 2.2954
73-              2.3633 2.4448 2.5127 2.5874 2.6689 2.7436 2.8115 2.8795 2.9542
74-              3.0289 3.1104 3.1783 3.2530 3.3209 3.4024 3.4703
75-        sp1   0 0.01340 0.01720 0.02014 0.02239 0.02429 0.02584 0.02731 0.02878
76-              0.02999 0.03094 0.03189 0.03267 0.03362 0.03405 0.03457 0.03509
77-              0.03518 0.03492 0.03492 0.03440 0.03319 0.03241 0.03129 0.02982
```

```
 78-             0.02809 0.02679 0.02498 0.02316 0.02092 0.01919 0.01711 0.01513
 79-             0.01305 0.01098 0.00916 0.00717 0.00553 0.00415 0.00285 0.00190
 80-             0.00112 0.00069 0.00026
 81-       si2   -7.9375 7.9375
 82-       sp2   0 1
 83-       si3   s 5 6 7 8 9 10 11 12 13 14 15
 84-       sp3   3.11 2.38 1.82 1.39 1.07 .826 .640 .498 .389 .304 .240
 85-       si4   -7.9375 7.9375
 86-       sp4   0 1
 87-       si5   2.38125 3.01625
 88-       sp5   0 1
 89-       si6   3.33375 3.96875
 90-       sp6   0 1
 91-       si7   4.28625 4.92125
 92-       sp7   0 1
 93-       si8   5.23875 5.87375
 94-       sp8   0 1
 95-       si9   6.19125 6.82625
 96-       sp9   0 1
 97-       si10  7.14375 7.77875
 98-       sp10  0 1
 99-       si11  8.09625 8.73125
100-       sp11  0 1
101-       si12  9.04875 9.68375
102-       sp12  0 1
103-       si13  10.00125 10.63625
104-       sp13  0 1
105-       si14  10.95375 11.58875
106-       sp14  0 1
107-       si15  11.90625 12.54125
108-       sp15  0 1
109-       m100 4009 1                  $ Beryllium rho=1.848 g/cc
110-       m200 6000  0.47              $ BC-404, rho=1.032 g/cc
111-            1001  0.53
```

```
     112-       m300 13027 1                 $ Aluminum, rho=2.7 g/cc
 warning.  material      300 is not used in the problem.
     113-       m400 6000   -0.0008          $ Stainless Steel 304 rho=8.03 g/cc
     114-            25055      -0.0200
     115-            24000  -0.1900
     116-            28000  -0.1000
     117-            14000  -0.0075
     118-            15031  -0.00045
     119-            16000  -0.0003
     120-            7014   -0.0010
     121-            26000  -0.67995
     122-       m500 6000   -0.625017       $ mylar
 warning.  material      500 is not used in the problem.
     123-            8016   -0.333024
     124-            1001   -0.041959
     125-       m600 6000   -0.50       $ cardboard from 1984 forestry pub.
     126-            8016   -0.44
     127-            1001   -0.06
     128-       f8:e,p  5 7 9 11 13 15 17 19 21 23 t
     129-       e8    0  0.001  27i  1.4 1.9 2.4 2.9 3.5
     130-       prdmp 1e15 1e15 1e15
     131-       nps 1e6
     132-

****************************************************
* Random Number Generator  =                     1 *
* Random Number Seed       =       19073486328125 *
* Random Number Multiplier =       19073486328125 *
* Random Number Adder      =                     0 *
* Random Number Bits Used  =                    48 *
* Random Number Stride     =               152917 *
****************************************************
```

```
         2 warning messages so far.
1cross-section tables
print table 100

     table    length

                        tables from file mcplib04

   1000.04p    1898  ENDF/B-VI Release 8 Photoatomic Data for 1-H    mat 100      02/07/03
   4000.04p    2363  ENDF/B-VI Release 8 Photoatomic Data for 4-BE   mat 400      02/07/03
   6000.04p    3152  ENDF/B-VI Release 8 Photoatomic Data for 6-C    mat 600      02/07/03
   7000.04p    3194  ENDF/B-VI Release 8 Photoatomic Data for 7-N    mat 700      02/07/03
   8000.04p    3272  ENDF/B-VI Release 8 Photoatomic Data for 8-O    mat 800      02/07/03
  14000.04p    4792  ENDF/B-VI Release 8 Photoatomic Data for 14-SI  mat1400      02/07/03
  15000.04p    4498  ENDF/B-VI Release 8 Photoatomic Data for 15-P   mat1500      02/07/03
  16000.04p    4654  ENDF/B-VI Release 8 Photoatomic Data for 16-S   mat1600      02/07/03
  24000.04p    5682  ENDF/B-VI Release 8 Photoatomic Data for 24-CR  mat2400      02/07/03
  25000.04p    5598  ENDF/B-VI Release 8 Photoatomic Data for 25-MN  mat2500      02/07/03
  26000.04p    5718  ENDF/B-VI Release 8 Photoatomic Data for 26-FE  mat2600      02/07/03
  28000.04p    5826  ENDF/B-VI Release 8 Photoatomic Data for 28-NI  mat2800      02/07/03

  total       50647

 maximum photon energy set to  100.0 mev (maximum electron energy)

                        tables from file el03

   1000.03e    2329      6/6/98
   4000.03e    2331      6/6/98
   6000.03e    2333      6/6/98
   7000.03e    2333      6/6/98
   8000.03e    2333      6/6/98
  14000.03e    2339      6/6/98
  15000.03e    2339      6/6/98
```

```
  16000.03e    2339      6/6/98
  24000.03e    2345      6/6/98
  25000.03e    2345      6/6/98
  26000.03e    2345      6/6/98
  28000.03e    2347      6/6/98

  warning.  material      100 has been set to a conductor.


*******************************************************************************************
*********************

 dump no.    1 on file runtph     nps =     0     coll =     0     ctm =    0.00   nrn =  0

         3 warning messages so far.
 warning.  tally not scored beyond last energy bin.
 nps =       91246     nrn =               77436 tal =    8     erg = 4.0427E+00
1problem summary

      run terminated when     1000000  particle histories were done.
+
10/10/14 08:20:12
      c    *** Detector Cell Cards ***      probid =  10/10/14 08:11:32
0
 photon creation     tracks   weight    energy        photon loss   tracks   weight     energy
 (per source particle)                                          (per source particle)

 source                   0    0.         0.          escape         27744  2.7744E-02  4.0903E-03
                                                       energy cutoff      0  0.          3.4958E-05
                                                       time cutoff        0  0.          0.
 weight window            0    0.         0.          weight window      0  0.          0.
 cell importance          0    0.         0.          cell importance    0  0.          0.
 weight cutoff            0    0.         0.          weight cutoff      0  0.          0.
 e or t importance        0    0.         0.          e or t importance  0  0.          0.
```

```
 dxtran                    0    0.          0.           dxtran              0  0.           0.
 forced collisions         0    0.          0.           forced collisions   0  0.           0.
 exp. transform            0    0.          0.           exp. transform      0  0.           0.
 from neutrons             0    0.          0.           compton scatter     0  0.           1.9825E-03
 bremsstrahlung       139927    1.3993E-01 7.9356E-03   capture       115743  1.1574E-01  1.8518E-03
 p-annihilation            0    0.          0.           pair production     0  0.           0.
 photonuclear              0    0.          0.           photonuclear abs    0  0.           0.
 electron x-rays         987   9.8700E-04  7.4077E-06
 1st fluorescence       2573   2.5730E-03  1.6480E-05
 2nd fluorescence          0    0.          0.
     total            143487    1.4349E-01 7.9595E-03               total           143487
1.4349E-01    7.9595E-03

   number of photons banked                    140914        average time of (shakes)
cutoffs
   photon tracks per source particle      1.4349E-01          escape            4.7995E-02
tco   1.0000E+33
   photon collisions per source particle  2.3081E-01          capture           9.2617E-03
eco   1.0000E-03
   total photon collisions                     230808          capture or escape 1.6751E-02
wc1   0.0000E+00
                                                               any termination   1.6751E-02
wc2   0.0000E+00
0
 electron creation   tracks      weight        energy            electron loss       tracks
weight        energy
                                 (per source particle)
(per source particle)

 source             1000000    1.0000E+00    1.5648E+00          escape               11566
1.1566E-02    1.1697E-02
                                                     energy cutoff  113769408 1.1377E+02 1.1024E-01
                                                     time cutoff            0 0.         0.
 weight window       0   0.           0.             weight window          0 0.         0.
```

```
 cell importance     0   0.           0.          cell importance        0 0.         0.
 weight cutoff       0   0.           0.          weight cutoff          0 0.         0.
 e or t importance   0   0.           0.          e or t importance      0 0.         0.
 pair production     0   0.           0.          scattering             0 0.         1.9897E+00
 compton recoil  75249   7.5249E-02   1.9712E-03  bremsstrahlung         0 0.         7.9356E-03
 photo-electric 114977   1.1498E-01   1.7972E-03  p-annihilation         0 0.         0.
 photon auger     3937   3.9370E-03   2.9764E-05
 electron auger   1791   1.7910E-03   1.3540E-05
 knock-on    112585020   1.1259E+02   5.5094E-01
     total   113780974   1.1378E+02   2.1196E+00  total          113780974 1.1378E+02 2.1196E+00

   number of electrons banked              112780974
cutoffs
   electron tracks per source particle    1.1378E+02
tco   1.0000E+33
   electron sub-steps per source particle 3.1127E+03
eco   1.0000E-03
   total electron sub-steps               3112734300
wc1   0.0000E+00

wc2   0.0000E+00

 computer time so far in this run   422.93 minutes            maximum number ever in bank
254
 computer time in mcrun             422.88 minutes            bank overflows to backup file
0
 source particles per minute            2.3647E+03
 random numbers generated              24848154032            most random numbers used was
199904 in history      594089

  warning.   random number stride   152917 exceeded       35 times.

 range of sampled source weights = 1.0000E+00 to 1.0000E+00
```

```
 number of histories processed by each thread
      143541      142886      143041      143002      141705      142471      143354

1tally        8        nps =     1000000
           tally type 8    pulse height distribution.                   units   number
           tally for  photons   electrons

 cell  5
      energy
    0.0000E+00   3.20000E-05 0.1768
    1.0000E-03   1.46310E-02 0.0082
    5.0964E-02   3.48400E-03 0.0169
    1.0093E-01   1.18800E-03 0.0290
    1.5089E-01   1.49900E-03 0.0258
    2.0086E-01   1.64600E-03 0.0246
    2.5082E-01   1.85600E-03 0.0232
    3.0079E-01   1.94900E-03 0.0226
    3.5075E-01   2.14700E-03 0.0216
    4.0071E-01   2.27600E-03 0.0209
    4.5068E-01   2.26100E-03 0.0210
    5.0064E-01   2.58100E-03 0.0197
    5.5061E-01   3.60200E-03 0.0166
    6.0057E-01   4.53200E-03 0.0148
    6.5054E-01   5.13800E-03 0.0139
    7.0050E-01   4.79600E-03 0.0144
    7.5046E-01   4.71200E-03 0.0145
    8.0043E-01   4.11600E-03 0.0156
    8.5039E-01   3.98200E-03 0.0158
    9.0036E-01   3.54100E-03 0.0168
    9.5032E-01   3.16300E-03 0.0178
    1.0003E+00   2.73300E-03 0.0191
    1.0502E+00   2.51100E-03 0.0199
    1.1002E+00   2.06100E-03 0.0220
    1.1502E+00   1.88200E-03 0.0230
    1.2001E+00   1.62500E-03 0.0248
```

```
   1.2501E+00   1.44900E-03 0.0263
   1.3001E+00   1.28200E-03 0.0279
   1.3500E+00   1.11300E-03 0.0300
   1.4000E+00   9.43000E-04 0.0325
   1.9000E+00   5.28500E-03 0.0137
   2.4000E+00   1.21500E-03 0.0287
   2.9000E+00   2.01000E-04 0.0705
   3.5000E+00   1.40000E-05 0.2673
     total      9.54460E-02 0.0031

cell  7
     energy
   0.0000E+00   3.60000E-05 0.1667
   1.0000E-03   1.56060E-02 0.0079
   5.0964E-02   3.49100E-03 0.0169
   1.0093E-01   9.51000E-04 0.0324
   1.5089E-01   1.06800E-03 0.0306
   2.0086E-01   1.29900E-03 0.0277
   2.5082E-01   1.41600E-03 0.0266
   3.0079E-01   1.52100E-03 0.0256
   3.5075E-01   1.69200E-03 0.0243
   4.0071E-01   1.75100E-03 0.0239
   4.5068E-01   1.88700E-03 0.0230
   5.0064E-01   1.91500E-03 0.0228
   5.5061E-01   2.70900E-03 0.0192
   6.0057E-01   3.36300E-03 0.0172
   6.5054E-01   3.86300E-03 0.0161
   7.0050E-01   3.75000E-03 0.0163
   7.5046E-01   3.58800E-03 0.0167
   8.0043E-01   3.26400E-03 0.0175
   8.5039E-01   3.01200E-03 0.0182
   9.0036E-01   2.67200E-03 0.0193
   9.5032E-01   2.44100E-03 0.0202
   1.0003E+00   2.04800E-03 0.0221
```

```
   1.0502E+00   1.92200E-03 0.0228
   1.1002E+00   1.73700E-03 0.0240
   1.1502E+00   1.43600E-03 0.0264
   1.2001E+00   1.20400E-03 0.0288
   1.2501E+00   1.12900E-03 0.0297
   1.3001E+00   9.19000E-04 0.0330
   1.3500E+00   8.09000E-04 0.0351
   1.4000E+00   7.28000E-04 0.0370
   1.9000E+00   3.89700E-03 0.0160
   2.4000E+00   9.43000E-04 0.0325
   2.9000E+00   1.54000E-04 0.0806
   3.5000E+00   1.40000E-05 0.2673
     total      7.82350E-02 0.0034

cell  9
     energy
   0.0000E+00   3.00000E-05 0.1826
   1.0000E-03   1.55900E-02 0.0079
   5.0964E-02   3.14900E-03 0.0178
   1.0093E-01   7.97000E-04 0.0354
   1.5089E-01   9.22000E-04 0.0329
   2.0086E-01   9.89000E-04 0.0318
   2.5082E-01   1.07300E-03 0.0305
   3.0079E-01   1.19800E-03 0.0289
   3.5075E-01   1.27600E-03 0.0280
   4.0071E-01   1.33100E-03 0.0274
   4.5068E-01   1.36000E-03 0.0271
   5.0064E-01   1.57800E-03 0.0252
   5.5061E-01   2.08300E-03 0.0219
   6.0057E-01   2.74700E-03 0.0191
   6.5054E-01   2.83700E-03 0.0187
   7.0050E-01   2.86400E-03 0.0187
   7.5046E-01   2.69300E-03 0.0192
   8.0043E-01   2.57700E-03 0.0197
```

```
   8.5039E-01   2.33100E-03 0.0207
   9.0036E-01   2.08400E-03 0.0219
   9.5032E-01   1.90400E-03 0.0229
   1.0003E+00   1.64000E-03 0.0247
   1.0502E+00   1.45400E-03 0.0262
   1.1002E+00   1.25900E-03 0.0282
   1.1502E+00   1.12200E-03 0.0298
   1.2001E+00   9.37000E-04 0.0327
   1.2501E+00   8.47000E-04 0.0343
   1.3001E+00   6.70000E-04 0.0386
   1.3500E+00   6.28000E-04 0.0399
   1.4000E+00   5.57000E-04 0.0424
   1.9000E+00   3.09500E-03 0.0179
   2.4000E+00   7.17000E-04 0.0373
   2.9000E+00   1.17000E-04 0.0924
   3.5000E+00   1.20000E-05 0.2887
     total      6.44680E-02 0.0038

cell  11
     energy
   0.0000E+00   1.80000E-05 0.2357
   1.0000E-03   1.46130E-02 0.0082
   5.0964E-02   2.80400E-03 0.0189
   1.0093E-01   5.22000E-04 0.0438
   1.5089E-01   6.75000E-04 0.0385
   2.0086E-01   7.20000E-04 0.0373
   2.5082E-01   8.07000E-04 0.0352
   3.0079E-01   9.35000E-04 0.0327
   3.5075E-01   9.63000E-04 0.0322
   4.0071E-01   9.55000E-04 0.0323
   4.5068E-01   1.06500E-03 0.0306
   5.0064E-01   1.18000E-03 0.0291
   5.5061E-01   1.57800E-03 0.0252
   6.0057E-01   2.06500E-03 0.0220
```

```
   6.5054E-01   2.20100E-03 0.0213
   7.0050E-01   2.31600E-03 0.0208
   7.5046E-01   2.11400E-03 0.0217
   8.0043E-01   1.99500E-03 0.0224
   8.5039E-01   1.70000E-03 0.0242
   9.0036E-01   1.67800E-03 0.0244
   9.5032E-01   1.45100E-03 0.0262
   1.0003E+00   1.24400E-03 0.0283
   1.0502E+00   1.13400E-03 0.0297
   1.1002E+00   9.96000E-04 0.0317
   1.1502E+00   8.43000E-04 0.0344
   1.2001E+00   7.47000E-04 0.0366
   1.2501E+00   6.39000E-04 0.0395
   1.3001E+00   5.09000E-04 0.0443
   1.3500E+00   4.78000E-04 0.0457
   1.4000E+00   3.99000E-04 0.0501
   1.9000E+00   2.39300E-03 0.0204
   2.4000E+00   5.74000E-04 0.0417
   2.9000E+00   9.30000E-05 0.1037
   3.5000E+00   7.00000E-06 0.3780
     total      5.24110E-02 0.0043

cell  13
     energy
   0.0000E+00   1.40000E-05 0.2673
   1.0000E-03   1.33390E-02 0.0086
   5.0964E-02   2.43000E-03 0.0203
   1.0093E-01   4.51000E-04 0.0471
   1.5089E-01   5.42000E-04 0.0429
   2.0086E-01   6.05000E-04 0.0406
   2.5082E-01   6.51000E-04 0.0392
   3.0079E-01   7.60000E-04 0.0363
   3.5075E-01   7.68000E-04 0.0361
   4.0071E-01   8.18000E-04 0.0349
```

```
   4.5068E-01   8.03000E-04 0.0353
   5.0064E-01   9.38000E-04 0.0326
   5.5061E-01   1.28000E-03 0.0279
   6.0057E-01   1.64600E-03 0.0246
   6.5054E-01   1.63900E-03 0.0247
   7.0050E-01   1.68100E-03 0.0244
   7.5046E-01   1.63600E-03 0.0247
   8.0043E-01   1.49100E-03 0.0259
   8.5039E-01   1.34000E-03 0.0273
   9.0036E-01   1.23200E-03 0.0285
   9.5032E-01   1.07500E-03 0.0305
   1.0003E+00   9.87000E-04 0.0318
   1.0502E+00   8.01000E-04 0.0353
   1.1002E+00   7.05000E-04 0.0376
   1.1502E+00   5.90000E-04 0.0412
   1.2001E+00   5.47000E-04 0.0427
   1.2501E+00   5.21000E-04 0.0438
   1.3001E+00   4.42000E-04 0.0476
   1.3500E+00   3.68000E-04 0.0521
   1.4000E+00   3.28000E-04 0.0552
   1.9000E+00   1.76500E-03 0.0238
   2.4000E+00   4.03000E-04 0.0498
   2.9000E+00   8.20000E-05 0.1104
   3.5000E+00   4.00000E-06 0.5000
     total      4.26820E-02 0.0047

cell  15
     energy
   0.0000E+00   5.00000E-06 0.4472
   1.0000E-03   1.18920E-02 0.0091
   5.0964E-02   2.06400E-03 0.0220
   1.0093E-01   3.84000E-04 0.0510
   1.5089E-01   3.78000E-04 0.0514
   2.0086E-01   4.53000E-04 0.0470
```

```
   2.5082E-01   4.76000E-04 0.0458
   3.0079E-01   5.75000E-04 0.0417
   3.5075E-01   5.67000E-04 0.0420
   4.0071E-01   6.00000E-04 0.0408
   4.5068E-01   6.28000E-04 0.0399
   5.0064E-01   7.18000E-04 0.0373
   5.5061E-01   9.27000E-04 0.0328
   6.0057E-01   1.21700E-03 0.0286
   6.5054E-01   1.37300E-03 0.0270
   7.0050E-01   1.35300E-03 0.0272
   7.5046E-01   1.17200E-03 0.0292
   8.0043E-01   1.14600E-03 0.0295
   8.5039E-01   1.05800E-03 0.0307
   9.0036E-01   9.49000E-04 0.0324
   9.5032E-01   8.65000E-04 0.0340
   1.0003E+00   7.20000E-04 0.0373
   1.0502E+00   6.76000E-04 0.0384
   1.1002E+00   6.10000E-04 0.0405
   1.1502E+00   5.09000E-04 0.0443
   1.2001E+00   4.53000E-04 0.0470
   1.2501E+00   3.96000E-04 0.0502
   1.3001E+00   3.07000E-04 0.0571
   1.3500E+00   2.98000E-04 0.0579
   1.4000E+00   2.87000E-04 0.0590
   1.9000E+00   1.31600E-03 0.0275
   2.4000E+00   3.57000E-04 0.0529
   2.9000E+00   4.60000E-05 0.1474
   3.5000E+00   2.00000E-06 0.7071
     total      3.47770E-02 0.0053

cell  17
     energy
   0.0000E+00   7.00000E-06 0.3780
   1.0000E-03   1.06090E-02 0.0097
```

5.0964E-02	1.67200E-03	0.0244
1.0093E-01	3.05000E-04	0.0573
1.5089E-01	3.25000E-04	0.0555
2.0086E-01	3.87000E-04	0.0508
2.5082E-01	3.39000E-04	0.0543
3.0079E-01	4.17000E-04	0.0490
3.5075E-01	4.34000E-04	0.0480
4.0071E-01	4.71000E-04	0.0461
4.5068E-01	4.74000E-04	0.0459
5.0064E-01	5.46000E-04	0.0428
5.5061E-01	7.34000E-04	0.0369
6.0057E-01	9.45000E-04	0.0325
6.5054E-01	1.03000E-03	0.0311
7.0050E-01	1.01200E-03	0.0314
7.5046E-01	9.80000E-04	0.0319
8.0043E-01	8.99000E-04	0.0333
8.5039E-01	8.62000E-04	0.0340
9.0036E-01	7.19000E-04	0.0373
9.5032E-01	6.04000E-04	0.0407
1.0003E+00	5.61000E-04	0.0422
1.0502E+00	4.83000E-04	0.0455
1.1002E+00	4.52000E-04	0.0470
1.1502E+00	3.85000E-04	0.0510
1.2001E+00	3.02000E-04	0.0575
1.2501E+00	3.55000E-04	0.0531
1.3001E+00	2.67000E-04	0.0612
1.3500E+00	2.19000E-04	0.0676
1.4000E+00	2.07000E-04	0.0695
1.9000E+00	1.09300E-03	0.0302
2.4000E+00	2.61000E-04	0.0619
2.9000E+00	4.40000E-05	0.1508
3.5000E+00	3.00000E-06	0.5773
total	2.84030E-02	0.0058

```
cell  19
     energy
   0.0000E+00   7.00000E-06 0.3780
   1.0000E-03   9.18800E-03 0.0104
   5.0964E-02   1.43700E-03 0.0264
   1.0093E-01   2.23000E-04 0.0670
   1.5089E-01   2.70000E-04 0.0608
   2.0086E-01   2.78000E-04 0.0600
   2.5082E-01   2.94000E-04 0.0583
   3.0079E-01   3.31000E-04 0.0550
   3.5075E-01   3.78000E-04 0.0514
   4.0071E-01   3.47000E-04 0.0537
   4.5068E-01   3.73000E-04 0.0518
   5.0064E-01   4.02000E-04 0.0499
   5.5061E-01   5.38000E-04 0.0431
   6.0057E-01   7.51000E-04 0.0365
   6.5054E-01   7.69000E-04 0.0360
   7.0050E-01   7.82000E-04 0.0357
   7.5046E-01   8.02000E-04 0.0353
   8.0043E-01   7.29000E-04 0.0370
   8.5039E-01   6.59000E-04 0.0389
   9.0036E-01   5.87000E-04 0.0413
   9.5032E-01   5.11000E-04 0.0442
   1.0003E+00   4.17000E-04 0.0490
   1.0502E+00   4.24000E-04 0.0486
   1.1002E+00   3.79000E-04 0.0514
   1.1502E+00   3.03000E-04 0.0574
   1.2001E+00   2.41000E-04 0.0644
   1.2501E+00   2.41000E-04 0.0644
   1.3001E+00   1.99000E-04 0.0709
   1.3500E+00   1.69000E-04 0.0769
   1.4000E+00   1.30000E-04 0.0877
   1.9000E+00   8.62000E-04 0.0340
   2.4000E+00   2.19000E-04 0.0676
```

```
   2.9000E+00   3.90000E-05 0.1601
   3.5000E+00   7.00000E-06 0.3780
     total      2.32860E-02 0.0065

cell  21
     energy
   0.0000E+00   6.00000E-06 0.4082
   1.0000E-03   7.83600E-03 0.0113
   5.0964E-02   1.16500E-03 0.0293
   1.0093E-01   1.69000E-04 0.0769
   1.5089E-01   1.82000E-04 0.0741
   2.0086E-01   2.20000E-04 0.0674
   2.5082E-01   2.57000E-04 0.0624
   3.0079E-01   2.82000E-04 0.0595
   3.5075E-01   2.80000E-04 0.0598
   4.0071E-01   3.03000E-04 0.0574
   4.5068E-01   2.97000E-04 0.0580
   5.0064E-01   3.36000E-04 0.0545
   5.5061E-01   4.36000E-04 0.0479
   6.0057E-01   5.84000E-04 0.0414
   6.5054E-01   5.83000E-04 0.0414
   7.0050E-01   6.02000E-04 0.0407
   7.5046E-01   5.97000E-04 0.0409
   8.0043E-01   5.69000E-04 0.0419
   8.5039E-01   4.86000E-04 0.0453
   9.0036E-01   4.72000E-04 0.0460
   9.5032E-01   3.68000E-04 0.0521
   1.0003E+00   3.38000E-04 0.0544
   1.0502E+00   2.96000E-04 0.0581
   1.1002E+00   2.84000E-04 0.0593
   1.1502E+00   2.32000E-04 0.0656
   1.2001E+00   2.27000E-04 0.0664
   1.2501E+00   2.02000E-04 0.0704
   1.3001E+00   1.47000E-04 0.0825
```

```
   1.3500E+00   1.47000E-04 0.0825
   1.4000E+00   1.18000E-04 0.0921
   1.9000E+00   6.34000E-04 0.0397
   2.4000E+00   1.42000E-04 0.0839
   2.9000E+00   2.80000E-05 0.1890
   3.5000E+00   2.00000E-06 0.7071
     total      1.88270E-02 0.0072

cell  23
     energy
   0.0000E+00   5.00000E-06 0.4472
   1.0000E-03   6.69500E-03 0.0122
   5.0964E-02   8.72000E-04 0.0338
   1.0093E-01   1.38000E-04 0.0851
   1.5089E-01   1.62000E-04 0.0786
   2.0086E-01   1.59000E-04 0.0793
   2.5082E-01   2.00000E-04 0.0707
   3.0079E-01   2.15000E-04 0.0682
   3.5075E-01   2.27000E-04 0.0664
   4.0071E-01   2.18000E-04 0.0677
   4.5068E-01   2.43000E-04 0.0641
   5.0064E-01   2.63000E-04 0.0617
   5.5061E-01   3.04000E-04 0.0573
   6.0057E-01   4.29000E-04 0.0483
   6.5054E-01   5.03000E-04 0.0446
   7.0050E-01   4.83000E-04 0.0455
   7.5046E-01   4.54000E-04 0.0469
   8.0043E-01   4.38000E-04 0.0478
   8.5039E-01   3.45000E-04 0.0538
   9.0036E-01   3.53000E-04 0.0532
   9.5032E-01   3.29000E-04 0.0551
   1.0003E+00   2.77000E-04 0.0601
   1.0502E+00   2.54000E-04 0.0627
   1.1002E+00   2.17000E-04 0.0679
```

```
   1.1502E+00   1.89000E-04 0.0727
   1.2001E+00   1.55000E-04 0.0803
   1.2501E+00   1.32000E-04 0.0870
   1.3001E+00   1.20000E-04 0.0913
   1.3500E+00   1.09000E-04 0.0958
   1.4000E+00   9.90000E-05 0.1005
   1.9000E+00   5.43000E-04 0.0429
   2.4000E+00   9.70000E-05 0.1015
   2.9000E+00   1.80000E-05 0.2357
   3.5000E+00   1.00000E-06 1.0000
     total      1.52460E-02 0.0080

cell union total   *** Total number of He-6 beta particles that interact in the scintillator ***
     energy
   0.0000E+00   1.59000E-04 0.0793
   1.0000E-03   1.66230E-02 0.0077
   5.0964E-02   1.38000E-02 0.0085
   1.0093E-01   4.88300E-03 0.0143
   1.5089E-01   5.92300E-03 0.0130
   2.0086E-01   6.69900E-03 0.0122
   2.5082E-01   7.32000E-03 0.0116
   3.0079E-01   8.12700E-03 0.0110
   3.5075E-01   8.68500E-03 0.0107
   4.0071E-01   9.05200E-03 0.0105
   4.5068E-01   9.35900E-03 0.0103
   5.0064E-01   1.03890E-02 0.0098
   5.5061E-01   1.40360E-02 0.0084
   6.0057E-01   1.81580E-02 0.0074
   6.5054E-01   1.98570E-02 0.0070
   7.0050E-01   1.96130E-02 0.0071
   7.5046E-01   1.87510E-02 0.0072
   8.0043E-01   1.72450E-02 0.0075
   8.5039E-01   1.58120E-02 0.0079
   9.0036E-01   1.43080E-02 0.0083
```

```
    9.5032E-01   1.27090E-02 0.0088
    1.0003E+00   1.10040E-02 0.0095
    1.0502E+00   9.99900E-03 0.0100
    1.1002E+00   8.74000E-03 0.0106
    1.1502E+00   7.50100E-03 0.0115
    1.2001E+00   6.47800E-03 0.0124
    1.2501E+00   5.92500E-03 0.0130
    1.3001E+00   4.87900E-03 0.0143
    1.3500E+00   4.36300E-03 0.0151
    1.4000E+00   3.81200E-03 0.0162
    1.9000E+00   2.09290E-02 0.0068
    2.4000E+00   4.94500E-03 0.0142
    2.9000E+00   8.25000E-04 0.0348
    3.5000E+00   6.60000E-05 0.1231
      total      3.40974E-01 0.0014


==================================================================================================
==================================

          results of 10 statistical checks for the estimated answer for the tally fluctuation
chart (tfc) bin of tally        8

 tfc bin     --mean--      ---------relative error---------      ----variance of the variance----
--figure of merit--     -pdf-
 behavior    behavior      value   decrease   decrease rate      value   decrease   decrease rate
value     behavior     slope

 desired      random       <0.10      yes      1/sqrt(nps)       <0.10      yes        1/nps
constant    random      >3.00
 observed     random        0.00      yes          yes            0.00      yes         yes
constant    random      10.00
```

```
 passed?        yes          yes      yes          yes             yes      yes         yes
yes        yes         yes


==========================================================================================
==================================


 this tally meets the statistical criteria used to form confidence intervals: check the tally
fluctuation chart to verify.
 the results in other bins associated with this tally may not meet these statistical criteria.

 ----- estimated confidence intervals:  -----

 estimated asymmetric confidence interval(1,2,3 sigma): 9.5153E-02 to 9.5740E-02; 9.4859E-02 to
9.6034E-02; 9.4565E-02 to 9.6328E-02
 estimated  symmetric confidence interval(1,2,3 sigma): 9.5152E-02 to 9.5740E-02; 9.4858E-02 to
9.6034E-02; 9.4565E-02 to 9.6327E-02

1analysis of the results in the tally fluctuation chart bin (tfc) for tally        8 with nps=
1000000 print table 160


 normed average tally per history  = 9.54460E-02          unnormed average tally per history  =
9.54460E-02
 estimated tally relative error    = 0.0031               estimated variance of the variance  =
0.0000
 relative error from zero tallies  = 0.0031               relative error from nonzero scores  =
0.0000

 number of nonzero history tallies =       95446          efficiency for the nonzero tallies  =
0.0954
 history number of largest  tally  =          31          largest  unnormalized history tally =
1.00000E+00
```

```
 (largest  tally)/(average tally)  = 1.04771E+01          (largest  tally)/(avg nonzero tally)=
1.00000E+00

 (confidence interval shift)/mean  = 0.0000               shifted confidence interval center  =
9.54464E-02


 if the largest  history score sampled so far were to occur on the next history, the tfc bin
quantities would change as follows:

      estimated quantities           value at nps           value at nps+1
value(nps+1)/value(nps)-1.

      mean                            9.54460E-02            9.54469E-02
0.000009
      relative error                  3.07849E-03            3.07848E-03                    -
0.000006
      variance of the variance        7.58265E-06            7.58254E-06                    -
0.000014
      shifted center                  9.54464E-02            9.54464E-02
0.000000
      figure of merit                 2.49521E+02            2.49523E+02
0.000011

 the 100 largest  history tallies appear to have a  maximum value of about 1.00000E+00
 the large score tail of the empirical history score probability density function appears to have
no unsampled regions.

 fom = (histories/minute)*(f(x) signal-to-noise ratio)**2 = (2.365E+03)*( 3.248E-01)**2 =
(2.365E+03)*(1.055E-01) = 2.495E+02

1    some tally scores were not made for various reasons:

                                  beyond last bin     not in
```

```
                  tally      angle   energy   time    user
                     8          0       6       0       0

1status of the statistical checks used to form confidence intervals for the mean for each tally
bin


 tally   result of statistical checks for the tfc bin (the first check not passed is listed) and
error magnitude check for all bins

        8   passed the 10 statistical checks for the tally fluctuation chart bin result
         missed all bin error check:   385 tally bins had     0 bins with zeros and    30 bins
with relative errors exceeding 0.10


 the 10 statistical checks are only for the tally fluctuation chart bin and do not apply to other
tally bins.

 warning.       1 of the     1 tallies had bins with relative errors greater than recommended.
1tally fluctuation charts

                           tally        8
          nps      mean     error   vov  slope    fom
        64000   9.5859E-02 0.0121 0.0001 10.0     250
       128000   9.6695E-02 0.0085 0.0001 10.0     253
       192000   9.5802E-02 0.0070 0.0000 10.0     250
       256000   9.6016E-02 0.0061 0.0000 10.0     251
       320000   9.6344E-02 0.0054 0.0000 10.0     252
       384000   9.6396E-02 0.0049 0.0000 10.0     252
       448000   9.6125E-02 0.0046 0.0000 10.0     251
       512000   9.5877E-02 0.0043 0.0000 10.0     251
       576000   9.5648E-02 0.0041 0.0000 10.0     250
       640000   9.5733E-02 0.0038 0.0000 10.0     250
       704000   9.5587E-02 0.0037 0.0000 10.0     250
```

```
       768000   9.5637E-02 0.0035 0.0000 10.0     250
       832000   9.5501E-02 0.0034 0.0000 10.0     250
       896000   9.5452E-02 0.0033 0.0000 10.0     249
       960000   9.5486E-02 0.0031 0.0000 10.0     250
      1000000   9.5446E-02 0.0031 0.0000 10.0     250


*******************************************************************************************
*********************

 dump no.    2 on file runtph     nps =     1000000     coll =     3112965108     ctm =
422.88   nrn =
 24848154032

         6 warning messages so far.

 run terminated when     1000000  particle histories were done.

 computer time =  422.94 minutes

 mcnp     version 5     09282010                      10/10/14 08:20:12                      probid
=  10/10/14 08:11:3
```

Appendix E Source Data Sheets

Cs-137 (IPL)

CERTIFICATE OF CALIBRATION
GAMMA STANDARD SOURCE

Radionuclide:	Cs-137	Customer:	UNIVERSITY OF NEW MEXICO	
Half Life:	30.0 ± 0.2 years	P.O.No.:	740552	
Catalog No.:	GF-137	Reference Date:	March 1 1994	12:00 PST.
Source No.:	449-56-2	Contained Radioactivity:	10.61	μCi.
		Contained Radioactivity:	393	kBq.

Description of Source

a. Capsule type:	M
b. Nature of active deposit:	Evaporated metallic salts
c. Active diameter/volume:	3 mm
d. Backing:	9.23 mg/cm² kapton
e. Cover:	0.254 mm aluminized mylar

Radioimpurities

None detected

Method of Calibration

The source was assayed by gamma spectrometry:

Energy peak(s) integrated under:	662	keV.
Branching ratio(s) used:	0.8521	gamma rays per decay.

Uncertainty of Measurement

a. Systematic uncertainty in instrument calibration:	± 3.0%
b. Random uncertainty in assay:	± 1.6%
c. Random uncertainty in weighing(s):	± 0.0%
d. Total uncertainty at the 99% confidence level:	± 3.4%

NIST Traceability

This calibration is implicitly traceable to the National Institute of Standards and Technology.

Leak Test(s)

See reverse side for Leak Test(s) applied to this source.

Notes

1. Nuclear data were taken from "Table of Radioactive Isotopes", edited by Virginia S. Shirley, 1986.
2. IPL participates in an NIST measurement assurance program to establish and maintain implicit traceability for a number of nuclides, based on the blind assay (and later NIST certification) of Standard Reference Materials (As in NRC Regulatory Guide 4.15).

Anna U. Kwa
QUALITY CONTROL

Mar. 9, 1994
Date Signed

ISOTOPE PRODUCTS LABORATORIES
1800 North Keystone Street
Burbank, California 91504
(818) 843 - 7000

IPL Ref. No.: 449-56-2

Cs-137 (Baird-Atomic)

BAIRD-ATOMIC, INC. 33 UNIVERSITY ROAD, CAMBRIDGE, MASSACHUSETTS 02138, Telephone: 617 864-7420, Cable Address BAIRDCO

TELEX 894-541

GAMMA SPECTROSCOPY REFERENCE SOURCE

MODEL CT-200-4 DISC SOURCE

CESIUM-137

Half-Life 30 years Gamma Photopeak(s)

32 Kev - Ba x-Ray
662 Kev - 86%
(From Ba-137^{m})

PREPARATION: An volume of nuclide solution was dispensed into the 1.5 mm dia. x 0.5 mm centered recess of the yellow disc and evaporated to dryness. The two discs were then chemically sealed and tested. Nominal diameter-one inch Nominal thickness-.062

CALIBRATION: Calibration was accomplished by direct measurement with a gamma ray scintillation spectrometer for which the intrinsic source activity response function had been precisely determined with standards from The National Bureau of Standards of The National Physical Laboratory (England). The maximum overall error associated with the radioactivity content value given herein is estimated to be within the limits of ± 5% of the given value. The photopeak value given is calculated based on intrinsic photofraction values derived for the measurement system.

Calibration Date 8/69 Serial No 31102-7

Radioactivity Content 1.35 Microcurie (s)

662 Kev gamma photons per second: 4.29 x 10^4

CERTIFICATION: Date 8/1/69

by RRD

30 YEARS OF SCIENTIFIC ACHIEVEMENT

Cl-36

CERTIFICATE OF RADIOACTIVITY CALIBRATION

Chlorine-36 Reference Source
NES-2000

Half-Life: 3.0×10^5 years
Lot Number: 285-275

The activity of Chlorine-36 was found to be,
0.0209 microcuries on November 21, 1977

DESCRIPTION OF THE SOURCE

The activity was deposited in a 5 mm diameter active area on a 0.25 mm thick stainless steel planchet, covered with a 0.90 mg/cm^2 aluminized mylar window, and sealed into the aluminum mount. The overall dimensions of the source are 3.2 mm in height and 25 mm in diameter. The mass of the deposit was less than 0.01 mg and self-absorption was considered negligible.

DECAY SCHEME		Intensity (%)
β^-	0.7089 MeV maximum	98.1
	0.2514 average	

Reference: Nuclear Data Tables, Vol. 8, Nos. 1-2, Academic Press, New York, October, 1970.

METHOD OF CALIBRATION

An aliquot was taken of a solution calibrated by liquid scintillation counting. The counting efficiency was determined using standards based on National Bureau of Standards assays.

IMPURITIES

Less than 1%.

RADIOACTIVE MATERIAL

The radioactive material described or contained herein is exempt from NRC or agreement state licensing requirements. Not for human use. Introduction into foods, beverages, cosmetics, drugs or medicinals, or into products manufactured for commercial distribution is prohibited. Exempt quantities should not be combined.

ERRORS

Random Errors (99% confidence level)

Precision of the NEN measurement	± 2.5%

Systematic Errors

Estimated maximum error in efficiency determination	± 0.5%
Error in pipetting	± 0.2%

Overall Error

2.5 + 0.5 + 0.2 = ± 3.2%

Percentage of radiation absorbed by window: 6%

NEN New England Nuclear
549 Albany Street, Boston, Mass. 02118
CUSTOMER SERVICE: (617) 482-9595

Mary E. Dumanoski

Co-60

CERTIFICATE OF CALIBRATION

MODEL CAL2600 GAMMA STANDARD

Radionuclide:	Co-60	**Activity:**	396.1 kBq (10.71 μCi)
Serial Number:	96052	**Reference Date:**	1200 PDT August 1, 2006
Half Life[1]**:**	5.271 ± 0.001 years		

PRINCIPAL EMISSIONS[1]

Type	Energy (keV)	Intensity (%)
gamma	1173.237	99.90
gamma	1332.501	99.9824

SOURCE DESCRIPTION

Active Diameter:	1 mm	**Backing:**	1 mm plastic
Overall Diameter:	25.4 mm	**Cover:**	1 mm plastic
Thickness:	3.2 mm		

METHOD OF CALIBRATION

The source was calibrated on a high purity germanium detector against a Co-60 standard at 1173.237 keV. The activity of the standard was determined using an efficiency established and verified through ongoing intercomparisons with the National Institute of Standards and Technology. This standard is indirectly (implicitly) traceable to the National Institute of Standards and Technology.

North American Scientific, Inc. participates in the Radioactivity Measurements Assurance Program conducted by the National Institute of Standards and Technology in cooperation with the Nuclear Energy Institute.

TOTAL UNCERTAINTY (99% Confidence Level)

Systematic uncertainty	3.85%
Random uncertainty	1.24%
Total uncertainty (quadratic sum)	± 4.04%

Amy Chen
Calibration Laboratory

July 20, 2006
Date

REFERENCES

(1) Table of Radioactive Isotopes, 7th edition, 1986.

•LEAK TEST CERTIFICATION ON REVERSE•

North American Scientific, Inc. 7435 Greenbush Ave., North Hollywood, CA 91605 (818) 734-8600 Fax (818) 734-5200

Na-22

CERTIFICATE OF CALIBRATION

MODEL CAL2600 GAMMA STANDARD

Radionuclide:	Na-22	**Activity:**	374.5 kBq (10.12 µCi)
Serial Number:	96049	**Reference Date:**	1200 PDT August 1, 2006
Half Life[1]:	2.602 ± 0.002 years		

PRINCIPAL EMISSIONS[1]

Type	Energy (keV)	Intensity (%)
gamma	1274.53	99.937
annihilation gamma	511	178.8

SOURCE DESCRIPTION

Active Diameter:	1 mm	**Backing:**	1 mm plastic
Overall Diameter:	25.4 mm	**Cover:**	1 mm plastic
Thickness:	3.2 mm		

METHOD OF CALIBRATION

The source was calibrated on a high purity germanium detector using a Na-22 efficiency at 1274.53 keV. This efficiency was established and verified through ongoing intercomparisons with the National Institute of Standards and Technology. This standard is indirectly (implicitly) traceable to the National Institute of Standards and Technology.

North American Scientific, Inc. participates in the Radioactivity Measurements Assurance Program conducted by the National Institute of Standards and Technology in cooperation with the Nuclear Energy Institute.

TOTAL UNCERTAINTY (99% Confidence Level)

Systematic uncertainty	3.54%
Random uncertainty	0.86%
Total uncertainty (quadratic sum)	± 3.64%

Amy Chen
Calibration Laboratory

July 21, 2006
Date

REFERENCES

(1) Table of Radioactive Isotopes, 7th edition, 1986.

• LEAK TEST CERTIFICATION ON REVERSE •

North American Scientific, Inc. 7435 Greenbush Ave., North Hollywood, CA 91605 (818) 734-8600 Fax (818) 734-5200

Pb-210/Bi-210

CERTIFICATE OF CALIBRATION
BETA STANDARD SOURCE

Radionuclide:	Pb-210	Customer:	UNIVERSITY OF NEW MEXICO
Half Life:	22.3 ± 0.2 years	P.O.No.:	740552
Catalog No.:	BF-200	Reference Date:	March 15 1994 12:00 PST.
Source No.:	449-53-1	Contained Radioactivity:	(Pb-210) 0.01007 μCi.
		Contained Radioactivity:	(Pb-210) 0.372 kBq.

Description of Source

a. Capsule type:	A
b. Nature of active deposit:	Distributed and evaporated metallic salts
c. Active diameter/volume:	22 mm
d. Backing:	0.254 mm stainless steel
e. Cover:	0.0254 mm aluminum

Radioimpurities

None detected (Bi-210 and Po-210 daughters are in equilibrium)

Method of Calibration

The source was prepared from a weighed aliquot of solution whose concentration in μCi/gram was determined by a windowless internal gas flow proportional counter.

Uncertainty of Measurement

a. Systematic uncertainty in instrument calibration:	± 5.0%
b. Random uncertainty in assay:	± 2.9%
c. Random uncertainty in weighing(s):	± 4.0%
d. Total uncertainty at the 99% confidence level:	± 5.8%

NIST Traceability

This calibration is not traceable to the National Institute of Standards and Technology.

Leak Test(s)

See reverse side for Leak Test(s) applied to this source

Notes

1. Nuclear data were taken from "Table of Radioactive Isotopes", edited by Virginia S. Shirley, 1986.
2. IPL participates in an NIST measurement assurance program to establish and maintain implicit traceability for a number of nuclides, based on the blind assay (and later NIST certification) of Standard Reference Materials (As in NRC Regulatory Guide 4.15).

QUALITY CONTROL

Mar 10, 1994

Date Signed

ISOTOPE PRODUCTS LABORATORIES
1800 North Keystone Street
Burbank, California 91504
(818) 843 - 7000

IPL Ref. No.: 449-53-1

Sr-90/Y-90

CERTIFICATE OF CALIBRATION
BETA STANDARD SOURCE

Radionuclide:	Sr-90	Customer:	UNIVERSITY OF NEW MEXICO
Half Life:	28.5 ± 0.2 years	P.O.No.:	740552
Catalog No.:	BF-200	Reference Date:	March 15 1994 12:00 PST.
Source No.:	449-53-3	Contained Radioactivity:	(Sr-90) 0.00993 μCi
		Contained Radioactivity:	(Sr-90) 0.367 kBq

Description of Source

a. Capsule type:	A
b. Nature of active deposit:	Distributed and evaporated metallic salts
c. Active diameter/volume:	22 mm
d. Backing:	0.254 mm stainless steel
e. Cover:	0.9 mg/cm² aluminized mylar

Radioimpurities

None detected (Y-90 daughter in equilibrium)

Method of Calibration

The source was prepared from a weighed aliquot of solution whose concentration in μCi/gram was determined by a liquid scintillation counter.

Uncertainty of Measurement

a. Systematic uncertainty in instrument calibration:	± 2.0%
b. Random uncertainty in assay:	± 1.5%
c. Random uncertainty in weighing(s):	± 0.6%
d. Total uncertainty at the 99% confidence level:	± 2.6%

NIST Traceability

This calibration is implicitly traceable to the National Institute of Standards and Technology.

Leak Test(s)

See reverse side for Leak Test(s) applied to this source

Notes

1. Nuclear data were taken from "Table of Radioactive Isotopes", edited by Virginia S. Shirley, 1986.
2. IPL participates in an NIST measurement assurance program to establish and maintain implicit traceability for a number of nuclides, based on the blind assay (and later NIST certification) of Standard Reference Materials (As in NRC Regulatory Guide 4.15).

Anna H. Huer
QUALITY CONTROL

Mar 10, 1994
Date Signed

ISOTOPE PRODUCTS LABORATORIES
1800 North Keystone Street
Burbank, California 91504
(818) 843 - 7000

IPL Ref. No.: 449-53-3

Appendix F Beta Source Spectral Data

He-6							
Energy (MeV)	Emission Probability	Energy (MeV)	Emission Probability	Energy (MeV)	Emission Probability	Energy (MeV)	Emission Probability
0.285	1.34E-02	1.107	3.27E-02	2.003	3.13E-02	2.812	1.10E-02
0.367	1.72E-02	1.175	3.36E-02	2.071	2.98E-02	2.879	9.16E-03
0.441	2.01E-02	1.256	3.41E-02	2.146	2.81E-02	2.954	7.17E-03
0.516	2.24E-02	1.331	3.46E-02	2.221	2.68E-02	3.029	5.53E-03
0.584	2.43E-02	1.480	3.51E-02	2.295	2.50E-02	3.110	4.15E-03
0.652	2.58E-02	1.555	3.52E-02	2.363	2.32E-02	3.178	2.85E-03
0.727	2.73E-02	1.630	3.49E-02	2.445	2.09E-02	3.253	1.90E-03
0.801	2.88E-02	1.705	3.49E-02	2.513	1.92E-02	3.321	1.12E-03
0.876	3.00E-02	1.779	3.44E-02	2.587	1.71E-02	3.402	6.91E-04
0.958	3.09E-02	1.854	3.32E-02	2.669	1.51E-02	3.470	2.59E-04
1.032	3.19E-02	1.922	3.24E-02	2.744	1.31E-02		

Co-60		cs-137		na-22		cl-36	
Energy (MeV)	Emission Probability	Energy (MeV)	Emission Probability	Energy (MeV)	Emission Probability	Energy (MeV)	Emission Probability
0.0746	4.45E-01	0.0587	1.93E-01	0.091	1.46E-01	0.0355	5.23E-02
0.1491	3.30E-01	0.1173	1.76E-01	0.182	2.75E-01	0.0709	5.81E-02
0.2237	1.78E-01	0.176	1.61E-01	0.273	2.71E-01	0.1064	6.26E-02
0.2982	4.58E-02	0.2346	1.44E-01	0.364	1.96E-01	0.1419	6.58E-02
0.3728	6.36E-04	0.2933	1.22E-01	0.455	9.46E-02	0.1774	6.80E-02
0.4473	5.99E-05	0.352	9.38E-02	0.546	1.67E-02	0.2129	6.94E-02
0.5219	5.96E-05	0.4106	6.01E-02	0.637	4.85E-05	0.2483	7.00E-02
0.5964	5.77E-05	0.4693	2.64E-02	0.728	4.84E-05	0.2838	6.98E-02
0.6710	5.54E-05	0.5279	5.70E-03	0.819	4.92E-05	0.3193	6.87E-02
0.7455	5.40E-05	0.5866	3.31E-03	0.9101	4.92E-05	0.3547	6.66E-02
0.8201	5.23E-05	0.6453	3.08E-03	1.0011	4.84E-05	0.3902	6.34E-02
0.8947	4.99E-05	0.7039	2.83E-03	1.0921	4.67E-05	0.4257	5.90E-02
0.9692	4.66E-05	0.7626	2.54E-03	1.1831	4.41E-05	0.4612	5.34E-02

1.0438	4.24E-05	0.8212	2.20E-03	1.2741	4.05E-05	0.4966	4.65E-02
1.1183	3.71E-05	0.8799	1.83E-03	1.3651	3.58E-05	0.5321	3.86E-02
1.1929	3.06E-05	0.9386	1.42E-03	1.4561	2.99E-05	0.5676	2.99E-02
1.2674	2.31E-05	0.9972	9.92E-04	1.5471	2.27E-05	0.6031	2.08E-02
1.3420	1.47E-05	1.0559	5.91E-04	1.6381	1.47E-05	0.6386	1.22E-02
1.4165	6.66E-06	1.1145	2.45E-04	1.7291	6.92E-06	0.674	5.23E-03
1.4911	1.57E-06	1.1732	5.38E-05	1.8201	1.14E-06	0.7095	8.47E-04

sr90		y90		pb210		bi210	
Energy (MeV)	Emission Probability	Energy (MeV)	Emission Probability	Energy (MeV)	Emission Probability	Energy (MeV)	Emission Probability
0.0273	7.79E-02	0.1140	4.26E-02	0.0032	4.02E-01	0.0581	7.59E-02
0.0546	7.60E-02	0.2284	5.18E-02	0.0063	2.60E-01	0.1162	7.96E-02
0.0819	7.50E-02	0.3426	5.94E-02	0.0095	1.50E-01	0.1742	8.20E-02
0.1092	7.40E-02	0.4568	6.50E-02	0.0126	7.26E-02	0.2323	8.29E-02
0.1365	7.30E-02	0.571	6.87E-02	0.0158	2.85E-02	0.2904	8.25E-02
0.1638	7.17E-02	0.6852	7.08E-02	0.0189	1.59E-02	0.3484	8.06E-02
0.1911	7.01E-02	0.7994	7.17E-02	0.0221	1.38E-02	0.4065	7.75E-02
0.2184	6.80E-02	0.9136	7.15E-02	0.0252	1.19E-02	0.4646	7.32E-02
0.2457	6.53E-02	1.0278	7.04E-02	0.0284	1.02E-02	0.5227	6.79E-02
0.273	6.19E-02	1.142	6.85E-02	0.0315	8.58E-03	0.5807	6.17E-02
0.3003	5.78E-02	1.2562	6.57E-02	0.0347	7.08E-03	0.6388	5.48E-02
0.3276	5.27E-02	1.3704	6.19E-02	0.0378	5.72E-03	0.6969	4.74E-02
0.3549	4.68E-02	1.4846	5.69E-02	0.041	4.49E-03	0.755	3.97E-02
0.3822	4.01E-02	1.5988	5.07E-02	0.0441	3.41E-03	0.8131	3.20E-02
0.4095	3.27E-02	1.713	4.30E-02	0.0473	2.46E-03	0.8711	2.45E-02
0.4368	2.48E-02	1.8272	3.42E-02	0.0504	1.66E-03	0.9292	1.75E-02
0.4641	1.71E-02	1.9414	2.46E-02	0.0536	1.02E-03	0.9873	1.12E-02
0.4914	9.75E-03	2.0556	1.50E-02	0.0567	5.28E-04	1.0454	6.16E-03
0.5187	4.28E-03	2.1698	6.43E-03	0.0599	1.93E-04	1.1034	2.33E-03
0.546	1.01E-03	2.284	1.13E-03	0.063	3.13E-05	1.1615	4.22E-04

Appendix G Scintillator Data Sheets

Bc-404 Scintillator (St. Gobain Crystals)

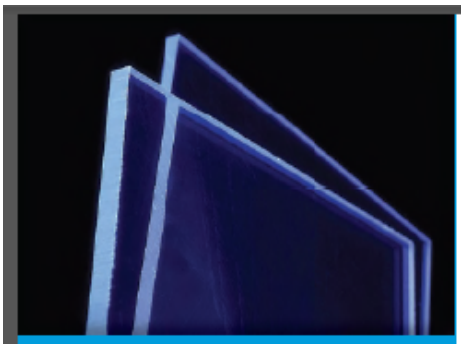

Plastic Scintillators

Plastic sheets cast from the monomer ensure the highest light yield and best internal light transmission. All raw materials undergo extensive purification prior to polymerization and the finished sheets exhibit highly uniform scintillation and optical properties. Scintillators are machined to final dimensions using diamond tooling to provide optimum quality surfaces for total internal reflection.

Thin Films –

Thin films are ideally suited for charged particle detection and fast timing applications. We supply thin films in the following blue-emitting (410 to 430 nm) scintillator formulations:

- BC-400 General purpose
- BC-404 Highest light output; ideal for beta detection
- BC-418 Fast timing material with decay time of 1.4 ns
- BC-422 Fast timing material with decay time of 1.6 ns

BC-490 Plastic Scintillator Casting Resin –

BC-490 is a partially polymerized plastic scintillator that can be cured to full hardness by the end user. The scintillator thus formed is clear, with scintillation and mechanical properties similar to those of our general purpose plastic scintillators. It is most frequently used in applications that require other materials to be imbedded in the scintillator and those that require unique shapes to be cast, often in special holders.

BC-490 is supplied in complete kits with detailed instructions. Each kit contains three parts: partially polymerized scintillator resin, catalyst and catalyst solvent.

A green-emitting version, BC-490G, is also available.

Standard Cast Sheet Sizes

Thickness*	Thickness Tolerance (nominal)	Routine Maximum**
1 mm	± 0.1 mm	30 x 60 cm
1.5 mm	± 0.25 mm	30 x 101 cm
2 mm	± 0.25 /- 0.3 mm	45 x 101 cm
3 mm	0.38 mm	63 x 101 cm
5 mm	+ 0.56 / - 0.46 mm	63 x 203 cm
6.4 mm	+ 0.64 / - 0.51 mm	63 x 203 cm
10 mm	± 0.51 mm	63 x 203 cm
12.7 mm	± 0.64 mm	63 x 203 cm
20 mm	± 0.73 mm	63 x 203 cm
25 mm	+ 0.76 / - 1 mm	63 x 203 cm
38 mm	± 0.76 mm	63 x 203 cm
50 mm	± 2 mm	63 x 203 cm
75 mm	± 2.5 mm	60 x 101 cm
100 mm	± 3.8 mm	60 x 101 cm
125 mm	± 6 mm	60 x 101 cm
150 mm	± 6 mm	60 x 101 cm

* This dimension is controlled during the casting process

** Large sizes available, but with different tolerances

Special Large Cast Sheet

Thickness Range	Maximum Width	Maximum Length
1 - 5 cm	30 cm	500 cm
0.5 - 5 cm	45 cm	400 cm
0.5 - 5 cm	60 cm	300 cm
1 - 2.5 cm	100 cm	200 cm
1 - 3.8 cm	120 cm	120 cm

Please ask about other speical sizes you may need

Thin Film Specifications (Typical Size)

Thickness Range	Tolerance Range	Sheet Size W x L
.5 - 1.0 mm	± 10%	250 x 250 mm
.22 - .49 mm	± 10%	225 x 225 mm
.11 - .24 mm	± 10%	150 x 200 mm
.04 - .10 mm	± 15%	150 x 200 mm
.010 - .039 mm	± 20%	150 x 200 mm

- Edges are trimmed or polished (upon request)
- Other scintillators available

3

Technical Data
Light Output, Light Collection

Range of Atomic Particles in Premium Plastic Scintillator

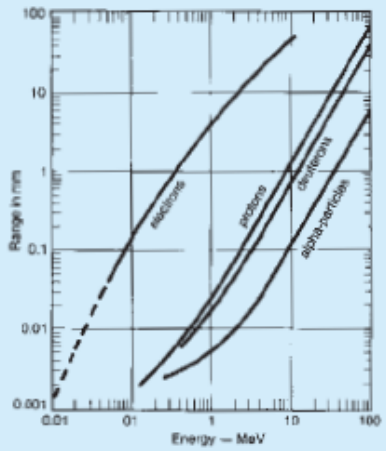

Premium Plastic Scintillator Response to Atomic Particles

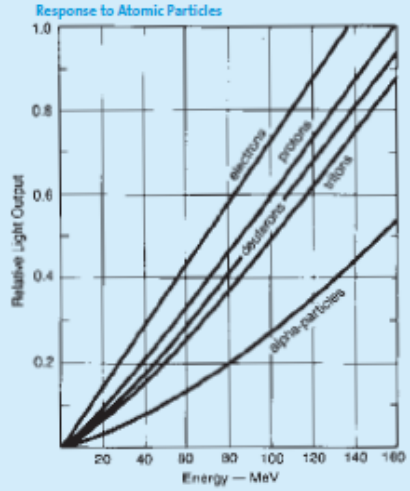

Light Collection in BC-412 Cast Sheet

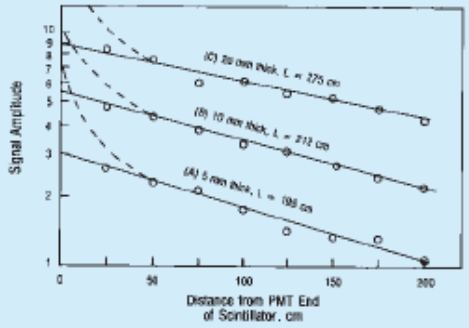

Sheet Size: 120 mm x 2000 mm (4.71" x 80")

- Plot of Technical Attenuation Length using a 150 mm (6") long, triangular light guide connecting the scintillator to the phototube.
- Approximate result when the phototube is coupled directly to the scintillator.

Physical Constants of SGC Plastic Scintillators

Scintillator	Light Output % Anthracene[1]	Wavelength of Maximum Emission, nm	Decay Constant, Main Component, ns	Bulk Light Attenuation Length, cm	Refractive Index	H:C Ratio	Loading Element % by weight	Density	Softening Point °C
BC-400	65	423	2.4	250	1.58	1.103		1.032	70
BC-404	68	408	1.8	160	1.58	1.107		1.032	70
BC-408	64	425	2.1	380	1.58	1.104		1.032	70
BC-412	60	434	3.3	400	1.58	1.104		1.032	70
BC-414	68	392	1.8	100	1.58	1.110		1.032	70
BC-416	38	434	4.0	400	1.58	1.110		1.032	70
BC-418	67	391	1.4	100	1.58	1.100		1.032	70
BC-420	64	391	1.5	110	1.58	1.102		1.032	70
BC-422	55	370	1.6	8	1.58	1.102		1.032	70
BC-422Q	11	370	0.7	<8	1.58	1.102	Benzephenone,0.5%*	1.032	70
BC-428	36	480	12.5	150	1.58	1.103		1.032	70
BC-430	45	580	16.8	NA	1.58	1.108		1.032	70
BC-436	52	425	2.2	NA	1.61	0.960 D:C	Deuterium,13.8%	1.130	100
BC-440	60	434	3.3	400	1.58	1.104		1.032	99
BC-440M	60	434	3.3	380	1.58	1.104		1.039	100
BC-444	41	428	285	180	1.58	1.109		1.032	70
BC-452	32	424	2.1	150	1.58	1.134	Lead,5%	1.080	60
BC-454	48	425	2.2	120	1.58	1.169	Boron,5%	1.026	60
BC-480	**	425	–	400	1.58	1.100		1.032	70
BC-482A	QE=.86	494	12.0	300	1.58	1.110		1.032	70
BC-490	55	425	2.3	NA	1.58	1.107		1.032	70
BC-498	65	423	2.4	NA	1.58	1.103		1.032	70

[1] Anthracene light output = 40-50% of NaI(Tl) * 0.1 to 5 weight % also available ** Ratio of Cerenkov light to scintillator light = 10:1

Physical Constants of SGC Liquid Scintillators

Scintillator	Light Output % Anthracene[1]	Wavelength of Maximum Emission, nm	Decay Constant, ns	H:C Ratio	Loading Element	Density	Flash Point °C
BC-501A	78	425	3.2[2]	1.212		0.87	26
BC-505	80	425	2.5	1.331		0.877	48
BC-509	20	425	3.1	.0035	F	1.61	10
BC-517L	39	425	2	2.01		0.86	102
BC-517H	52	425	2	1.89		0.86	81
BC-517P	28	425	2.2	2.05		0.85	115
BC-517S	66	425	2	1.70		0.87	53
BC-519	60	425	4	1.73		0.87	63
BC-521	60	425	4	1.31	Gd (to 1%)	0.89	44
BC-523	65	425	3.7	1.74	Nat. ^{10}B (5%)	0.916	-8
BC-523A	65	425	3.7	1.67	Enr. ^{10}B (5%)	0.916	-8
BC-525	55	425	3.8	1.56	Gd (to 1%)	0.88	91
BC-531	59	425	3.5	1.63		0.87	93
BC-533	51	425	3	1.96		0.80	65
BC-537	61	425	2.8	0.99 (D:C)	^2H	0.954	-11

* Anthracene light output = 40-50% of NaI(Tl) [2] Fast component; mean decay times of first 3 components = 3.16, 32.3 and 270 ns

EJ-204 (Eljen Technologies)

Physical Constants of Plastic Scintillators

Scintillator	Light Output, % Anthracene[1]	Wavelength of Maximum Emission nm	Decay Constant Main Component ns	Typical Light Attenuation Length cm	H : C Atomic Ratio	Refractive Index	Softening Point °C	Density	Principal Applications
EJ-200	64	425	2.1	380	1.104	1.58	75	1.02	Best overall properties, TOF Counters, large area, p+, e-, etc.
EJ-204	68	408	1.8	160	1.107	1.58	75	1.02	Good general properties
EJ-208	60	434	3.3	400	1.104	1.58	75	1.02	Large area, protons, electrons, etc.
EJ-212	65	423	2.4	250	1.103	1.58	75	1.02	General Purpose, Thin Films
EJ-228	67	391	1.4			1.58		1.02	Very fast timing, high pulse pair resolution
EJ-230	64	391	1.5			1.58		1.02	Variant EJ-228 optimized for detector dimensions over 10 cm
EJ-232	55	370	1.4	N/A	1.102	1.58	75	1.023	Ultra fast timing
EJ-232Q (0.5%)	19	370	700ps	N/A	1.102	1.58	75	1.023	Ultra fast timing, Quenched with Benzophenone for Shortening timing properties to achieve high counting
EJ-240	41	435	~230	240	1.109	1.58	75	1.02	Long decay time, phoswich detectors
EJ-244	56	434	3.3	380	0.995	1.58	100	1.02	Elevated temperatures, general purpose
EJ-248	54	425	2.1	350	0.995	1.58	100	1.02	Elevated temperatures, general purpose
EJ-252	46	423	2.4	N/A	1.098	1.58	75	1.037	Dosimetry, air-equivalent
EJ-254 (5%)	48	425	2.2		1.167	1.58	75	1.026	Boron Loaded, Fast Neutron Spectroscopy
EJ-256	32	425	2.1	N/A	1.134	1.58	75	1.08	Lead-Loaded, (5% standard), X-ray Dosimetry
EJ-260	60	490	9.2	N/A	1.102	1.58	75	1.02	Green Emitting, Longer wavelengths, Solid State Photosensors
EJ-264	50	580	16.8	N/A	1.105	1.58	75	1.023	Orange emitting, Longer wavelengths, Solid State Photosensors
EJ-299-07		435	2	N/A	1.123	1.58	70	1.02	Ultra thin Films (5 microns to 25 microns)

[1] 1 MeV of energy deposited in EJ-200 from an energetic electron produces approximately 10,000 blue photons

ELJEN TECHNOLOGY
Charles Hurlbut, General Manager
Chris Maxwell, Sales Manager
1300 W. Broadway
Sweetwater, Texas 79556
Tel: (325) 235-4276
Toll Free: (888) 800-8771
Fax: (325) 235-0701

Appendix H PMT Data Sheets

Hamamatsu R5946 PMT

HAMAMATSU

PHOTOMULTIPLIER TUBE
R5946

Stable Operation in High Magnetic Fields beyond 1 Tesla
38mm(1–1/2 Inch) Diameter, Proximity Photocathode and Fine Mesh Dynodes

GENERAL

Parameter		Description/Value	Unit
Spectral Response		300 to 650	nm
Wavelength of Maximum Response		420 ± 50	nm
Photocathode	Material	Bialkali	–
	Minimum Effective Area	27	mm dia.
Window	Material	Borosilicate glass	–
	Shape	Plano–plano	–
Dynode	Secondary Emitting Surface	Bialkali	–
	Structure	Fine mesh	–
	Number of Stages	16	–
Base		19–pin glass base	–
Suitable Socket		E678–19D (supplied)	–

MAXIMUM RATINGS (Absolute Maximum Values)

Parameter		Value	Unit
Supply Voltage	Between Anode and Cathode	2300	Vdc
	Between Anode and Last Dynode	200	Vdc
Average Anode Current		0.01	mA

CHARACTERISTICS (at 25℃)

Parameter		Min.	Typ.	Max.	Unit
Cathode Sensitivity	Luminous (2856K)	–	80	–	μA/lm
	Blue (CS–5–58 filter)	–	9.5	–	μA/lm–b
	Quantum Efficiency at 390nm	–	23	–	%
Anode Sensitivity	Luminous (2856K)	–	80	–	A/lm
Gain	At 0 tesla	–	1.0×10^6	–	–
	At 1 tesla	–	2.9×10^4	–	–
Anode Dark Current (after 30min. storage in darkness)		–	5.0	30	nA
Time Response	Anode Pulse Rise Time	–	1.9	–	ns
	Transit Time	–	7.2	–	ns
	Transit Time Spread (FWHM)	–	0.35	–	ns

NOTE: Anode characteristics are measured with the voltage distribution ratio shown below.

VOLTAGE DISTRIBUTION RATIO AND SUPPLY VOLTAGE

Electrodes	K	Dy1	Dy2	Dy3	Dy4	Dy5	Dy6	.....	Dy16	P
Ratio	2	1	1	1	1	1	.....		1	1

Supply Voltage : 2000Vdc, K : Cathode, Dy : Dynode, P : Anode

Subject to local technical requirements and regulations, availability of products included in this promotional material may vary. Please consult with our sales office.
Information furnished by HAMAMATSU is believed to be reliable. However, no responsibility is assumed for possible inaccuracies or commission. Specifications are subjected to change without notice. No patent right are granted to any of the circuits described herein. © 1994 Hamamatsu Photonics K.K.

PHOTOMULTIPLIER TUBE R5946

Figure 1: Typical Spectral Response

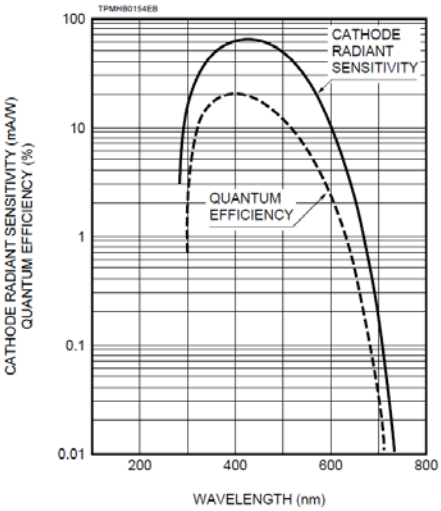

Figure 2: Typical Gain in Magnetic Fields (Parallel to Tube Axis)

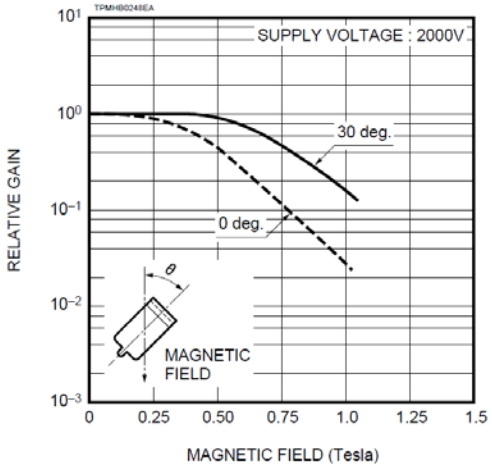

Figure 3: Dimensional Outline and Basing Diagram (Unit : mm)

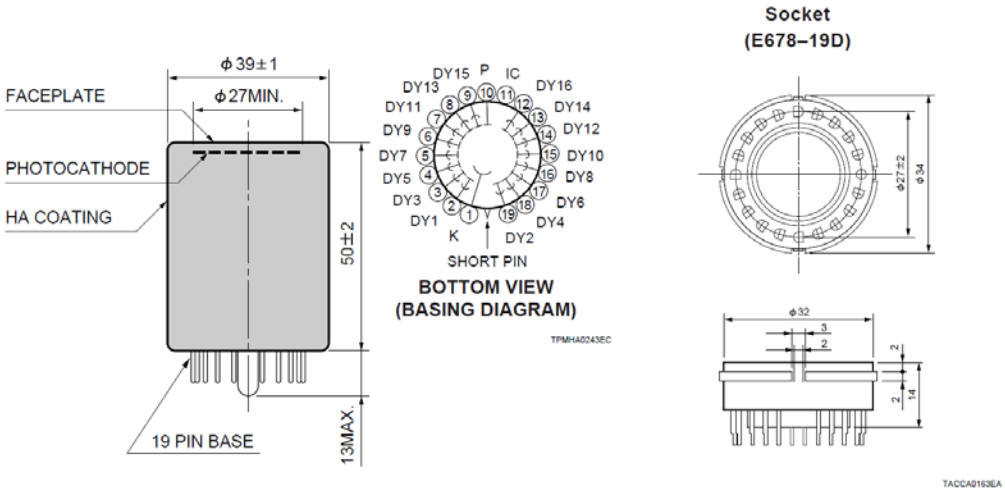

HAMAMATSU

HAMAMATSU PHOTONICS K.K., Electoron Tube Center
314-5, Shimokanzo, Toyooka-village, Iwata-gun, Shizuoka-ken, 438-0193, Japan, Telephone: (81)539/62-5248, Fax: (81)539/62-2205
U.S.A.: Hamamatsu Corporation: 360 Foothill Road, Bridgewater, N.J. 08807-0910, U.S.A., Telephone: (1)908-231-0960, Fax: (1)908-231-1218
Germany: Hamamatsu Photonics Deutschland GmbH: Arzbergerstr. 10, D-82211 Herrsching am Ammersee, Germany, Telephone: (49)8152-375-0, Fax: (49)8152-2658
France: Hamamatsu Photonics France S.A.R.L.: 8, Rue du Saule Trapu, Parc du Moulin de Massy, 91882 Massy Cedex, France, Telephone: (33)1 69 53 71 00, Fax: (33)1 69 53 71 10
United Kingdom: Hamamatsu Photonics UK Limited: Lough Point, 2 Gladbeck Way, Windmill Hill, Enfield, Middlesex EN2 7JA, United Kingdom, Telephone: (44)181-367-3560, Fax: (44)181-367-6384
North Europe: Hamamatsu Photonics Norden AB: Färögatan 7, S-164-40 Kista Sweden, Telephone: (46)8-703-29-50, Fax: (46)8-750-58-95
Italy: Hamamatsu Photonics Italia: S.R.L.: Via Della Moia, 1/E, 20020 Arese, (Milano), Italy, Telephone: (39)2-935 81 733, Fax: (39)2-935 81 741

TPMH1097E04
JUL. 1994

Hamamatsu R1250 PMT

HAMAMATSU

PHOTOMULTIPLIER TUBE R1250

For High Energy Physics, Fast Time Response, High Pulse Linearity 127mm (5 Inch) Diameter, Bialkali Photocathode, 14-Stage, Head-on Type

GENERAL

Parameter		Description/Value	Unit
Spectral Response		300 to 650	nm
Wavelength of Maximum Response		420	nm
Photocathode	Material	Bialkali	—
	Minimum Useful Diameter	120	mm dia.
Window	Material	Borosilicate glass	—
Dynode	Structure	Linear focused	—
	Number of Stages	14	—
Base		20-pin base	—
Suitable Socket		E678-20A (supplied)	—

MAXIMUM RATINGS (Absolute Maximum Values)

Parameter		Value	Unit
Supply Voltage	Between Anode and Cathode	3000	Vdc
	Between Anode and Last Dynode	500	Vdc
Average Anode Current		0.2	mA
Ambient Temperature		-30 to +50	°C

CHARACTERISTICS (at 25°C)

Parameter		Min.	Typ.	Max.	Unit
Cathode Sensitivity	Luminous (2856K)	55	70	—	μA/lm
	Blue (with CS 5-58 filter)	7.0	9.0	—	μA/lm-b
	Quantum Efficiency at 390nm	—	22	—	%
Anode Sensitivity	Luminous (2856K)	300	1000	—	A/lm
	Blue (with CS 5-58 filter)	—	130	—	A/lm-b
Gain		—	1.4×10^7	—	—
Anode Dark Current (after 30min. storage in darkness)		—	50	300	nA
Time Response	Anode Pulse Rise Time	—	2.5	—	ns
	Electron Transit Time	—	54	—	ns
	Transit Time Spread	—	1.2	—	ns
Pulse Height Resolution with ^{137}Cs		—	8.3	—	%
Gain Deviation	Long Term	—	1.0	—	%
	Short Term	—	1.0	—	%
Pulse Linearity *	2% Deviation	—	160	—	%
	5% Deviation	—	250	—	%

* Measured with special voltage distribution ratios shown in the Table 2.

Table 1: VOLTAGE DISTRIBUTION RATIO AND SUPPLY VOLTAGE

Electrode	K	G1	G2	Dy1	Dy2	Dy3	Dy4	Dy5	Dy6	Dy7	Dy8	Dy9	Dy10	Dy11	Dy12	Dy13	Dy14	P
Ratio	2.5	7.5	0	1.2	1.8	1	1	1	1	1	1	1	1	1.5	1.5	3	2.5	

Supply Voltage: 2000Vdc, K: Cathode, Dy: Dynode, P: Anode, G: Grid

Table 2: SPECIAL VOLTAGE DISTRIBUTION RATIO AND SUPPLY VOLTAGE FOR PULSE LINEARITY MEASUREMENT

Electrode	K	G1	G2	Dy1	Dy2	Dy3	Dy4	Dy5	Dy6	Dy7	Dy8	Dy9	Dy10	Dy11	Dy12	Dy13	Dy14	P
Ratio	2.5	7.5	0	1.2	1.8	1	1	1	1	1.2	1.5	2	2.8	4	5.7	8	5	
Capacitors in μF											0.01	0.01	0.02	0.02	0.02	0.04	0.06	

Supply Voltage: 2500Vdc, K: Cathode, Dy: Dynode, P: Anode, G: Grid

Subject to local technical requirements and regulations, availability of products included in this promotional material may vary. Please consult with our sales office. Information furnished by HAMAMATSU is believed to be reliable. However, no responsibility is assumed for possible inaccuracies or omissions. Specifications are subject to change without notice. No patent rights are granted to any of the circuits described herein. © 1999 Hamamatsu Photonics K.K.

PHOTOMULTIPLIER TUBE R1250

Figure 1: Typical Spectral Response

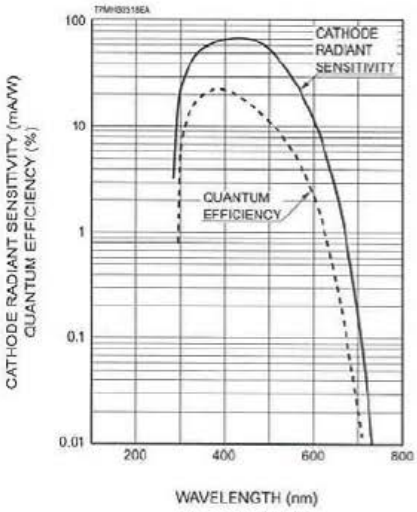

Figure 2: Typical Gain Characteristics

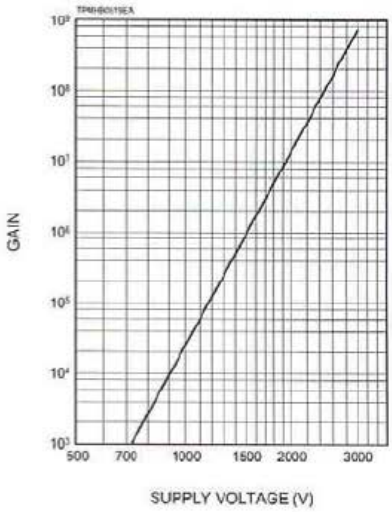

Figure 3: Dimensional Outline and Basing Diagram (Unit: mm)

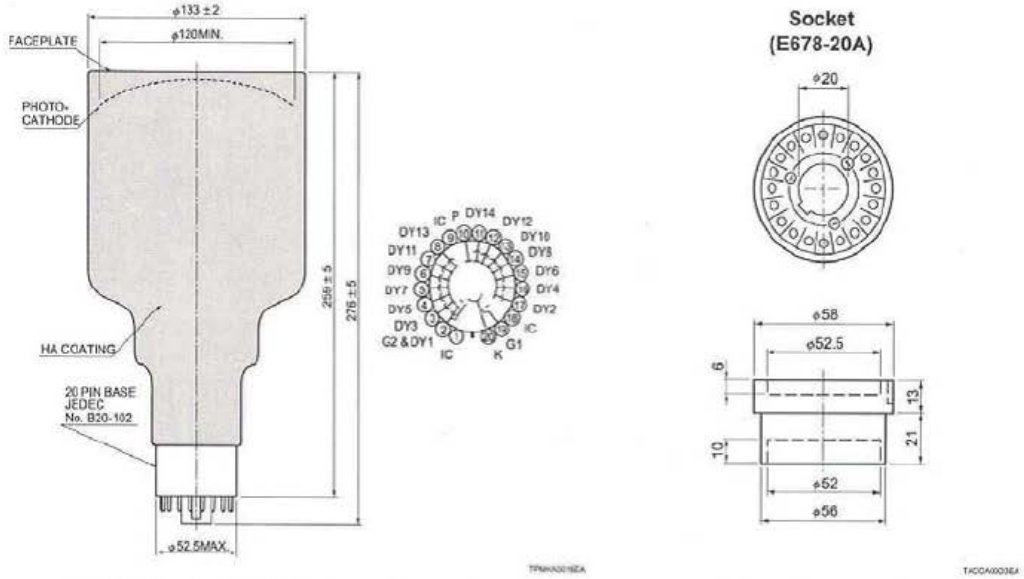

HAMAMATSU HOMEPAGE URL http://www.hamamatsu.com

HAMAMATSU PHOTONICS K.K., Electron Tube Center
314-5, Shimokanzo, Toyooka-village, Iwata-gun, Shizuoka-ken, 438-0193, Japan, Telephone: (81)539/62-5248, Fax: (81)539/62-2205
U.S.A.: Hamamatsu Corporation: 360 Foothill Road, P. O. Box 6910, Bridgewater, N.J. 08807-0910, U.S.A., Telephone: (1)908-231-0960, Fax: (1)908-231-1218
Germany: Hamamatsu Photonics Deutschland GmbH: Arzbergerstr. 10, D-82211 Herrsching am Ammersee, Germany, Telephone: (49)8152-375-0, Fax: (49)8152-2658
France: Hamamatsu Photonics France S.A.R.L.: 8, Rue du Saule Trapu, Parc du Moulin de Massy, 91882 Massy Cedex France, Telephone: (33)1 69 53 71 00, Fax: (33)1 69 53 71 10
United Kingdom: Hamamatsu Photonics UK Limited: Lough Point, 2 Gladbeck Way, Windmill Hill, Enfield, Middlesex EN2 7JA, United Kingdom, Telephone: 44(20)8-367-3560, Fax: 44(20)8-367-6384
North Europe: Hamamatsu Photonics Norden AB: Smidesvägen 12, SE-171-41 SOLNA, Sweden, Telephone: (46)8-509-031-00, Fax: (46)8-509-031-01

Appendix J Review of Scientific Instruments Publication (Draft)

Predicting the Sensitivity of the Beryllium/Scintillator Layer Neutron Detector Using Monte Carlo and Experimental Response Functions

J.D. Styron[1a, b], G.W. Cooper[1], C.L. Ruiz[2], K.D. Hahn[2], G.A. Chandler[2], A.J. Nelson[1], J.A. Torres[2], B.R. McWatters[2], Ken Carpenter[1], and M.A. Bonura[1]

[1]*Dept. of Chemical and Nuclear Engineering, University of New Mexico, Albuquerque, NM 87131, USA*

[2]*Sandia National Laboratories, Albuquerque, New Mexico 87185, USA*

(Presented XXXXX; received XXXXX; accepted XXXXX; published online XXXXX)

A methodology for obtaining empirical curves relating absolute measured scintillation light output to beta energy deposited are presented. Output signals were measured from thin plastic scintillator using NIST traceable beta and gamma sources and MCNP5 was used to model the energy deposition from each source. Combining the experimental and calculated results gives the desired empirical relationships. To validate, the sensitivity of a beryllium/scintillator-layer neutron activation detector was predicted and then exposed to a known DD neutron fluence. The predicted and the measured sensitivity were in statistical agreement.

I. Introduction

The physical relationship between beta energy deposition and the resulting light output for organic scintillators is well known and described in detail by Birks.[1] Birks' formula predicts the light output in the absence of quenching, which is the case for energetic electrons, and is directly proportional to the beta energy deposition. In addition, the detector response will be characterized absolutely by a system specific proportionality constant[2]. There are two types of experimental techniques commonly discussed in the literature to determine this constant: the Compton Coincidence Technique (CCT)[3] and the Compton Edge Method (CEM).[4-5] In CCT, the electron energy is inferred by exposing the scintillator to a collimated gamma source and measuring the kinematic relationship of scattered photon and electron pairs. This requires a coincidence measurement between the scintillator detector of interest and a calibrated photon detector, typically a high-purity germanium detector at a known angle and location. The CEM method is used to determine the response of the detector at the maximum obtainable energy of a recoil electron from a collision with a gamma of known energy. This energy corresponds to the half-height of the Compton edge that can be determined from a differential spectrum. This method requires several known gamma sources of varying energies and some knowledge of the detector resolution.

In this work, we are interested in the response function of a fusion neutron detector which is based on the ^{9}Be (n, α) ^{6}He reaction. The neutron yield is inferred by measuring the beta decay of the ^{6}He nucleus, which has a half-life of 807 ms and a beta end-point energy of 3.51 MeV.[6] The beta particle is detected by intimately coupling a thin layer of plastic scintillator to a beryllium layer, similar to the original design proposed by Rowland.[7] Any or all of the betas' energy is deposited within the scintillator and the resulting scintillation photons are collected using a photomultiplier tube (PMT) that views the scintillator on edge. It has been well established in the literature that the parameters that affect the magnitude of the pulse measured from the PMT are the scintillator type, the reflectivity of materials surrounding the scintillator, the location of scintillation event, the system electronics, and the solid angle subtended by the scintillator on the photocathode.[8-10] This work quantifies these parameters and develops a detector response function for a simple detector system using a semi-empirical formulation that combines experimental data and Monte Carlo calculations.[11]

II. Experimental Set-Up

For this work, an existing cylindrical beryllium detector was adopted. The housing is a steel tube (4.215 cm in diameter by 11.9 cm in height) that houses a Hamamatsu R5946 PMT and was retrofitted to accept, 5.5 mm below the PMT, rectangular geometries. Figure 1 shows the variations of beryllium-scintillator options investigated and the three possible source positions. The left image is the primary geometry for which the response function is desired. It consists of alternating 30 x 65 mm layers of 3.175 mm thick beryllium metal (3 total) and 1.0 mm thick Bicron BC-404 plastic scintillator (4 total). The two inner scintillator layers have beryllium on both sides of the scintillator

[a)]Contributed paper published as part of the Proceedings of the 20th Topical Conference on High-Temperature Plasma Diagnostics, Atlanta, Georgia, June, 2014.
[b)]Author to whom correspondence should be addressed: jdstyro@sandia.gov

and the outermost scintillator layers are reflected with beryllium and a 1.0 mm white polypropylene layer. These two geometries, shown with a source in place, are labeled case 1 and case 2 and are shown in the center and right images, respectively.

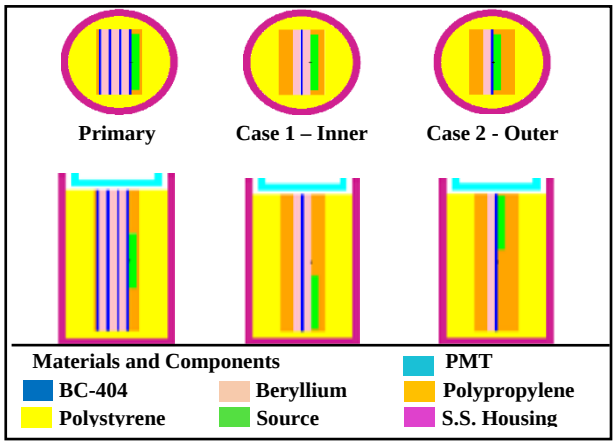

Figure 38 Experimental Geometries, Top-Radial View, Bottom-Axial View. For perspective, three different source locations are shown.

Data were collected with several NIST traceable beta and gamma sources for cases 1 and 2 to develop the response for the primary detector geometry. The isotopes used throughout were Co-60, Cl-36, Cs-137, Sr-90/Y-90, and Na-22. Each source has a known activity (~10 nCi and < 3% uncertainty) and a well-defined geometry.[12] Sources could be positioned on the face of the scintillator at one of three locations: at the center or 1.37 cm from either end as shown in Figure 1. The detector efficiency was inferred for each source at a given location by taking measurements using standard NIM electronics at the recommended bias of -2 kV. The output signal of the detector was routed through a 5 Volt clipper circuit and then split to an Ortec 584 Constant Fraction Discriminator (CFD) and a Tektronix DPO 3032 digitizer. The positive TTL output signal of the 584 was processed with an Ortec Easy-MCS for monitoring signal drift and the negative logic output was processed through a Tennelec TC 536 counter/timer. For each source-geometry combination, counts were first measured at a minimum CFD setting of 20 mV and then at 20 mV increments until the number of counts in a 300 second interval diminished to background.

III. MCNP 5 model

For every experiment conducted, the specific geometry and the source used were modeled using the transport code MCNP5.[13] Materials used in the models were of theoretical density and the compositions were obtained from the NIST database.[14] The beta and gamma sources are planar geometries, with the beta and gamma sources distributed over 22.0 mm and 5.0 mm diameter circular regions, respectively. Specifics of the geometric configuration for each source type can be found in ref. 12. Discreet photon energies and branching ratios for each source were found in ref. 15. The spectral data for the beta emissions were found in ref. 16 and were modeled as a probability function continuous between points. The output quantity calculated using the MCNP F8 pulse-height tally was the number of events that occur within user-defined energy bins. In this case, the energy bins were divided into 50 keV increments ranging from the MCNP threshold limit of 1 keV to a maximum energy that was source dependent. A separate MCNP model was developed for each type of emission having a branching ratio >0.001%. The total differential spectrum for each isotope was found by taking the product of the F8 result and the branching ratio and summing over all possible decay modes. The overall statistical uncertainty for the MCNP calculations was < 1%.

IV. Results

For each case, an integral spectrum was obtained by measuring the counts as a function of CFD setting. Background counts were subtracted from the total counts to obtain the number of net events, which were normalized to the decay corrected source activity. Predicted integral spectra were also calculated from the MCNP results as a function of tallied energy bins. A data set for one experiment and the corresponding MCNP calculation are shown in Fig. 2. The results shown are typical of all experiments. The vertical axis has units of counts per decay and can be expressed as a function of CFD threshold in mV for the experimental result and as a function of energy deposition in MeV (shown in parentheses) for the MCNP result.

The dependent variable for both functions are the same, therefore the independent variable for one function can be solved in terms of the other. Since the shapes of the curves are unique, a point-wise interpolation method was used to obtain a discrete energy deposition value for each CFD threshold level at every experimental data point that was bounded by two values from the MCNP calculation. These points can then be plotted for a specific case to produce an analytical expression for the expected discriminator value for a given energy deposition. This method is similar to the CEM method except the whole range of data is used instead of just the Compton edges. Correlations are shown in Fig. 3 for case 1 and 2 for several sources. In each case, the source was centered on the scintillator and the scintillator axially centered under the PMT. For comparison, the relationship developed by Pozzi et al using the CEM method[17] is also shown.

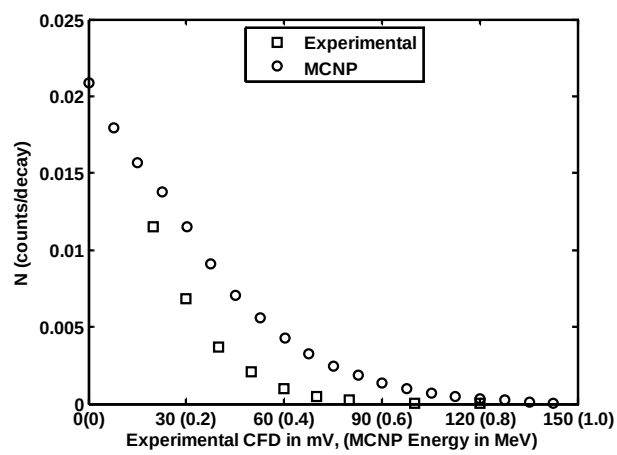

Figure 2 Experimental and MCNP data for the Case 1 geometry and a Co-60 source. (MCNP data is shifted slightly to show similarities)

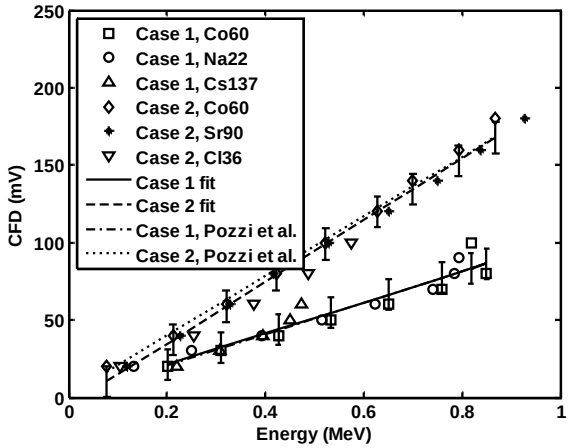

Figure 3 CFD to Energy Deposited Correlation for Case 1 and 2 geometries. Least squares fit using various beta and gamma sources.

In a correlation developed by Schonfelder[10], the light yield changes by a view factor, the fraction of light incident on the face of the photocathode emitted from the edge of the scintillator. To confirm their findings, data were taken using case 1 and 2, with the source centered on the scintillator at five scintillator positions: on axis and 2, 4, 6, and 8 mm off-axis. Assuming that light is isotropically emitted from the scintillator, the corresponding view factors were calculated to be 0.503, 0.500, 0.478, 0.447, and 0.398 with an uncertainty at the one sigma level of 3%[18]. Curves were generated, similar to that shown in Fig. 3, for each data set except the CFD level was divided by the view factor to account for this dependency. With the view factor included in the correlation, the curves yielded the same result, thus confirming the findings of Schonfelder.

Data were taken individually at three source locations, with the scintillator on axis, for cases 1 and 2. Each data set was resolved into the view-factor-dependent discriminator-level to energy-deposition correlation using the methodology established. The data were then averaged, point-wise, over the three source locations to obtain an average energy deposition for each discriminator level in either case. The average accounts for the size ratio of the source distribution to the scintillator, which is ~ 1/3. This could, however, be easily adapted to an analytical form for post processing if a collimated source or a larger scintillator is used. Shown in equations 1 and 2 are the final correlations for cases 1 and 2, respectively. The final correlation can be described as the average energy deposition in MeV, from an MCNP calculation, needed to reach a discreet discriminator level in mV at a known view factor, Ω. These equations are only valid for this detector at beta energies between 125 and 960 keV. The standard deviation for these equations at the one sigma level is +/- 8 mV.

$$CFD = \Omega\,(182.74E_{avg} + 12.88) \qquad (1)$$

$$CFD = \Omega\,(426.06E_{avg} - 15.52) \qquad (2)$$

V. Validation

The primary geometry was placed in the detector and then exposed to a known neutron fluence at the Ion Beam Laboratory located at Sandia National Laboratories. D-D neutrons were generated by accelerating 175 keV D^+ ions into a thin erbium deuteride target using a 350 keV Cockroft-Walton accelerator. The general experimental set-up and the calculation of the neutron fluence using the Associated Particle Method (APM) is described in detail by Ruiz *et al.* and Cooper *et al.*[19,20] For this experiment, the center of the detector active region was placed on the outside of the thin-walled, 3-inch radius, aluminum target chamber at 90 degrees. Data were taken at a CFD level of 40 mV and the detector bias was -2kV. The beam was cycled in 20 second intervals, where the beam was on target for four seconds and then off target for sixteen seconds. Counts were taken for the first 12 seconds the beam was off. This cycling was repeated until ~ 10,000 counts were obtained in the first time bin. An average background was obtained after ten half-lives (~ 8 sec) and deducted from the total counts. The net counts were divided by the number of neutrons incident at the average detector solid angle, 1.57 +/- 0.09 x 10^7, which corresponds to the midway point of the detector. This yielded an experimental sensitivity of 0.0033 +/- 0.0003 counts per incident neutron at the average solid angle.[21]

The prediction of the detector sensitivity required two Monte Carlo calculations to model the production and decay of ^{6}He. The source modeled was a distributed energy neutron source consistent with the kinematics of accelerating 175 keV D^+ ions into an erbium deuteride target.[22] The neutron flux, within the beryllium layers, was multiplied by the energy dependent ^{9}Be (n, α) ^{6}He cross-section to define the spatial distribution of ^{6}He beta particles. The beta particle energy was sampled using spectral data from previous work.[23] Five F8 tallies were taken, one for each scintillator layer and one that treats all four layers as a single unit. The individual layer tallies were used to determine the fraction of total events that occurred per layer. Since the problem is symmetric the fraction of events per the outer and inner layers are 0.353+/-0.001 and 0.647+/- 0.002, respectively. The minimum energy deposition was found by taking the inverse of equations 1 and 2 at a CFD setting of 40 mV and applying the appropriate view factors. The minimum energy deposition was found to be 0.37 +/- 0.08 MeV for the two inner layers and 0.24 +/- 0.05 MeV for the two outer layers. A weighted average energy deposition of 0.31 +/- 0.06 MeV was found by adding the quotients of the fractional events and the energy deposition per layer and taking the inverse. The corresponding counts per source neutron at that energy was 4.1 +/- 0.1 x 10^{-6} and the number of neutrons at the average solid angle per source neutron was 0.01530+/- 0.00001. Dividing the two values, the source term falls out and gives a sensitivity of 0.0027 +/- 0.0006 counts per incident neutron at the average solid angle, which is in statistical agreement with the APM. The 20% uncertainty in the sensitivity prediction corresponds to the +/- 8 mV uncertainty in the correlation. This uncertainty is mainly driven by poor energy resolution, so it seems reasonable for a thin plastic scintillator. Even with large uncertainties this methodology provides results that are consistent with previous work and could prove to be a useful tool when trying to design future scintillation detectors. Work is ongoing with a more complex detector, with more data points, to further validate this methodology.

VI. Acknowledgements

Sandia National Laboratories is a multi-program laboratory operated by Sandia Corporation, a wholly owned subsidiary of Lockheed Martin Company, for the U.S. Department of Energy's National Nuclear Security Administration under contract DE-AC04-94AL85000.

VII. References

[1]J.B. Birks, "The Theory and Practice of Scintillation Counting," Pergamon Press, Oxford, (1964).

[2]G.F. Knoll, "Radiation Detection and Measurement", Fourth Ed., Wiley,New York, (2010), pg. 231.

[3]D.L. Smith, R.G. Polk,T.G. Miller, Nucl. Instr. Meth., **64**, (1968), 157.

[4]G. Dietze and H. Klein, Nucl. Instr. Meth., **193**, (1982), 549.

[5]Lisa G. Chiang, Richard B. Oberer, Sara A. Pozzi , "Method to Correlate CFD Discriminator Level and Energy Deposition by Neutrons and Photons in A Fast Plastic Scintillating Detector", ORNL/TM-2000/193, (2000).

[6]Chart of the Nuclides,16 ed.,Bechtel, (2002).

[7]M.S. Rowland and J.C. Roberson, Nucl. Instr. Meth., **224**, (1984), 322.

[8]P. Kuijper, C.J. Tiesinga, C.C. Jonker, Nucl. Instr. Meth., **42**, (1966), 56.

[9]G. Keil, Nucl. Instr. And Meth., **87,** (1970), 111.

[10]V.Schonfelder, Nucl. Instr. And Meth., **86**, (1970), 327.

[11]Sarah A. Pozzi, Marek Flaska, Andreas Enqvist, Imre Pazsit, Nucl. Instr. Meth. **582**, (2007), 629.

[12]Eckert & Ziegler, "Reference and Calibration Sources Catalog vers. 1.0", (2007), http://www.ezag.com

[13]X-5 Monte Carlo Team, "MCNP - A General Monte Carlo N-Particle Transport Code, Version 5," LA-UR-03-1987, Los Alamos National Laboratory (2008).

[14]NIST, ESTAR, Database, http://physics.nist.gov, (2013).

[15]Brookhaven National Laboratories, http://www.nndc.bnl.gov/nudat2/.

[16]M.G. Stabin and C.Q. da Luz, Health Phys., 83, (2002), 471 http://www.doseinfo-radar.com/RADARDecay.html.

[17]Sarah A. Pozzi, James A. Mullens, John T. Mihalczo, Nucl. Instr. Meth., **524**, (2004), 92.

[18]Howell, J.R., "A catalog of radiation configuration factors", McGraw-Hill, (1982).

[19]C.L. Ruiz et al, Rev. Sci. Instr. **83**, (2012), 10D913, http://dx.doi.org/10.1063/1.4729495.

[20]G.W. Cooper et al, Rev. Sci. Instr. **83**, (2012), 10D918, http://dx.doi.org/10.1063/1.4746999.

[21]C.L. Ruiz, Manuscript in preparation (2014).

[22]C.L. Ruiz et. al., Rev. Sci. Instr., **63**, (1992), 4889, http://dx.doi.org/10.1063/1.1143541.

[23]J.B. Vise and B.M. Rustad, Phys. Rev., **132,** (1963), 2573.